THE UNIVERSITY
of EDINBURGH

SCHOOL OF CHEMISTRY

THE UNIVERSITY *of* EDINBURGH

Triptycene-based Polymers of Intrinsic Microporosity for membrane applications

Thesis submitted for the degree of Doctor of Philosophy by:

Ian James Rose

Supervisor: Neil B. McKeown

2016

Declaration

This work has not been submitted in substance for any other degree or award at this or any other university or place of learning, nor is it being submitted concurrently in candidature for any degree or other award.

Signed …… (candidate)

Date …12/09/2016……

Statement 1

This thesis is being submitted in partial fulfilment of the requirements for the degree of Doctor of Philosophy.

Signed …… (candidate)

Date …12/09/2016……

Statement 2

This thesis is the result of my own independent work/investigation, except where otherwise stated. Other sources are acknowledged by explicit references. Any views expressed are my own.

Signed …… (candidate)

Date …12/09/2016……

Statement 3

I hereby give consent for my thesis, if accepted, to be available for photocopying and for inter-library loan, and for the title and summary to be made available to outside organisations.

Signed …… (candidate)

Date …12/09/2016……

Acknowledgments

First of all I would like to thank my supervisor, Professor Neil McKeown, for giving me the opportunity to join his research group and for his continued support and guidance throughout my entire PhD. I would also like to give a special thanks to Lino and Grazia for their constant support and help they have given me over the past four years.

I would also like to thank everyone who has worked with me during my PhD: Rich, Kadhum, Rupert, Matt, Sabeeha, Mike, Ali, Bibianna, Sadiq, Sarah, Rich II, Luke, Rhodri and Ariana for making the lab such a great place to work and also enabling the formation of some great friendships.

I would like to thank our collaborators, especially Johannes (John) Jansen and everyone at ITM CNR for measuring the transport parameters for our membranes. I would also like to show my appreciation to all the technical staff at Cardiff University and Edinburgh for their expertise and willingness to help me at any given moment.

I would like to thank my family, in particular, my parents for their constant love and support (financial), not just during my PhD, but throughout my entire life.

Finally, I would like to give a heart filled thank you to my partner, Kelsey and my beautiful daughters, Autumn and Blossom, for all of your love, care and support, making those hard, stressful days that much easier. Words are not enough to express my gratitude, thank you.

Abstract

This project was focused on the synthesis of novel Polymers of Intrinsic Microporosity (PIMs) that are soluble in common low boiling point solvents so that self-standing films can be prepared for gas permeability measurements. The common building unit of these novel PIMs was triptycene and its derivatives. Modification of these triptycene compounds enabled the alteration of the polymeric backbone, so that we could tune the gas permeability properties. Modifications included the substitution of different functional groups (e.g. addition of methyl groups) and also the extension via benzoannulation of the triptycene structure.

The synthesis of the PIMs was based around three different polymerisation techniques. The first one involved the formation of triptycene-based polyimides (PIs) using a triptycene based dianhydride, prepared in a multistep synthesis. Shorter and cheaper synthetic routes were attempted, but all to no avail. The resulting triptycene monomer was reacted with a variety of commercial and non-commercial bisanilines for the formation of several PIM-PIs, all exhibiting different performances. Robust self-standing films were obtained for two of these PIM polyimides.

In addition to the formation of polyimides, the synthesis of Tröger's Base (TB) polymers, also based on triptycene components, were achieved. This type of polymerisation involves the reaction between a "bisaniline" monomer and a source of "formaldehyde", such as dimethoxymethane (DMM), in a strong acid media, typically trifluoroacetic acid (TFA). Modification of these triptycene-based bisanilines has led to the formation of TB-PIMs, all with distinctive gas permeation properties. TB-PIM copolymers (reaction between two different bisaniline monomers with DMM and TFA) were synthesised in an attempt to further tune the performance of the polymers.

Finally, the preparation of polybenzodioxan polymers based around extended triptycene monomers (i.e. benzotriptycenes) was studied. By using a variety of substituted benzotriptycene biscatechol monomers and performing the polymerisation using tetrafluoroterephthalonitrile, in the presence of K_2CO_3, the synthesis of a series of substituted benzotriptycene polybenzodioxane polymers was successfully achieved and the polymers showed enhanced gas permeation properties.

Overall aim of the project

Since the discovery of Polymers of Intrinsic Microporosity (PIMs) as microporous materials with a variety of potential uses, there has been a continued effort to ever increase their performance. This project focuses on the target of creating novel PIMs with enhanced gas separation properties. The performance of these materials for separating a pair of gases X and Y are typically analysed and compared with other previously synthesised polymers, by plotting their gas permeability (P_x) and selectivity (P_x/P_y) data on double logarithmic graphs. This comparison was first conducted by Robeson in 1991[1] (and later updated in 2008)[2] and his diagram is today known as a "Robeson plot". In 1991, Robeson delineated a trade-off relationship between the permeability of a polymer to its selectivity, termed an upper bound limit, which represents the state-of-the-art for polymers for gas separation. The discovery of Polymers of Intrinsic Microporosity, starting from PIM-1[3] in 2004, followed by PIM-EA-TB[4] in 2013 and PIM-Trip-TB[5] in 2014, showed an improvement in the performance of these materials as summarised in **Figure Xi.1**.

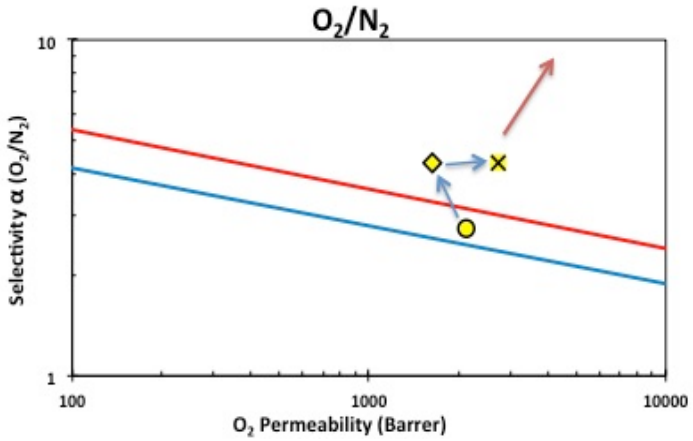

Figure Xi.1. Robeson plot of O_2/N_2 gas pair showing the overall increase in performance from PIM-1 (○), PIM-EA-TB (◇) and PIM-Trip-TB (×) with 1991 (—) and 2008 (—) upper bounds.

The aim of this project is the design and synthesis of novel polymers that are optimised for gas separation by further pushing their gas permeability data over the Robeson 2008 upper bound, in the direction as shown by the red arrow in **Figure Xi.1**.

Abbreviations

Atm	Atmospheres	**$NaBH_4$**	Sodium borohydride
BBr_3	Boron tribromide	**NMP**	N-methyl pyrrolidone
BET	Brunauer-Emmett-Teller	**NMR**	Nuclear Magnetic Resonance
Cy-6	2,2,4,4-Tetramethyl cyclohexane	**PAF**	Porous Aromatic Framework
DCM	Dichloromethane	**PALS**	Positron Annihilation Lifetime Spectroscopy
DCX	Dichloroxylene	**PDI**	Polydispersity Index
DMF	N,N-Dimethylformamide	**PI**	Polyimide
DMM	Dimethoxymethane	**PIM**	Polymer of Intrinsic Microporosity
EA	Ethanoanthracene	**POC**	Porous Organic Cage
FFV	Fractional Free Volume	**PTMSP**	Poly[1-(trimethylsilyl)-1-propyne)]
GPC	Gel Permeation Chromatography	**S.A**	Surface Area
h	Hours	**STP**	Standard temperature and pressure
HCP	Hyper-cross-linked Polymer	**TB**	Tröger's Base
HRMS	High Resolution Mass Spectrometry	***t*-Bu**	Tertiary-butyl group
IFV	Internal Free Volume	**T_d**	Temperature of decomposition
IUPAC	International Union of Pure and Applied Chemistry	**TFA**	Trifluoroacetic acid
KAUST	King Abdullah University of Science and Technology	**TFAA**	Trifluoroacetic anhydride
$KMnO_4$	Potassium permanganate	**T_g**	Glass Transition Temperature
LRMS	Low Resolution Mass Spectrometry	**TGA**	Thermogravimetric analysis
$MgSO_4$	Magnesium sulphate	**THF**	Tetrahydrofuran
MMM	Mixed Matrix Membranes	**Trip**	Triptycene
M_n	Number average molecular weight	**WAXS**	Wide-angle X-ray Scattering
M_p	Melting point	**XRD**	X-ray Diffraction
M_w	Weight average molecular weight		

Table of Contents

Chapter 1: Introduction

1.1 Porous Materials

A porous material can be described as a solid that contains pores (voids), i.e. cavities or channels. These pores can exist as three different types, (i) *closed pores* (ii) *open pores* (iii) *roughness*, and each pore must obey the rule that they are deeper than they are wide.[6]

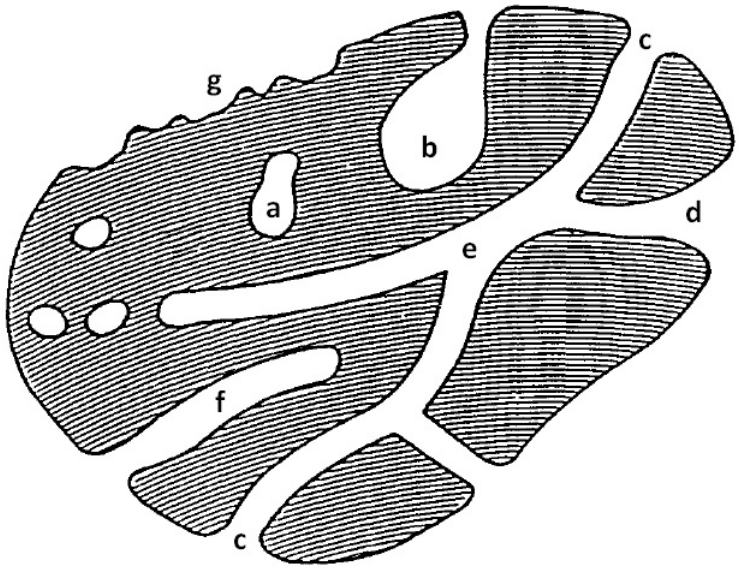

Figure 1.1[6] Schematic cross-section of a porous solid

The classification of these three types of pores can´´´ be determined by their *availability to an external fluid*. Using this model, the type of pore that can be seen at point (a) (**Figure 1.1**) can be described as a *closed pore*. These pores are fully secluded from any other pores and can influence the macroscopic properties of the material, such as; bulk density, thermal conductivity and mechanical strength.[6] *Open pores* can exist as many different types, (b, c, d, e, f) in which these pores are continually open to the external surface of the porous material. These pores can be open at one end only (b and f) and are described as *blind* (*dead-end***)** pores and some pores (c, d and e) are open at both ends and can be described as *through pores*.[6] The shape of the pores can also provide another means of classification. *Blind* or *through pores* (c and f) can both be *cylindrical* in shape, (b) type pores are characterized as *ink-bottle* shaped, (d) being *funnel* shaped and (e) *slit* shaped. The pores that are represented at (g) are not directly linked to porosity and are called *roughness*. For a rough surface to be porous, the pores must follow the rule, already stated, in which the

pore must be deeper than they are wide.[6] Apart from their type and shape, pores can also be classified by their size into three categories according to IUPAC; (i) macropores – pores that are larger than 50 nm, (ii) mesopores – between 2 and 50 nm in size and (iii) micropore – less than 2 nm in size.[7] The *pore width* is generally taken when describing the *pore size*. This *pore width* is the smallest measured dimension between two opposite walls of the pore and it is this limiting factor that is taken to represent the effective pore size.[8]

1.2 Surface area measurement

The porosity of a material is usually measured in terms of its *surface area* (i.e. the total area of the material that is accessible to a probe. Over time, there have been several techniques that have been utilized to determine the surface area of a material, mercury porosimetry[9] which uses mercury as a non-wetting liquid, optical methods[10] and computational methods[11,12]. However, the most commonly exploited method to date is the use of gas sorption. There are two types of gas sorption: (i) adsorption which involves interactions between solid and a probe molecule in the fluid phase[8] and (ii) desorption where the probe molecule is released from the solid in the fluid phase. There are two types of interaction that can occur between a solid and probe molecule in the fluid phase during the process of adsorption: (i) physisorption – involves only weak van der Waals forces between the solid and probe molecule, which as a result leads to a reversible process and (ii) chemisorption, which occurs when the probe molecule becomes linked to the reactive parts of the solid surface and gives rise to an irreversible process.[8] By using the process of physisorption, the surface area of a porous material can be determined. By injecting a small, known volume of gas onto a solid and measuring the uptake of gas (by gravimetric or volumetric analysis), the surface area can be determined from the number of gas molecules that are needed to cover the available surface.

An extension of the Langmuir theory for monolayer molecular adsorption,[13] BET (Brunauer-Emmett-Teller) theory,[14] is currently the most widely used method to determine the surface area of a porous material. A popular choice of probe gas is nitrogen, in which the measurement is carried out at 77 K. The sample being studied is evacuated and a small, known volume of nitrogen is injected onto the sample. The sample is allowed to equilibrate and the resulting pressure in the sample vessel is measured. Using the ideal gas equation, the recorded pressure is converted to volume. This injection of nitrogen is repeated until the sample reaches saturation. Other gases such as carbon dioxide, hydrogen, argon and krypton may be used for this technique. The Langmuir isotherm model was developed by

Irving Langmuir in 1916[13] and uses a number of assumptions in the calculation of an adsorption isotherm.

1) Adsorption cannot proceed beyond monolayer coverage.
2) There are no interactions between neighboring adsorbate molecules
3) All surface sites are equivalent and can only play host to one adsorbed molecule.
4) An adsorbed molecule is immobile.
5) The adsorbate behaves ideally in the gas phase.

This model considers the equilibrium between a gas molecule (*A*), a free surface site (*S*) and an adsorbed molecule (*AS*).

$$A + S \rightleftharpoons AS \qquad K = \frac{[AS]}{[A][S]}$$

As this process is in a dynamic equilibrium, the rate of adsorption and desorption are equal. The equilibrium constant for this system, K, can be expressed in terms of the fraction of occupied sites, [*AS*] (θ) and the concentration of available sites, [*S*] (1- θ).

$$K = \frac{\theta}{(1-\theta)P}$$

By rearranging this equation for θ, as *P* represents the concentration of adsorbed gas molecules [*AS*] (partial pressure), the volume of gas adsorbed (V_A) can be determined in relation to the volume of gas required to form a monolayer (V_M):

$$\theta = \frac{KP}{1+KP} = \frac{V_A}{V_M}$$

When this equation is applied in the form $y = mx + c$, the partial pressure, (*P*) and volume of adsorbed gas, (V_A) can be plotted to allow for the calculation of the volume of gas in one monolayer (V_M) which can be extrapolated from the straight line graph.

$$\frac{1}{V_A} = \frac{1}{KV_M}\left[\frac{1}{P}\right] + \frac{1}{V_M}$$

As the assumptions used in this model do not really apply to 'real' systems, the BET theory[14] builds on these ideas, but takes into account multilayer adsorption. Applying this approach to the above Langmuir equation, a new modified BET equation is generated:

$$\frac{P}{V_A(P - P_O)} = \frac{C - 1}{CV_M}\left[\frac{P}{P_O}\right] + \frac{1}{CV_M}$$

where: P = partial pressure of sample, P_O = saturation pressure, V_M = monolayer volume, V_A = volume adsorbed, C = BET constant. Over the range $0.05 \leq P/P_O \leq 0.35$ a $y = mx + c$ plot of $P/[V_A(P\text{-}P_O)]$ against P/P_O (called the adsorption isotherm) has been experimentally shown to generate a linear plot.[14] Thus, from this linear plot the gradient (A) and intercept (I) can be obtained by the rearrangement of the BET equation to the form:

$$V_M = \frac{1}{A + I}$$

By calculating V_M (monolayer volume) in moles, the BET surface area can be obtained, S_{BET} in $m^2\ g^{-1}$ using the equation:

$$S_{BET} = \frac{N_A V_M \sigma}{W_S M_V}$$

where N_A = Avogadro's number ($6.022 \times 10^{23}\ mol^{-1}$), σ = effective cross-sectional area of probe molecule (16.2 Å for nitrogen),[15] W_S = sample weight (g) and M_V = molar volume of adsorbate gas at STP (22.4 L).

IUPAC has classified six different adsorption isotherms (**Figure 1.2.1**)[16] which give an accurate indication on the porosity of the material being studied.

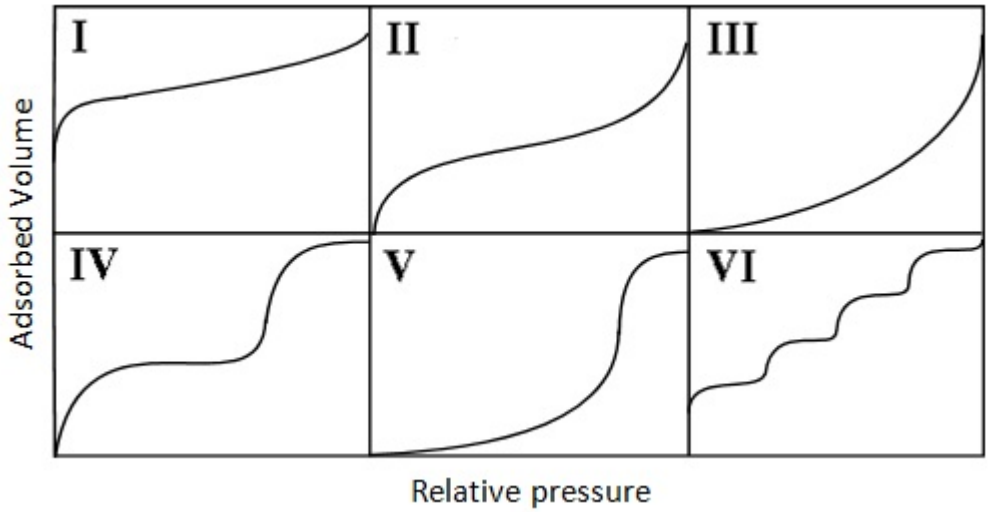

Figure 1.2.1 IUPAC defined isotherms: *Type I*: Microporous, *Type II*: Non-porous/ Macroporous, *Type III*, *V*: Non-porous, *Type IV*, *VI*: Mesoporous.

1.3 Introduction to Microporous Materials

1.3.1 Zeolites

The term *zeolite* has been derived from two Greek words, *zeo* and *lithos,* which are translated as "to boil" and "a stone" respectively. In 1756, a Swedish mineralogist Cronstedt noticed, upon heating of the natural occurring stilbite with a flame blowpipe, a large amount of steam was released which was due to the large amount of water that had been adsorbed.[17] Zeolites are crystalline aluminosilicates that are based upon an infinitely extending three-dimensional, four-connected framework of AlO_4 and SiO_4 tetrahedra, in which they are linked together by the sharing of oxygen ions (**Figure 1.3.1.1**) (**Figure 1.3.1.2**).[17] They have defined channels and cavities which have a size range ca. 3 – 15 Å.[18]

Zeolites have many different applications worldwide to date, but they are more commonly used for sorbants, ion-exchange materials and catalysts.[19,20,21]. Due to the presence of $[AlO_4]^-$ units, these materials possess a net negative structural charge and thus have a strong affinity for metal cations,[22] thus making them suitable choices for ion-exchange materials. Due to their ordered structure, zeolites have high surface areas (900 $m^2\ g^{-1}$)[22,23] and also have demonstrated high thermal stabilities.[24] Due to their uniform pore size they behave as molecular sieves, which enables them to separate molecules based only on their size.

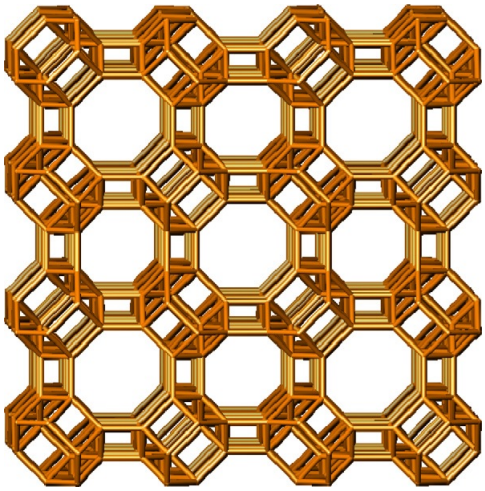

Figure 1.3.1.1 The *n*Si/*n*Al framework of zeolite ZK-5.[25]

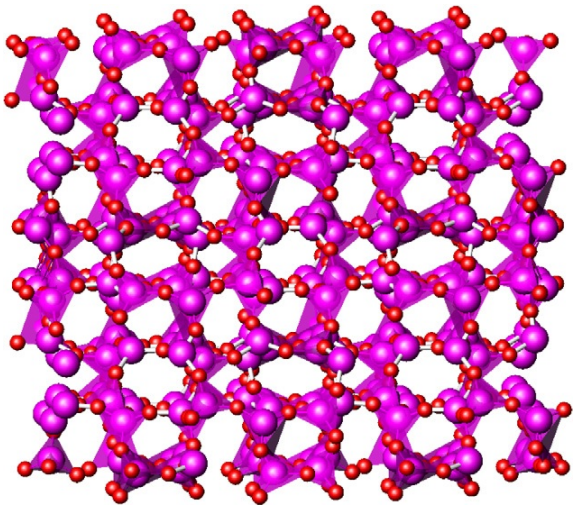

Figure 1.3.1.2 Structure of analcime, as condensed tetrahedra.[26]

1.3.2 Activated Carbons

In comparison with zeolites, activated carbons are amorphous porous solids which are generally produced from physical and/or chemical activation from a variety of materials (wood, coal, polymers).[27,28] Physical activation involves heating the carbon source up to a temperature between 700-1200°C in the presence of oxidizing gases such as steam, CO_2 or air. Chemical activation usually involves the heating of the carbon source (400-700°C) in the presence of an activating agent such as; KOH, NaOH, phosphoric acid and zinc chloride. It has been well documented that activated carbons have demonstrated BET surface areas as high as 3000 $m^2\ g^{-1}$.[27] The microporosity in activated carbons is derived from a network polymer structure, which can be described as the arrangement of planar graphene sheets that are cross-linked together by nongraphitized aliphatic units (**Figure 1.3.2.1**).[29] The surface of activated carbons is chemically ill-defined with a large variety of functional groups that contain both oxygen and nitrogen.[30] Due to these tunable properties, activated carbons have been used for a variety of different applications such as; CO_2 capture,[31] fuel cells,[32] gas separation, water purification, catalyst supports and electrodes for electrochemical double layer capacitors.[33]

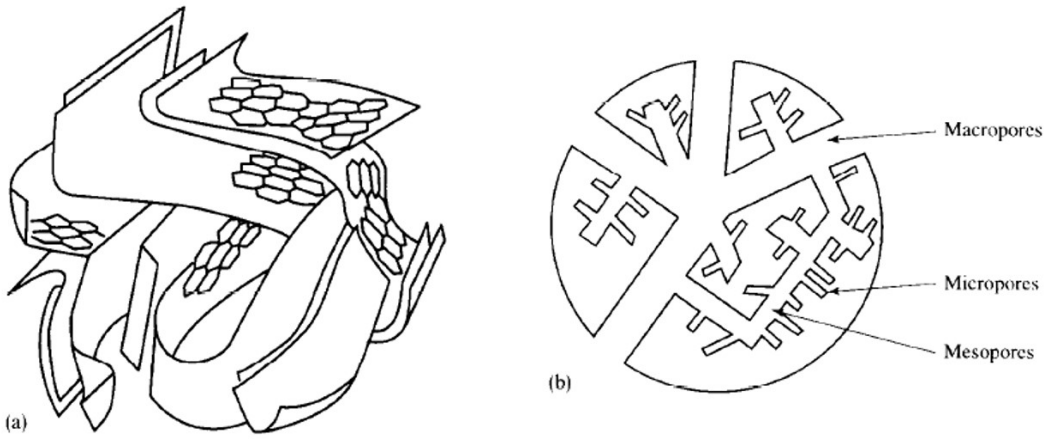

Figure 1.3.2.1 (a) Schematic representation of the structure of activated carbon; (b) schematic representation of an activated carbon granule.[34]

1.3.3 Porous Aromatic Frameworks (PAFs)

PAFs are a new class of porous material that are prepared through irreversible cross-coupling reactions that generate stable and robust materials that demonstrate ultra-high BET surface areas.[35] Ben *et al.* suggested that by replacing the C–C covalent bonds of diamond with rigid phenyl rings, the basic structure of diamond should remain but now would allow sufficient exposure of the faces and edges of the phenyl rings, so that the internal surface area of this material should increase.[36] With this in mind, Ben *et al.* successfully synthesised the first example of a porous aromatic framework called PAF-1 (**Figure 1.3.3.1**).[36] This revolutionary porous material had a BET surface area of 5640 m^2 g^{-1} and demonstrated exceptional thermal and physicochemical stability via a nickel(0)-mediated Yamamoto-type Ullmann cross-coupling reaction.[37] PAF-1 also exhibited high uptake capacities for hydrogen (10.7 wt% at 77 K, 48 bar) and carbon dioxide (1300 mg g^{-1} at 298 K, 40 bar), which when combined with its ultra high surface area, makes it a candidate for hydrogen gas and carbon dioxide storage.[36] It has been demonstrated by Trewin and Cooper that the powder X-ray diffraction pattern of PAF-1 revealed a broad peak, which suggests that PAF-1 is amorphous.[38] This experimental data suggests that the average size of any ordered domains in PAF-1 is very small,[37] thus long range crystallinity is not required to generate a porous material that demonstrates ultra high BET surface areas.

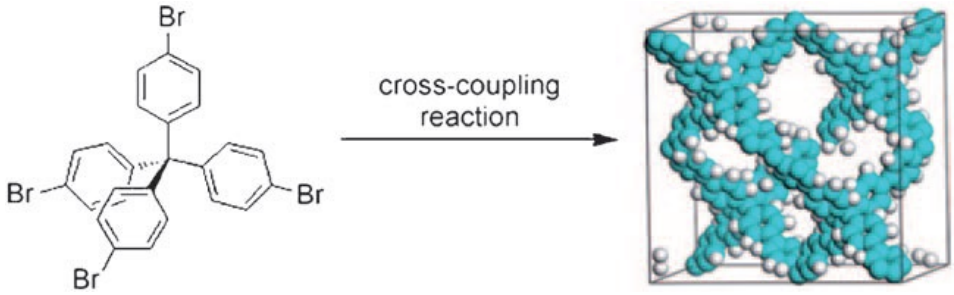

Figure 1.3.3.1 Synthesis of the microporous polymer network PAF-1 by Yamamoto cross-coupling reaction.[38]

By using PAF-1 as a scaffold, further computational studies have been performed in an attempt to unearth new potential PAFs for new applications (**Figure 1.3.3.2**). Lan *et al*.[39] simulated the hydrogen storage capacity for several PAF structures, whereas Sun *et al*.[40] used lithium tetrazolide linkers to propose new PAFs for hydrogen storage applications.

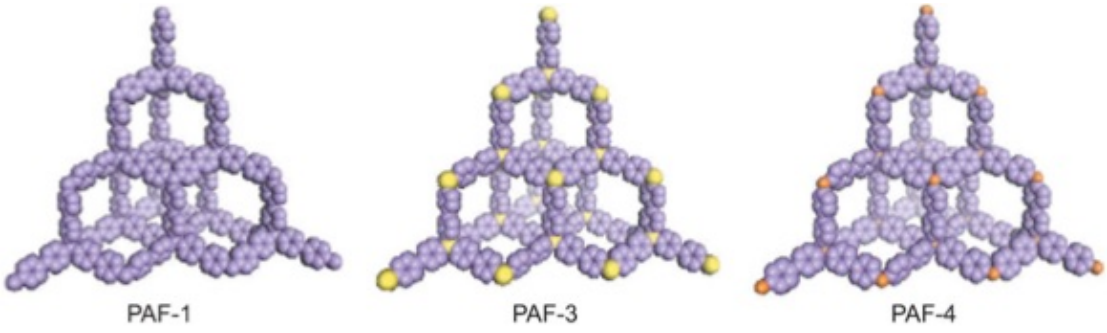

Figure 1.3.3.2 Structure model of synthesized and simulated PAF. (C, purple; Si, yellow; Ge. brown).[37]

1.3.4 Hyper-Cross-linked Polymers (HCPs)

Hyper-cross-linked polystyrene networks and sorbents were first described in the literature in 1969[41] and were commercially available at the end of the 1990s.[42] These "Davankov-type" resins[43,44] are prepared by a Friedel-Crafts-type post-cross-linking reaction of polystyrenic networks, which are catalyzed by a Lewis acid such as $FeCl_3$ (**Figure 1.3.4.1**).[45]

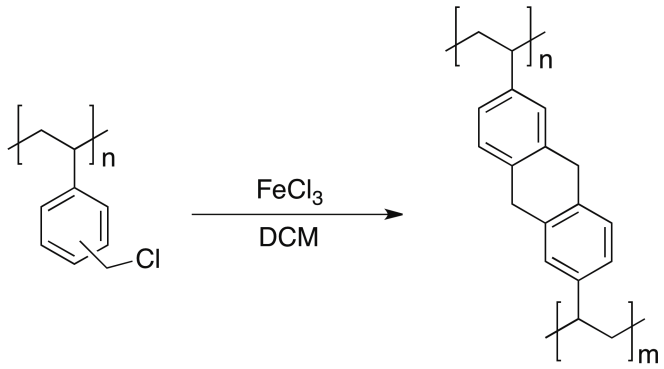

Figure 1.3.4.1 Preparation of hypercrosslinked styrenic Polymer from poly-(vinylbenzyl chloride)- gel-typre resin Precursor.[45]

During these reactions, the microporosity of these materials can be thought to arise from the trapped solvent molecules within the polymer network that originate from the synthesis of HCPs (i.e. a template effect)[46] (**Figure 1.3.4.2**).

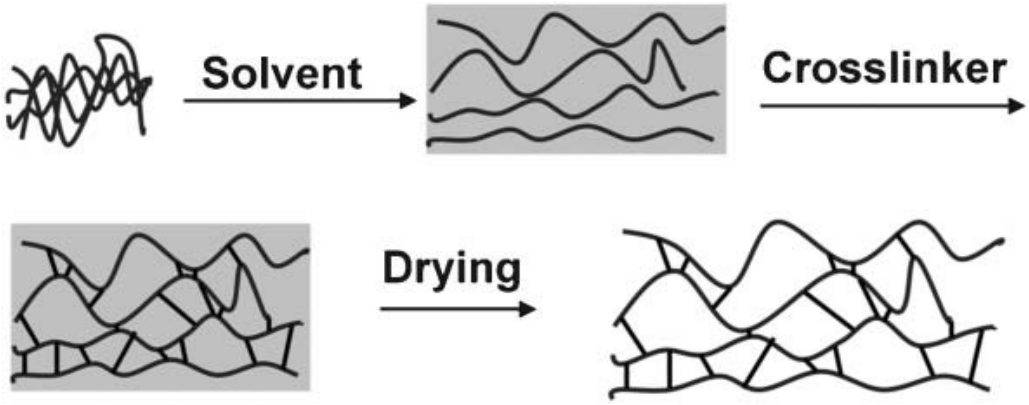

Figure 1.3.4.2 Schematic representation of the hyper-cross-linking process. First, swelling is achieved through dissolution in a solvent. Once swollen, the polymer is cross-linked. Finally, solvent removed whilst HCP maintains its permanent porosity.[47]

These robust microporous organic materials exhibit high apparent BET surface areas (up to 2090 $m^2 g^{-1}$)[48] and have been used in applications such as sorbents for organic vapours,[49] water treatment (specifically the removal of organic compounds from water)[50] and in chromatography.[51] HCPs exhibit permanent porosity due to the extensive cross-linking reactions, which as a consequence prevent the polymer chains from collapsing into a dense, non-porous state (aging).[52] HCPs offer many advantages such as excellent chemical robustness (stable against strong acid and bases), good thermal stability and can also be produced on a large scale.[52] Examples in the literature[53,54] have demonstrated the synthesis

of a HCP based on the step growth polycondensation of dichloroxylene (DCX) and other bischloromethyl monomers. These materials have been shown to exhibit high apparent BET surface areas (~1900 $m^2 g^{-1}$) and can adsorb up to around 3.7 wt% H_2 at 77 K and 15 bar.[54]

1.3.5 Porous Organic Cages (POCs)

Recently, shape-persistent organic cage molecules which are wholly organic and composed entirely of covalent C—C, C—H, N—H and C—N bonds, have gained significant interest in the field of novel porous materials.[55,56] This class of material offer ultra-high BET surface areas (**Figure 1.3.5.1**) but also maintain their molecular identity, i.e. are fully soluble and thus processable.[57] Due to the processability of these porous materials, they have been extensively used for a variety of different applications[58] such as sensors, nanoreactors, delivery vehicles, gas storage and separation materials.[59,60,61,62,63] There are two main synthetic approaches to generating these cage structures: (i) stepwise irreversible bond formation and (ii) thermodynamically preferred reversible bond formation.[55] Both of these methods have their advantages and disadvantages. The stepwise irreversible bond formation process involves low yielding reactions that have long reaction times but however generate cages that have high chemical stability and robustness. The synthesis of these cages via thermodynamic reversible reactions generally provides high yielding reactions, which are usually conducted in a single step. However, such cages have relatively low chemical stability.[55]

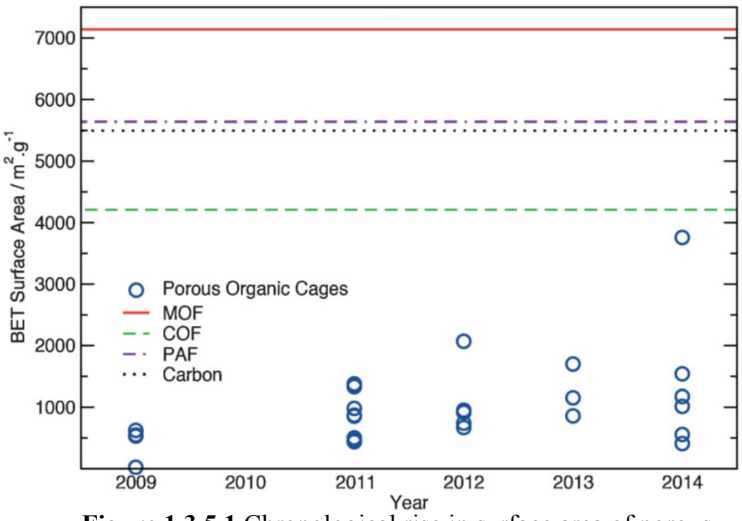

Figure 1.3.5.1 Chronological rise in surface area of porous organic cages.[57]

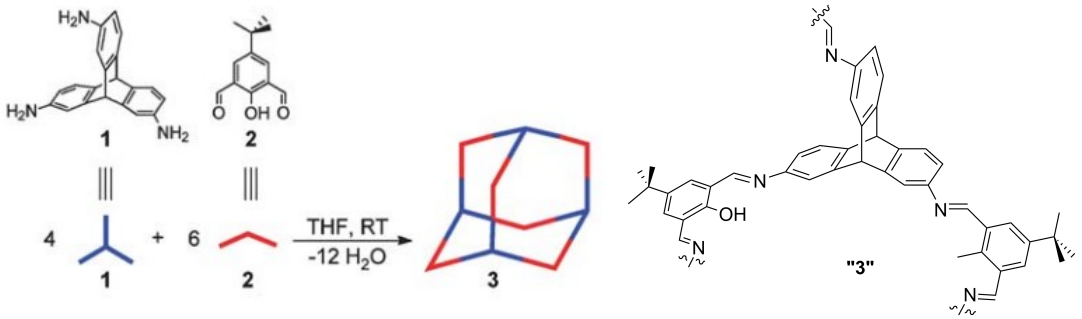

Figure 1.3.5.2 One-pot synthesis of the adamantoid cage compound **3**. "**3**" is a part of the cage structure to clearly depict the formed imine bonds.[64]

(**Figure 1.3.5.2**) shows the general synthesis of these porous cage materials via a "one-pot" synthetic approach, which involves the reaction between triaminotriptycene (**1**) and salicylic dialdehyde (**2**) in the ratio 4:6 respectively to yield the endo-functionalised adamantoid nanocage compound (**3**).[64] Due to the straight-forward synthesis depicted (**Figure 1.3.5.2**) the room for functionality in this field is vast. Thus, by varying the size and functionality of these cage components, one can fine-tune the properties of the POCs for a variety of applications.[58] A study by Budd *et al.*[65] has demonstrated the use of POCs in mix-matrix membranes (MMM). The study has shown that incorporating a particular POC into PIM-1 can substantially enhance the gas permeability and maintain good selectivity, but also provides better resistance towards physical ageing.[65]

1.4 Polymers of Intrinsic Microporosity (PIMs)

Polymers of Intrinsic Microporosity (PIMs), first developed by McKeown *et al.* in 2004,[3] are described as rigid and contorted macromolecules which are wholly composed of fused-ring components. Generally, polymers pack space efficiently, thus allowing them to maximize attractive interactions between the constituent macromolecules.[46] However, due to the composition of PIMs, these materials form microporous organic materials due to their inability to pack space efficiently.[66] Hence, in this context, Intrinsic Microporosity (IM), has been defined as "*a continuous network of interconnected intermolecular voids that forms as a direct consequence of the shape and rigidity of the component macromolecules*".[67] These polymers are designed with the key goal in mind of generating a rigid and contorted structure, such that they possess large amounts of free volume.[68] There are many other types of polymers that possess high free volume and also exhibit

significant IM (demonstrated by their very fast gas permeabilities) such as polyacetylenes,[69,70] fluorinated polymers,[71,72] polynorbornenes,[73,74] polyimides[75] and polymer membranes.[46]

1.4.1 Polyacetylenes

The first reported study of a polyacetylene was in 1866 by Berthelot.[76] Since the extensive investigations by Natta *et al.* in 1958 on the polymerisation of acetylene,[76] a variety of polyacetylenes have been investigated for an array of different applications such as optoelectronics, stimuli-responsive materials and gas separation membranes.[77] Since 1975, the synthesis of polyacetylenes have been performed using so-called metathesis catalysts based on the following metals: W, Mo, Ta and Nb. The use of these catalysts has led to the discovery of poly[1-(trimethylsilyl)-1-propyne)] (PTMSP) (**Figure 1.4.1.1(a)**) in 1983, which involves the polymerisation of 1-(trimethylsilyl)-1-propyne in the presence of the catalyst $TaCl_5$ or $NbCl_5$.[70,78] During the synthesis of a polyacetylene, *cis*- and *trans*-arrangements at each of the double bonds are possible and the choice of catalyst may give rise to the selective synthesis of one isomer over the other.[79] PTMSP was found to be soluble in many common organic solvents and exhibits high molecular weights. Due to the high molecular weight of this polymer, self-standing films were successfully fabricated and gas permeability studies were performed. Interestingly, up until 2008, PTMSP exhibited the highest oxygen permeability of all known polymers.[70] Due to these exciting properties, the synthesis and characterisation of other substituted polyacetylenes increased rapidly (**Figure 1.4.1.1(b)(c)**), which lead to the discovery of an indan-containing poly(diphenylacetylene), which is to date, the most permeable polymer for oxygen in the literature (P_{O_2} = 15000 Barrer; **Figure 1.4.1.1(d)**).[69] The high permeabilities associated with these polymers arise from the bulky side groups that inhibit the efficient packing of the polymer chains in the solid state.[80] Polyacetylenes exhibit properties that are associated with glassy polymers and also that of rubber polymers. When polyacetylene polymer chains are packed in the solid state, they display large amounts of free volume and the free volume distribution includes both small disconnected elements, as seen for glassy polymers, but also display larger continuous microvoids.[79] These properties have been confirmed by positron annihilation lifetime spectroscopy (PALS).[81,82]

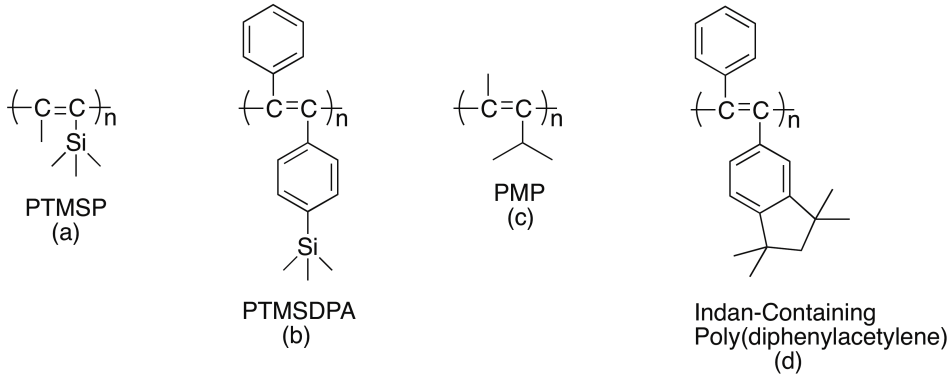

Figure 1.4.1.1 Polyacetylenes (a-d).

1.4.2 PIM-1

PIM-1, first synthesised by McKeown *et al.*[3] in 2004, was the first example of a Polymer of Intrinsic Microporosity (PIM). This involves a dibenzodioxan-forming reaction between commercially available 2,4,5,6-tetrafluoroterephthalonitrile and 5,5′,6,6′-tetrahydroxy-3,3,3′,3′-tetramethyl-1,1′-spirobisindane (**Scheme 1.4.2**).[3]

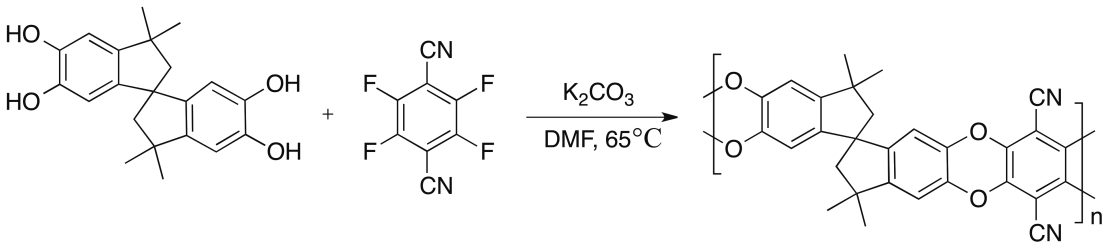

Scheme 1.4.2.1 Synthesis of PIM-1 via an aromatic nucleophilic substitution reaction.

This non-network, fluorescent ladder polymer, was fully soluble in polar aprotic solvents such as THF or chloroform and due to its high molar mass (270,000 g mol^{-1}) the fabrication of a robust, self-standing film was successful. Due to its highly rigid and contorted structure PIM-1 exhibits a high BET surface area (860 $m^2 g^{-1}$). The rigidity arises from the fused five and six membered of the polymer backbone and the contorted nature is generated from the spiro-centre of the spirobisindane molecule (**Figure 1.4.2.2**). Gas permeation studies were performed on PIM-1, which revealed a highly permeable polymer, with only few polymers such as PTMSP,[70] PMP[83] and Teflon AF[72] that exhibit higher permeabilities.[84] However, methanol-treated PIM-1 demonstrated significantly high selectivities for the gas pairs O_2/N_2 and CO_2/N_2 and placed the performance of PIM-1 over the 1991 Robeson upper bound. These enhanced properties has made PIM-1 an attractive

material, which has been used for a variety of different applications such as sensors[85] and gas separation membranes.[86]

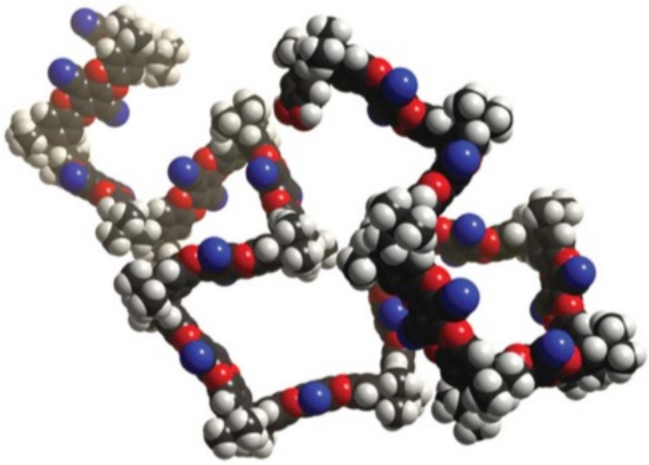

Figure 1.4.2.2 A molecular model of a small fragment of PIM-1 showing its rigid and contorted structure.[87]

1.4.3 PIM-Polyimides

Since the discovery of the archetypal PIM-1 in 2004, the last decade has seen the advancement of state-of-the-art materials for the use in the rapidly growing field of industrial membrane-based gas separations.[2,88] In particular, polyimides are one of the most studied classes of polymers for membrane materials.[89] They are growing in importance due to their excellent balance of mechanical and thermal properties, which include thermoxidative stability, electrical properties, chemical resistance, mechanical robustness and structural diversity.[90,91,92] The first breakthrough in polyimide chemistry can be traced back to the 1950s and 1960s[93,94] where research at DuPont led to the development of a range of polyimides, for a variety of different applications, e.g. Pyralin™ soluble polyimides were used as wire coatings and Kapton-H™ polyimide films were also synthesised.[95] The production of polyimides involves a two-step process (**Scheme 1.4.3.1**): (i) condensation reaction of an aromatic bisaniline (**1**) and dianhydride (**2**) to generate the corresponding poly(amic acid) (**3**), (ii) cyclodehydration of (**3**) to yield the polyimide (**4**).

As previously mentioned in this chapter, polymers that contain rigid and contorted structures give rise to microporous materials. Freeman states that increasing the stiffness of the polymer backbone, results in increased selectivity but lower diffusivity whereas increasing the interchain separation results in an increase in permeability.[96] By following these general guidelines, the past decade has seen the synthesis of polyimides that have increased in performance, from the synthesis of PIM-PI-1 and PIM-PI-8 in 2008,[92] PIM-

PI-9, PIM-PI-10 and PIM-PI-11 in 2013 (**Figure 1.4.3.2**)[89] and up to the current highest performing polymers in the literature, KAUST-PI-1 and KAUST-PI-2 in 2014 (**Figure 1.4.3.3**).[88]

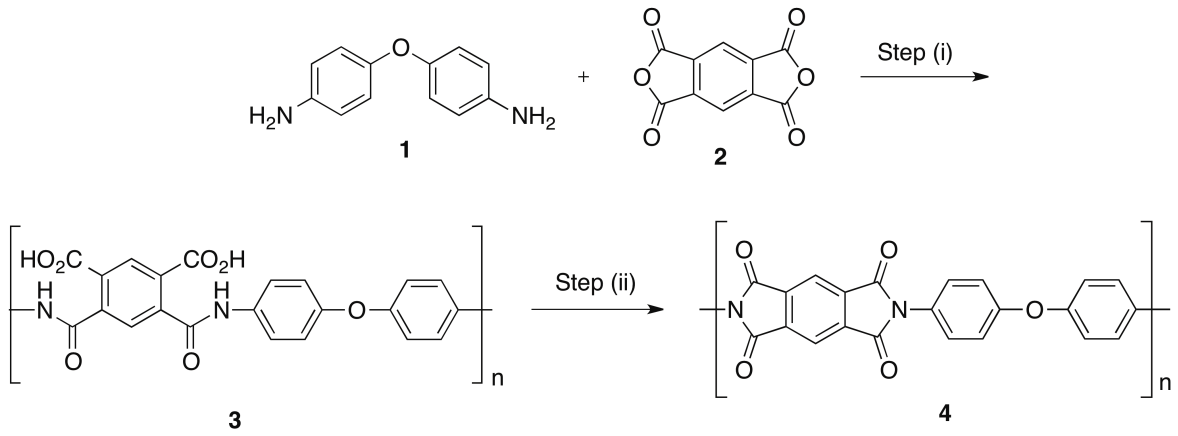

Scheme 1.4.3.1 Two-step condensation polyimide synthesis of Kapton™.[95] (i) Base, (ii) Increase heat.

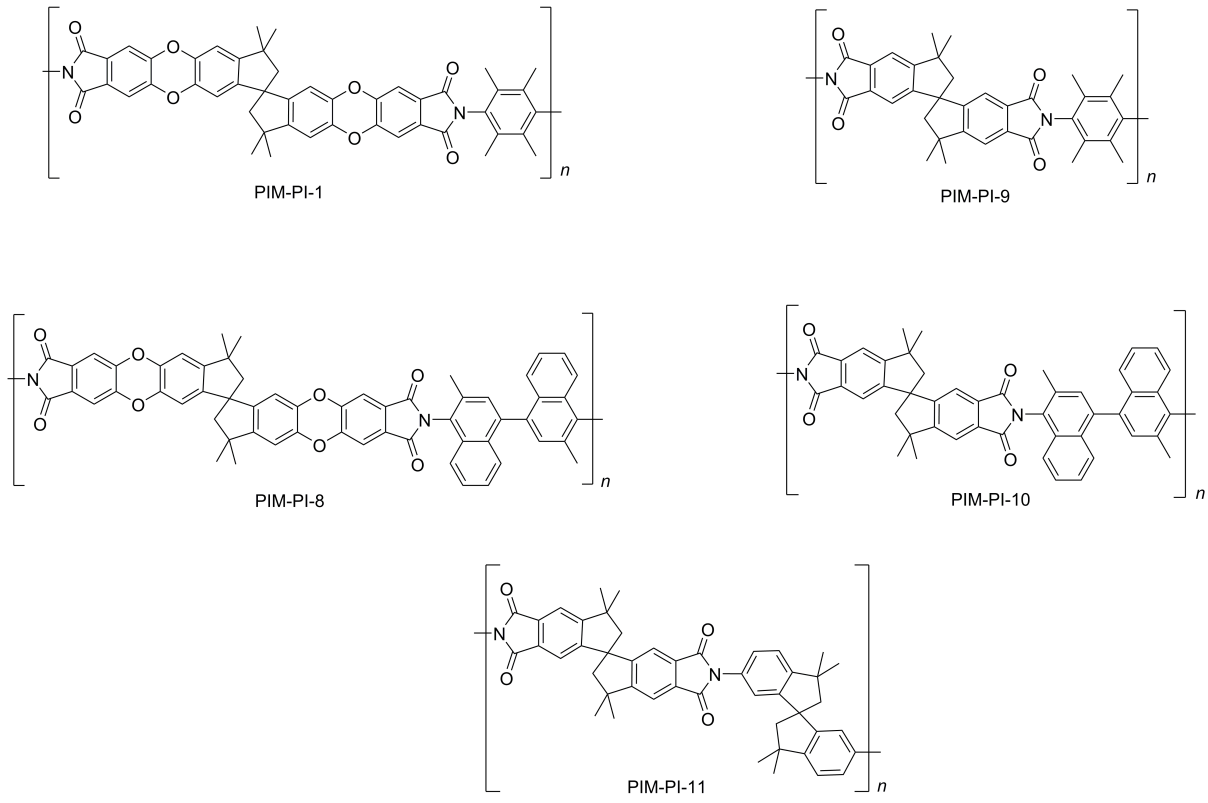

Figure 1.4.3.2 PIM-PI-1, PIM-PI-8, PIM-PI-9, PIM-PI-10 and PIM-PI-11.

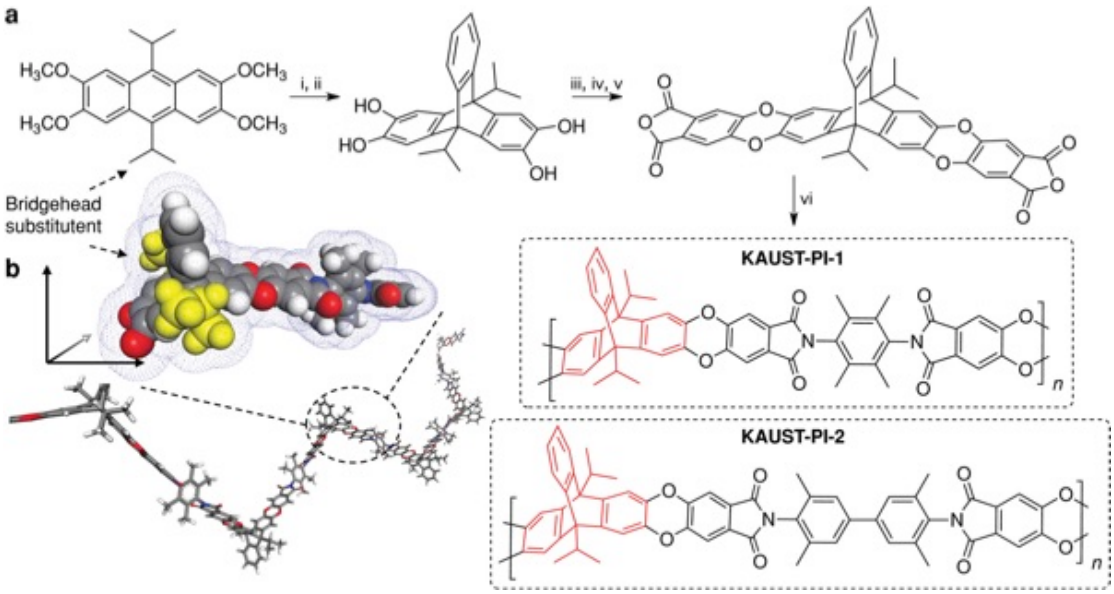

Figure 1.4.3.3 (a) Synthesis of KAUST-PI-1; (b) geometrically optimised KAUST-PI-1 demonstrating contorted, ribbon-like growth and enhanced three-dimensionality afforded by the 9,10-diisopropyl-triptycene.[88]

1.4.4 Tröger's Base (TB) polymers

In 1887 Julius Tröger discovered 2,8-dimethyl-6*H*,12*H*-5,11-methanodibenzo[*b*,*f*][1,5]diazocine, which has become known as Tröger's Base (TB).[97] The first reported synthesis of TB involved the reaction between *p*-toluidine and dimethoxymethane (DMM) in aqueous HCl (**Figure 1.4.4.1**).

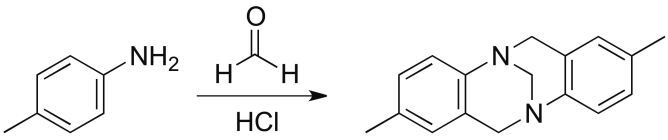

Figure 1.4.4.1 The synthesis of TB.

However, during this time Tröger described this unexpected product as a 'base $C_{17}H_{18}N_2$' but was not able to assign a plausible structure to it.[98] However, nearly 50 years later, work by Spielman[99] in 1935 assigned the chemical structure of racemic TB (**Figure 1.4.4.2**). Around the same time, the mechanism for the synthesis of TB was first proposed by Wagner[100] and confirmed later by mass spectrometry in 2007 by Abella et al.[101]

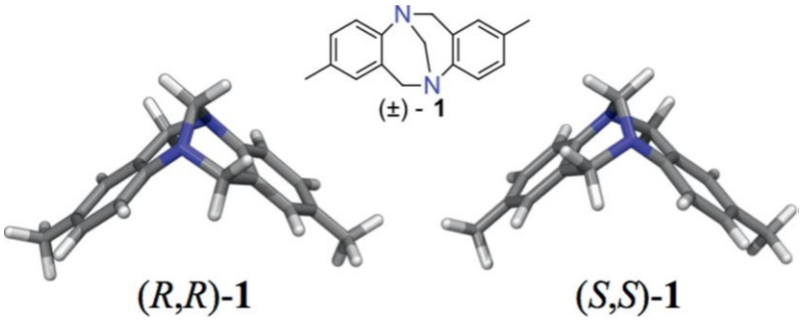

Figure 1.4.4.2 TB [(±)-1] and the MMFFs-optimised structures of Its two enantiomers.[102]

In 1986 the structure of TB was fully confirmed by single-crystal X-ray-diffraction (XRD) analysis by Larson and Wilcox.[103] This molecule features a central bicyclic aliphatic unit fused with two aromatic rings. These two aromatic rings are projected nearly perpendicular to each other, due to the methanodiazocine unit, which generates a V-shaped molecule which possesses a hydrophobic cavity that is around 1 nm in size between the two extremities.[102,98] The structure of TB is C_2-symmetric and thus a chiral molecule. The nitrogen atoms in this molecule are configurationally stable stereogenic centres, due to the presence of the methylene bridge that prevents the inversion of these nitrogen atoms.[102] In 1944, pioneering work by Prelog and Wieland successfully performed the separation of the two enantiomers of TB (**Figure 1.4.4.2**) by chromatographic methods, using (+)-α-lactose hydrate as the chiral stationary phase.[104] As Tröger described this molecule as a base, the basic nature of this molecule has been studied. Work by Wepster in 1953 concluded that the TB molecule was only a weak base.[105] However, a more recent study on hydrogen bonding acceptor strength by Marquis in 2004, determined that on comparison with other aromatic amines, it is strongly basic ($pK_{HB}(N) = 1.15$).[106] The basic nature of TB arises due to the V-shape structure of this molecule. The V-shaped structure forces the free electron lone pairs out of conjugation with electron density that is associated with the aromatic rings.[102] The basicity of this molecule has been utilised in different applications such as heterogeneous organocatalysis.[107,108,109] Another successful application of TB has been in the use of this molecule for the formation of polymers, which will be discussed and demonstrated during this thesis. Reacting suitable aromatic bisaniline monomers with dimethoxymethane in the presence of trifluoroacetic acid (TFA) generates the corresponding TB homopolymer. The first successful polymerisation involving the utilisation of the TB molecule was synthesised (PIM-EA-TB) by McKeown *et al*.[4] PIM-

EA-TB was found to demonstrate very fast gas permeabilities and good selectivity, so that its data lay well over the Robeson 2008 upper bound. These enhanced properties arise from the rigid structure of the ethanoanthracene molecule and the V-shaped TB unit generates the contorted nature of the polymer. These enhanced properties formed the basis for further study of this novel class of PIM, which has led to the synthesis of polymers with even more promising data for gas separation: PIM-Trip-TB[5] and PIM-BTrip-TB.[110]

1.5 Membrane theory

1.5.1 Membrane properties and gas transport mechanisms

A membrane has been generally defined as *"A phase or a group of phases that lies between two different phases which is physically and/or chemically distinctive from both of them and which, due to its properties and force field applied, it is able to control mass transport between these phases"*.[111] In 1866, Graham[112] first proposed the concept of membrane separation and it was not until 1977 where the first commercialised gas separation membrane became available when Monsanto/Perma released their hydrogen recovery system.[113] There are a number of different *"forces"* that can drive the permeate to flow through the membrane: difference in temperature, pressure, concentration or electric potential across the membrane.[114] In principle, a membrane acts as a filter that separates one or more gases from a feed mixture, thus generating a purified permeate on the other side of the membrane (**Figure 1.5.1.1**).

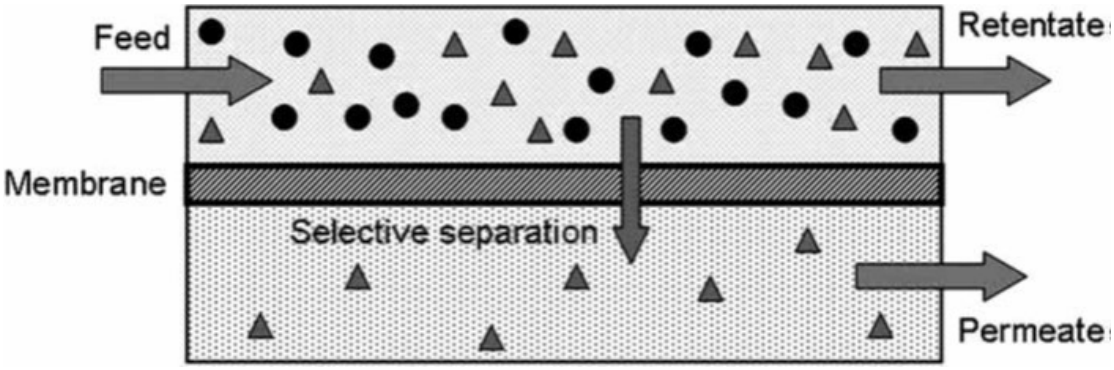

Figure 1.5.1.1 Schematic of membrane gas separation.[115]

The performance of these membranes is determined by two factors: (i) permeance (flux) of one specific gas through the membrane and (ii) selectivity which is the ability of the

membrane to allow the permeation of one gas species over the other.[115] Membrane separation can take place via five different possible mechanisms; (i) Knudson diffusion, (ii) molecular sieving, (iii) solution-diffusion, (iv) surface diffusion, and (v) capillary condensation.[116,117] The separation mechanism that governs the properties of the polymers that are going to be described in this thesis are based around the solution-diffusion model with a contribution from molecular sieving (**Figure 1.5.1.2**).

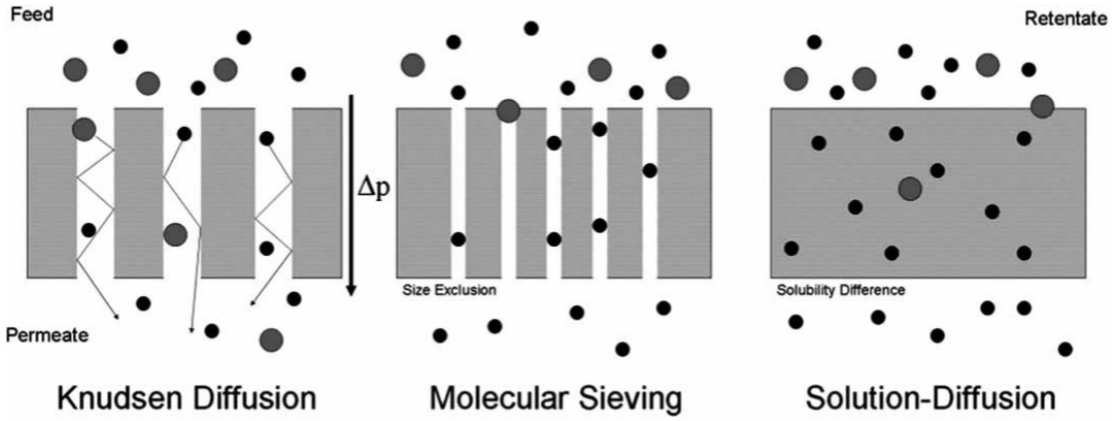

Figure 1.5.1.2 Schematic representation of Knudsen Diffusion, Molecular Sieving and Solution-Diffusion separation mechanisms.[115]

Knudsen diffusion takes place in membrane materials when the range of pore size is 5 – 2000 Å. As the gas particles permeate through the membrane, they collide with the pore walls, becoming momentarily adsorbed and then reflected in random directions. As molecule – molecule interactions are rare, each gas molecule moves independently, and thus due to the differences in average velocities, gas mixtures are separated. Molecular sieving takes place when the pore size ranges between 5 – 20 Å. Transport through this type of membrane involves two processes: (i) diffusion in the gas phase, (ii) diffusion of adsorbed species on the surface of the pores (surface diffusion).[118] This process relies on size exclusion to separate gas mixtures and one can tailor a membrane, based on the relative kinetic diameters of the gases, for the selective separation of one gas from another.[115] The solution-diffusion model separates gas mixtures based on interactions with the membrane material. Upon dissolution of the permeates into the membrane material, they diffuse through the membrane down a concentration or pressure gradient.[115] Due to the differences in solubility of specific gases and their diffusion rates through the membrane material, a separation of gas mixtures occurs.

Polymer materials can be sub-divided into rubbery or glassy. This classification depends on the operating temperature being either above (rubbery) or below (glassy) the glass transition temperature (T_g).[115] Rubbery polymer membranes have been found to obey Henry's Law, where the gas solubility within the polymer is linearly proportional to the partial pressure, whereas, as described by Meares,[119,120,121] glassy polymer membranes have been found to contain a distribution of microvoids that are frozen into the structure. These "holes" may act to immobilise a portion of the permeate molecules by either entrapment or binding at high energy states.[122] Continued work by Vieth, Michaels and Barrie[123,124] discovered that glassy polymers have an abnormally high solubility for inert gases. By plotting the adsorption isotherms for these systems, it was discovered that they were highly non-linear i.e. not only following Henry's Law, but can be explained as to follow a combination of Henry's Law and the Langmuir adsorption model.[122] Then in 1965, Vieth and Sladek[125] postulated a mathematical explanation of these processes, which has today become known as the Dual Sorption Theory.[122] This model postulates that the diffusion of gas molecules in the polymer membrane can be divided into two phases: (i) Henry's law type sorption and (ii) Langmuir type sorption. As already mentioned, the gas solubility within the polymer membrane follows Henry's Law and is linearly proportional to the partial pressure. However, in glassy type polymers, due to the excess free volume in the form of microscopic voids, the gas molecules can become immobilised inside these voids (Langmuir type sorption). During this type of sorption, the gas molecules diffuse through the membrane material by "hopping" from one Langmuir sorption site to the next and for this process of diffusion to take place there is an energy barrier that has to be overcome.[126]

1.5.2 Transport parameters

The solution-diffusion model postulates that the permeability (P) of a diffusing gas through a membrane is a result of the product of the solubility coefficient (S) and the diffusivity coefficient (D).

$$P = SD \qquad Eq.\,1.5.1$$

The solubility coefficient is an equilibrium component that describes the concentration of gas molecules within the polymer membrane ($cm^3\,cm^{-3}\,bar^{-1}$). The diffusivity coefficient is

a dynamic component that describes the mobility of the diffusing gas in the polymer membrane (10^{-12} m^{-1} s^{-1}).[127] This equation can be utilised for the characterisation of the permeability properties of a polymer membrane. The separation of a gas mixture that is composed of gas molecules A and gas molecules B is characterised by the selectivity or ideal separation factor:

$$\alpha_{A/B} = \frac{P(A)}{P(B)} \qquad Eq.\,1.5.2$$

This equation (1.5.2) can be explained as the ratio of the permeability of A over the permeability of B. From equation (1.5.1) it is also possible to characterise the separation of gas molecule A from gas molecule B from the diffusivity selectivity or solubility selectivity:

$$D\alpha_{A/B} = \frac{D(A)}{D(B)} \qquad S\alpha_{A/B} = \frac{S(A)}{S(B)} \qquad Eq.\,1.5.3$$

During the separation process, the limiting factor that governs the performance of the membrane is overcoming the diffusion energy barrier. As this is a temperature dependent process, the diffusivity and permeability coefficients are described by the Arrhenius and van't Hoff equations (Eq. 1.5.4, Eq. 1.5.5, Eq. 1.5.6). This energy barrier arises from the kinetic energy that the diffusing gas molecule requires for the successful diffusive jumps across the membrane.[127]

$$D_A = D_A^* \, exp\left(\frac{-\Delta E_a}{RT}\right) \qquad Eq.\,1.5.4$$

The van't Hoff equation holds for the solubility coefficient:

$$S_A = S_A^* \, exp\left(\frac{-\Delta H_a}{RT}\right) \qquad Eq.\,1.5.5$$

Where $\Delta H_a < 0$ is the enthalpy or sorption.

With respect to equation (Eq. 1.5.1)

$$P_A = P_A^* \, exp\left(\frac{-\Delta E_P}{RT}\right) \qquad Eq.\,1.5.6$$

Where $\Delta E_p = \Delta E_a + \Delta H_a$

1.6 Robeson plots and upper bounds

Due to the vast number of different polymers considered for gas separation membranes that has been published in the literature to date, the need for a universal system for the comparison of performance needed to be devised. The performance of a gas separation membrane is ultimately determined by how permeable the membrane is to the relevant gases and how selective it is towards one gas over another (i.e. selectivity). In 1991 Robeson cumulated over 300 different literature results for the gas separation properties of different membranes and plotted these results on a double logarithmic plot of selectivity against permeability ($log\ P_x$ vs $log\ \alpha_{xy}$) (**Figure 1.6.1**). From this data, Robeson determined that a "trade-off" relationship existed and from this data originates the 1991 Robeson upper bounds for each important gas pair.[1] However, due to the significant progress in polymeric material design and synthesis, particularly the development of PIMs, the performance of these new materials surpassed the 1991 upper bounds. This new data allowed Robeson to revise his original 1991 upper bounds, to give the 2008 upper bounds,[2] and it is these upper bounds that are currently used today for the comparison of gas separation membranes. During this project, the gas permeabilities that were calculated for each polymer film were conducted by single gas measurements. This represents the ideal gas separation when two gases are compared with each other. The basic set-up measures the transport of a variety of different gases across a polymer membrane, in which the computer plots a graph of permeate pressure against time (**Figure 1.6.2(a)**). When the feed volume and pressure is much larger than that of the permeate, it can be assumed that there is a constant feed pressure. This will cause the permeate pressure to increase asymptotically to the feed pressure. When a pure gas "feed gas" is exposed to the membrane, there is a "time-lag" that occurs from when the membrane is exposed to the feed gas to when the permeate pressure starts to increase. This phase is known as the "transient state" (**Figure 1.6.2 (b)**) which then leads to the second phase which is the linear region known as the "steady state". At this point, a straight line tangent can be drawn which obeys the following "quasi steady state condition".[128]

$$P_t = P_0 + \left(\frac{dP}{dt}\right)_o . t + \left(\frac{RT.A}{V_p V_m} . \frac{P_f . P}{l}\right)\left(t - \frac{l^2}{6D}\right)$$

P_t = Permeate pressure at time t, P_0 = Starting pressure, $(dP/dt)_0$ = Baseline gradient, P_f = Feed pressure, P = Permeability coefficient, R = Universal gas constant (8.3144 JK^{-1} mol^{-1}), T = Absolute temperature (298.15 K), A = Exposed membrane area (2.14 cm^2), V_p = Permeate volume, V_m = Molar volume of permeate gas at STP (0 ° C and 1 atm) and l = Membrane thickness.

From (**Figure 1.6.2 (b)**), extrapolation of the tangent line to the *x*-axis generates a value for the time-lag (θ), which by using the following equation, the diffusion coefficient (D) can be calculated:

$$D = \frac{l^2}{6\theta}$$

The permeability coefficient (P) is then calculated from the rate of steady state pressure increase:

$$P = \frac{V_p . V_m . l}{RT . A . P_f} . \left[\left(\frac{dp}{dt}\right) . \left(\frac{dp}{dt}\right)_0\right]$$

The solubility coefficient can then be calculated according the solution-diffusion model transport mechanism:

$$S = \frac{P}{D}$$

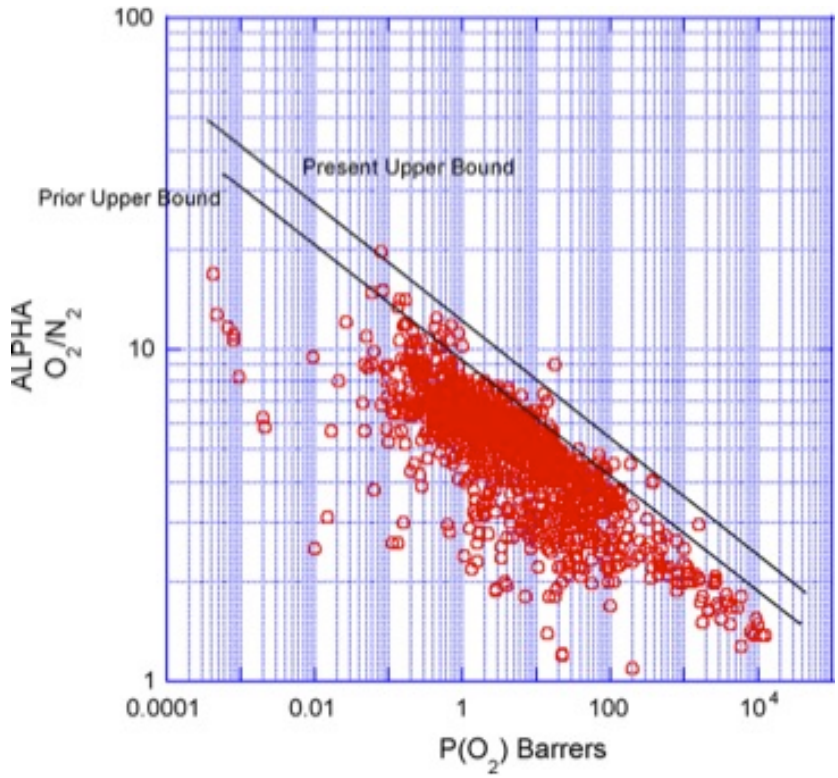

Figure 1.6.1 Robeson plot of $\alpha O_2/N_2$ vs PO_2 demonstrating 1991 and 2008 upper bounds.[2]

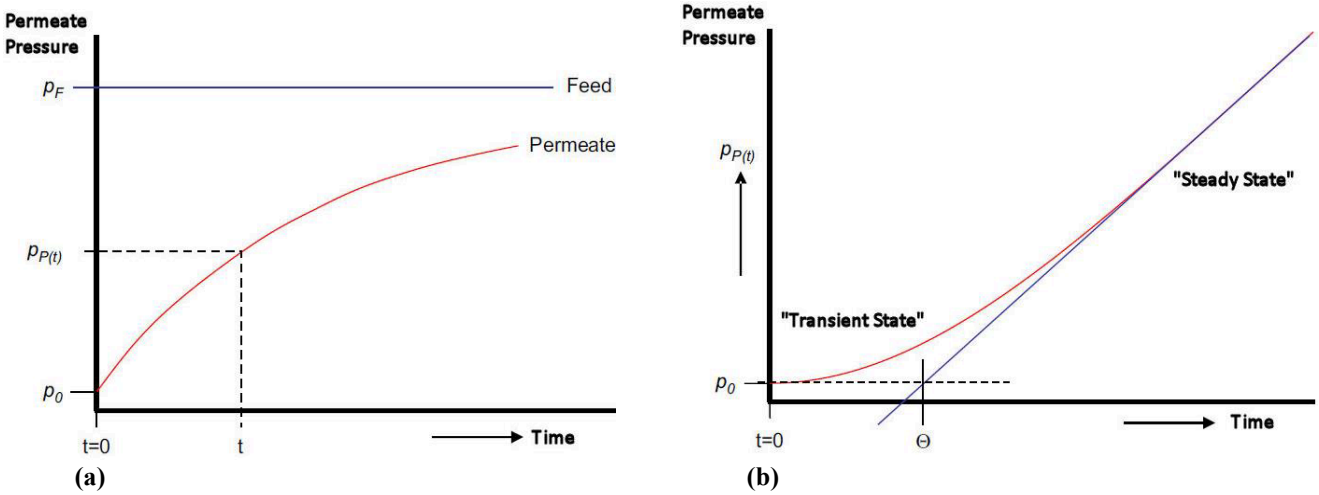

Figure 1.6.2 (a) A graph of permeate pressure *vs* time, demonstrating the increase in permeate pressure, (b) Time-lag curve with steady state tangent line.[129]

Chapter 2: Triptycene derived polyimides

2.1 Introduction

In an attempt to provide a potential solution to greenhouse gas driven climate change, the capture and storage of carbon dioxide has been identified as one of the most challenging environmental issues that face industrialised countries today.[115,130] The use of an energy efficient membrane provides a simplistic method for the capture of carbon dioxide. A perfect membrane can be described as one that selectively allows the passage of one component while rejecting another.[115] Polyimides are one of the most studied classes of polymers for membrane materials.[89] They are growing in importance due to their excellent balance of mechanical and thermal properties, which include thermoxidative stability, electrical properties, chemical resistance, mechanical robustness and structural diversity.[90,91,92] This chapter focuses on the synthesis of polyimides for use as gas separation membranes. There have been many promising examples for this purpose from within our group PIM-PI-1 and PIM-PI-8 in 2008[131], PIM-PI-9, PIM-PI-10, and PIM-PI-11 in 2013 (**Figure 1.4.3.2**)[89] and more recently, work by Pinnau *et al*, KAUST-PI-1 and KAUST-PI-2 in 2014 (**Figure 1.4.3.3**)[88] have demonstrated excellent gas separation properties. As noted by Freeman, increasing the stiffness of the polymer backbone results in increased selectivity and by increasing the interchain separation results in an increase in permeability. Therefore by combining these two factors, a polymer with enhanced gas permselectivities should result.[96] Following on from the success of PIM-PI-1 and PIM-PI-8, the aim was to increase the rigidity of the polymer backbone and also to increase the interchain separation by the use of triptycene as the main component of the polyimide.

2.2 Synthesis of triptycene bisanhydride monomer

Typically, for the synthesis of new polyimides it is possible to work on the preparation of either novel bisanilines or bisanhydrides, as they are the two components of the polymer. The most common approach focuses on the synthesis of bisanilines. [132,133,134] In this project, instead, we decided to attempt the synthesis of a new bisanhydride based monomer, being a lesser studied field. Since triptycenes have always been reported as very successful monomers for the synthesis of microporous polymers, in particular polyimides,[88] we decided to prepare the triptycene molecule (**8**). The retrosynthetic analysis is shown in (**Figure 2.2.1**).

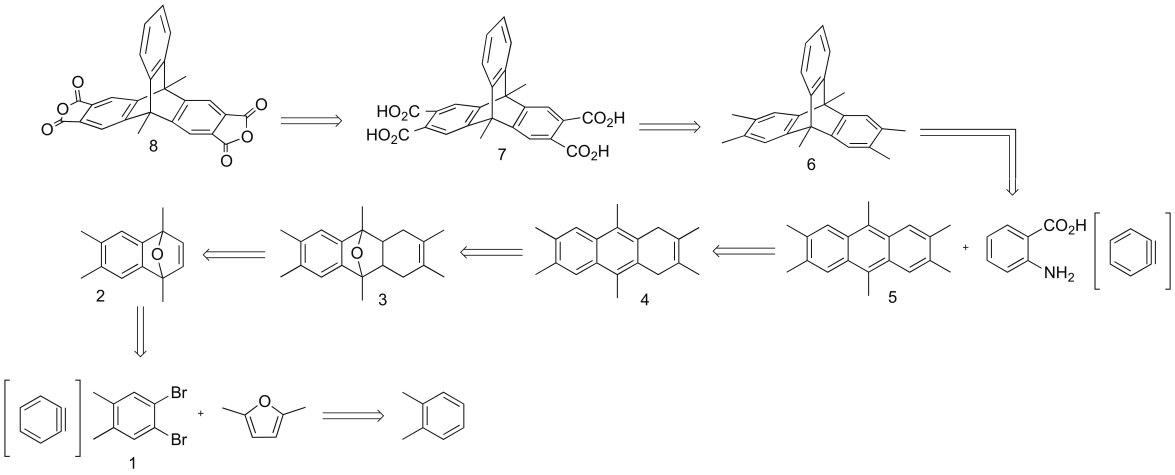

Scheme 2.2.1 Retrosynthesis of target molecule (**8**).

This eight-step synthesis starts with the preparation of 1,2-dibromo-4,5-dimethylbenzene (**1**) which was conducted by the drop-wise addition of bromine to *o*-xylene. The synthesis of tetramethyl-epoxynaphthalene (**2**) involves the Diels-Alder reaction between (**1**), anhydrous furan in a solution of anhydrous toluene and *n*-BuLi at -78 ºC. The crude product was purified by column chromatography to yield (**2**). Epoxyanthracene (**3**) was synthesised according to a modified procedure that was originally reported by Wolthius.[135] The reaction involves a Diels-Alder attack between (**2**) and the commercial 2,3-dimethyl-1,3-butadiene. The original procedure conducted the Diels-Alder step using the conventional reflux conditions, whereas the procedure reported here used a microwave reactor. There have been many examples in which the use of microwave irradiation has been used over conventional heating due to the improvement of yields, lowering of reaction times and simplicity of use.[136,137,138] The removal of the oxygen bridge from (**3**) was performed by the addition of concentrated HCl to yield hexamethyl-dihydroanthracene (**4**). The aromatisation of (**4**) to yield hexamethylanthracene (**5**) was performed by the addition of *p*-chloranil to a refluxing solution of *o*-xylene. The triptycene core (**6**) was obtained by Diels-Alder reaction between (**5**) and anthranilic acid. The preferred choice of benzyne precursor was in this case anthranilic acid, as the very reactive intermediate can be generated in situ at elevated temperatures and in dilute conditions, to obtain the desired precursor (**6**).[139,140] Previous attempts at using 1,2-dibromobenzene, as in the step to form (**2**), proved unsuccessful.[141] Despite the use of 1,2,4,5-tetrabromobenzene, as the benzyne precursor for the synthesis of 2,3-dibromotriptycene, proving successful in previously reported studies,[142] in our case it failed. The oxidation of the external methyl groups of (**6**) was performed by the portion wise addition of $KMnO_4$ to a refluxing solution of (**6**) in

pyridine/water, to yield triptycene-tetracarboxylic acid (**7**), followed by its dehydration by heating to 220 ºC under reduced pressure in a Kugelrohr apparatus, to form the final triptycene-bisanhydride monomer (**8**).

2.3 Synthesis of the triptycene based polyimides

The synthesis of four polyimides based on the newly synthesised triptycene bisanhydride (**8**) was conducted according to the procedure reported by Ghanem et al.[143] Usually polyimides do not possess very high apparent BET surface areas, as the free rotation around the imide link allows the polymer to pack very efficiently, reducing the possibility of generating pores when packing in the solid state, which is the typical characteristic of high performing PIMs. Keeping this in mind, we decided to add more bulky groups to the polymer and the chosen bisanilines were the commercially available 3,3′-dimethylnaphthidine, 2,3,5,6-tetramethyl-*p*-phenylenediamine, 2,4,6-trimethyl-*m*-phenylenediamine and the Tröger's Base bisaniline (**9**) (prepared by Michael Lee in our group). The three commercially available bisanilines are widely reported to hinder free rotation around the imide link and to increase permeability of polyimide films,[88,89,144] and the latter possesses the Tröger's base core which confers high BET surface areas to the resulting polymers, as demonstrated in several studies within our group.[4,5,110] The properties of these four polymers are provided in (**Table 2.3.1**). As previously stated,[92,96] by increasing the rigidity and contorted nature of the polymer backbone gives rise to highly permeable polymers. By hindering the rotation around the imide bond, generally the BET surface area (determined from isothermal nitrogen adsorption at 77 K) increases. With this in mind, the two commercial bisanilines that were first used were 2,4,6-trimethyl-*m*-phenylenediamine and 2,3,5,6-tetramethyl-*p*-phenylenediamine. The synthesis of **P1** was attempted multiple times, however, the resulting polymer did not provide a sufficiently high molecular mass to allow the formation of a robust, self-standing film, as evident from the gel permeation chromatography (GPC) results (see **Table 2.3.1**). The synthesis of **P2** also gave a disappointing result as the polymer precipitated out during the reaction and proved insoluble in most common organic solvents, preventing again the formation of a good film. It is also worth noticing, from the BET analysis, (see **Figure 2.3.2**) that these two polyimides did not generate the high apparent surface area, which was expected. In a continued effort to improve these results, the use of the commercially available 3,3′-dimethylnaphthidine and the synthetic Tröger's Base bisaniline (**9**) was attempted. Unlike

the bisanilines used for **P1** and **P2**, the two used to synthesise **P3** and **P4** possess very different structures. In fact, the monomer used to prepare **P3** does not contain substituents at both positions around the imide bond but the Tröger's base core adds an extra "site of contortion" to the polymer. The bisaniline employed for **P4** places an extra aromatic substituent adjacent to the imide bond to further inhibit the free rotation around the imide bond. As anticipated this results in a higher apparent BET surface area (646 $m^2 g^{-1}$ **Table 2.3.1**). Apart from the evaluation of their BET surface areas, all four polymers were studied by infra-red spectroscopy, in which the presence of the imide bond can be detected at ~3500 cm^{-1}, thermal gravimetric analysis (TGA) which revealed great stability at high temperatures and by gel permeation chromatography (GPC), for the soluble polymers (**P1, P3** and **P4**), which revealed average molecular masses (M_w) in the range 4500-40000 Da – the results of which are shown in (**Table 2.3.3**). For repeat attempts of polymerisations, the highest molecular masses obtained have been recorded (**Table 2.3.3**).

Polymer	Yield	BET		TGA	GPC		Film
	(%)	S.A ($m^2 g^{-1}$)	Pore Volume ($cm^3 g^{-1}$) (P/P_o = 0.9814)	T_d (ºC)	M_w x 10^{-3} (g mol^{-1})	Đ	
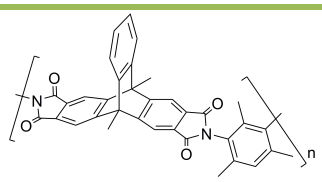 **P1**	36	703	0.48	518	4500	1.49	x
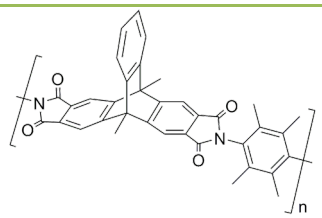 **P2**	11	352	0.21	464	-	-	x
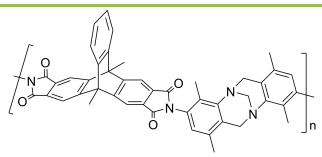 **P3**	58	560	0.45	435	39	1.82	✓
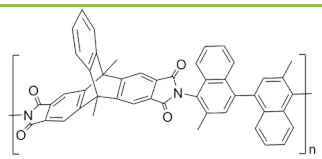 **P4**	27	646	0.43	539	34	1.29	✓

Table 2.3.1 Characterisation of novel PIM-PIs. GPC values calibrated against polystyrene standards using chloroform as eluent.

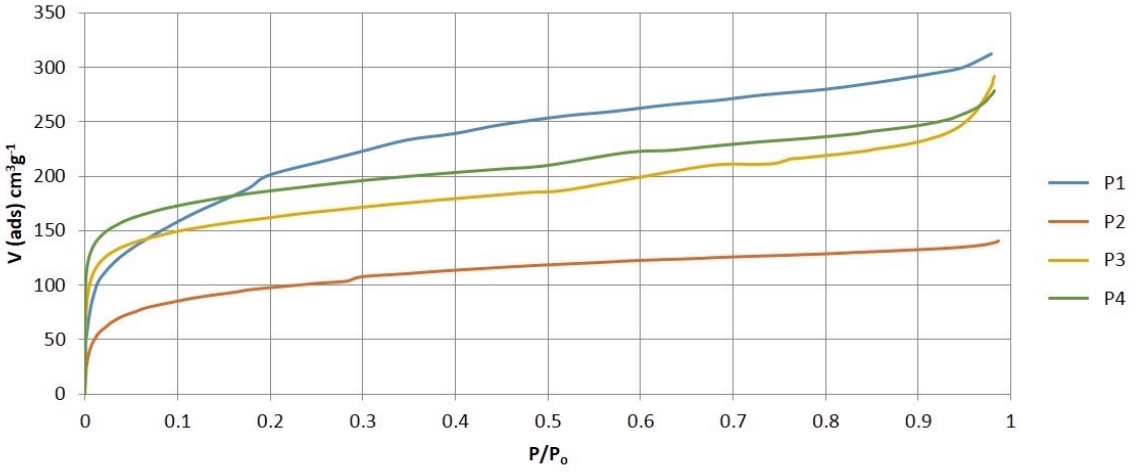

Figure 2.3.2 BET isotherms determined by N_2 adsorption at 77 K.

Large apparent surface area is not the only factor that results in high permeability in a polymer. As discussed in Chapter 1, the solution-diffusion model ($P = SD$) postulates that the permeability is determined by the product of the solubility coefficient (S) and the diffusion coefficient (D). The kinetic diameters of common gas molecules are CH_4 = 3.9 Å > N_2 = 3.7 Å > O_2 = 3.5 Å > CO_2 = 3.3. Å > H_2 = 2.8 Å > He = 2.7 Å. The order of gas permeabilities for the two polyimides synthesised (**P3, P4**) are the same (CO_2 > H_2 > He > O_2 > CH_4 > N_2). In these polyimides, the gas permeabilities do not follow the conventional size-selective polymers, also known as the "molecular sieving behavior". **P3** and **P4** exhibit what is known as "reverse-selectivity" which is typical of PIMs and PIM-PIs as reported in previous work.[131,143,145] This behavior allows some larger gas molecules to permeate quicker than smaller gas molecules,[146] due to the higher affinity of these gases for the polymer composition, as shown by higher solubility coefficients. Thus, in the case of **P3** and **P4**, CO_2 permeates through the polymer membrane quicker than H_2, even though the diffusion coefficient of H_2 is higher than that of CO_2 (see **Table 2.3.3**). As previously described in Chapter 1, the performance of a polymer membrane can be evaluated by placing the data of the permeability (P_x) of the fastest gas and the selectivity ($\alpha_{xy} = (P_x/P_y)$ towards a second gas in the so-called Robeson plot for that particular gas pair and noting the position of the data relative to the 1991 and 2008 upper-bounds for commercially important gas pairs (O_2/N_2, H_2/CH_4, CO_2/CH_4, H_2/N_2, He/CH_4, He/N_2, He/H_2, He/O_2 and H_2/O_2). Despite **P3** demonstrating higher gas permeability values compared to **P4**, the latter exhibits better performance for some important gas pairs such as CO_2/CH_4, CO_2/N_2 and O_2/N_2 which lie over the Robeson 1991 upper bound but below the 2008 one (see **Figure 2.3.4**). In contrast **P3** demonstrates better performance for the H_2/N_2 gas pair, for

which separation is crucial for the purification of H_2 during ammonia production, with data placed on the 2008 upper bound. The performance of **P3** can be related to that of other TB-based polymers which demonstrate relatively low CO_2 permeability perhaps due to carbonic acid formation caused by some residual water attached to the basic TB component. The rigidity of the TB enhances performance as a molecular sieve favouring the transport of small H_2 molecules. The performance of **P4** and PIM-PI-8 can also be compared as the same bisaniline was used for the synthesis of the both polymers (3,3′-dimethylnaphthidine). It can be seen from the Robeson plots (see **Figure 2.3.4**) that PIM-PI-8 performs slightly better than **P4** for the gas pairs in which CO_2 is involved.

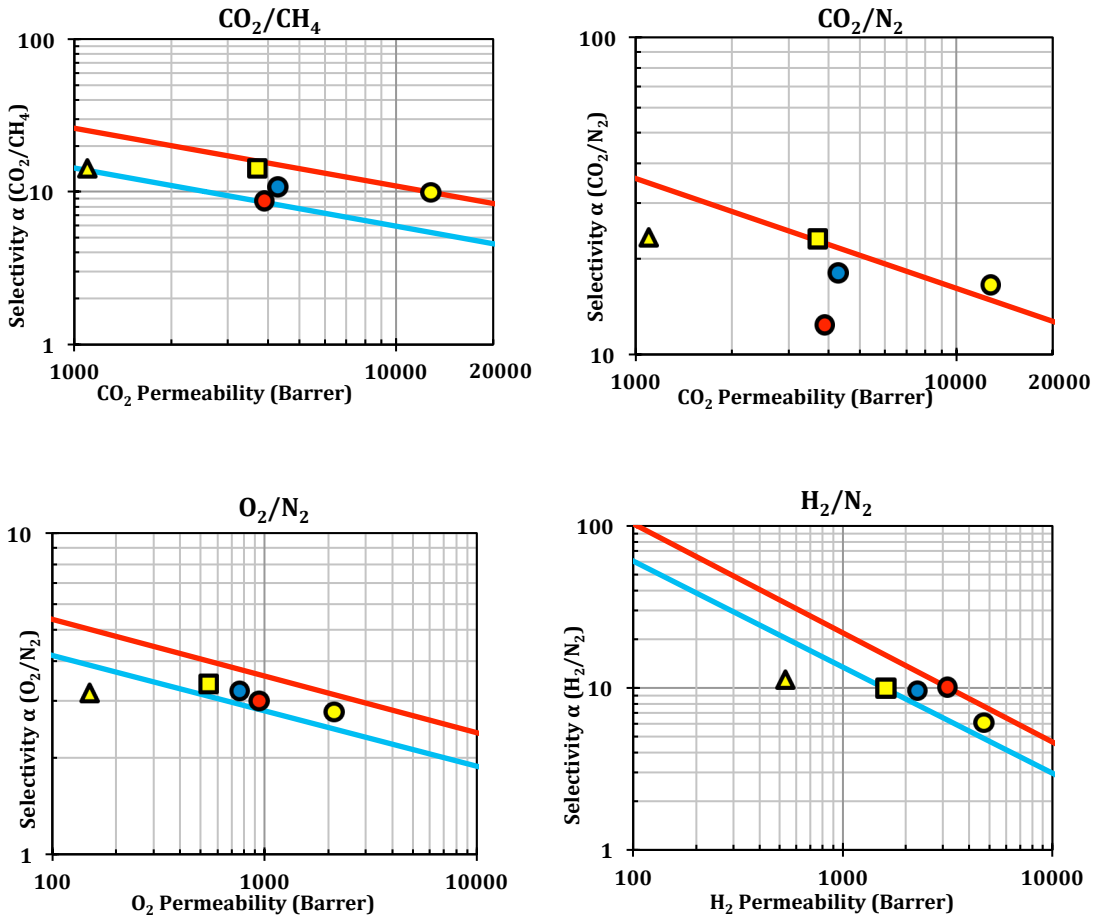

Figure 2.3.4 Robeson plots for CO_2/CH_4, CO_2/N_2, H_2/N_2 and O_2/N_2 gas pairs with 1991 (——) and 2008 (----) upper bounds; P3 (●), P4 (●) with literature data for PIM-1 (○),[131] PIM-PI-1 (△),[92] PIM-PI-8 (□).[92]

Sample	Transport Parameters	N_2	O_2	CO_2	CH_4	H_2	He	Selectivity α (x/y)			
								H_2/N_2	CO_2/N_2	CO_2/CH_4	O_2/N_2
P3	P_x **[Barrer]**	313	942	3887	445	3155	1154	10.1	12.4	8.7	3.0
	D_x **[10^{-12} m^2s^{-1}]**	51	161	55	19	3800	5800	75	1.1	2.8	3.2
	S_x **[cm^3 cm^{-1} bar^{-1}]**	4.6	4.4	52.4	17.5	0.6	0.2	0.1	11.4	3.0	1.0
P4	P_x **[Barrer]**	240	760	4280	400	2270	930	9.6	18.1	10.8	3.2
	D_x **[10^{-12} m^2s^{-1}]**	43	144	61	16	2739	4087	64	1.5	3.8	3.3
	S_x **[cm^3 cm^{-1} bar^{-1}]**	4.2	4.0	52.8	18.2	0.6	0.2	1.4	12.6	2.9	1.0
PIM-1	P_x **[Barrer]**	773	2135	12775	1281	4711	1830	6.1	16.5	10.0	2.8
	D_x **[10^{-12} m^2s^{-1}]**	165	452	199	70	5763	7120	34.9	1.2	2.8	2.7
	S_x **[cm^3 cm^{-1} bar^{-1}]**	3.5	3.5	48.1	13.7	0.6	0.2	0.17	13.7	3.5	1.0
PIM-PI-1	P_x **[Barrer]**	47	150	1100	77	530	260	11.3	23.4	14.3	3.2
	D_x **[10^{-12} m^2s^{-1}]**	20	56	17	7	1200	2000	60	0.9	2.4	2.8
	S_x **[cm^3 cm^{-1} bar^{-1}]**	24	28	620	110	4.5	1.3	0.2	25.8	5.6	1.2
PIM-PI-8	P_x **[Barrer]**	160	545	3700	260	1600	660	10.0	23.1	14.2	3.4
	D_x **[10^{-12} m^2s^{-1}]**	41	130	45	14	2600	3900	3.2	1.1	3.2	3.2
	S_x **[cm^3 cm^{-1} bar^{-1}]**	39	41	810	180	6.2	1.7	0.2	20.8	4.5	1.1

Table 2.3.3 Gas permeabilities P_x, diffusion D_x, solubility coefficient S_x, and ideal selectivities α (P_x/P_y) for methanol treated films of **P3, P4** in comparison to previously reported values of **PIM-1**,[131] **PIM-PI-1**[92] and **PIM-PI-8**.[92]

For the gas pairs shown (**Figure 2.3.4**) the performance of **P3** and **P4** lie over the 1991 Robeson upper bound, but below the updated 2008 upper bound with the exception of **P3** for the gas pair H_2/N_2. With this performance in mind, the need to synthesise new polymers that were based on the triptycene structure which also incorporated the TB unit was desirable.

Chapter 3: Triptycene derived Tröger's Base (TB) polymers

3.1 Introduction

Use of the bridge bicyclic Tröger's Base (TB) unit for the synthesis of PIMs has been previously described in Chapter 1. Utilising the efficient reaction between a 'bisaniline' and a methylene precursor (e.g. dimethoxymethane, DMM) enables the formation of the related TB polymer. Previous examples, such as, PIM-EA-TB[4], PIM-Trip-TB[5] (see p.35) have demonstrated excellent gas separation properties that lie over the 2008 Robeson upper bound for many important gas pairs (O_2/N_2, H_2/N_2, H_2/CH_4, H_2/CO_2 and CO_2/CH_4).[4,5] With the latter demonstrating the greatest performance and also being more permeable overall, the attempt to explain the increase in performance relative to PIM-EA-TB was desirable. Unpublished work in our group has resulted in the synthesis of PIM-EA(H_2)-TB, which is similar to the previously reported PIM-EA(Me)-TB but does not possess the bridgehead methyl. PIM-EA(H_2)-TB shows a slight decrease in permeability, but a significant increase in selectivity, which leads to overall better performance over PIM-EA(Me)-TB. In an attempt to prove that change in performance was indeed due to the presence of hydrogen instead of methyl groups on the bridgehead positions of the ethanoanthracene, the synthesis of the PIM-Trip(Me)-TB was attempted.

3.2 Synthesis of 2,6(7)-diamino-9,10-dimethyl-triptycene monomer

The synthesis of 9,10-dimethyl-diamino-triptycene (**13**) was performed in four-steps (**Scheme 3.2.1**).

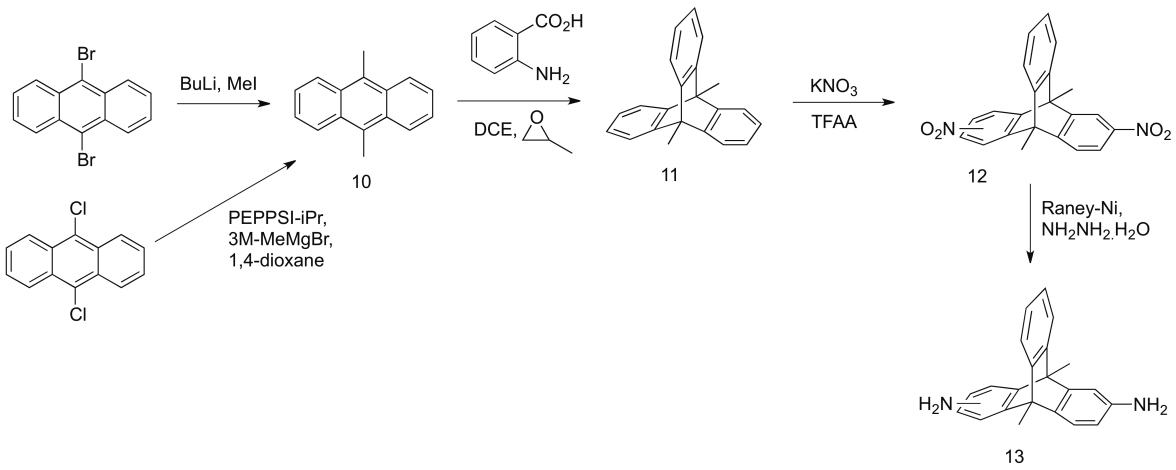

Scheme 3.2.1 Synthesis of 2,6(7)-diamino-9,10-dimethyl-triptycene.

Precursor 9,10-dimethylanthracene (**10**) was prepared using two different methods. The procedure that generated the highest yield involved the reaction between 9,10-dichloroanthracene and the commercially available methyl magnesium bromide (MeMgBr) in the presence of PEPPSI-*i*Pr, which is a commercial but very expensive catalyst. The second method involves the reaction between 9,10-dibromoanthracene and methyl iodide in the presence of *n*-butyl lithium. Even though the yield for the second procedure was only 50%, the cost of the starting materials outweighed the lower yield, thus the reaction between 9,10-dibromoanthracene and MeI was used as the most economic route. The intermediate 9,10-dimethyltriptycene (**11**) was prepared via Diels-Alder reaction between **10** and the commercially available anthranilic acid. The presence of the methyl groups at the 9,10-positions activates the anthracene towards the Diels-Alder reaction. Indeed, the reaction of anthracene with anthranilic acid can lead to a variety of products, where the Diels-Alder adduct can statistically add over each one of the three benzene rings that make up anthracene.[147] The increase in electron density at the 9,10-positions of **10** directs the Diels-Alder reaction to the middle ring, thus increasing the yield of the desired product and facilitating the purification. Nitration of **11** using KNO_3 and trifluoroacetic anhydride (TFAA) gave **12** and reduction of the nitro groups by the use of Raney-Ni® and $NH_2NH_2.H_2O$ gave the corresponding 2,6(7)-diamino-9,10-dimethyltriptycene (**13**).

3.3 Synthesis of polymer PIM-Trip(Me)-TB (P5)

The synthesis of **P5** was conducted according to the general TB polymerisation procedure reported in 2013.[4] This involved the reaction between **13** and five equivalents of dimethoxymethane (DMM) in trifluoroacetic acid (TFA), which was left at room temperature for 5 days. The polymer proved highly soluble in chloroform, which allowed for the analysis of the molecular mass by gel permeation chromatography (GPC), which showed a value of M_w = 116,000 (relative to polystyrene standards, see **Table 3.3.1**). As previously discussed in Chapter 1, the structure of the Tröger's base core induces high microporosity to the resulting polymers.[4,5,110] Thus, a freshly purified polymer powder **P5** demonstrated an apparent BET surface area of 926 $m^2 g^{-1}$ (calculated from isothermal N_2 adsorption at 77 K (error ± 50 $m^2 g^{-1}$), see **Table 3.3.1, Figure 3.3.2**). Comparing this result with that from the previously prepared TB polymers it can be concluded that methyl groups at the bridgehead positions of the triptycene or ethanoanthracene units enhances microporosity, perhaps due to their role as "chain-separators". As all four polymers

demonstrated complete solubility in chloroform and a high molecular mass, the preparation of robust self-standing films for gas permeation studies was successful. For all polymers the order of gas permeability is $H_2 > CO_2 > O_2 > CH_4 > N_2$. As noted previously, PIMs containing the TB unit display relatively low permeability for CO_2.

Polymer	Yield	BET		TGA	GPC		Film
	(%)	S.A ($m^2 g^{-1}$)	Pore Volume ($cm^3 g^{-1}$) ($P_s/P_o = 0.9814$)	T_d (°C)	M_w x 10^{-3} (g mol^{-1})	Đ	
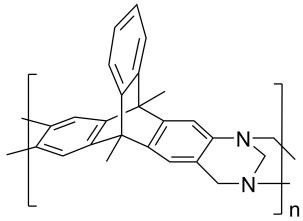 **P5**	83	926	0.6532	413	116	2.51	✓
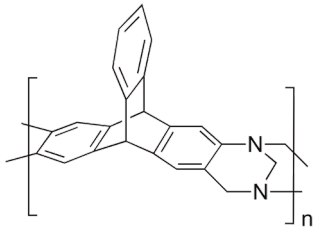 **PIM-Trip(H_2)-TB**	82	899	0.5705	400	51	2.39	✓
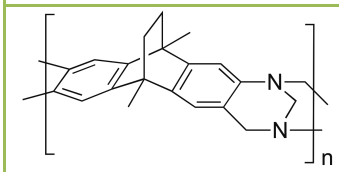 **PIM-EA(Me)-TB**	76	1028	0.7500	260	156	2.50	✓
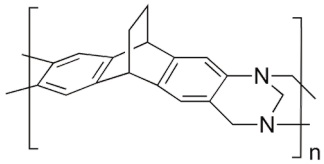 **PIM-EA(H_2)-TB**	91	845	0.6200	260	50	5.36	✓

Table 3.3.1 Characterisation of PIM-TBs. GPC measured against polystyrene standard using chloroform as eluent. **P5**, PIM-Trip(H_2)-TB data,[5] PIM-EA(Me)-TB data,[4] and PIM-EA(H_2)-TB data.[148]

Overall, the order of permeability is PIM-Trip(H_2)-TB > PIM-EA(Me)-TB > PIM-EA(H_2)-TB > PIM-Trip(Me)-TB (**P5**) showing that the addition of methyl groups onto the bridgehead positions of the triptycene unit does not enhance permeability. It can also be seen from the respective Robeson plots (**Figure 3.3.3**) that all four polymers display impressive data relative to the upper bounds but that methyl substitution of the triptycene does not enhance selectivity – with the possible exception of the H_2/N_2 gas pair.

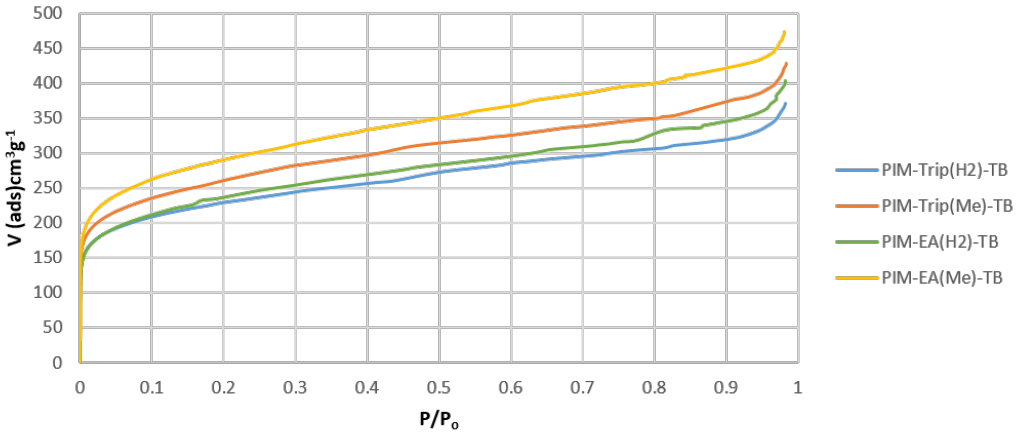

Figure 3.3.2 BET isotherms determined from N_2 adsorption at 77 K. PIM-Trip(Me)-TB (**P5**), PIM-Trip(H_2)-TB,[5] PIM-EA(H_2)-TB,[148] PIM-EA(Me)-TB.[4]

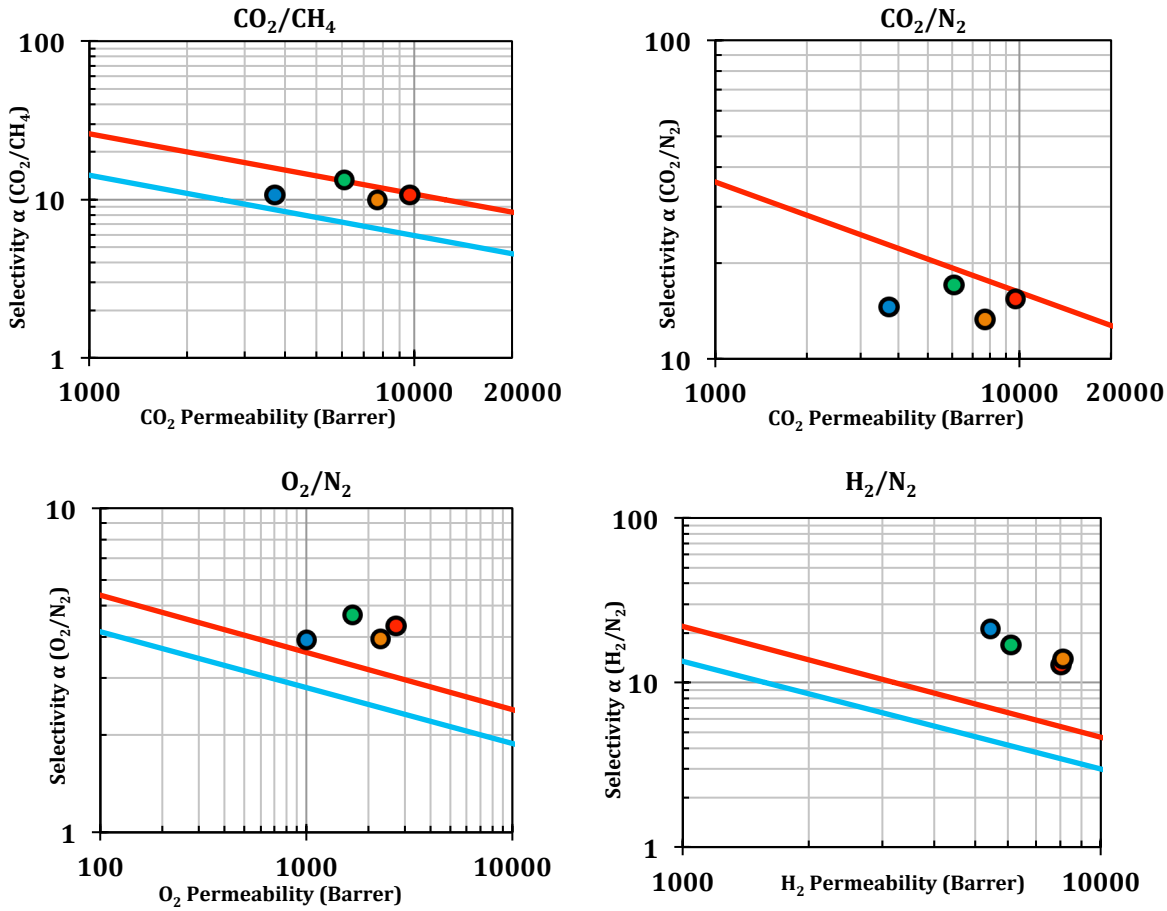

Figure 3.3.3 Robeson plots for CO_2/CH_4, CO_2/N_2, O_2/N_2 and H_2/N_2 gas pairs with 1991 (----) and 2008 (----) upper bounds; **P5** (●), with literature data for PIM-Trip(H_2)-TB (●),[5] PIM-EA(H_2)-TB (●),[148] PIM-EA(Me)-TB (●).[4]

Sample	Transport Parameters	N_2	O_2	CO_2	CH_4	H_2	He	Selectivity $\alpha(x/y)$			
								H_2/N_2	CO_2/N_2	CO_2/CH_4	O_2/N_2
PIM-EA(H_2)-TB	P_x **[Barrer]**	358	1673	6097	458	6088	1938	17.0	17.0	13.3	4.7
	D_x **[10^{-12} m^2 s^{-1}]**	48	216	66	15	5635	7822	117	1.4	4.4	4.5
	S_x **[cm^3 cm^{-1} bar^{-1}]**	5.6	5.8	69.0	22.8	0.8	0.2	0.1	12.3	3.0	1.0
PIM-EA(Me)-TB	P_x **[Barrer]**	580	2294	7696	774	8114	2685	14.0	13.3	9.9	4.0
	D_x **[10^{-12} m^2 s^{-1}]**	100	318	87	36	>7000	>10000	70.0	0.9	2.4	3.2
	S_x **[cm^3 cm^{-1} bar^{-1}]**	4.4	7.3	47.0	17.2	1.1	0.3	0.3	10.7	2.7	1.7
PIM-Trip(H_2)-TB	P_x **[Barrer]**	629	2718	9709	905	8039	2500	12.8	15.4	10.7	4.3
	D_x **[10^{-12} m^2 s^{-1}]**	135	462	111	48.9	7800	>10000	57.8	0.8	2.3	3.4
	S_x **[cm^3 cm^{-1} bar^{-1}]**	3.5	4.4	65.6	13.9	0.8	0.2	0.2	18.7	4.7	1.3
P5	P_x **[Barrer]**	255	1002	3718	347	5446	2178	21.4	14.6	10.7	3.9
	D_x **[10^{-12} m^2 s^{-1}]**	25	106	24	8.0	4393	7580	176	1.0	3.0	4.2
	S_x **[cm^3 cm^{-1} bar^{-1}]**	7.5	7.1	117	34	0.9	0.2	0.1	15.6	3.4	0.9

Table 3.3.4 Gas permeabilities P_x, diffusivity D_x, solubility coefficient S_x, and ideal selectivities α (P_x/P_y) for methanol treated films of PIM-EA(H_2)-TB,[148] PIM-EA(Me)-TB,[4] PIM-Trip(H_2)-TB,[5] and **P5**.

3.4 Synthesis of Triptycene/Ethanoanthracene Co-polymers

Due to the excellent properties observed with the four TB polymers described in the previous section, the preparation of co-polymers of each of the four bisaniline monomers was desired, especially to evaluate better the influence of the methyl groups on the bridgehead positions. Initial attempts used 50:50 combination of a triptycene bisamine with an ethanoanthracene bisamine reacted together using the typical TB polymerisation technique. Each combination of co-polymer was successfully synthesised (see **Table 3.4.1**) and ^{1}H NMR, TGA and BET analysis techniques were used to ensure the 50:50 composition of the resulting co-polymer was obtained.

Polymer	Yield	BET		TGA	GPC		Film
	(%)	S.A ($m^2 g^{-1}$)	Pore Volume ($cm^3 g^{-1}$) ($P_s/P_o = 0.9814$)	T_d (°C)	M_w x 10^{-3} (g mol^{-1})	Đ	
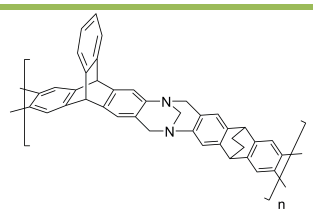 **P6**	73	855	0.6212	289	191	2.51	✓
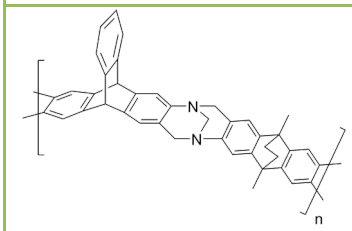 **P7**	51	896	0.7110	311	117	2.85	✓
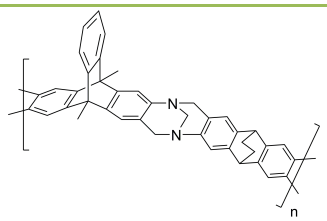 **P8**	83	888	0.6401	300	160	2.01	✓
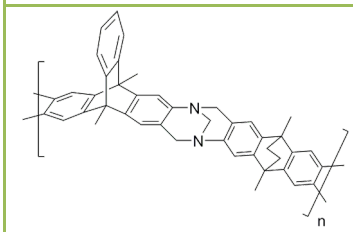 **P9**	69	952	0.7672	311	188	4.49	✓

Table 3.4.1 Characterisation of **P6**, **P7**, **P8** and **P9** Co-Polymers**.** GPC measured against polystyrene standard using chloroform as eluent.

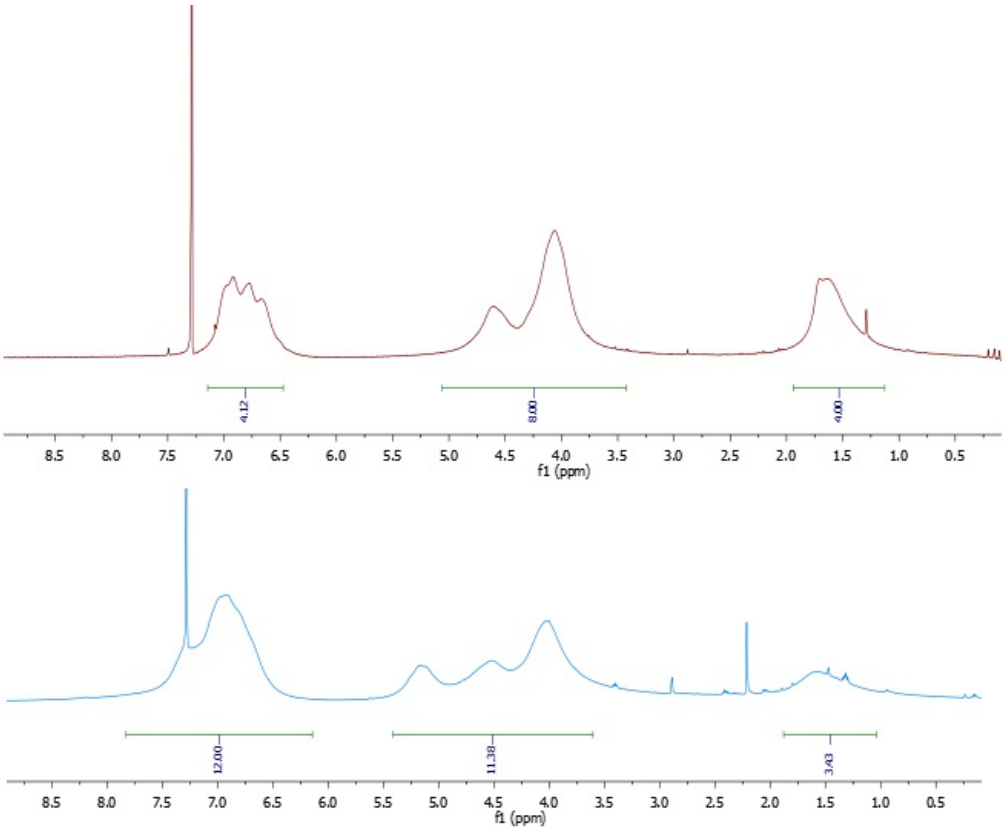

Figure 3.4.2 ^{1}H NMR spectrum of **P6 (—)** and PIM-EA(H_2)-TB[148] (—) in $CDCl_3$.

As a typical example of the characterisation of these co-polymers, in (**Figure 3.4.2**) is shown the Trip(H_2)-EA(H_2)-TB 50/50 co-polymer. From a comparison of the ^{1}H NMR of **P6** and the homo-polymer PIM-EA(H_2)-TB (see **Figure 3.4.2**), there can be seen an extra signal between δ5.25 – 5.00 ppm, corresponding to the bridgehead protons of the Trip(H_2)-component. The presence of the Trip(H_2) unit in **P6** can also be inferred from the greater relative intensity of the aromatic peak (δ7.5 – 6.0 ppm) as compared with that of the homo-polymer of PIM-EA(H_2)-TB. The integration values are slightly incorrect, but this due to any unremoved impurities from the polymer sample, thus causing the integration values to differ.

The composition of **P6** can also be confirmed from the TGA analysis of **P6** and PIM-EA(H_2)-TB (see **Figure 3.4.3** and **Figure 3.4.4**). From the TGA analysis of PIM-EA(H_2)-TB (**Figure 3.4.3**) we can evaluate the retro-Diels-Alder loss of the ethano-bridge, which occurs at a temperature of 289°C and results in an 8 % reduction in mass. As expected the analogous loss in mass for **P6**, corresponds to 4% (**Figure 3.4.4**) thus confirming the 50:50 composition of **P6**. Similar NMR and TGA analysis analysis confirmed the composition of all four co-polymers **P6**, **P7**, **P8** and **P9**.

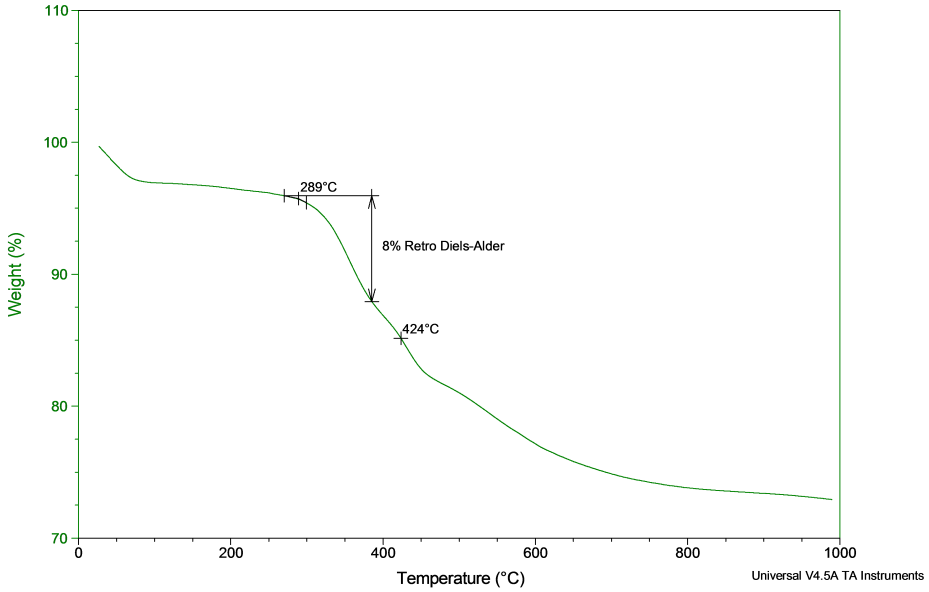

Figure 3.4.3 TGA analysis of PIM-EA(H_2)-TB. Highlighted is the reverse Diels-Alder reaction that allows polymer composition calculation.

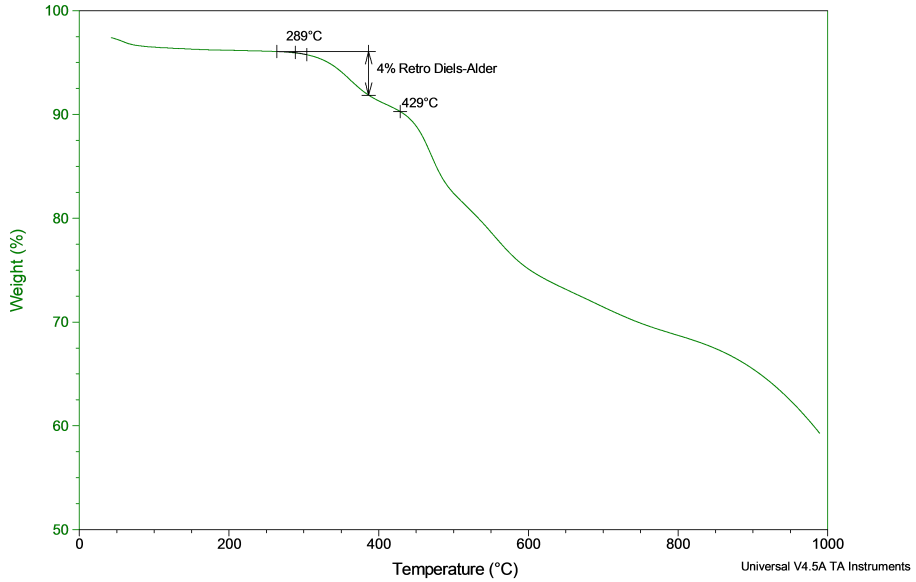

Figure 3.4.4 TGA analysis of **P6**. Highlighted is the reverse Diels-Alder reaction that allows polymer composition calculation.

Surface area analysis (**Figure 3.4.5**) confirmed the trend seen for the homopolymers that methyl substitution of the bridgehead positions enhances microporosity, although the differences are not significant.

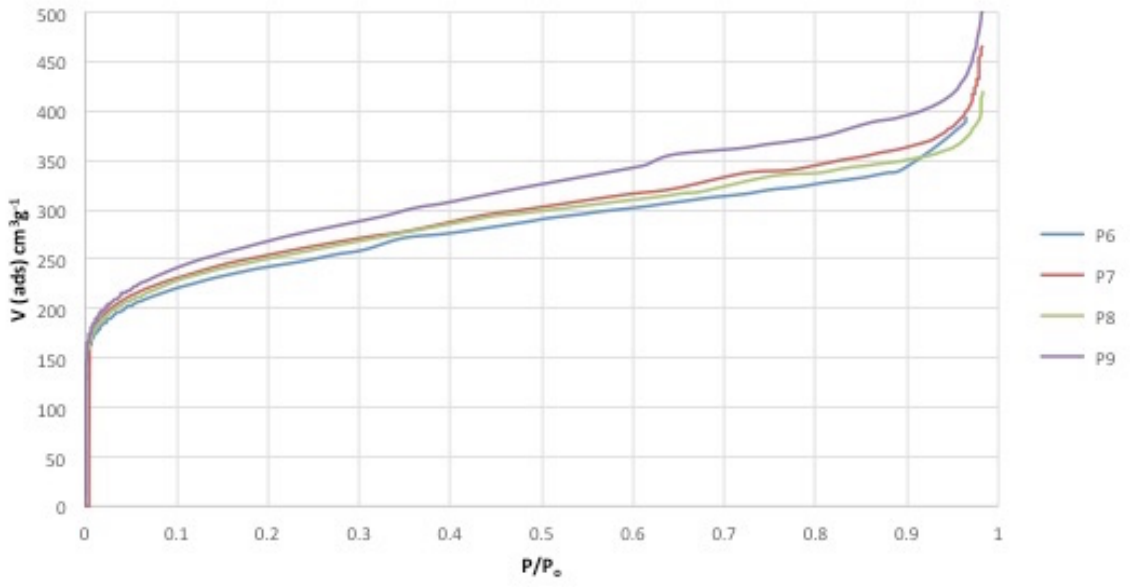

Figure 3.4.5 BET isotherms determined from N_2 adsorption at 77 K of **P6**, **P7**, **P8** and **P9**.

The Robeson plots of CO_2/CH_4, CO_2/N_2, O_2/N_2 and H_2/N_2 (**Figure 3.4.6**) show that the gas permeabilities of the copolymers are roughly as anticipated from predictions based upon their composition. Unsurprisingly, the co-polymer **P7** containing the same components as the two best performing homopolymers (i.e. EA(Me) and Trip(H_2)) showed the best results and indeed slightly out-perform the homopolymers with regards data position relative to the upper bounds, especially for CO_2/N_2 and CO_2/CH_4 for which the data lie above the 2008 upper bounds. Data for O_2/N_2 are also impressive due to the significant advancement above the upper bounds.

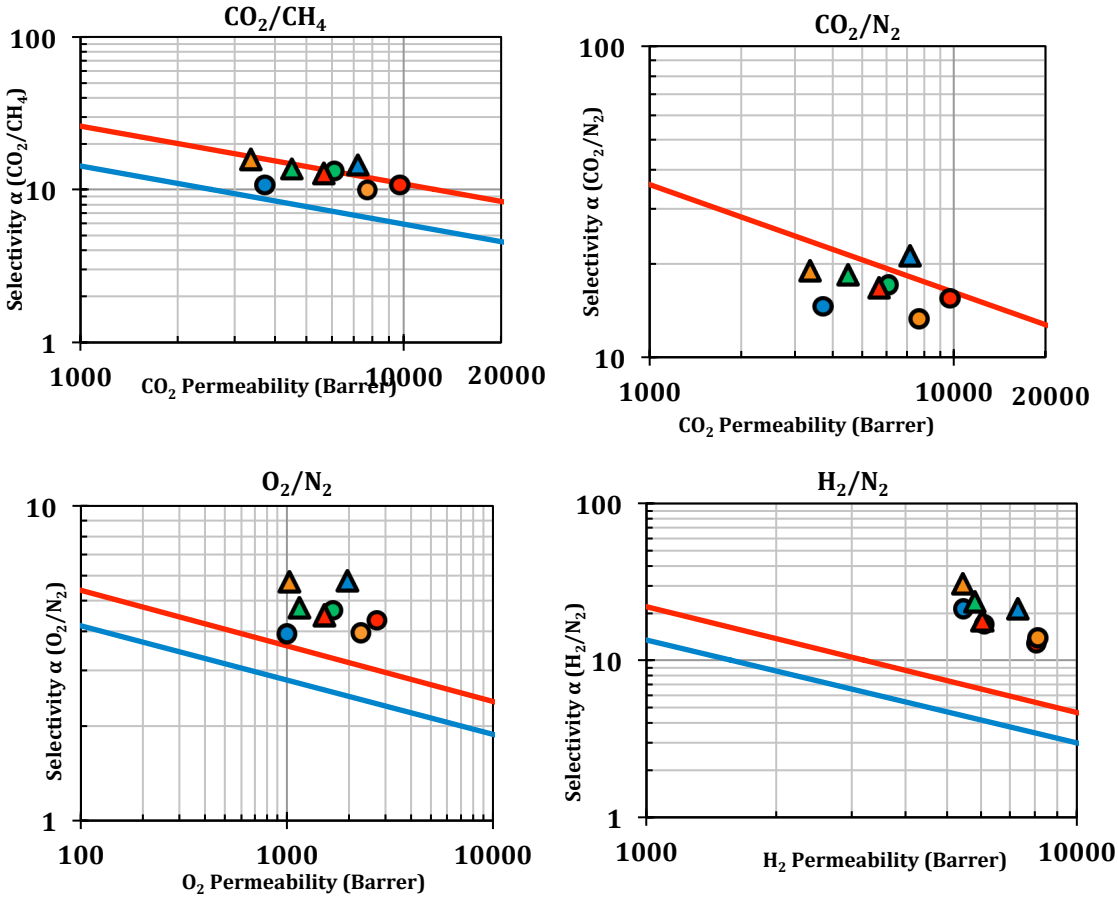

Figure 3.4.6 Robeson plots for CO_2/CH_4, CO_2/N_2, O_2/N_2 and H_2/N_2 gas pairs with 1991 (—) and 2008 (—) upper bounds; **P5** (●), with literature data for PIM-Trip(H_2)-TB (●),[5] PIM-EA(H_2)-TB (●),[148] PIM-EA(Me)-TB (●),[4] **P6** (▲), **P7** (▲), **P8** (▲) and **P9** (▲).

Sample	Transport Parameters	N_2	O_2	CO_2	CH_4	H_2	He	Selectivity $\alpha(x/y)$			
								H_2/N_2	CO_2/N_2	CO_2/CH_4	O_2/N_2
P6	P_x **[Barrer]**	338	1521	5667	445	6041	1949	17.9	16.8	12.7	4.5
	D_x **[10^{-12} m^2s^{-1}]**	35	188	46	10	5785	8459	165	1.3	4.6	5.4
	S_x **[cm^3cm^{-1} bar^{-1}]**	7.3	6.1	92.0	34.6	0.8	0.2	0.1	12.6	2.7	0.8
P7	P_x **[Barrer]**	341	1974	7192	494	7274	2464	21.3	21.1	14.6	5.8
	D_x **[10^{-12} m^2s^{-1}]**	60	297	48	16	4053	4240	68	0.8	3	5
	S_x **[cm^3cm^{-1} bar^{-1}]**	4.2	5.0	113	22.7	1.4	0.4	0.3	26.9	5.0	1.2
P8	P_x **[Barrer]**	244	1157	4497	329	5788	2077	23.7	18.4	13.7	4.7
	D_x **[10^{-12} m^2s^{-1}]**	25	130	13	1.2	4586	7294	183	0.5	10.8	5.2
	S_x **[cm^3cm^{-1} bar^{-1}]**	7.4	6.7	253	198	0.9	0.2	0.1	34	1.3	0.9
P9	P_x **[Barrer]**	178	1027	3370	213	5443	1938	30.6	18.9	15.8	5.8
	D_x **[10^{-12} m^2s^{-1}]**	23	124	20	5	3224	6702	140	0.9	4	5.4
	S_x **[cm^3cm^{-1} bar^{-1}]**	5.8	6.2	124	31.2	1.3	0.2	0.2	21.4	4	1.1

Table 3.4.7 Gas permeabilities P_x, diffusivity D_x, solubility coefficient S_x, and ideal selectivities α (P_x/P_y) for methanol treated films of **P6**, **P7**, **P8**, **P9**.

3.5.1 Benzotriptycene as component of PIMs

Due to the excellent gas permeation properties showed by the use of triptycene as the main component for the synthesis of PIMs, the further enhancement of these properties was desirable. It has already been demonstrated in Chapter 3.3 that by inhibiting the efficient packing of the polymer chains by the addition of methyl groups, the interchain separation is increased, which in-turn, generated higher free volume. Thus it was suggested that by adding another aromatic ring to one arm of the triptycene unit, i.e. to use benzotriptycene units, would inhibit even further the efficient packing of the polymer chains. This phenomenon has recently been demonstrated for polyimides by Pinnau et al.[149] and Swager et al.[150] According to these earlier studies, the structure of benzotriptycene possesses higher internal free volume (IFV) than that of triptycene (see **Figure 3.5.1**).

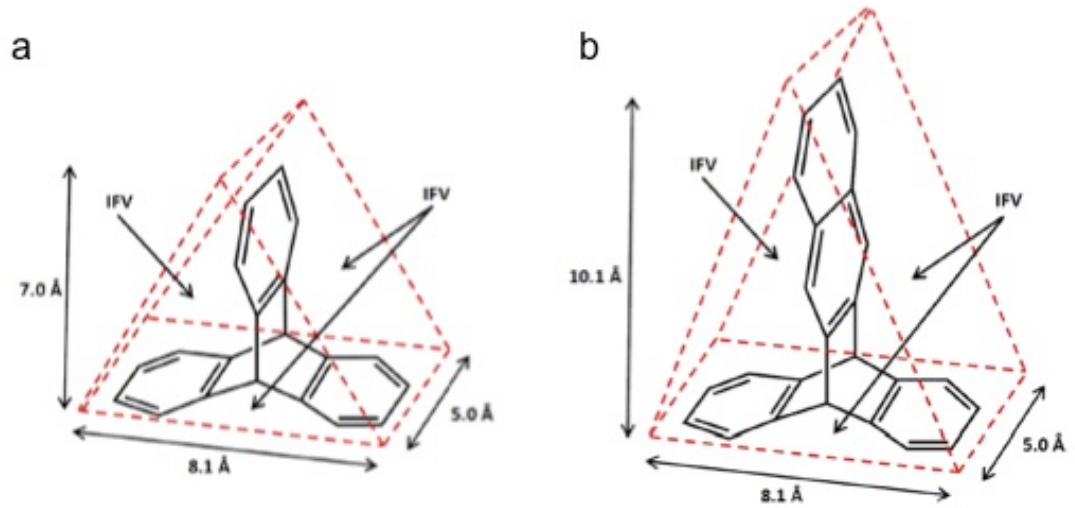

Figure 3.5.1 Chemical structures of (a) triptycene (b) benzotriptycene to demonstrate the internal free volume (IFV) between both structures.[149]

3.5.2 Synthesis of Benzotriptycene TB polymer

The synthesis of the required diaminobenzotriptycene monomer (**Scheme 3.5.2.1**) was conducted according to a slightly modified procedure reported by Swager et al.[150] The intermediate 2,6-diaminoanthracene (**14**) was prepared via the two-step reduction of 2,6-diaminoanthraquinone. Alternative, commonly-used reagents such as zinc were reported to over-reduce 2,6-diaminoanthraquinone to yield the non-aromatic dihydro analogue by Kantam et al.[151] The Diels-Alder reaction between **15** and **16** was conducted using microwave irradiation as a means to improve the yield and lower the reaction times (from 4 days to 2.5 h). The removal of the oxygen bridge from **17** was achieved by the reaction with a strong acid to yield 2,6-diaminobenzotriptycene (**18**). This synthetic method allows the formation of the final monomer as a single product, in contrast to those used for the synthesis of PIM-EA-TB and PIM-Trip-TB, for which the bisamino monomers are synthesised as regioisomers, via a nitration method from their respective hydrocarbons. In a recent publication it was demonstrated that the use of a single isomer benefits the polymerisation of a PIM, which improves the physical properties of solvent cast films.[152]

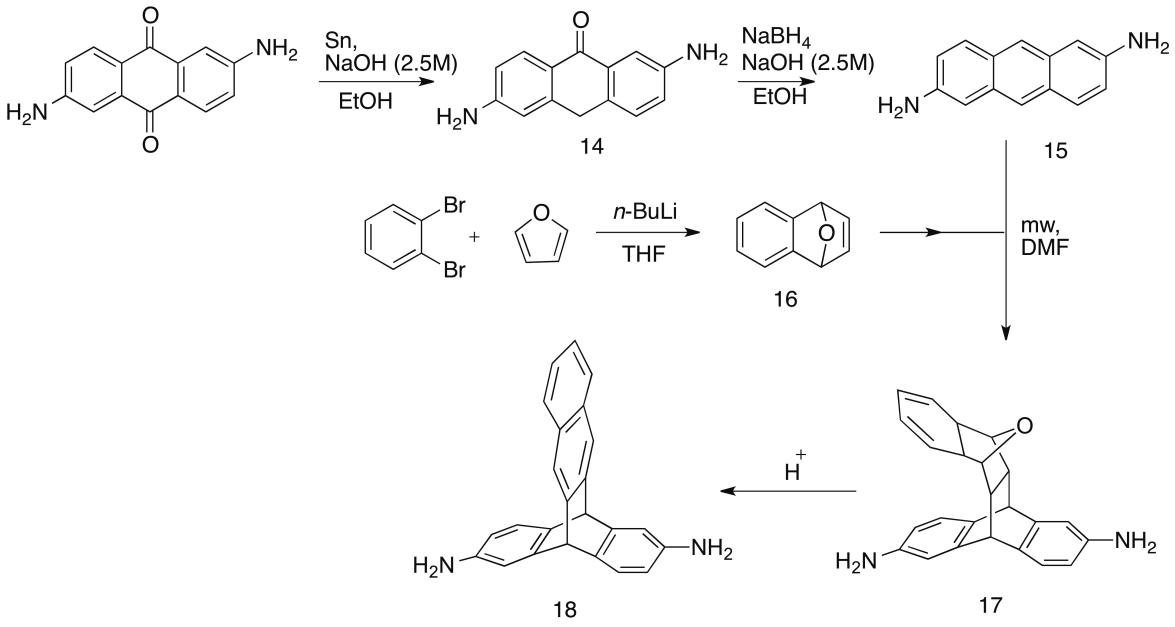

Scheme 3.5.2.1 Synthesis of diaminobenzotriptycene monomer 18.

The synthesis of the benzotriptycene TB polymer **P10** was conducted according to the general TB polymerisation described in chapter 3.3, which involves the reaction between **18** and DMM in the presence of TFA. The resulting mixture was left at room temperature for 24 h, before being poured into aqueous ammonium hydroxide solution to quench the reaction. The resulting cream-coloured polymer was highly soluble in chloroform, which allowed for its analysis by NMR and GPC, which gave a value of M_w = 103,500 (relative to polystyrene standards) (see **Table 3.5.2.2**). A model of **P10** (**Figure 3.5.2.3**) indicates that its macromolecular structure is contorted in three dimensions, combined with its rigid and contorted nature, the shape of the resulting TB polymer should generate intrinsic microporosity. From a fresh, methanol-treated and dried polymer **P10**, the BET surface area was calculated from the isothermal N_2 adsorption at 77 K (see **Table 3.5.2.2**), demonstrating a similar BET surface area to that of PIM-Trip(H_2)-TB. The T_d of **P10** was measured to be 465 °C by TGA analysis – an increase in the thermal stability of 65°C relative to PIM-Trip(H_2)-TB (see **Table 3.5.2.2**).

Polymer	Yield	BET		TGA	GPC		Film
	(%)	S.A ($m^2 g^{-1}$)	Pore Volume ($cm^3 g^{-1}$) ($P_s/P_o = 0.9814$)	T_d (°C)	M_w x 10^{-3} (g mol^{-1})	Đ	
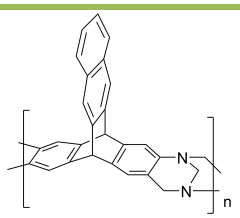 **P10**	81	868	0.6189	465	103	3.55	✓
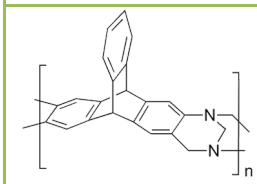 **PIM-Trip(H_2)-TB**	82	899	0.5705	400	51	2.39	✓

Table 3.5.2.2 Characterisation of **P10**[110] and PIM-Trip(H_2)-TB.[5] GPC measured against polystyrene standards using chloroform as eluent.

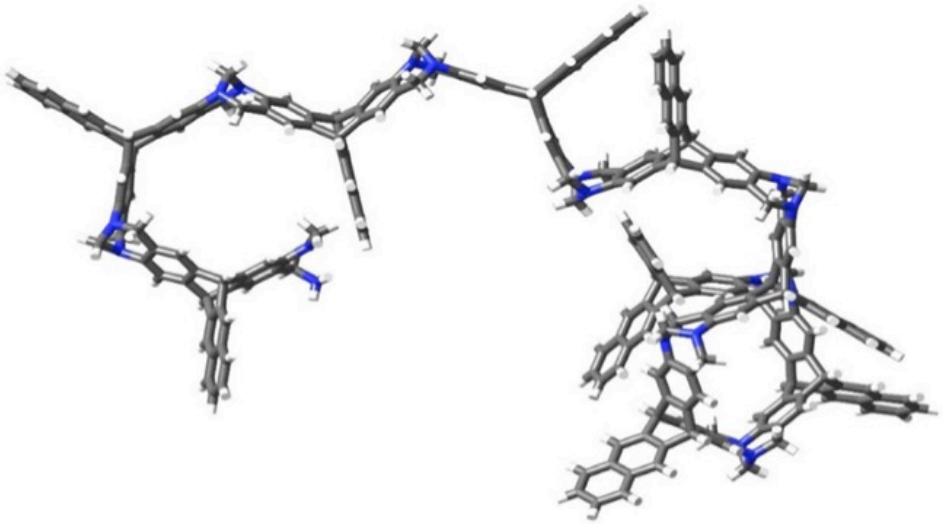

Figure 3.5.2.3 Molecular model of a fragment of **P10** (made with Spartan 10 vVersion 1.1.0; Wave function Inc., Irvine, CA, USA).[110]

Due to the high molecular mass and complete solubility in chloroform, the preparation of robust self-standing films for gas permeation studies was successful. For all gas pairs, **P10** demonstrates enhanced permeability when compared to PIM-Trip(H_2)-TB (**Table 3.5.2.5**) (see **Figure 3.5.2.4**), which is consistent with the anticipated higher free volume that is generated from the benzotriptycene structure. This is also confirmed from the higher pore volume obtained for **P10** (0.62 $cm^3 g^{-1}$) than that of PIM-Trip(H_2)-TB (0.57

$cm^3 g^{-1}$). The order of the gas permeabilities is $CO_2 > H_2 > O_2 > He > CH_4 > N_2$ which is the typical behaviour of "reverse-selective" polymers which has been previously described in chapter 1 and chapter 2. This enhancement in permeability of **P10** against PIM-Trip(H_2)-TB is due to the improved solubility coefficients (see **Table 3.5.2.5**). Even though PIM-Trip(H_2)-TB exhibits greater diffusivity coefficients, the enhancement in the solubility coefficients of **P10** outweigh the difference, thus generating a more permeable polymer for each probe gas tested. For the gas pairs CO_2/CH_4, CO_2/N_2 and H_2/N_2 the performance of **P10** is comparable with that of PIM-Trip(H_2)-TB, in that the data points approach the CO_2/CH_4 and CO_2/N_2 upper bounds but lie well over the 2008 upper bound for H_2/N_2. For the gas pair O_2/N_2 **P10** is less selective than PIM-Trip(H_2)-TB.

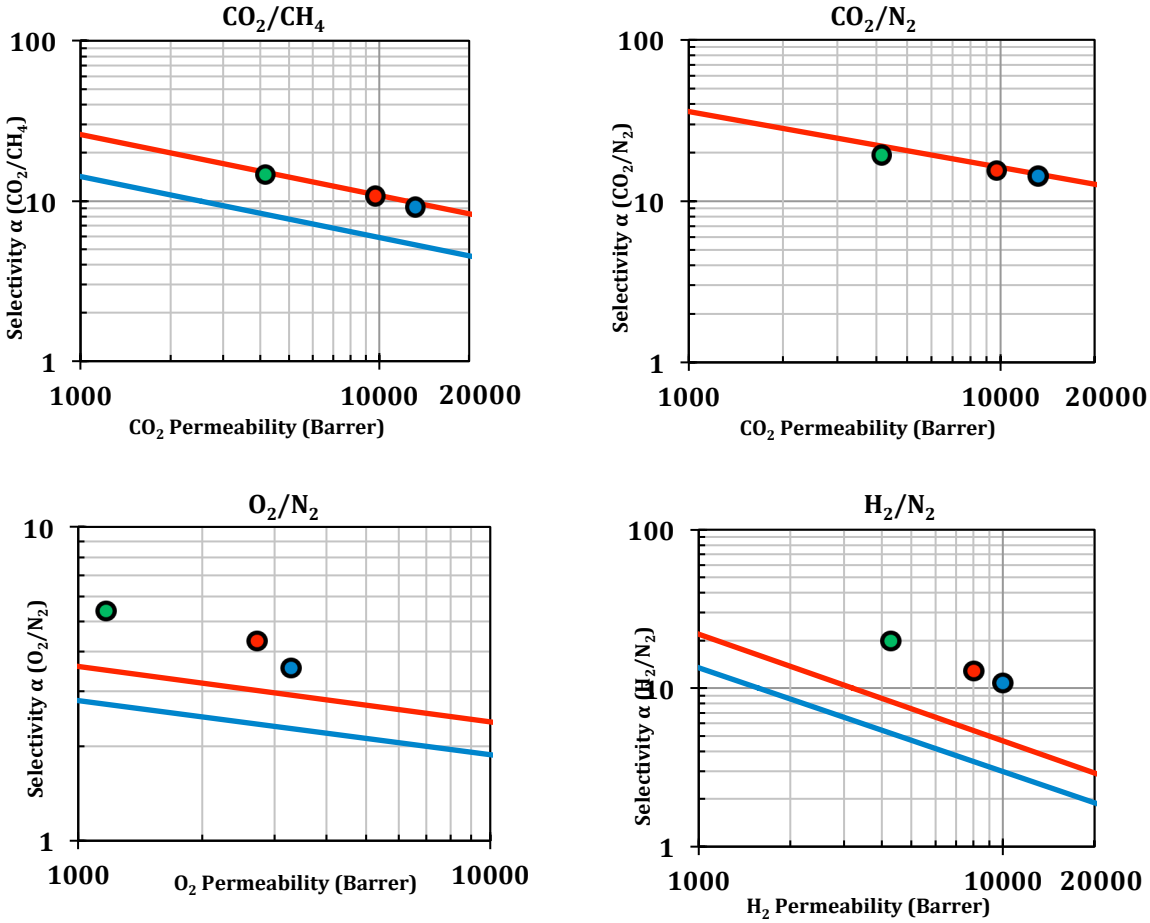

Figure 3.5.2.4 Robeson plots for CO_2/CH_4, CO_2/N_2, O_2/N_2 and H_2/N_2 gas pairs with 1991 (——) and 2008 (– –) upper bounds; **P10** (●),[110] **P10** (aged 166 days) (●) with literature data for PIM-Trip(H_2)-TB (●).[5]

As previously described in chapter 2, physical aging is a typical feature of glassy polymers, which leads to a loss of permeability, but subsequently generates an increase in selectivity which is in accordance with the Robeson trade-off.[1] Upon aging of a freshly treated

methanol film of **P10** for 166 days, the expected loss in permeability and corresponding increase in selectivity was noted (**Figure 3.5.2.4**). Hence for the gas pair O_2/N_2 the effect of aging has caused PO_2 to decrease from 3290 to 1170 Barrer, but results in an increase in selectivity from PO_2/PN_2 = 3.6 to a remarkably high value of 5.4. This performance is comparable to some of the best performing PIMs such as PIM-Trip-TB, TPIM-1 and KAUST-PI-1.[153,88]

Sample	Transport Parameters	N_2	O_2	CO_2	CH_4	H_2	He	Selectivity $\alpha(x/y)$			
								H_2/N_2	CO_2/N_2	CO_2/CH_4	O_2/N_2
P10	P_x **[Barrer]**	926	3292	13205	1440	9976	2932	10.8	14.3	9.2	3.6
	D_x **[10^{-12} m^2s^{-1}]**	70	347	43	28	8493	10800	121	0.6	1.5	5.0
	S_x **[cm^3 cm^{-1} bar^{-1}]**	10	7	230	39	0.9	0.2	0.1	23	6.0	0.7
P10 (aged 166 days)	P_x **[Barrer]**	216	1166	4147	283	4280	1470	19.8	19.2	14.7	5.4
	D_x **[10^{-12} m^2s^{-1}]**	34	159	41	10	4780	6720	141	1.2	4.1	4.7
	S_x **[cm^3 cm^{-1} bar^{-1}]**	5	6	77	21	0.7	0.2	0.1	15	3.6	1.2
PIM-Trip(H_2)-TB	P_x **[Barrer]**	629	2718	9709	905	8039	2500	12.8	15.4	10.7	4.3
	D_x **[10^{-12} m^2s^{-1}]**	135	462	111	49	7800	>10000	58	0.8	2.3	3.4
	S_x **[cm^3 cm^{-1} bar^{-1}]**	3.5	4.4	66	14	0.8	0.2	0.2	19	5	1.3

Table 3.5.2.5 Gas permeabilities P_x, diffusivity D_x, solubility coefficient S_x, and ideal selectivities α (P_x/P_y) for methanol treated films of **P10**,[110] PIM-Trip(H_2)-TB[5] and **P10** (aged for 166 days).[110]

3.5.3 Synthesis of substituted Benzotriptycene TB polymers

The naphthalene moiety of the benzotriptycene structure provides an ideal location for the addition of different functional groups, so that the properties of the final TB polymer can be tuned. The synthesis of the diaminobenzotriptycene described above (**Scheme 3.5.2**) can be adapted to allow this functionalisation. By changing the 1,4-epoxynaphthalene adduct for the Diels-Alder reaction with diaminoanthracene, a variety of substituted

monomers can be synthesised (**Figure 3.5.3.1**). In the following sections the synthesis of a variety of substituted diaminobenzotriptycene monomers (see **Table 3.5.3.2**) and their corresponding TB polymers (see **Table 3.5.3.3**) will be discussed.

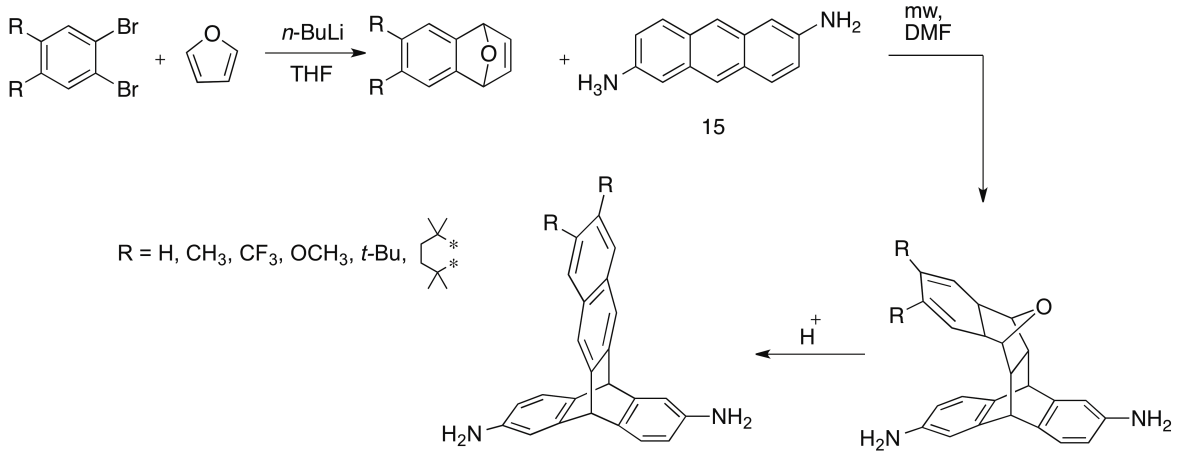

Figure 3.5.3.1 General synthesis of substituted diaminobenzotriptycene monomers.

For each monomer, the synthesis began with the preparation of the 1,4-epoxynaphthalene units (**19**, **22**, **25**, **28** and **31**), which were subsequently reacted in a Diels-Alder reaction with **15** to form the corresponding oxygen-bridge species (**20**, **23**, **26**, **29** and **32**). Note that 1,4-epoxynaphthalene **31** was reacted with an amide protected diaminoanthracene (**61**) as the free bisamine monomer (**33**) proved too unstable without the protecting groups. The bisamine monomers (**21**, **24**, **27**, **30**, and **33**) were obtained by the removal of the oxygen-bridge using a strong acid.

Using the TB polymerisation method reported by McKeown *et al*.,[4] the resulting TB polymers (**P11**, **P12**, **P13**, **P14** and **P15**) were synthesised from their corresponding bisanilines and their basic properties were determined (**Table 3.5.3.3**). Both polymers **P11** and **P12**, unfortunately, cross-linked during the polymerisation reaction, probably due to a Friedel-Crafts alkylation reaction between two naphthalene moieties promoted by the electron-donating effects of the methoxy and methyl groups.

1,4-Epoxynaphthalene	Oxygen-bridged species	Bisaniline derivative	TB Polymer
16 	**17** 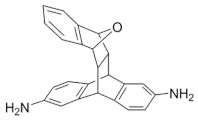	**18** 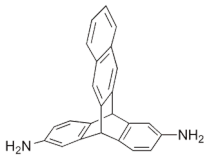	**P10** 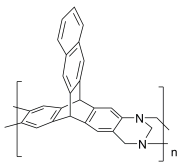
19 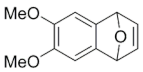	**20** 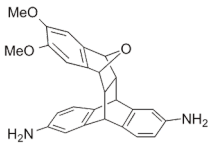	**21** 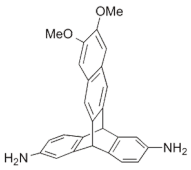	**P11** 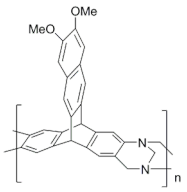
22 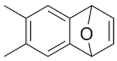	**23** 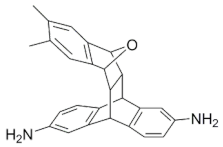	**24** 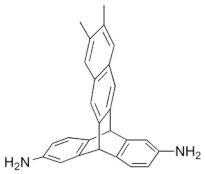	**P12** 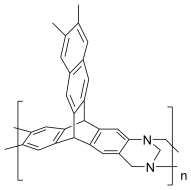
25 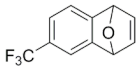	**26** 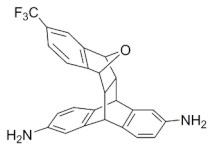	**27** 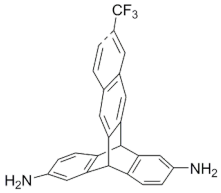	**P13** 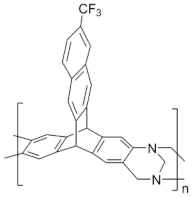
28 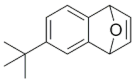	**29** 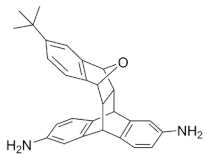	**30** 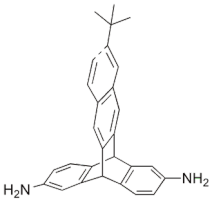	**P14** 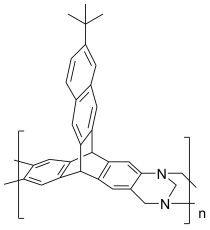
31 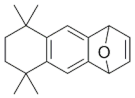	**32** 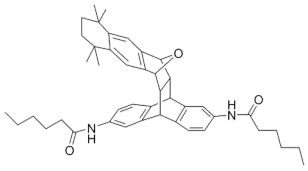	**33** 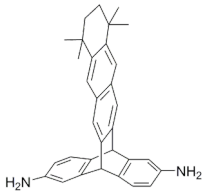	**P15** 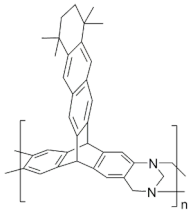

Table 3.5.3.2 Substituted 1,4-epoxynaphthalenes, the corresponding oxygen-bridged species and final substituted diaminobenzotriptycene monomers.

The synthesis of **P13** led to the formation of a TB polymer from which films could not be prepared from solution casting perhaps due to the strongly electron-withdrawing nature of the CF_3 group hindering polymerisation, despite its long distance from the aromatic amines. The successful synthesis of **P14** and **P15** led to the creation of TB polymers that were fully soluble in chloroform and both also demonstrated sufficiently high M_w for the formation of self-standing films for gas permeability studies. BET surface area analysis, at 77 K, was carried out for all of the substituted benzotriptycene TB polymers (**P11**, **P12**, **P13**, **P14** and **P15**) (**Table 3.5.3.3**) (**Figure 3.5.3.4**). From the BET analysis, it can be seen that as the substitution of the benzotriptycene structure increases, the resulting apparent BET surface area decreases. **P11**, **P12**, **P13**, **P14** and **P15** have also been analysed by TGA which reveals a series of polymers that have high thermal stabilities, all of which have T_d greater than 400°C.

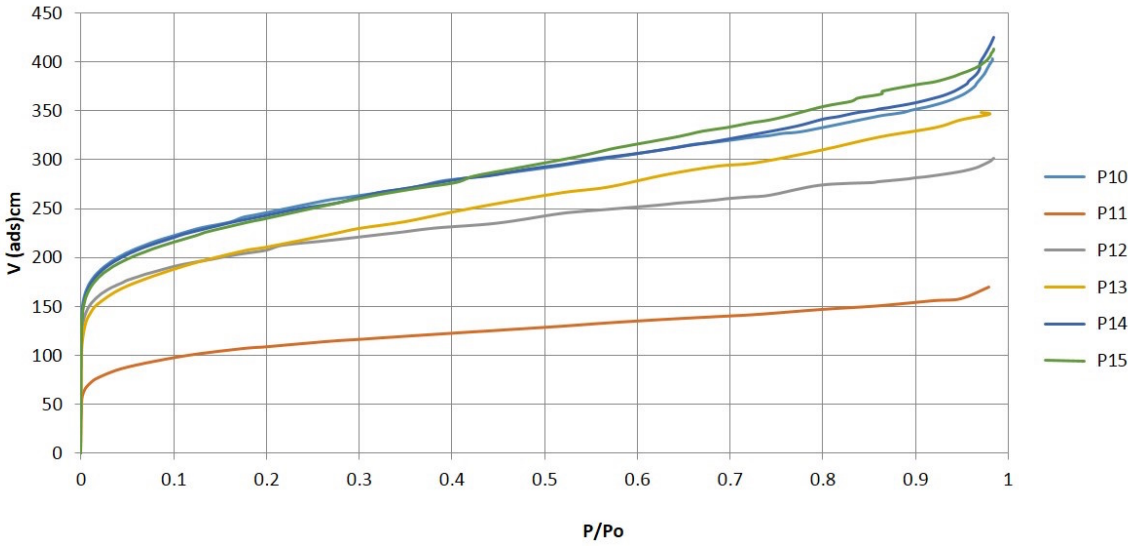

Figure 3.5.3.4 BET isotherms determined from N_2 adsorption at 77 K of **P10**[110], **P11**, **P12**, **P13**, **P14** and **P15**.

Polymer	Yield	BET		TGA	GPC		Film
	(%)	S.A ($m^2 g^{-1}$)	Pore Volume ($cm^3 g^{-1}$) (P_s/P_o = 0.9814)	T_d (°C)	M_w x 10^{-3} (g mol^{-1})	Đ	
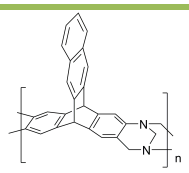 **P10**	81	868	0.6189	465	103	3.55	✓
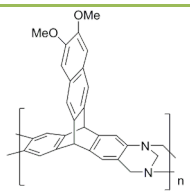 **P11**	77	384	0.2631	410	-	-	x
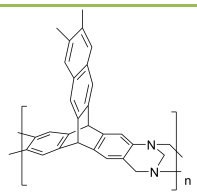 **P12**	48	729	0.4627	421	-	-	x
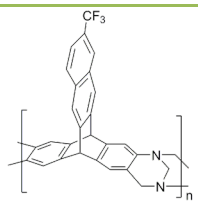 **P13**	90	742	0.5398	458	-	-	x
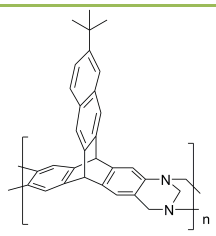 **P14**	70	856	0.6475	446	45	3.72	✓
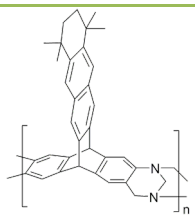 **P15**	40	847	0.6312	446	-	-	✓

Table 3.5.3.3 Characterisation of **P10**[110] and **P11**, **P12**, **P13**, **P14** and **P15**. GPC measured against polystyrene standards using chloroform as eluent.

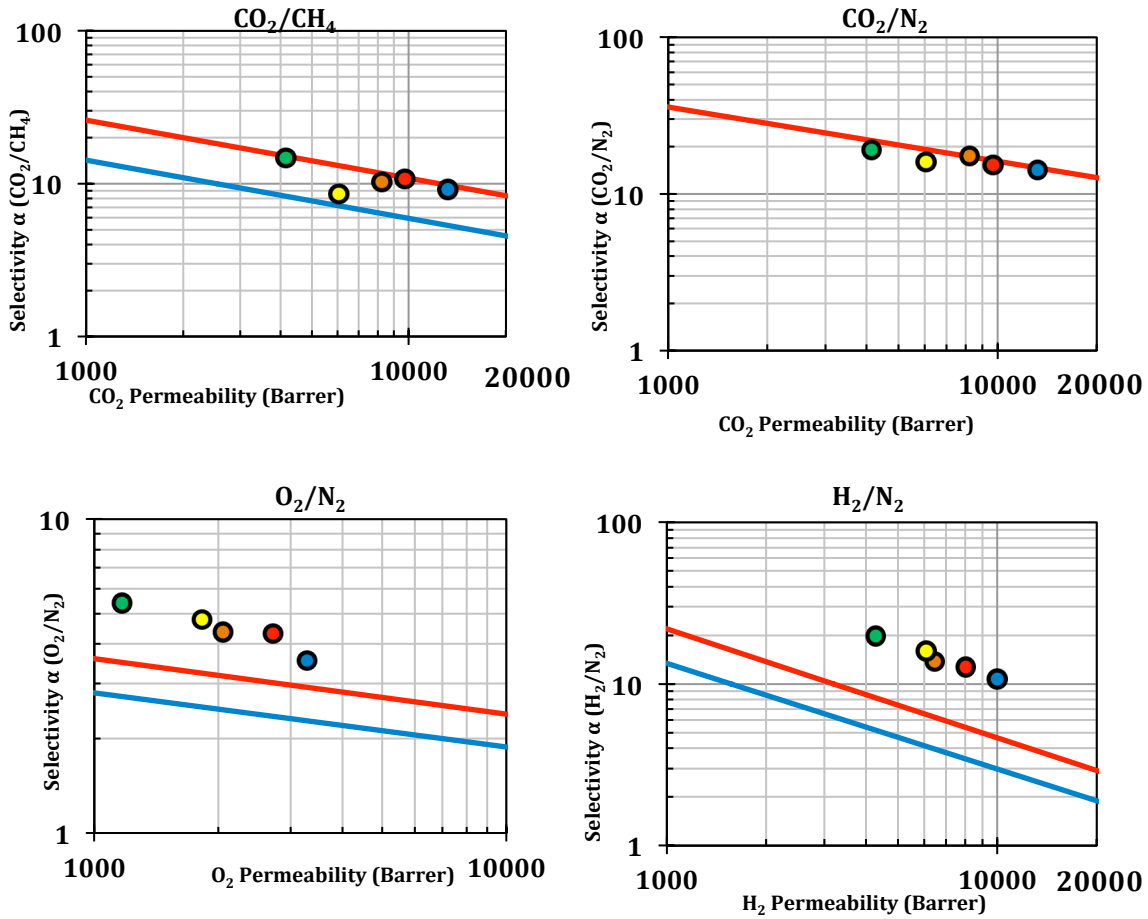

Figure 3.5.3.3 Robeson plots for CO_2/CH_4, CO_2/N_2, O_2/N_2 and H_2/N_2 gas pairs with 1991 (----) and 2008 (----) upper bounds; **P10** (●),[110] **P10** (aged 166 days) (●),[110] **P14** (●), **P15** (●) with literature data for PIM-Trip(H_2)-TB (●).[5]

Gas permeability measurements show that permeability of the substituted benzotriptycene TB polymers is generally reduced (with the exception of helium) relative to the unsubstituted polymer as anticipated from the apparent BET surface areas. Robeson plots of O_2/N_2 and H_2/N_2 (**Figure 3.5.3.3**) show that all data points for the triptycene or benzotriptycene TB polymers are of a similar distance above the 2008 upper bounds indicating that they all behave as efficient molecular sieves.

Sample	Transport Parameters	N_2	O_2	CO_2	CH_4	H_2	He	Selectivity $\alpha(x/y)$			
								H_2/N_2	CO_2/N_2	CO_2/CH_4	O_2/N_2
P14	P_x **[Barrer]**	470	2051	8227	798	6468	2277	13.8	17.5	10.3	4.4
	D_x **[10^{-12} m^2s^{-1}]**	67	309	58	26	5590	6298	83	0.9	2.2	4.6
	S_x **[cm^3cm^{-1} bar^{-1}]**	5.2	5.0	106	23.3	0.9	0.3	0.2	20	4.5	1.0
P15	P_x **[Barrer]**	379	1820	6068	710	6078	2287	16.0	16.0	8.5	4.8
	D_x **[10^{-12} m^2s^{-1}]**	51	235	69	14	6068	11832	119	1.4	5.0	4.6
	S_x **[cm^3cm^{-1} bar^{-1}]**	5.6	5.8	66	38	0.8	0.1	0.1	11.8	1.7	1.0

Table 3.5.3.4 Gas permeabilities P_x, diffusivity D_x, solubility coefficient S_x, and ideal selectivities α (P_x/P_y) for methanol treated films of **P14** and **P15**.

The synthesis of **P5** and **PIM-EA(H_2)-TB** showed that by adding methyl groups to the bridgehead positions of each monomer, polymers were generated that generally displayed decreased performance. This decrease in performance was seen for the gas pairs that have been compared (**Figure 3.3.3**), with the exception of H_2/N_2, in which the methyl substituted versions slightly out-performed their methyl-less counterparts. With this in mind, the generation of four co-polymers was conducted in an attempt to generate a combination that would out-perform the corresponding homopolymers. From the resulting analysis of these co-polymers (BET, TGA and NMR data) it was confirmed that 50:50 combinations were obtained all of which produced self-standing films. It was not surprising that the combination of **PIM-Trip(H_2)-TB** and **PIM-EA(Me)-TB** generated the best performing copolymer that out-performed both of the corresponding homopolymers, as each homopolymer from this combination demonstrated the higher BET surface areas when compared with their respective methyl and methyl-less versions. As the BET surface area results plays an integral role in the performance of these polymer materials, the need to synthesise a monomer, that could be used for the synthesis of a novel TB polymer that had a high BET surface area, was desirable. The use of the diaminobenzotriptycene molecule that had previously been synthesised by Swager et al, was thought to generate a TB polymer that had increased BET surface areas when compared to **PIM-Trip(H_2)-TB**. As a self-standing film was successfully formed for **P10** the gas permeabilities was measure for this polymer. For the Robeson plots shown (**Figure 3.5.2.4**) it can be seen that the performance of **P10** is comparable with that of **PIM-Trip(H_2)-TB**, however **P10** has

increased permeability. This increase in permeability arises from the increase in the solubility coefficients for the gas pairs studied. The unsubstituted naphthalene moiety of **P10** provided an ideal location for the modification of the benzotriptycene structure. A variety of different functional groups were used in an attempt to synthesised modified, novel benzotriptycene monomers, which were then used to generate the subsequent TB polymers. It can be seen from (**Figure 3.5.3.3**) that this modification led to the formation of novel TB polymers (**P14** and **P15**) that overall has lower gas permeabilities when compared to the unsubstituted **P10**. The lowering of permeability towards the gas pairs tested (with exception to He) was also confirmed by a decrease of the BET surface areas.

Chapter 4: Benzotriptycene derived polybenzodioxan polymers

4.1 Introduction

Since the synthesis of archetypal PIM-1 in 2004,[3] the efficient benzodioxan formation has been extensively used in the preparation of PIMs.[154,155,152,156,157] Previous work in the McKeown group attempted to use this polymerisation technique to make a triptycene-based PIM but an insoluble polymer resulted. In order to overcome this solubility problem, it was thought to attempt to prepare a series of PIMs using benzotriptycene-based biscatechols as monomers.

4.2 Synthesis of substituted Benzotriptycene biscatechols

The general synthesis of the substituted benzotriptycene biscatechols is shown (**Scheme 4.2.1**). As shown in (**Scheme 4.2.2**), the synthesis of 1,4-epoxynaphthalene allows the preparation of a variety of substituted structures. The synthesis begins with the Diels-Alder reaction between a substituted dibromobenzene, or a substituted chlorobenzene precursor, and anhydrous furan in the presence of *n*-BuLi at -78 °C. The substituted 1,4-epoxynaphthalenes (**16**, **25**, **28**, **31**, **46**, **53**) were combined via a Diels-Alder reaction with anthracene **34**, as previously described in chapter 3, using microwave heating in DMF. Also in this series of reactions, the use of microwave chemistry over conventional heating conditions provided greater yields and lower reaction times. The removal of the oxygen bridge was achieved in acidic media, and subsequent demethylation was performed using boron tribromide (BBr_3) in DCM, to yield the corresponding biscatechol monomers (**Table 4.2.3**).

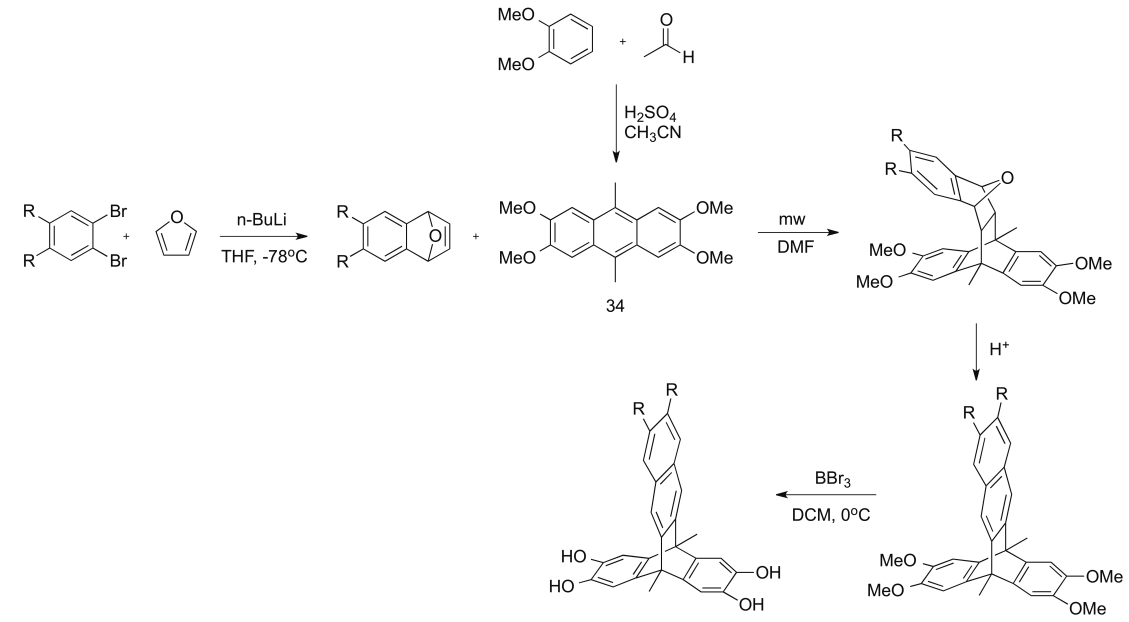

Scheme 4.2.1 General synthesis of substituted benzotriptycene biscatechol monomers.

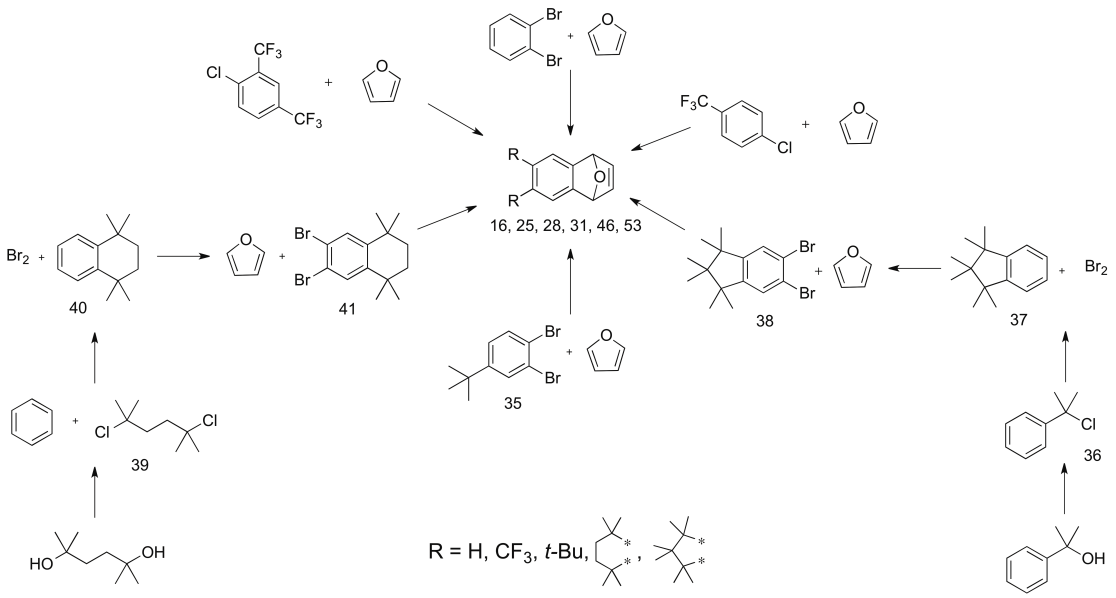

Scheme 4.2.2 General synthesis of substituted 1,4-epoxynaphthalenes **16**, **25**, **28**, **31**, **46**, **53**.

1,4-Epoxynaphthalene	Oxygen-bridged species	Biscatechol derivative	Polybenzodioxane Polymer
16 	**42** 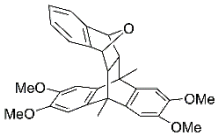	**43** 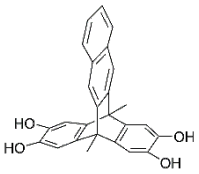	**P16** 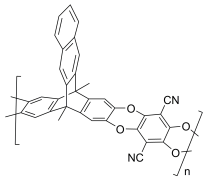
28 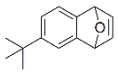	**44** 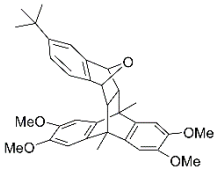	**45** 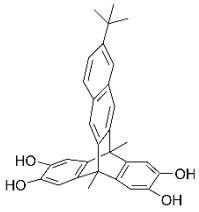	**P17** 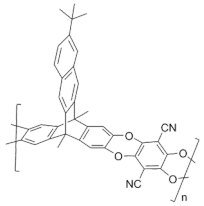
46 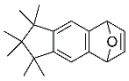	**47** 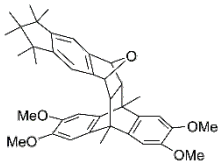	**48** 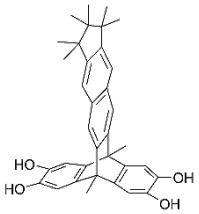	**P18** 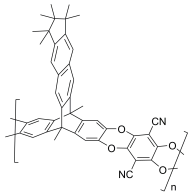
31 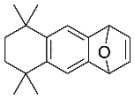	**49** 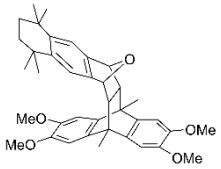	**50** 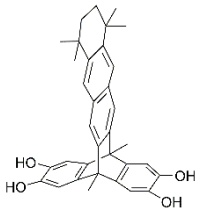	**P19** 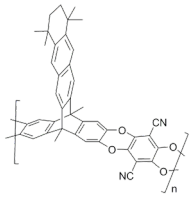
25 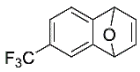	**51** 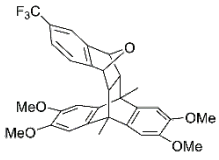	**52** 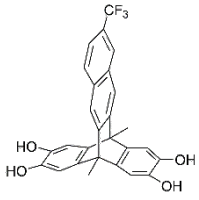	**P20** 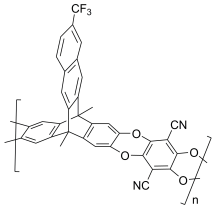
53 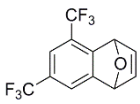	**54** 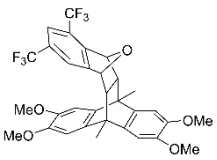	**55** 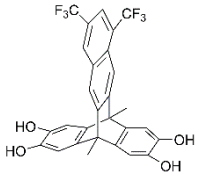	**P21** 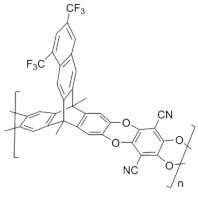

Table 4.2.3 Substituted 1,4-epoxynaphthalenes, the corresponding oxygen-bridged species and final substituted biscatechol monomers.

4.3 Synthesis of Benzotriptycene polybenzodioxan polymers

The preparation of the benzotriptycene polybenzodioxan polymers was conducted according to the procedure that was originally published by our group in 2004 for the formation of PIM-1.[3] By reacting the benzotriptycene biscatechol monomers (**Table 4.2.3**) with tetrafluoroterephthalonitrile, in DMF with an exact one-to-one stoichiometry and in the presence of K_2CO_3, we obtained a series of polybenzodioxane based polymers (**P16**, **P17**, **P18**, **P19**, **P20** and **P21**). Their corresponding physical properties are reported in (**Table 4.3.3**).

The synthesis of **P16**, **P17** and **P18** led to the formation of polymers that were only soluble in high boiling point solvents such as quinoline or N-methyl-2-pyrrolidone (NMP) and, unfortunately, the preparation of self-standing films proved unsuccessful. However, the synthesis of **P19**, **P20** and **P21** led to polymers that proved fully soluble in chloroform, quinoline and THF respectively and, in addition, demonstrated sufficiently high molecular weight for the formation of self-standing films. Apparent BET surface areas, based on nitrogen adsorption at 77 K, were measured for all of the synthesised benzotriptycene polybenzodioxane polymers (**Figure 4.3.1**) (**Table 4.3.3**).

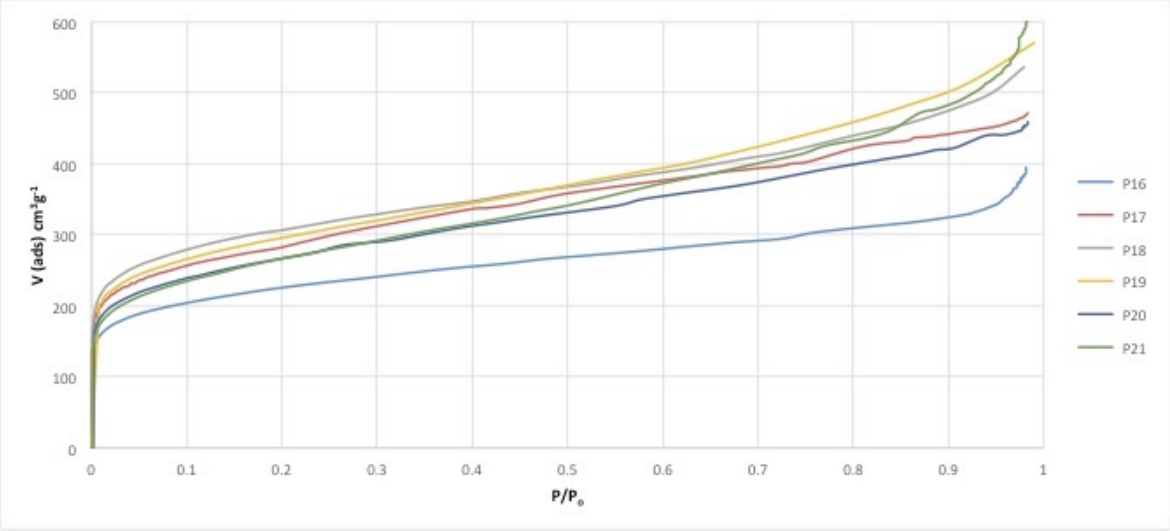

Figure 4.3.1 BET isotherms determined from N_2 adsorption at 77 K for **P16**, **P17**, **P18**, **P19**, **P20** and **P21**.

BET analysis revealed that these polymers possess high surface areas, with **P16** demonstrating the lowest and **P18** the highest. From these results a general trend can be seen, in which the substituted polymers have greater apparent BET surface areas when compared with the unsubstituted **P16**. This observed trend is the opposite to that noted in Chapter 3, in which greater substitution of the benzotriptycene-TB polymers resulted in

lower calculated apparent BET surface areas. This is probably due to the different, two-dimensional, conformation of the polymeric chain of the benzodioxan based PIMs, compared to that of the TB ones. The TGA analysis was also conducted and indicates the high thermal stability that is associated with each of these polybenzodioxane polymers.

Facilitated by the successful preparation of self-standing films for **P19**, **P20** and **P21**, gas permeability studies of these polymers were carried out (**Table 4.3.7**) and the analysis of the performance of these polymers for the gas pairs CO_2/CH_4, CO_2/N_2, O_2/N_2 and H_2/N_2 was achieved by placing the data on appropriate Robeson plots (**Figure 4.3.2**).

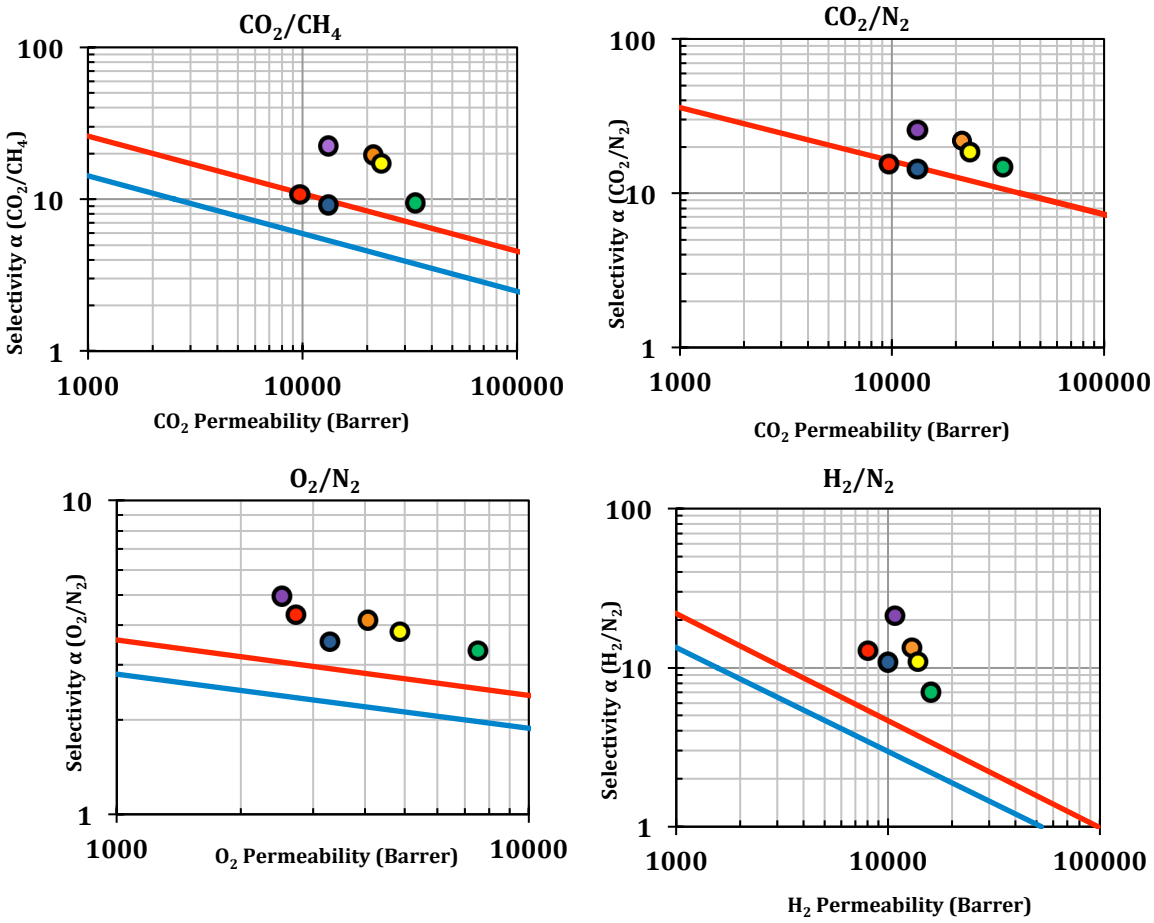

Figure 4.3.2 Robeson plots for CO_2/CH_4, CO_2/N_2, O_2/N_2 and H_2/N_2 gas pairs with 1991 (----) and 2008 (----) upper bounds; **P19** (●), **P20** (●) **P20** (aged 97 days) (●), **P21** (●), **P10** (●)[110] with literature data for PIM-Trip(H_2)-TB (●).[5]

Polymer	Yield	BET		TGA	GPC		Film
	(%)	S.A ($m^2 g^{-1}$)	Pore Volume ($cm^3 g^{-1}$) (P_s/P_o = 0.9814)	T_d (°C)	M_w x 10^{-3} (g mol^{-1})	Đ	
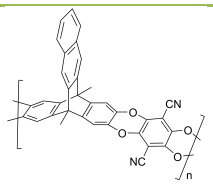 **P16**	78	791	0.6050	436	-	-	*x*
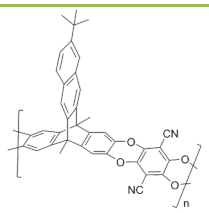 **P17**	75	1009	0.7264	437	-	-	*x*
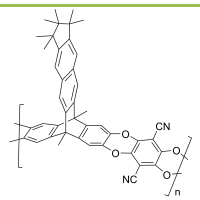 **P18**	58	1105	0.8325	435	-	-	*x*
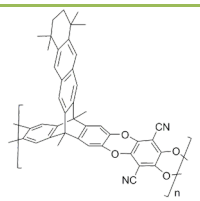 **P19**	67	1034	0.8739	474	140	2.39	✓
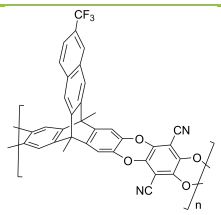 **P20**	79	944	0.7048	442	-	-	✓
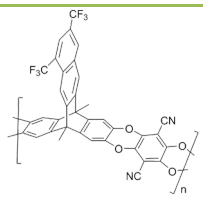 **P21**	84	1074	1.021	488	-	-	✓

Table 4.3.3 Characterisation of PIM-benzotriptycene polybenzodioxane polymers: **P16**, **P17**, **P18**, **P19**, **P20** and **P21**. GPC measured against polystyrene standards using chloroform as eluent.

Each of the polymers **P19**, **P20** and **P21** demonstrate performances that lie significantly over the 2008 upper bounds with all demonstrating "reverse-selective" properties (i.e. the permeability of CO_2 is significantly higher than H_2, despite its larger kinetic diameter). The permeability that is associated with **P19** arises from the diffusivity coefficients for each gas probe being greater than the correspondent diffusivity coefficients of **P20** and **P21**. Upon further analysis of **P19**, computational modelling shows that the structure of this rigid polymer is two-dimensional (**Figure 4.3.4**), in contrast with that of **P10** (**Figure 3.5.2.2** - Chapter 3) for which the structure is contorted in three-dimensions. From this model, it is anticipated that the individual polymer chains can align, thus generating a more interconnected pore structure and thus giving rise to an ultra-permeable polymer.

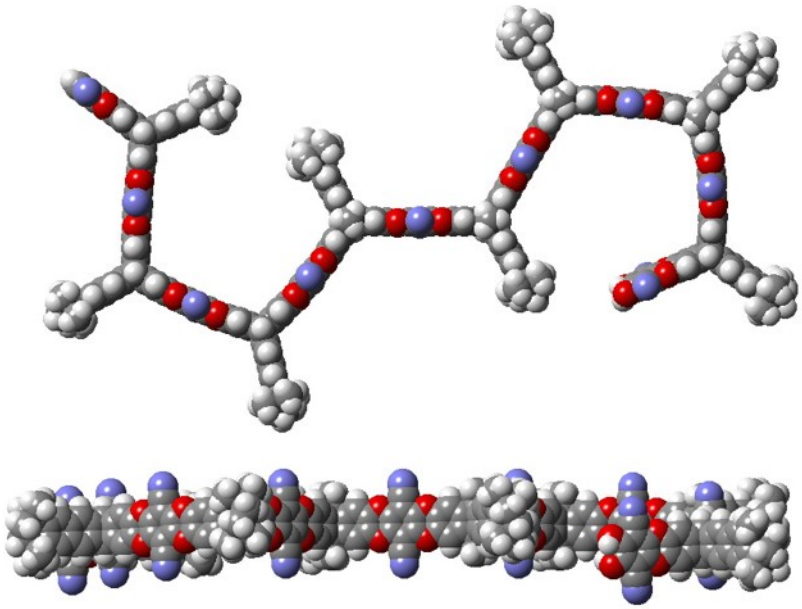

Figure 4.3.4 Molecular model of a fragment of **P19** (made with Spartan 10 vVersion 1.1.0; Wave function Inc., Irvine, CA, USA).

In an attempt to prove this theory, wide-angle X-ray scattering (WAXS) experiments have been conducted on self-standing films of **P19** and PIM-1 for comparative purposes. The data collected confirmed the amorphous nature of both polymers but it also showed two different preferential intersegmental distances (**Figure 4.3.5**), which indicates that there is a certain degree of local order in the polymeric chains. By using Bragg's equation, the average *d*-spacing can be extrapolated:

$$n\lambda = 2d\ sin\ \theta$$

n = integer number related to Bragg order

d = d-spacing

λ = scattering angle

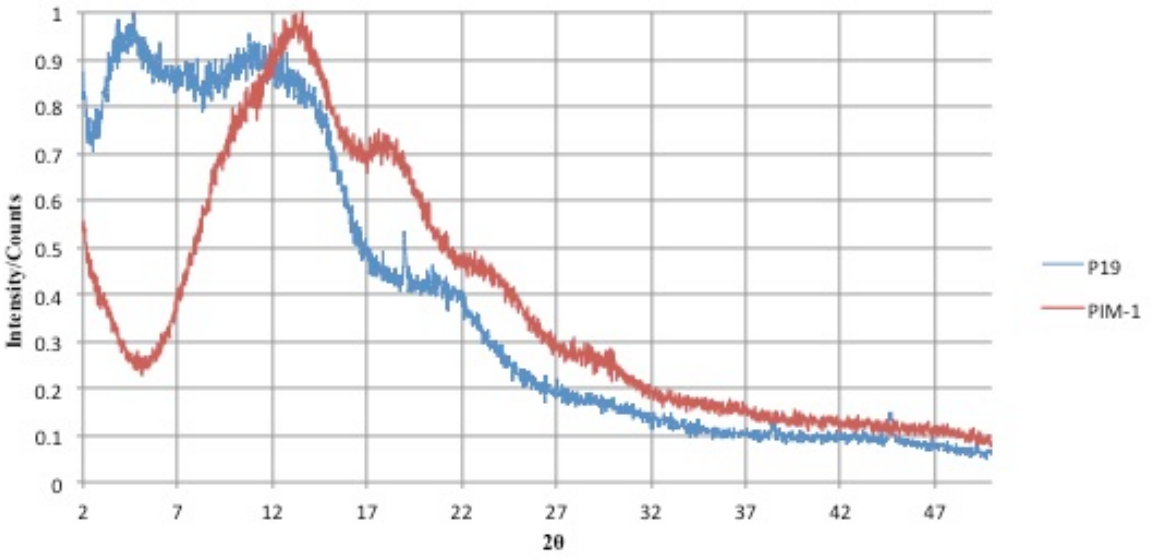

Figure 4.3.5 WAXS data for **P19** and PIM-1.

It can be calculated that **P19** shows higher inter-segmental distances (19.4 Å and 8.0Å) than that of PIM-1 (6.5 Å and 4.9 Å) (**Table 4.3.6**). The distances obtained for **P19** can be ascribed to the diameter of the in-plane pore and the inter-chain packing distance. As the in-plane pore and inter-chain packing distances of **P19** are much larger than that of PIM-1, this in-turn results in larger fractional free volume (FFV) and as a result indicates the origin of the ultra-high permeability that is associated with **P19**.

Membrane	Larger *d*-spacing (Å)	Smaller *d*-spacing (Å)
P19	19.4	8.0
PIM-1	6.5	4.9

Table 4.3.6 *d*-spacing values obtained for **P19** and PIM-1.

The large inter-chain separation seems to arise due to the large bulky tetramethyl-cyclohexane ring, which pushes the polymer chains apart. **P20** demonstrates much lower gas permeabilities as compared to **P19** but the latter demonstrates much higher

selectivities. As a result it outperforms **P19** relative to the Robeson 2008 upper bounds (**Figure 4.3.2**). The performance of **P20** has been studied on aging for 97 days, which has revealed a major loss in permeability over this time, as expected from this class of polymer.[158,159] However, due to the corresponding increase in selectivity due to ageing, the overall performance of aged **P20** has shown a comparable performance with the freshly methanol treated **P20** for the gas pairs CO_2/CH_4, CO_2/N_2 and O_2/N_2 but has also demonstrated an increase in performance for the separation of H_2/N_2. This improvement is generated from the significant increase in diffusivity selectivity, which has doubled upon the aging of this polymer membrane, with only the slight decrease in solubility selectivity. With the synthesis of **P21** it can be seen from the Robeson plots (**Figure 4.3.2**) that for each gas pair, it demonstrates higher gas permeabilities when compared with **P20**. This increase in permeability is due to the presence of the extra CF_3 group, which results in an increase of the solubility coefficients for each probe gas (**Table 4.3.7**). This increase clearly outweighs the lower diffusivity coefficients and thus generates a more permeable polymer. However, as seen from (**Figure 4.3.2**) the overall performance of **P21**, relative to the upper bound position, is slightly lower than that of **P20.**

Sample	Transport Parameters	N_2	O_2	CO_2	CH_4	H_2	He	Selectivity $\alpha(x/y)$			
								H_2/N_2	CO_2/N_2	CO_2/CH_4	O_2/N_2
P19	P_x **[Barrer]**	2267	7518	33466	3533	15909	6344	7.0	14.8	9.5	3.3
	D_x **[10^{-12} m^2 s^{-1}]**	511	1088	411	253	13722	13438	27	0.8	1.6	2.1
	S_x **[cm^3 cm^{-1} bar^{-1}]**	3.3	5.2	61	10.5	0.9	0.4	0.3	18	5.8	1.6
P20	P_x **[Barrer]**	973	4059	21377	1087	13000	5457	13.4	22.0	19.7	4.2
	D_x **[10^{-12} m^2 s^{-1}]**	183	597	221	53	8506	7541	46	1.2	4.2	3.3
	S_x **[cm^3 cm^{-1} bar^{-1}]**	4.0	5.1	76.0	15.5	1.2	0.5	0.3	19	4.9	1.3
P20 (aged 97 days)	P_x **[Barrer]**	508	2510	13129	585	10770	5164	21.2	25.8	22.4	4.9
	D_x **[10^{-12} m^2 s^{-1}]**	93	374	142	30	8916	6135	96	1.5	4.7	4.0
	S_x **[cm^3 cm^{-1} bar^{-1}]**	4.1	5.0	69.5	14.8	0.9	0.6	0.2	17	4.7	1.2
P21	P_x **[Barrer]**	1283	4848	23335	1357	13887	6389	10.8	18.2	17.2	3.8
	D_x **[10^{-12} m^2 s^{-1}]**	157	508	192	44	4732	4149	30	1.2	4.4	3.2
	S_x **[cm^3 cm^{-1} bar^{-1}]**	6.1	7.2	91	23	2.2	1.2	0.4	14.9	4.0	1.2

Table 4.3.7 Gas permeabilities P_x, diffusivity D_x, solubility coefficient S_x and ideal selectivities α (P_x/P_y) for methanol treated films of **P19**, **P20**, **P20** (aged 97 days) and **P21**.

From a previous study within our group, the synthesis of a triptycene polybenzodioxane polymer yielded one that was insoluble in common organic solvents. Due to this, it was thought that by generating a benzotriptycene biscatechol monomer so the resulting polybenzodioxane polymer could be synthesised, may have led to a polymer that was soluble in common organic solvents. With the inability to form a self-standing film for **P16**, as for the previous chapter (3), the naphthalene moiety provides an excellent location for the modification of the benzotriptycene unit. The modification of this structure led to the formation of a variety of different novel polymers that were soluble in a common organic solvents, in which the BET surface areas were overall higher than that of **P16** and also led to high performing polymers when their subsequent gas permeabilities were measured and compared (**Figure 4.3.2**). With the significant increase in permeability for **P19**, WAXS measurements were undertaken to determine a reason for this large increase in

permeability. When compared to PIM-1, the amorphous nature of both polymers was confirmed, but **P19** contains two different preferential intersegmental distances (**Figure 4.3.5**) which indicates that there is a certain degree of local order in the polymeric chains.

Chapter 5: Future Work and Conclusions

5.1 Polyimides

Further attempts to synthesise a robust self-standing film of **P1** are required due to the polymer displaying the highest calculated BET surface area of the PIM-PIs studied in this research programme. It has also been demonstrated in the literature that the use of 2,3,5,6-tetramethyl-*p*-phenylenediamine with a particular bisanhydride monomer generates a polymer with excellent perm-selectivities.[88] The continued efforts in preparing triptycene-bisanhydride monomer need to be improved in order to generate the required monomer more efficiently. A proposed improvement for this synthetic route is based on the efficient production of **5**.[160] By generating it using the proposed one-step synthesis (**Figure 5.1.1**) would greatly improve the efficiency of this synthetic procedure, cutting the overall synthesis of **8** from eight steps down to four steps.

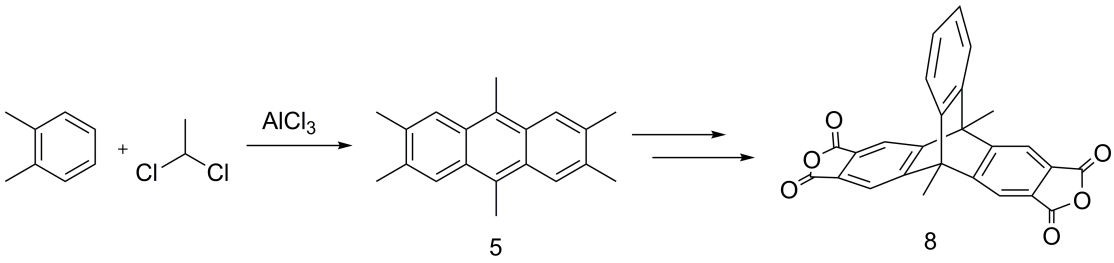

Figure 5.1.1 Proposed synthesis of **5**.

5.2 Tröger's Base (TB) polymers

Further work for the synthesis of Tröger's Base (TB) can be based around the substitution of the 2,6-diaminobenzotriptycene monomer. As already mentioned, substitution at the bridgehead position of the benzotriptycene structure can potentially generate a series of different TB polymers with enhanced properties, as has already been demonstrated in the literature.[88,153,156] Also the addition of functionalisation around the naphthalene unit of the benzotriptycene structure can also generate a series of TB polymers with different properties. Of interest for enhancing permeability would be to add methyl groups to the (a) and (b) positions of the benzotriptycene molecule (**Figure 5.2.1**).

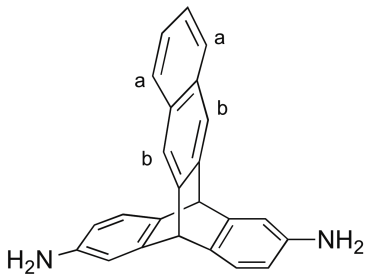

Figure 5.2.1. Substituion of 2,6-diaminobenzotriptycene

Another possible future endeavour would be the synthesis of 2,6-diaminotriptycene with the addition of a tetramethyl-cyclohexane ring to one of the benzene rings (**Scheme 5.2.2**). This can be achieved through the Diels-Alder reaction between the cyclo-6-anthranilic acid (a**)** with 2,6-diaminoanthracene (b) (**Scheme 5.2.2**).

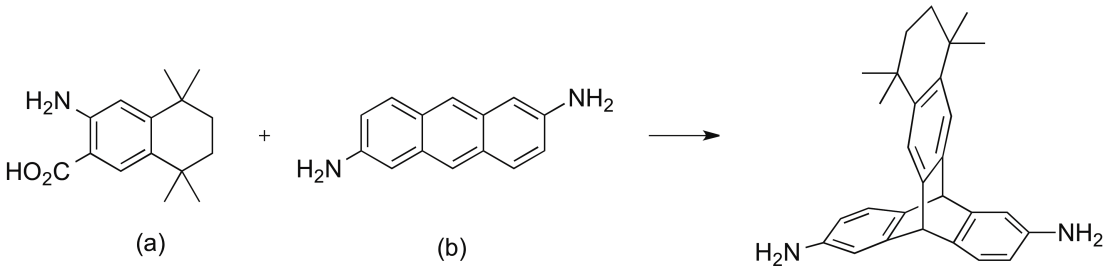

Scheme 5.2.2. Proposed synthetic scheme.

5.3 Polybenzodioxan polymers

Future work based around the formation of substituted benzotriptycene polybenzodioxan polymers is also desirable. The continued efforts to achieve a polymer capable of forming robust self-standing films for **P17** and **P18** are of importance due to the high BET surface areas that were obtained for these polymers. Additional urgency arises because it has been demonstrated previously[69] that the use of a tetramethyl-indane group (**Figure 5.3.1**) attached to a polyacetylene backbone generated a polymer with the highest gas permeabilities recorded so far. As described above for TB polymers, the substitution at the bridgehead or naphthalene positions of the benzotriptycene structure could again lead to a series of different polybenzodioxan polymers with enhanced permeability.

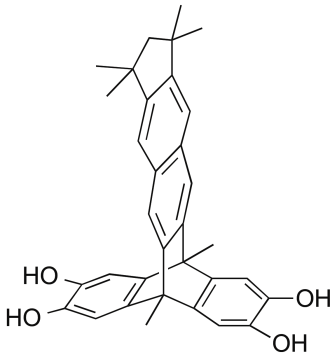

Figure 5.3.1. Tetramethylindan-benzotriptycene biscatechol monomer.

Chapter 6: Conclusions

During this project, three different classes of polymers have been investigated and assessed for their gas separation properties. In each case the main structural feature of these polymers is their rigidity and contortion that enables the formation of polymers that cannot pack space efficiently and thus generates a large quantity of free volume, which as a consequence, leads to high BET surface areas.

A series of polyimides were successfully synthesised demonstrating a wide range of properties, such as high thermal stabilities and high BET surface areas (352-703 $m^2 g^{-1}$). Having prepared robust self-standing films of two examples, **P3** and **P4**, gas permeability studies were performed which reveal gas perm-selectivies that lie over the Robeson 1991 upper bound for the gas pairs CO_2/CH_4, O_2/N_2 and H_2/N_2. It has been shown that the performance of **P3** lies on the Robeson 2008 upper bound for the gas pair H_2/N_2.

The use of a relatively new polymerisation technique for the formation of Tröger's base polymers provided materials which demonstrate high thermal stability and several examples that were fully processable in common low boiling point chloroform. Importantly the preparation of TB polymer **P5** provided evidence regarding the effects that methyl groups have when placed on the bridgehead positions of triptycene or ethanoanthracene units. It was found that methyl groups at these positions generated polymers that possess higher BET surface areas when compared to their H_2 counterparts, but significantly lowered the overall gas separation performance. By forming co-polymers using the ethanoanthracene and triptycene units, with or without methyl groups at the bridgehead, led to TB polymers that possess similar properties to those of the respective homo-polymers. The performance of the co-polymers (**P6**, **P7**, **P8** and **P9**) lie greatly over the Robeson 2008 upper bound for the gas pairs CO_2/CH_4, O_2/N_2 and H_2/N_2, and, unusually for TB polymers, **P7** also lies above the 2008 upper bound for the CO_2/N_2 gas pair. The synthesis of a series of benzotriptycene TB polymers, for which the majority were processable in common organic solvents, provided polymers with high thermal stabilities and apparent BET surface areas ranging from 384-868 $m^2 g^{-1}$. The parent benzotriptycene TB polymer is highly permeable but substitution of the benzotriptycene unit generally reduces permeability.

The third and final class of polymerisation reaction that was used during this project was the formation of polybenzodioxan polymers using monomers based on benzotriptycene. The benzotriptycene polybenzodioxan polymers (**P16** – **P21**), all

demonstrated high BET surface areas (791-1105 $m^2 g^{-1}$) and high thermal stabilities. Three of the six polybenzodioxane polymers prepared resulted in fully soluble polymers, which facilitated the preparation of robust self-standing films. The gas permeability studies revealed that **P19**, **P20** and **P21** possess excellent perm-selectivities that place them well over the Robeson 2008 upper bound for the gas pairs CO_2/CH_4, CO_2/N_2, O_2/N_2 and H_2/N_2. Indeed, **P19** has demonstrated the highest gas permeability of any PIM with values that are comparable to those of certain polyacetylenes, which are the most gas permeable polymers reported to date. The CF_3 substituted polymer **P20** demonstrates both high permeability and high selectivity, the latter being greatly enhanced after aging for 97 days.

This project confirms recent reports on the ability of the triptycene component to enhance the performance of PIMs due to its rigidity. The most important finding of this research programme is that the two-dimensional shape imposed on polybenzodioxan-based PIMs by the triptycene unit, extended by the use of benzo-substitution, enhances gas permeability by increasing the interconnectivity of the intrinsic microporosity as the polymer packs in the solid state. This is a novel design concept for producing ultrapermeable polymers. By further addition of substituents onto such polymers, PIMs with even higher permeability are likely to be achieved.

Chapter 7: Experimental

7.1 Techniques

Where possible reagents were purchased from commercial sources and used without further purification unless stated otherwise. Air/moisture sensitive reactions were carried out under a nitrogen atmosphere using glassware dried in an oven prior to use. TLC analysis refers to analytical thin layer chromatography, using aluminium-backed plates coated with Merck TLC silica gel 60 F_{254}. Column chromatography was performed over a silica gel (pore size 60 Å, particle size 40-63 μm) stationary phase. Anhydrous solvents were obtained following passage through a column of activated molecular sieves (hexane) or through activated alumina (diethyl ether, THF, toluene).

Infrared Spectroscopy (IR)

Infrared adsorption spectra were recorded in the range 4000-400 cm^{-1} using a Shimadzu IR Affinity-1S FTIR spectrophotometer as a powder.

Melting Point (Mp)

Melting points were recorded using a Stuart SMP10 melting point apparatus and are uncorrected; (dec.) refers to a decomposition temperature.

Wide Angle X-Ray Scattering (WAXS)

Intermolecular distances of the membranes was proved by WAXS. Performed in reflection mode at room temperature by using a Bruker D8 Advance system fitted with a Goebel mirror and provided with a PSD Vantec detector. Cu K radiation source of wavelength 1.54 Å was used, operating in a 2θ range of 2-55° with a scan rate of 0.5 s per step. The WAXS analysis was conducted and analysed by a member of our group, Bibiana Comesaña.

Nuclear Magnetic Resonance (NMR)

^{1}H and ^{13}C NMR spectra were recorded in a suitable deuterated solvent using an Avance Bruker DPX 400 instrument (400 MHz) or an Avance Bruker DPX 500 instrument (500 MHz) (Cardiff University) or a Bruker AVA 400, AVA 500, PRO 500 or AVA 600

intrument (Edinburgh University). Solid state ^{13}C NMR spectra were recorded by the EPSRC funded solid state NMR service at Durham University.

Mass spectrometry

Small molecule (M_w < 1000 $gmol^{-1}$) low-resolution mass spectrometry (LRMS) and high resolution mass spectrometry (HRMS) was performed by using Waters GCT Premier E1 instrument (Cardiff University) or a Fisonsn VG Platform II quadrupole instrument plus Thermo finnigan MAT 900 XP, Electron Ionisation Sector MS (Edinburgh University) utilising electron impact (EI).

Gel permeation chromatography (GPC)

Gel permeation chromatography (GPC) was carried out on chloroform solutions (1mg ml^{-1}) using a GPC MAX variable loop equipped with two KF-805L SHODEX columns and a RI(VE3580) detector, operating at a flow rate of 1 ml min^{-1}. Calibration was achieved using Viscotek polystyrene standards (M_w 1,000-1,000,000 $gmol^{-1}$).

Thermo-Gravimetric Analysis (TGA)

Thermo-gravimetric analysis (TGA) was conducted using a Thermal Analysis SDT Q600 system with a sample heating rate of 10°C min^{-1} up to 1000°C.

Brunauer-Emmett-Teller (BET) theory

Low-temperature (77 K) nitrogen adsorption/desorption isotherms were obtained using a Coulter SA3100 surface area analyser or a Quantachrome Quadrasorb*evo* automated surface area analyser. Accurately weighed powdered samples of roughly 100 mg were degassed for 16 h at 125°C under high vacuum prior to analysis.

7.2 Experimental procedures

General procedure 1 (G.P.1)

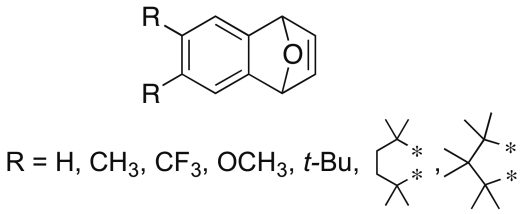

The 1,4-expoxynaphthalene compounds were prepared according to the general procedure reported by Luo et al.[161] 1,2-Dibromo species and anhydrous furan was dissolved in anhydrous THF and cooled to -78 ºC. To this, a solution of n-BuLi in anhydrous THF was added drop wise and left to stir at -78 ºC for 1.5 h. The resulting solution was allowed to warm to room temperature and water added. The organic layer was extracted with DCM (3 x 100.0 mL) and dried over $MgSO_4$. The solvent was removed under vacuum and precipitated solid from oil/washed solid with hexane, filtered off and dried to yield corresponding 1,4-epoxynaphthalene.

General procedure 2 (G.P.2)

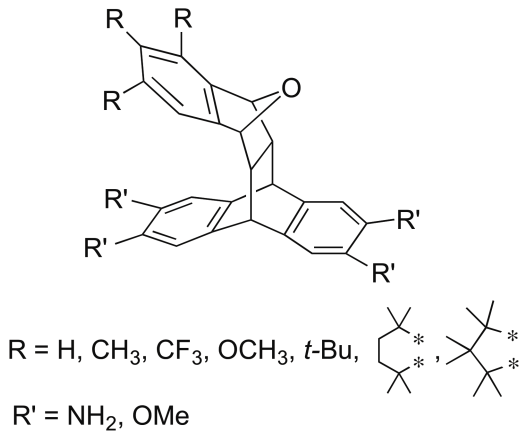

The oxygen-bridged benzotriptycenes were synthesised according to a modified procedure reported by Swager et al.[150] 2,6-diaminoanthracene or 9,10-dimethyl-tetramethoxy

anthracene and the required 1,4-epoxynaphthalene was dissolved in DMF and heated in microwave reactor at 250 ºC for 2.5 h. Solvent was removed under vacuum and the residue was purified by column chromatography to yield desired product.

General procedure 3 (G.P.3)

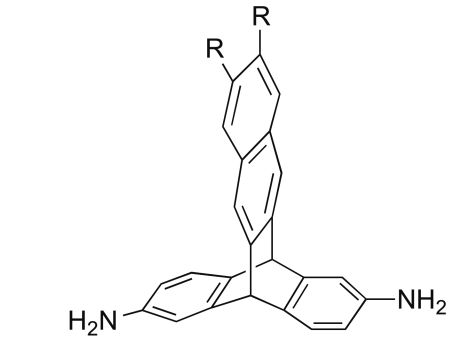

R = H, CH_3, CF_3, OCH_3, *t*-Bu,

Synthesis was conducted according to the general procedure reported by Swager et al.[150] The desired expoxynaphthalene, ethanol and perchloric acid (70 %) were combined and heated to reflux for 24 h. The resulting mixture was cooled and poured into ice/ water and neutralised with aqueous 2M NaOH solution. Extracted with $CHCl_3$ (3 x 100 mL), dried over $MgSO_4$ and removed solvent under vacuum. Crude product was purified by column chromatography $CHCl_3$/ ethyl acetate (7:3, v/v), washed with cold DCM and dried to yield the desired product.

General procedure 4 (G.P.4)

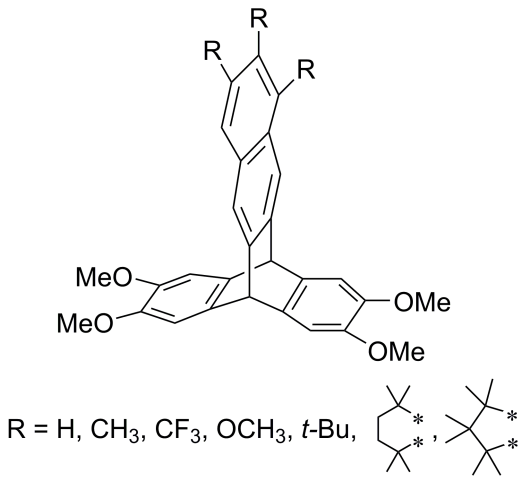

Required oxygen-bridged tetramethoxy benzotriptycene was dissolved in TFA or $MeSO_4H$ and left at room temperature for 24 h. The reaction mixture was poured into water, neutralised with ammonium hydroxide solution, extracted with DCM and dried over $MgSO_4$. Solvent removed under vacuum and crude product was purified by column chromatography to yield desired product.

General procedure 5 (G.P.5)

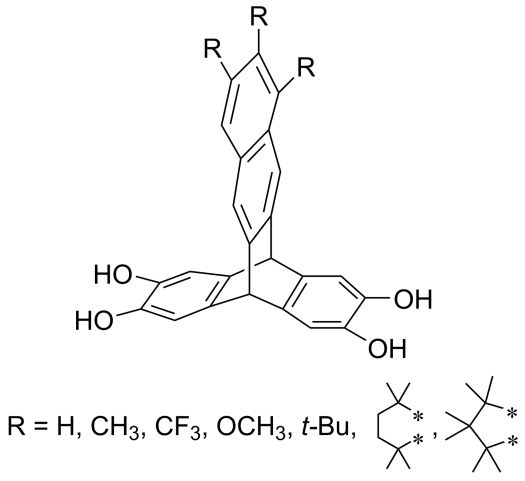

Biscatechol monomers were prepared according to the general procedure reported by McKeown et al.[156] Tetramethoxy-benzotriptycene species were dissolved in anhydrous DCM and cooled to 0 ºC. BBr_3 was added drop wise and left at 0 ºC for 30 mins, then

allowed to warm to room temperature for 2.5 h. Poured resulting reaction mixture into ice/water and allowed DCM to evaporate. Filtered off precipitate, washed with water and dried under N_2 to yield desired biscatechol monomer.

1,2-Dibromo-4,5-dimethylbenzene (1)

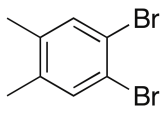

The compound 1,2-dibromo-4,5-dimethylbenzene (**1**) was synthesised according to the procedure reported by He.[162] Iodine (0.4 g, 1.60 mmol) was added to *o*-xylene (95 mL, 788 mmol) and cooled to 0°C. To this cooled solution, bromine (80 mL, 1575 mmol) was added dropwise. The resulting solution was gradually allowed to reach room temperature over 24 h. The orange solid was dissolved in diethyl ether (500 mL) and the organic layer washed with 2M NaOH (6 x 100 mL) and water (6 x 100 mL) then dried over $MgSO_4$, the solvent removed and solid washed with MeOH to afford 1,2-dibromo-4,5-dimethyl-benzene (**1**) (76.52 g, 290 mmol, 37 %) as white crystals. Mp 86-88°C (Lit[163] 88°C); IR (film)/cm^{-1}: 2974, 2947, 2912, 2361, 2340, 1738, 1470, 1437, 1402, 1373, 1341, 1258, 1115, 1009, 933, 889, 872, 799; ^{1}H NMR (400 MHz, $CDCl_3$) δ 7.15 (s, 2H, Ar *H*) 2.07 (s, 6H, C*H*$_3$); ^{13}C NMR (101 MHz, $CDCl_3$) δ 137.2, 134.2, 121.1, 19.0; LRMS (EI, m/z): Calculated 263.90, found 263.90 [M^+].

1,4-Dihydro-1,4,6,7-tetramethyl-1,4-epoxynaphthalene (2)

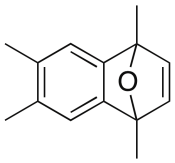

The compound 1,4-dihydro-1,4,6,7-tetramethyl-1,4-epoxynaphthalene (**2**) was synthesised according to the procedure reported by Meier and Rose.[164] 1,2-dibromo-4,5-dimethylbenzene (**1**) (14.75 g, 56.0 mmol) and 2,5-dimethylfuran (49 g, 510 mmol) was

dissolved in anhydrous toluene (200 mL) and cooled to -78°C. A solution of 2.5 M *n*-butyllithium (29.12 mL, 73.0 mmol) in anhydrous toluene (50 mL) was added drop wise. The resulting solution was allowed to gradually warm to room temperature over 24 h. The organic layer was washed with water (3 x 300 mL) and dried over $MgSO_4$, solvent removed under vacuum and product purified by column chromatography DCM/ Hexane (3:7, v/v) to yield 1,4-dihydro-1,4,6,7-tetramethyl-1,4-epoxynaphthalene (**2**) (5.36 g, 26.8 mmol, 36 %) as a yellow/orange oil. ν_{max} (cm^{-1}): 3076, 3009, 2970, 2928, 2866, 2361, 2342, 1450, 1381, 1344, 1304, 1233, 1142, 1032, 878, 858, 847, 700, 650; ^{1}H NMR (400 MHz, $CDCl_3$): δ_H (ppm) = 6.93 (s, 2H, Ar *H*), 6.76 (s, 2H, C*H*), 2.21 (s, 6H, CH_3), 1.87 (s, 6H, CH_3); ^{13}C NMR (126 MHz, $CDCl_3$) δ_C (ppm) = 150.5, 146.9, 134.2, 132.2, 120.4, 88.5, 19.7, 19.0, 15.3; LRMS (APCI, m/z): Calculated: 200.3 found: 201.1 [M^+ + H].

1,4,4a,9,9a,10-Hexahydro-2,3,6,7,9,10-hexamethyl-9,10-epoxyanthracene (3)

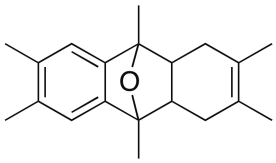

The compound 1,4,4a,9,9a,10-hexahydro-2,3,6,7,9,10-hexamethyl-9,10-epoxyanthracene (**3**) was synthesised according to a modified procedure reported by Wolthius.[135] 1,4-dihydro-1,4,6,7-tetramethyl-1,4-epoxynaphthalene (**2**) (2.85 g, 14.0 mmol), 2,3-dimethyl-1,3-butadiene (1.29 g, 15.4 mmol) and a small amount of hydroquinone crystals were dissolved in *o*-xylene (6.0 mL) and heated in microwave reactor at 150°C for 2.5 h. The solvent was removed under vacuum and the crude product was purified by recrystallisation from methanol to yield 1,4,4a,9,9a,10-hexahydro-2,3,6,7,9,10-hexamethyl-9,10-epoxyanthracene (**3**) (1.62 g, 5.73 mmol, 37 %) as a white solid. Mp: 139-141 ºC (Lit[135] 141.5-142°C); ν_{max} (cm^{-1}): 3728, 3701, 3630, 3599, 3017, 2986, 2932, 2889, 2832, 2361, 2342, 1445, 1381, 1234, 827, 658; ^{1}H NMR (400 MHz, $CDCl_3$): δ_H (ppm) = 6.87 (s, 2H, Ar *H*), 2.24 (s, 6H, CH_3), 2.01 (m, 4H, CH_2), 1.79 (m, 2H, C*H*), 1.68 (s, 6H, CH_3), 1.65 (s, 6H, CH_3); ^{13}C NMR (101 MHz, $CDCl_3$) δ_C (ppm) = 147.9, 134.1, 127.3, 118.9, 86.3, 47.1, 31.7, 19.9, 18.8, 14.2; LRMS (EI, m/z): Calculated: 282.20 found: 282.2 [M^+].

1,4-Dihydro-2,3,6,7,9,10-hexamethylanthracene (4)

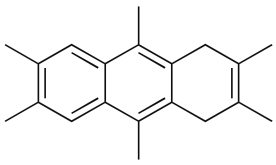

The compound 1,4-dihydro-2,3,6,7,9,10-hexamethylanthracene (**4**) was synthesised according to the procedure reported by Wolthuis.[135] 1,4,4a,9,9a,10-hexahydro-2,3,6,7,9,10-hexamethyl-9,10-epoxyanthracene (**3**) (3.10 g, 11.0 mmol) was dissolved in methanol (80 mL) and heated to reflux. *Conc.* HCL (9.07 mL, 110.0 mmol) was added drop wise and left at reflux for 3 h. After this time, the reaction mixture was cooled to -15°C for 24 h. 1,4-dihydro-2,3,6,7,9,10-hexamethylanthracene (**x4**) (2.80 g, 10.59 mmol, 96 %) was collected by filtration as a white powder. Mp: 208-210 ºC (Lit[135] 211-212°C); ν_{max} (cm^{-1}): 2913, 2853, 1499, 1445, 1425, 1022, 997, 858; ^{1}H NMR (400 MHz, $CDCl_3$): δ_H (ppm) = 7.78 (s, 2H, Ar *H*), 3.42 (s, 4H, CH_2), 2.55 (s, 6H, CH_3), 2.44 (s, 6H, CH_3), 1.83 (s, 6H, CH_3); ^{13}C NMR (101 MHz, $CDCl_3$) δ_C (ppm) = 133.7, 130.2, 130.1, 126.9, 123.9, 122.9, 36.1, 20.4, 18.7, 14.0; LRMS (EI, m/z): Calculated: 264.44 found: 264.2 [M^+].

2,3,6,7,9,10-Hexamethylanthracene (5)

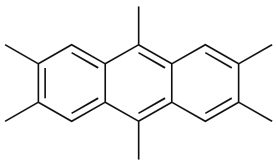

The compound 2,3,6,7,9,10-hexamethylanthracene (**5**) was synthesised according to the procedure reported by Wolthuis.[135] 1,4-dihydro-2,3,6,7,9,10-hexamethylanthracene (**4**) (2.53 g, 9.60 mmol) and chloranil (2.36 g, 9.60 mmol) was dissolved in anhydrous *o*-xylene (60 mL) and heated to reflux for 1 h. The resulting reaction mixture was cooled to room temperature and crude product filtered off. The crude product was washed with cold methanol (50 mL) to yield 2,3,6,7,9,10-hexamethylanthracene (**5**) (1.31 g, 5.00 mmol, 52 %) as a green powder. Mp: 220-222 ºC (Lit[135] 223-224°C); ν_{max} (cm^{-1}): 2911, 1445, 1369, 1026, 999, 889, 856; ^{1}H NMR (400 MHz, $CDCl_3$): δ_H (ppm) = 8.02 (s, 4H, Ar *H*),

3.02 (s, 6H, CH_3), 2.50 (s, 12H, CH_3); ^{13}C NMR (101 MHz, $CDCl_3$) δ_C (ppm) = 134.0, 128.9, 125.6, 124.3, 20.6, 13.9; LRMS (EI, m/z): Calculated: 262.42 found: 262.17 [M^+].

2,3,6,7,9,10-Hexamethyltriptycene (6)

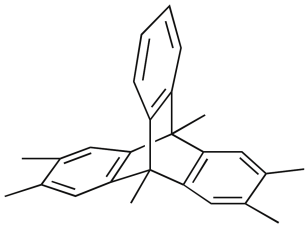

The compound 2,3,6,7,9,10-hexamethyltriptycene (**6**) was synthesised according to the general procedure reported by Rybáčková.[139] 2,3,6,7,9,10-hexamethylanthracene (**5**) (3.00 g, 11.4 mmol) was dissolved in dichloroethane (72 mL) and heated to reflux. A solution of anthranilic acid (3.14 g, 23.0 mmol) in anhydrous THF (60 mL) and a solution of isoamyl-nitrite (5.36 mL, 40.0 mmol) in dichloroethane (60 mL) was added drop wise to the refluxing solution of 2,3,6,7,9,10-hexamethylanthracene (**5**) and left to reflux for 24 h. The resulting reaction mixture was allowed to cool to room temperature and solvent was removed under vacuum. The black solid was dissolved in *o*-xylene (150 mL) and maleic anhydride (0.56 g, 5.70 mmol) was added and heated to reflux for 1 h. After this time, the solution was allowed to cool to room temperature before adding water (200 mL). The product was extracted with DCM (4 x 100 mL). The organic layer was washed with 15% w/w potassium hydroxide solution (200 mL). The organic layer was collected and the solvent removed under vacuum. The resulting dark brown solid was triturated in methanol (100 mL) for 24 h, filtered and purified by column chromatography DCM/ Hexane (1:9, v/v) to yield 2,3,6,7,9,10-hexamethyltriptycene (**6**) (2.38 g, 7.03 mmol, 61 %) as a white solid. Mp: 254-256 ºC; ν_{max} (cm^{-1}): 3061, 3017, 2963, 2938, 2916, 2878, 2361, 2342, 1449, 1377, 1020, 991, 880, 752, 737, 613; ^{1}H NMR (400 MHz, $CDCl_3$): δ_H (ppm) = 7.30 (m, 2H, Ar *H*), 7.09 (s, 4H, Ar *H*), 6.97 (m, 2H, Ar *H*), 2.36 (s, 6H, CH_3), 2.15 (s, 12H, CH_3); ^{13}C NMR (101 MHz, $CDCl_3$) δ_C (ppm) = 148.7, 146.2, 132.2, 124.5, 122.0, 120.1, 47.8, 19.5, 13.5; HRMS (EI, m/z): Calculated: 338.20 found: 338.2034 [M^+].

9,10-Dimethyltriptycene-2,3,6,7-tetracarboxylic acid (7)

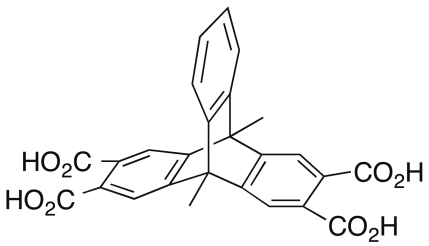

The compound 9,10-dimethyltriptycene-2,3,6,7-tetracarboxylic acid (**7**) was synthesised according to the general procedure reported Rybáčková.[139] To a refluxing solution of 2,3,6,7,9,10-hexamethyltriptycene (**6**) (3.65 g, 11.0 mmol) in pyridine (200 mL), $KMnO_4$ (61.10 g, 387 mmol) was added portion wise over 48 h. The precipitate MnO_2 was filtered off whilst hot and washed with hot water. Solvent removed under vacuum. To this, *conc.* HCl (~300 mL) was added and left to stir for 1 h. The precipitated was filtered, washed with water and dried to yield 9,10-dimethyltriptycene-2,3,6,7-tetracarboxylic acid (**7**) (4.60 g, 10.03 mmol, 91 %) as a white solid. Mp: Above 300 ºC; ν_{max} (cm^{-1}): 3574, 3451, 2361, 2342, 1688, 1682, 1611, 1566, 1381, 1217, 1078, 912, 768, 694; ^1H NMR (400 MHz, $(CD_3)_2CO$): δ_H (ppm) = 7.84 (s, 4H, Ar *H*), 7.55 (dd, 2H, *J* = 5.5, 3.2 Hz, Ar *H*), 7.15 (dd, 2H, *J* = 5.5, 3.2 Hz, Ar *H*), 2.62 (s, 6H, C*H*$_3$); ^{13}C NMR (101 MHz, $(CD_3)_2CO$) δ_C (ppm) = 169.1, 151.8, 131.5, 126.9, 122.7, 122.5, 50.3; HRMS (EI, m/z): Calculated: 458.09 found: 457.0927 [M^-].

9,10-Dimethyltriptycene-dianhydride (8)

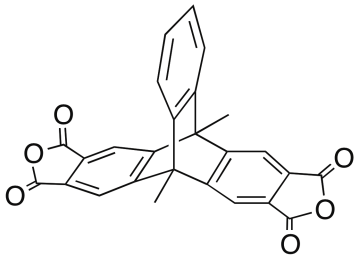

The compound 9,10-dimethyltriptycene-2,3,6,7-tetracarboxylic acid (**7**) (4.06 g, 8.90 mmol) was heated to 220 ºC under vacuum for 4 h using a Kugelrohr. The crude product was dissolved in acetone, filtered off insoluble material and removed solvent under

vacuum to yield 9,10-dimethyltriptycene-dianhydride (**8**) (2.01 g, 4.80 mmol, 54 %) as a white solid. Mp: Above 300 ºC; ν_{max} (cm^{-1}): 3601, 3080, 2978, 2361, 2342, 1838, 1776, 1699, 1452, 1277, 1234, 1175, 1103, 1084, 970, 887, 735, 719, 625; ^{1}H NMR (400 MHz, $(CD_3)_2CO$): δ_H (ppm) = 8.32 (s, 4H, Ar *H*), 7.83 (dd, 2H, *J* = 5.60, 3.20 Hz, Ar *H*), 7.42 (dd, 2H, *J* = 5.60, 3.20 Hz, Ar *H*), 2.98 (s, 6H, C*H*$_3$); ^{13}C NMR (101 MHz, $(CD_3)_2CO$) δ_C (ppm) = 164.1, 157.2, 131.3, 127.7, 123.3, 119.3, 51.9; HRMS (EI, m/z): Calculated: 422.07 found: 422.0796 [M^+].

2,8-Diamino-1,4,7,10-tetramethyl-6H,12H-5,11-methanodibenzo[b,f][1,5]diazocine (9) (Synthesised by Michael Lee)

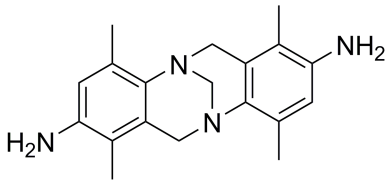

A solution of 2,8-diacetamido-1,4,7,10-tetramethyl-6H,12H-5,11-methanodibenzo[b,f][1,5]-diazocine (4.00 g, 10.2 mmol) dissolved in 6M hydrochloric acid solution (100 mL) was heated at 80°C with stirring for 4 h. The reaction was then cooled in an ice bath and ammonia solution was added dropwise until pH 8. The precipitate was extracted with dichloromethane and the solvent was removed under reduced pressure to yield 2,8-diamino-1,3,7,9-tetramethyl-6H,12H-5,11-methanodibenzo[b,f][1,5]diazocine (3.04 g, 97 %) as a beige solid. Mp: 111-115°C; ν_{max} (cm^{-1}): 3350, 3224, 2945, 2881, 1621, 1478, 1223, 754; ^{1}H NMR (400 MHz, $CDCl_3$): δ_H (ppm) = 6.41 (s, 2H, Ar *H*), 4.32 (d, *J* = 16.8 Hz, 2H, C*H*$_2$), 4.15 (s, 2H, C*H*$_2$), 3.83 (d, *J* = 16.8 Hz, 2H, C*H*$_2$), 3.28 (s, 4H, N*H*$_2$), 2.28 (s, 6H, C*H*$_3$), 1.78 (s, 6H, C*H*$_3$); ^{13}C NMR (126 MHz, $CDCl_3$) δ_C (ppm) = 140.3, 130.8, 126.9, 116.6, 116.5, 66.5, 54.6, 17.0, 11.0; HRMS (EI, m/z): Calculated: 308.2001 found: 308.1983 [M^+].

9,10-Dimethylanthracene (10)

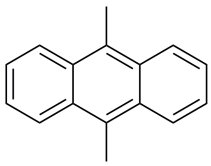

The compound 9,10-dimethylanthracene (**10**) was synthesised according to the procedure reported by Guenzi et al.[165] 9,10-Dichloroanthracene (7.50 g, 30.35 mmol) and PEPPSI-iPr catalyst (1.33 g, 1.96 mmol) were dissolved in 1,4-dioxane (400 mL) and stirred for 30 mins. To this, 3M methyl magnesium bromide in ether (60.70 mL, 182.0 mmol) was added dropwise and left at room temperature for 24 h. After this time, water (500 mL) was added, extracted with ethyl acetate (3 x 100 mL) and dried over $MgSO_4$. The solvent was removed under vacuum, the resulting solid triturated with acetone (70 mL) and filtered off to yield 9,10-dimethylanthracene (**10**) (5.95 g, 28.83 mmol, 95 %) as a yellow solid. Mp: 179-181 ºC (Lit[165] 181 - 183°C); ν_{max} (cm^{-1}): 3073, 2932, 1618, 1526, 1443, 1383, 1364, 1165, 1024, 988, 845, 816, 764, 741, 600, 581; ^1H NMR (400 MHz, $CDCl_3$): δ_H (ppm) = 8.35 (dd, 4H, *J* = 6.9, 3.3 Hz, Ar *H*), 7.53 (dd, 4H, *J* = 6.9, 3.3 Hz, Ar *H*), 3.11 (s, 6H, C*H*$_3$); ^{13}C NMR (101 MHz, $CDCl_3$) δ_C (ppm) = 129.9, 128.3, 125.3, 124.7, 14.1; LRMS (EI, m/z): Calculated: 206.11 found: 206.1 [M^+].

9,10-Dimethyltriptycene (11)

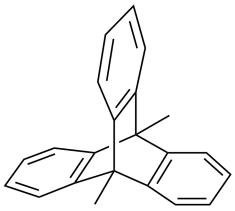

The compound 9,10-dimethyltriptycene (**11**) was synthesised according to the general procedure report by Friedman and Logullo.[166] 9,10-Dimethylanthracene (**10**) (2.45 g, 11.88 mmol) was dissolved in DCM (100 mL) and heated to 60°C. To this, 1,2-epoxypropane (80 mL) and benzenediazonium-2-carboxylatechloride (10.96 g, 59.38 mmol) was added portion wise over 30 min. The reaction mixture was then heated to 85°C for 24 h. The

resulting reaction was cooled to room temperature and solvent removed under vacuum. To the crude product, maleic anhydride (0.60 g, 5.94 mmol) and *o*-xylene (100 mL) was added and heated to 110°C for 1 h. The reaction was cooled to room temperature, solvent removed under vacuum and triturated in MeOH (150 mL) for 16 h. The resulting solid was filtered to yield 9,10-dimethyltriptycene (**11**) (2.47 g, 8.75 mmol, 74 %) as a light brown powder. Mp: Above 300 ºC (Lit[167] Above 300°C); ν_{max} (cm^{-1}): 3067, 2976, 1469, 1448, 1375, 1141, 1089, 1024; ^{1}H NMR (400 MHz, $CDCl_3$): δ_H (ppm) = 7.35 (dd, 6H, *J* = 5.5, 3.2 Hz, Ar *H*), 7.02 (dd, 6H, *J* = 5.5, 3.2 Hz, Ar *H*), 2.42 (s, 6H, C*H*$_3$); ^{13}C NMR (101 MHz, $CDCl_3$) δ_C (ppm) = 148.5, 125.0, 120.7, 48.8, 13.8; LRMS (EI, m/z): Calculated: 282.14 found: 282.1 [M^+].

2,6(7)-Dinito-9,10-dimethyltriptycene (12)

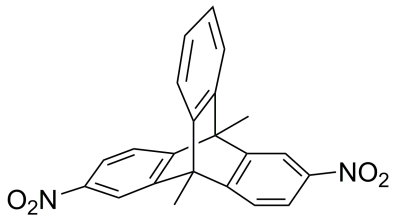

The compound 2,6(7)-dinito-9,10-dimethyltriptycene (**12**) was synthesised according to the general procedure reported by Crivello.[168] 9,10-Dimethyltriptycene (**11**) (2.83 g, 10.02 mmol) was dissolved in mixture of DCM (40 mL) and acetonitrile (160 mL) and heated to 50°C. Potassium nitrate (2.33 g, 23.05 mmol) and trifluoroacetic anhydride (9.88 mL, 70.15 mmol) was added and left at 50°C for 24 h. The resulting reaction was cooled to room temperature and solvent removed under vacuum. The oil was washed with water (300 mL), extracted with DCM (3 x 100 mL), dried over $MgSO_4$ and solvent removed under vacuum. The crude product was purified by column chromatography DCM/ hexane (4:1, v/v) to yield 2,6(7)-dinito-9,10-dimethyltriptycene (1.44 g, 3.87 mmol, 39 %) as a white solid. Mp: 222-224 ºC; ν_{max} (cm^{-1}): 3075, 3025, 2977, 2947, 2886, 1587, 1522, 1449, 1383, 1341, 1275, 1216, 1180, 1162, 1143, 1111, 1095, 1044, 1037; ^{1}H NMR (400 MHz, $CDCl_3$): δ_H (ppm) = 8.21 (m, 2H, Ar *H*), 8.01 (m, 2H, Ar *H*), 7.52 (m, 2H, Ar *H*), 7.44 (m, 2H, Ar *H*), 7.15 (m, 2H, Ar *H*), 2.54 (m, 6H, C*H*$_3$); ^{13}C NMR (101 MHz, $CDCl_3$) δ_C (ppm)

= 154.1, 153.7, 149.3, 148.9, 145.9, 145.5, 145.1, 126.1, 121.5, 121.4, 121.3, 116.1, 49.3, 13.5; LRMS (EI, m/z): Calculated: 372.11 found: 371.1 [M^+].

2,6(7)-Diamino-9,10-dimethyltriptycene (13)

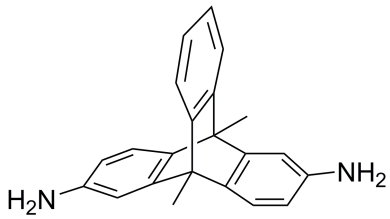

The compound 2,6(7)-diamino-9,10-dimethyltriptycene (**13**) was synthesised according to a modified procedure reported by Furst and Moore.[169] 2,6(7)-Dinitro-9,10-dimethyltriptycene (**12**) (1.44 g, 3.87 mmol) was dissolved in anhydrous, de-oxygenated THF (150 mL) and heated to 50 ºC. To this, Raney nickel (catalytic amount) and hydrazine monohydrate (2.48 mL, 77.34 mmol) was added and left at 50 ºC for 24 h. The resulting reaction mixture was cooled to room temperature, filtered off Raney nickel and removed solvent under vacuum. Washed the resulting oil with water, extracted with DCM (3 x 60.0 mL), dried over $MgSO_4$ and removed solvent under vacuum to yield 2,6(7)-diamino-9,10-dimethyltriptycene (**13**) (1.03 g, 3.31 mmol, 85 %) as a white powder. Mp: 293-295 ºC; ν_{max} (cm^{-1}): 3439, 3358, 2968, 1614, 1476, 1454, 1377, 1231, 1296, 1215, 1144, 1088, 1026, 845, 826, 810, 783, 748, 635, 621, 611, 581, 559, 538; ^{1}H NMR (500 MHz, $CDCl_3$): δ_H (ppm) = 7.28 (m, 2H, Ar *H*), 7.07 (s, 1H, Ar *H*), 7.06 (s, 1H, Ar *H*), 6.99 (m, 2H, Ar *H*), 6.70 (dd, 2H, Ar *H*), 6.29 (m, 2H, Ar *H*), 3.50 (*b*s, 4H, NH_2), 2.29 (m, 6H, CH_3); ^{13}C NMR (126 MHz, $CDCl_3$) δ_C (ppm) = 150.3, 149.6, 149.5, 148.8, 148.2, 143.6, 143.4, 139.6, 138.9, 124.9, 124.6, 124.4, 121.2, 120.9, 120.4, 120.1, 119.8, 110.6, 110.4, 109.2, 108.9, 48.4, 47.8, 47.2, 13.70; LRMS (EI, m/z): Calculated: 312.16 found: 312.2 [M^+].

2,6-Diaminoanthracen-9(10*H*)-one (14)

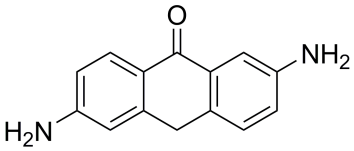

The compound 2,6-diaminoanthracen-9(10*H*)-one (**14**) was synthesised according to the procedure reported by K. D. Revelle et al.[151] 2,6-Diaminoanthraquinone (20.0 g, 83.95 mmol), tin powder (59.79 g, 503.70 mmol), ethanol (400 mL) and 2.5 M aq. NaOH (350 mL) were combined and heated to reflux for 24 h. The resulting reaction was cooled to room temperature, poured into water (1.0 L), filtered off and dried to yield 2,6-diaminoanthracen-9(10*H*)-one (**14**) (16.65 g, 74.24 mmol, 88 %) as a yellow solid. Mp: 280 ºC (dec); ν_{max} (cm^{-1}): 3421, 3331, 3196, 1645, 1564, 1322; ^{1}H NMR (500 MHz, $(CD_3)_2CO$): δ_H (ppm) = 7.87 (d, 1H, *J* = 8.6 Hz, Ar *H*), 7.32 (d, 1H, *J* = 2.6 Hz, Ar *H*), 7.16 (d, 1H, *J* = 8.2 Hz, Ar *H*), 6.85 (dd, 1H, *J* = 8.2, 2.6 Hz, Ar *H*), 6.62 (d, 1H, *J* = 6.4 Hz, Ar *H*), 6.54 (s, 1H, Ar *H*), 6.04 (s, 2H, C*H*), 5.19 (s, 2H, NH_2), 4.05 (s, 2H, NH_2); ^{13}C NMR (126 MHz, $(CD_3)_2CO$) δ_C (ppm) = 182.2, 153.4, 147.7, 144.1, 132.9, 129.4, 129.3, 128.2, 121.1, 119.5, 113.7, 111.0, 110.2, 31.5; LRMS (EI, m/z): Calculated: 224.09 found: 224.1 [M^+].

2,6-Diaminoanthracene (15)

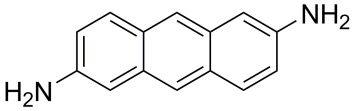

The compound 2,6-diaminoanthracene (**15**) was synthesised according to the procedure reported by K. D. Revelle et al.[151] 2,6-Diaminoanthranone (**14**) (16.0 g, 71.0 mmol), $NaBH_4$ (21.59 g, 571.0 mmol), ethanol (300 mL) and 2.5 M aq. NaOH (300 mL) were combined and heated to reflux for 6 h. The hot mixture was poured into water (1.0 L) and stirred for 20 min. The resulting solid was filtered and extracted with acetone. The solvent was removed under vacuum. Resulting solid was washed with small amount of cold acetone, filtered and dried to give 2,6-Diaminoanthracene (**15**) (8.0 g, 38.4 mmol, 54 %) as

a yellow solid. Mp: 231-232 ºC (Lit[170] 230 ºC); ν_{max} (cm^{-1}): 3403, 3326, 3204, 3009, 2957, 1635, 1475; ^1H NMR (400 MHz, $(CD_3)_2SO$): δ_H (ppm) =7.88 (s, 2H, Ar *H*), 7.64 (d, 2H, *J* = 8.9 Hz, Ar *H*), 6.93 (d, 2H, *J* = 8.9 Hz, Ar *H*), 6.80 (s, 2H, Ar *H*), 5.24 (*b*s, 4H, N*H*); ^{13}C NMR (101 MHz, $(CD_3)_2SO$) δ_C (ppm) = 144.0, 130.6, 127.9, 127.2, 121.3, 120.5, 103.7; LRMS (EI, m/z): Calculated: 208.1 found: 208.1 [M^+].

1,4-Dihydro-1,4-epoxynaphthalene (16)

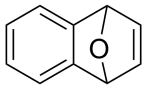

The compound 1,4-dihydro-1,4-epoxynaphthalene (**16**) prepared according to the general procedure G.P 1. 1,2-Dibromobenzene (30.0 g, 127.2 mmol) and anhydrous furan (64.73 mL, 890.1 mmol) dissolved in anhydrous THF (40 mL). n-BuLi (66.12 mL, 165.3 mmol) in anhydrous THF (20 mL) was added to yield desired product 1,4-dihydro-1,4-epoxynaphthalene (**16**) (7.34 g, 51.0 mmol, 40 %) as a white solid. Mp: 56-57 ºC (lit[135] 56 ºC); ν_{max} (cm^{-1}): 3021, 1450, 1279, 987, 871, 845; ^1H NMR (500 MHz, $CDCl_3$): δ_H (ppm) = 7.25 (dd, 2H, *J* = 5.1, 3.0 Hz, Ar *H*), 7.03 (t, 2H, *J* = 1.1 Hz, C*H*), 6.97 (dd, 2H, *J* = 5.1, 3.0 Hz, Ar *H*), 5.71 (t, 2H, *J* = 1.1 Hz, C*H*); ^{13}C NMR (126 MHz, $CDCl_3$) δ_C (ppm) = 149.2, 143.2, 125.2, 120.4, 82.5; LRMS (EI, m/z): Calculated: 144.06 found: 144.0 [M^+].

(5R,12R)-5,5a,6,11,11a,12-Hexahydro-5,12-[1,2]benzeno-6,11-epoxytetracene-2,16-diamine (17)

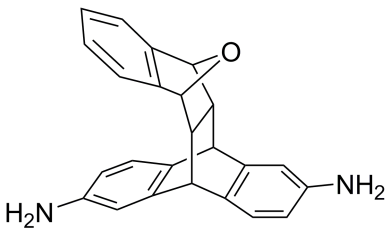

The compound (5R,12R)-5,5a,6,11,11a,12-hexahydro-5,12-[1,2]benzeno-6,11-epoxytetracene-2,16-diamine (**17**) was prepared according to the general procedure G.P 2. 2,6-Diaminoanthracene (**15**) (3.00 g, 14.4 mmol) and 1,4-dihydro-1,4-epoxynaphthalene (2.08 g, 14.4 mmol) dissolved in DMF (15.0 mL). Purified by column chromatography $CHCl_3$/ ethyl acetate (1:1, v/v) to yield (5R,12R)-5,5a,6,11,11a,12-hexahydro-5,12-[1,2]benzeno-6,11-epoxytetracene-2,16-diamine (**17**) (4.55 g, 12.9 mmol, 90 %) as a yellow/ brown solid. Mp: 250 ºC; ν_{max} (cm^{-1}): 3350, 3008, 2933, 1625, 1483, 1266; ^1H NMR (600 MHz, $CDCl_3$): δ_H (ppm) = 7.12 (dd, 2H, *J* = 5.2, 3.1 Hz, Ar *H*), 7.02 (m, 3H, Ar *H*), 6.96 (d, 1H, *J* = 7.8 Hz, Ar *H*), 6.67 (d, 1H, *J* = 2.2 Hz, Ar *H*), 6.60 (d, 1H, *J* = 2.2 Hz, Ar *H*), 6.44 (dd, 1H, *J* = 7.8, 2.2 Hz, Ar *H*), 6.30 (dd, 1H, *J* = 7.8, 2.2 Hz, Ar *H*), 4.90 (d, 2H, *J* = 4.1 Hz, C*H*), 4.17 (dd, 2H, *J* = 7.4, 2.7 Hz, C*H*), 3.46 (*b*s, 4H, NH_2), 2.18 (m, 2H, C*H*); ^{13}C NMR (126 MHz, $CDCl_3$) δ_C (ppm) =147.1, 147.0, 146.2, 144.5, 144.3, 143.3, 134.7, 131.8, 126.2, 124.1, 124.0, 118.6, 112.0, 111.5, 111.2, 81.4, 81.3, 49.5, 48.6, 46.9, 46.8; LRMS (EI, m/z): Calculated: 352.16 found: 352.1 [M^+].

(5*S*,12*S*)-5,12-Dihydro-5,12-[1,2]benzenotetracene-2,16-diamine (18)

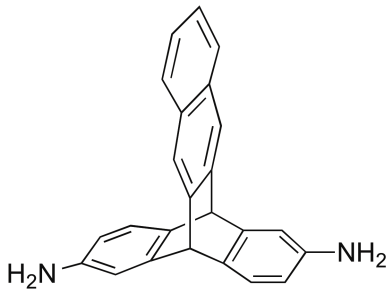

The compound (5*S*,12*S*)-5,12-dihydro-5,12-[1,2]benzenotetracene-2,16-diamine (**18)** was synthesised according to the general procedure G.P 3. (5R,12R)-5,5a,6,11,11a,12-Hexahydro-5,12-[1,2]benzeno-6,11-epoxytetracene-2,16-diamine (**17**) (3.03 g, 8.60 mmol), ethanol (120 mL) and perchloric acid (70 %, 40.0 mL) were combined. Desired product (5*S*,12*S*)-5,12-dihydro-5,12-[1,2]benzenotetracene-2,16-diamine (**18)** (1.31 g, 3.93 mmol, 46 %) collected as an off white solid. Mp: 235 ºC (lit[150] 233-235); ν_{max} (cm^{-1}): 3350, 3009, 1622, 1479; ^1H NMR (500 MHz, $CDCl_3$): δ_H (ppm) = 7.69 (s, 2H, Ar *H*), 7.67 (dd, 2H, *J* = 6.2, 3.4 Hz, Ar *H*), 7.34 (dd, 2H, *J* = 6.2, 3.4 Hz, Ar *H*), 7.14 (d, 2H, *J* = 7.8 Hz, Ar *H*),

6.78 (d, 2H, *J* = 2.2 Hz, Ar *H*), 6.29 (dd, 2H, *J* = 7.8, 2.2 Hz, Ar *H*), 5.27 (s, 2H, C*H*), 3.51 (*b*s, 4H, O*H*); ^{13}C NMR (126 MHz, $CDCl_3$) δ_C (ppm) = 146.5, 144.2, 142.8, 135.0, 131.8, 27.4, 125.4, 124.2, 121.1, 111.4, 111.1, 53.0; LRMS (EI, m/z): Calculated: 334.15 found: 334.1 [M^+].

6,7-Dimethoxy-1,4-dihydro-1,4-epoxynaphthalene (19)

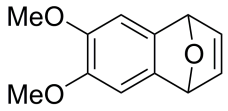

The compound 6,7-dimethoxy-1,4-dihydro-1,4-epoxynaphthalene (**19**) prepared according to the general procedure G.P 1. 1,2-Dibromo-4,5-dimethyl benzene (5.00 g, 16.90 mmol) and anhydrous furan (36.86 mL, 506.8 mmol) dissolved in anhydrous THF (20.0 mL). n-BuLi (8.78 mL, 21.96 mmol) in anhydrous THF (10.0 mL) was added to yield desired product 6,7-dimethoxy-1,4-dihydro-1,4-epoxynaphthalene (**19**) (3.22 g, 15.77 mmol, 93 %) as a white solid. Mp: 130-132 ºC (Lit[171] 147-149 ºC); ν_{max} (cm^{-1}): 2963, 1485, 1466, 1454, 1412, 1323, 1277, 1204, 1180, 1061, 964, 872, 856, 787, 733, 694, 637; ^{1}H NMR (400 MHz, $CDCl_3$): δ_H (ppm) = 7.04 (t, 2H, *J* = 1.0 Hz, C*H*), 6.97 (s, 2H, Ar *H*), 5.68 (t, 2H, *J* = 1.0 Hz, C*H*), 3.85 (s, 6H, CH_3); ^{13}C NMR (126 MHz, $CDCl_3$) δ_C (ppm) = 146.0, 143.5, 141.9, 107.0, 82.7, 56.7; LRMS (EI, m/z): Calculated: 204.08 found: 204.1 [M^+].

(5*R*,12*R*)-8,9-Dimethoxy-5,5a,6,11,11a,12-hexahydro-5,12-[1,2]benzeno-6,11-epoxytetracene-2,16-diamine (20)

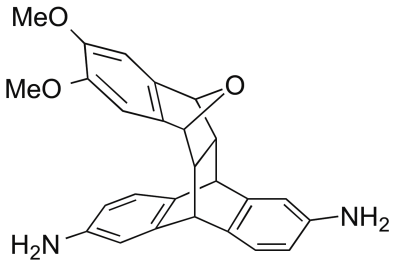

The compound (5*R*,12*R*)-8,9-dimethoxy-5,5a,6,11,11a,12-hexahydro-5,12-[1,2]benzeno-6,11-epoxytetracene-2,16-diamine (**20**) was synthesised according to the general procedure G.P 2. 2,6-Diaminoanthracene (**15**) (1.11 g, 5.33 mmol) and 6,7-dimethoxy-1,4-dihydro-1,4-epoxynaphthalene (**19**) (1.09 g, 5.33 mmol) was dissolved DMF (15.0 mL). Purified by column chromatography $CHCl_3$/ ethyl acetate (7:3, v/v) to yield (5*R*,12*R*)-8,9-dimethoxy-5,5a,6,11,11a,12-hexahydro-5,12-[1,2]benzeno-6,11-epoxytetracene-2,16-diamine (**20**) (1.10 g, 2.67 mmol, 50 %) as a light brown crystalline solid. Mp: 196-198 ºC; ν_{max} (cm^{-1}): 3348, 2932, 1620, 1481, 1331, 1300, 1269, 1246, 1211, 1080, 856, 799, 586; ^{1}H NMR (600 MHz, $CDCl_3$): δ_H (ppm) = 7.00 (d, 1H, *J* = 7.7 Hz, Ar *H*), 6.95 (d, 1H, *J* = 7.7 Hz, Ar *H*), 6.76 (s, 2H, Ar *H*), 6.66 (d, 1H, *J* = 2.3 Hz, Ar *H*), 6.59 (d, 1H, *J* = 2.3 Hz, Ar *H*), 6.43 (dd, 1H, *J* = 7.7, 2.3 Hz, Ar *H*), 6.30 (dd, 1H, *J* = 7.7, 2.3 Hz, Ar *H*), 4.84 (d, 2H, *J* = 4.0 Hz, C*H*), 4.14-4.12 (m, 2H, C*H*), 3.81 (s, 6H, CH_3), 3.49 (*b*s, 4H, O*H*), 2.17-2.11 (m, 2H, C*H*); ^{13}C NMR (126 MHz, $CDCl_3$) δ_C (ppm) = 147.6, 146.4, 144.6, 144.4, 143.5, 139.6, 139.5, 134.9, 131.9, 124.2, 124.1, 112.2, 112.1, 111.6, 111.4, 104.0, 103.9, 81.7, 81.6, 56.4, 50.1, 49.3, 47.1, 47.0; HRMS (EI, m/z): Calculated: 412.18 found: 412.1792 [M^+].

(5*S*,12*S*)-8,9-Dimethoxy-5,12-dihydro-5,12-[1,2]benzenotetracene-2,16-diamine (21)

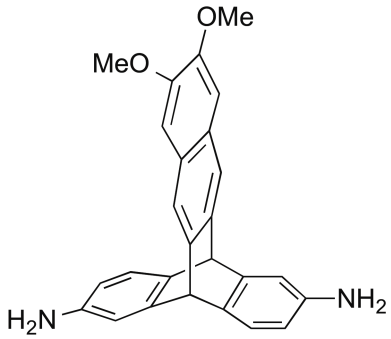

The compound (5*S*,12*S*)-8,9-dimethoxy-5,12-dihydro-5,12-[1,2]benzenotetracene-2,16-diamine (**21**) was synthesised according to the general procedure G.P 3. (5*R*,12*R*)-8,9-Dimethoxy-5,5a,6,11,11a,12-hexahydro-5,12-[1,2]benzeno-6,11-epoxytetracene-2,16-diamine (**20**) (2.00 g, 4.85 mmol), EtOH (130 mL) and perchloric acid (70 %, 30 mL) were combined. Desired product (5*S*,12*S*)-8,9-dimethoxy-5,12-dihydro-5,12-[1,2]benzenotetracene-2,16-diamine (**21)** (1.32 g, 3.35 mmol, 69 %) collected as a light

brown solid. Mp: Above 300 ºC; ν_{max} (cm^{-1}): 3360, 2951, 1616, 1504, 1477, 1435, 1416, 1250, 1200, 1138, 1099, 1003, 895, 868, 833, 536, 505; ^{1}H NMR (500 MHz, $(CD_3)_2SO$): δ_H (ppm) = 7.57 (s, 2H, Ar *H*), 7.13 (s, 2H, Ar *H*), 7.01 (d, 2H, *J* = 7.8 Hz, Ar *H*), 6.65 (d, 2H, *J* = 2.2 Hz, Ar *H*), 6.12 (dd, 2H, *J* = 7.8, 2.2 Hz, Ar *H*), 5.15 (s, 2H, C*H*), 4.83 (*b*s, 4H, NH_2), 3.81 (s, 6H, CH_3); ^{13}C NMR (126 MHz, $(CD_3)_2SO$) δ_C (ppm) = 148.7, 146.5, 146.0, 141.8, 132.6, 126.2, 123.6, 119.3, 110.0, 108.9, 106.6, 55.3, 51.8; HRMS (EI, m/z): Calculated: 394.17 found: 394.1665 [M^+].

6,7-Dimethyl-1,4-dihydro-1,4-epoxynaphthalene (22)

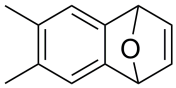

The compound 6,7-dimethyl-1,4-dihydro-1,4-epoxynaphthalene (**22**) prepared according to the general procedure G.P 2. (**1**) (20.0 g, 75.8 mmol) and anhydrous furan (49.59 mL, 681.9 mmol) dissolved in anhydrous THF (40.0 mL). n-BuLi (39.4 mL, 98.5 mmol) in anhydrous THF (10.0 mL) was added to yield desired product 6,7-dimethyl-1,4-dihydro-1,4-epoxynaphthalene (**22**) (5.90 g, 34.26 mmol, 45 %) as a white solid. Mp: 67-68 ºC (lit[135] 72-73 ºC); ν_{max} (cm^{-1}): 2920, 1458, 1389, 1277, 1072, 1038, 976, 868, 841, 694, 637; ^{1}H NMR (500 MHz, $CDCl_3$): δ_H (ppm) = 7.06 (s, 2H, Ar *H*), 7.00 (t, 2H, *J* = 1.0 Hz, C*H*), 5.66 (t, 2H, *J* = 1.0 Hz, C*H*), 2.20 (s, 6H, CH_3); ^{13}C NMR (126 MHz, $CDCl_3$) δ_C (ppm) = 146.8, 143.3, 132.7, 122.3, 82.4, 19.9; LRMS (EI, m/z): Calculated: 172.09 found: 172.1 [M^+].

(5*R*,12*R*)-8,9-Dimethyl-5,5a,6,11,11a,12-hexahydro-5,12-[1,2]benzeno-6,11-epoxytetracene-2,16-diamine (23)

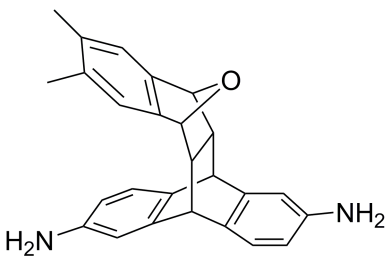

The compound (5*R*,12*R*)-8,9-dimethyl-5,5a,6,11,11a,12-hexahydro-5,12-[1,2]benzeno-6,11-epoxytetracene-2,16-diamin (**23**) was synthesised according to the general procedure G.P 2. (**15**) (1.50 g, 7.20 mmol) and (**22**) (1.49 g, 8.64 mmol) dissolved in DMF (15.0 mL). Purified by column chromatography $CHCl_3$/ ethyl acetate (7:3, v/v) to yield (**23**) (2.77 g, 7.28 mmol, 76 %) as a light brown crystalline solid. Mp: 216-218 ºC; ν_{max} (cm^{-1}): 3341, 2928, 1620, 1481, 1339, 1265, 1211, 1119, 856, 818, 799, 748, 664, 633, 586, 563, 540, 509; ^{1}H NMR (500 MHz, $CDCl_3$): δ_H (ppm) = 7.00 (d, 1H, *J* = 7.7 Hz, Ar *H*), 6.94 (d, 1H, *J* = 7.7 Hz, Ar *H*), 6.90 (s, 2H, Ar *H*), 6.66 (d, 1H, *J* = 2.3 Hz, Ar *H*), 6.58 (d, 1H, *J* = 2.3 Hz, Ar *H*), 6.43 (dd, 1H, *J* = 7.7, 2.3 Hz, Ar *H*), 6.29 (dd, 1H, *J* = 7.7, 2.3 Hz, Ar *H*), 4.84 (d, 2H, *J* = 3.5 Hz, C*H*), 4.15 (d, 1H, C*H*), 4.14 (d, 1H, C*H*), 3.53 (*b*s, 4H, NH_2), 2.16 (s, 6H, CH_3), 2.14 (m, 2H, C*H*); ^{13}C NMR (126 MHz, $CDCl_3$) δ_C (ppm) = 146.3, 145.1, 145.0, 144.6, 144.3, 143.5, 134.9, 134.2, 132.0, 124.2, 124.1, 120.2, 120.1, 112.2, 112.1, 111.6, 111.3, 81.4, 81.3, 50.0, 49.2, 47.1, 47.0, 31.7, 22.8, 20.0, 14.3; HRMS (EI, m/z): Calculated: 380.19 found: 380.1873 [M^+].

(5*S*,12*S*)-8,9-Dimethyl-5,12-dihydro-5,12-[1,2]benzenotetracene-2,16-diamine (24)

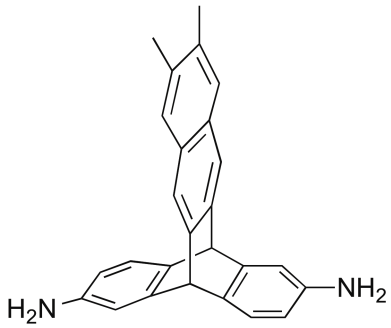

The compound (5*S*,12*S*)-8,9-dimethyl-5,12-dihydro-5,12-[1,2]benzenotetracene-2,16-diamine (**24**) was synthesised according to the general procedure G.P 3. (5*R*,12*R*)-8,9-Dimethyl-5,5a,6,11,11a,12-hexahydro-5,12-[1,2]benzeno-6,11-epoxytetracene-2,16-diamin (**23**) (2.77 g, 7.27 mmol) dissolved in EtOH (110 mL) and perchloric acid (40 mL). Afforded desired product (5*S*,12*S*)-8,9-dimethyl-5,12-dihydro-5,12-[1,2]benzenotetracene-2,16-diamine (**24**) (2.35 g, 6.48 mmol, 89 %) as a light brown solid. Mp: 224-226°C; ν_{max} (cm^{-1}): 3348, 3005, 2951, 1616, 1481, 1439, 1331, 1265, 1115, 907, 891, 876, 822, 810, 768, 590, 548, 523, 505; ^{1}H NMR (500 MHz, $CDCl_3$): δ_H (ppm) = 7.56 (s, 2H, Ar *H*), 7.40

(s, 2H, Ar *H*), 7.13 (d, 2H, *J* = 7.8 Hz, Ar *H*), 6.77 (d, 2H, *J* = 2.3 Hz, Ar *H*), 6.28 (dd, 2H, *J* = 7.8, 2.3 Hz, Ar *H*), 5.22 (s, 2H, C*H*), 3.43 (*b*s, 4H, NH_2), 2.34 (s, 6H, CH_3); ^{13}C NMR (126 MHz, $CDCl_3$) δ_C (ppm) = 146.8, 144.1, 141.9, 135.4, 134.9, 130.7, 127.2, 124.2, 120.3, 111.5, 111.1, 53.2, 20.2; HRMS (EI, m/z): Calculated: 362.18 found: 362.1759 [M^+].

6-(Trifluoromethyl)-1,4-dihydro-1,4-epoxynaphthalene (25)

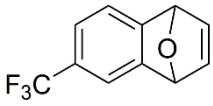

The compound 6-(trifluoromethyl)-1,4-dihydro-1,4-epoxynaphthalene (**25**) was synthesised according to the procedure reported by Bailly et al.[172] 4-Chlorobenzotrifluoride (10.0 g, 55.39 mmol) was dissolved in anhydrous THF (80 mL) and cooled to -78°C. *n*-BuLi (28.8 mL, 72.0 mmol) was added drop wise and left at -78°C for 1 h. The resulting solution was transferred drop wise to a solution of furan (121 mL, 1.66 mol) in anhydrous THF (20 mL) and left at room temperature for 2 h. After this time, the solvent was removed under vacuum, crude product was dissolved in ether (30 mL) and filtered through a pad of basic alumina. Washed through with ether and removed solvent under vacuum. The resulting oil was distilled under vacuum to yield 6-(trifluoromethyl)-1,4-dihydro-1,4-epoxynaphthalene (**25**) (6.08 g, 28.66 mmol, 52 %) as a colourless oil. ν_{max} (cm^{-1}): 3019, 2359, 2324, 1427, 1354, 1323, 1275, 1198, 1167, 1140, 1049, 995, 897, 872, 853, 839, 750, 700, 654, 637, 544; ^{1}H NMR (600 MHz, $CDCl_3$): δ_H (ppm) = 7.46 (s, 1H, Ar *H*), 7.32 (d, 1H, *J* = 7.5 Hz, Ar *H*), 7.29 (dd, 1H, *J* = 7.5, 0.8 Hz, Ar *H*), 7.07-7.03 (m, 2H, C*H*), 5.76 (m, 2H, C*H*); ^{13}C NMR (151 MHz, $CDCl_3$) δ_C (ppm) = 153.4, 150.5, 143.3, 142.8, 129.2, 128.0-127.1 (cluster of peaks), 125.3, 123.5, 123.2-123.1 (cluster of peaks), 120.1, 117.2-117.1 (cluster of peaks), 82.2; LRMS (EI, m/z): Calculated: 212.04 found: 212.0 [M^+].

(5*R*,12*R*)-8-(Trifluoromethyl)-5,5a,6,11,11a,12-hexahydro-5,12-[1,2]benzeno-6,11-epoxytetracene-2,16-diamine (26)

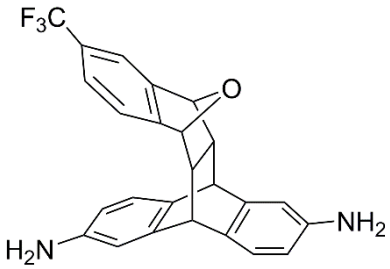

The compound (5*R*,12*R*)-8-(trifluoromethyl)-5,5a,6,11,11a,12-hexahydro-5,12-[1,2]benzeno-6,11-epoxytetracene-2,16-diamine (**26**) was synthesised according to the general procedure G.P 2. 2,6-Diaminoanthracene (**15**) (2.50 g, 12.0 mmol) and 6-(trifluoromethyl)-1,4-dihydro-1,4-epoxynaphthalene (**25**) (2.55 g, 12.0 mmol) dissolved in DMF (15.0 mL). Purified by column chromatography $CHCl_3$/ ethyl acetate (7:3, v/v) to yield (5*R*,12*R*)-8-(trifluoromethyl)-5,5a,6,11,11a,12-hexahydro-5,12-[1,2]benzeno-6,11-epoxytetracene-2,16-diamine (**26**) (4.08 g, 9.71 mmol, 81 %) as a brown solid. Mp: 195-197 ºC; ν_{max} (cm^{-1}): 3429, 3354, 3007, 2936, 2363, 2324, 1665, 1624, 1481, 1431, 1319, 1275, 1163, 1144, 111, 1053, 961, 839, 818, 797, 673, 662, 586; ^{1}H NMR (600 MHz, $CDCl_3$): δ_H (ppm) = 7.37 (s, 1H, Ar *H*), 7.33 (d, 1H, *J* = 7.5 Hz, Ar *H*), 7.22 (d, 1H, *J* = 7.5 Hz, Ar *H*), 7.02 (dd, 1H, *J* = 7.7, 3.8 Hz, Ar *H*), 6.96 (d, 1H, *J* = 7.7 Hz, Ar *H*), 6.68-6.66 (m, 1H, Ar *H*), 6.60 (d, 1H, *J* = 2.3 Hz, Ar *H*), 6.46-6.43 (m, 1H, Ar *H*), 6.33-6.30 (m, 1H, Ar *H*), 4.96 (d, 2H, *J* = 4.6 Hz, C*H*), 4.21-4.17 (m, 2H, C*H*), 3.51 (*b*s, 4H, NH_2), 2.24-2.16 (m, 2H, C*H*); ^{13}C NMR (126 MHz, $CDCl_3$) δ_C (ppm) = 124.0-123.5 (cluster of peaks), 119.4-119.3 (cluster of peaks), 116.5, 116.2, 115.9, 115.8-115.6 (cluster of peaks), 115.3, 111.6, 110.6, 81.0-80.8 (cluster of peaks), 54.1, 49.20-48.1 (cluster of peaks), 47.0-46.4 (cluster of peaks); HRMS (EI, m/z): Calculated: 420.14 found: 420.1461 [M^+].

(5*S*,12*S*)-8-(Trifluoromethyl)-5,12-dihydro-5,12-[1,2]benzenotetracene-2,16-diamine (27)

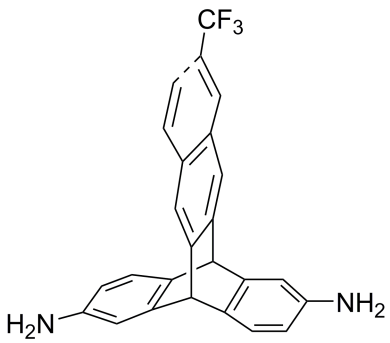

The compound (5*S*,12*S*)-8-(trifluoromethyl)-5,12-dihydro-5,12-[1,2]benzenotetracene-2,16-diamine (**27**) was synthesised according to the general procedure G.P 3. (5*R*,12*R*)-8-(Trifluoromethyl)-5,5a,6,11,11a,12-hexahydro-5,12-[1,2]benzeno-6,11-epoxytetracene-2,16-diamine (**26**) (3.50 g, 8.33 mmol) dissolved in EtOH (120 mL) and $HClO_4$ (50 mL). Afforded desired product (5*S*,12*S*)-8-(trifluoromethyl)-5,12-dihydro-5,12-[1,2]benzenotetracene-2,16-diamine (**27**) (1.14 g, 2.84 mmol, 34 %) as a cream powder. Mp: 198-200 ºC; ν_{max} (cm^{-1}): 3437, 3358, 3009, 2955, 2359, 1614, 1479, 1456, 1333, 1308, 1265, 1188, 1148, 1107, 1076, 1061, 932, 908, 810, 571; ^{1}H NMR (600 MHz, $CDCl_3$): δ_H (ppm) = 7.96 (s, 1H, Ar *H*), 7.76 (d, 1H, *J* = 8.6 Hz, Ar *H*), 7.74 (s, 1H, Ar *H*), 7.72 (s, 1H, Ar *H*), 7.52 (dd, 1H, *J* = 8.6, 1.8 Hz, Ar *H*), 7.17-7.15 (m, 2H, Ar *H*), 6.79 (m, 2H, Ar *H*), 6.31 (m, 2H, Ar *H*), 5.30 (s, 2H, C*H*), 3.54 (*b*s, 4H, NH_2); ^{13}C NMR (151 MHz, $CDCl_3$) δ_C (ppm) = 146.2, 146.2, 145.4, 144.5-144.4 (cluster of peaks), 134.6, 134.5, 133.4, 130.8, 128.4, 125.1, 125.1, 124.5, 121.9, 121.2, 121.2, 121.1, 111.5, 111.4, 111.4, 77.2, 53.1, 53.0; HRMS (EI, m/z): Calculated: 402.13 found: 402.1335 [M^+].

6-(*Tert*-butyl)-1,4-dihydro-1,4-epoxynaphthalene (28)

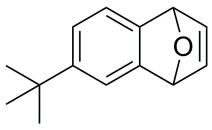

The compound 6-(*tert*-butyl)-1,4-dihydro-1,4-epoxynaphthalene (**28**) was prepared according to the general procedure G.P 1. 1,2-Dibromo-4-tert-butylbenzene (10.0 g, 34.24

mmol) and anhydrous furan (22.41 mL, 308 mmol) dissolved in anhydrous THF (30 mL). n-BuLi (17.81 mL, 44.5 mmol) in anhydrous THF (10.0 mL) was added to yield desired product 6-(*tert*-butyl)-1,4-dihydro-1,4-epoxynaphthalene (**28**) (4.50 g, 20.02, 58 %) as a white crystalline solid. Mp: 54-55 ºC; ν_{max} (cm^{-1}): 2963, 1474, 1362, 1281, 1254, 984, 872, 849, 837, 826, 748, 698, 652, 633, 571, 517; ^{1}H NMR (500 MHz, $CDCl_3$): δ_H (ppm) = 7.34 (d, 1H, *J* = 1.6 Hz, Ar *H*), 7.17 (d, 1H, *J* = 7.5 Hz, Ar *H*), 7.02 (m, 2H, C*H*), 6.97 (dd, 1H, *J* = 7.5, 1.6 Hz, Ar *H*), 5.69 (s, 2H, C*H*), 1.30 (s, 9H, CH_3); ^{13}C NMR (126 MHz, $CDCl_3$) δ_C (ppm) = 149.1, 148.5, 146.0, 143.1, 143.0, 121.3, 119.7, 118.3, 82.7, 82.3, 77.2, 34.8, 31.6; LRMS (EI, m/z): Calculated: 200.12 found: 200.1 [M^+].

(5*R*,12*R*)-8-(*Tert*-butyl)-5,5a,6,11,11a,12-hexahydro-5,12-[1,2]benzeno-6,11-epoxytetracene-2,16-diamine (29)

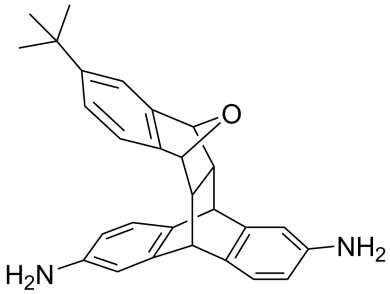

The compound (5*R*,12*R*)-8-(*tert*-butyl)-5,5a,6,11,11a,12-hexahydro-5,12-[1,2]benzeno-6,11-epoxytetracene-2,16-diamine (**29**) was synthesised according to the general procedure G.P.2. 2,6-Diaminoanthracene (**15**) (1.82 g, 8.75 mmol) and 6-(*tert*-butyl)-1,4-dihydro-1,4-epoxynaphthalene (**28**) (1.75 g, 8.75 mmol) dissolved in DMF (15.0 mL). Purified by column chromatography $CHCl_3$/ ethyl acetate (7:3, v/v) to yield (5*R*,12*R*)-8-(*tert*-butyl)-5,5a,6,11,11a,12-hexahydro-5,12-[1,2]benzeno-6,11-epoxytetracene-2,16-diamine (**29**) (2.20 g, 5.38 mmol, 62 %) as a yellow/brown solid. Mp: 165-167 ºC; ν_{max} (cm^{-1}): 3347, 2953, 1670, 1624, 1479, 1265, 1215, 889, 851, 835, 814, 797, 731, 584; ^{1}H NMR (500 MHz, $CDCl_3$): δ_H (ppm) = 7.16 (s, 1H, Ar *H*), 7.02 (m, 3H, Ar *H*), 6.95 (d, 1H, *J* = 7.7 Hz, Ar *H*), 6.67 (dd, 1H, *J* = 3.2, 2.3 Hz, Ar *H*), 6.59 (d, 1H, *J* = 2.3 Hz, Ar *H*), 6.43 (dd, 1H, *J* = 7.7, 2.3 Hz, Ar *H*), 6.29 (dd, 1H, *J* = 7.7, 2.3 Hz, Ar *H*), 4.87 (d, 2H, *J* = 3.2 Hz, C*H*), 4.16 (m, 2H, C*H*), 3.66-3.18 (*b*s, 4H, NH_2), 2.17 (m, 2H, C*H*), 1.24 (m, 9H, CH_3); ^{13}C

NMR (126 MHz, $CDCl_3$) δ_C (ppm) = 149.6, 147.2, 146.4, 144.6, 144.3, 143.5, 134.9, 132.0, 124.2, 124.1, 122.9, 118.1, 116.0, 112.2, 112.1, 111.5, 111.4, 49.9, 47.1, 46.9, 34.8, 31.7; HRMS (EI, m/z): Calculated: 408.22, found: 408.2193 [M^+].

(5*S*,12*S*)-8-(*Tert*-butyl)-5,12-dihydro-5,12-[1,2]benzenotetracene-2,16-diamine (30)

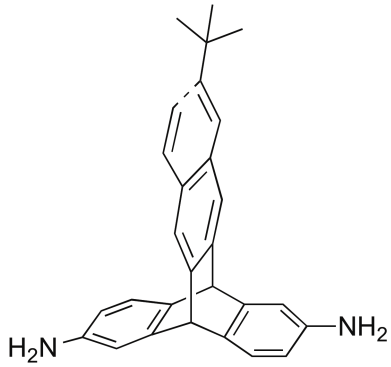

The compound (5*S*,12*S*)-8-(*tert*-butyl)-5,12-dihydro-5,12-[1,2]benzenotetracene-2,16-diamine (**30)** was synthesised according to the general procedure G.P 3. (5*R*,12*R*)-8-(*Tert*-butyl)-5,5a,6,11,11a,12-hexahydro-5,12-[1,2]benzeno-6,11-epoxytetracene-2,16-diamine (**29**) (2.20 g, 5.38 mmol) dissolved in ethanol (100 mL), perchloric acid (70 %, 35 mL). Purified by column chromatography $CHCl_3$/ ethyl acetate (7:3, v/v) to yield (5*S*,12*S*)-8-(*tert*-butyl)-5,12-dihydro-5,12-[1,2]benzenotetracene-2,16-diamine (**30**) (1.56 g, 3.99 mmol, 74 %) as a light yellow solid. Mp: 178-180 ºC; ν_{max} (cm^{-1}): 3443, 3348, 2951, 1614, 1479, 1329, 1263, 1184, 1111, 897, 824, 806, 762, 656, 646, 633, 596, 571, 538, 501; ^{1}H NMR (600 MHz, $CDCl_3$): δ_H (ppm) = 7.66 (s, 1H, Ar *H*), 7.64 (s, 1H, Ar *H*), 7.62 – 7.60 (m, 2H, Ar *H*), 7.43 (dd, 1H, *J* = 8.6, 1.9 Hz, Ar *H*), 7.13 (d, 2H, *J* = 7.8 Hz, Ar *H*), 6.77 (d, 2H, *J* = 2.2 Hz, Ar *H*), 6.28 (dd, 2H, *J* = 7.8, 2.2 Hz, Ar *H*), 5.25 (s, 1H, C*H*), 5.24 (s, 1H, C*H*), 3.49 (*b*s, 4H, NH_2), 1.35 (s, 9H, CH_3); ^{13}C NMR (151 MHz, $CDCl_3$) δ_C (ppm) = 148.1, 146.5, 144.0, 142.7, 142.2, 135.1, 131.7, 129.8, 124.1, 124.1, 122.6, 121.1, 120.5, 111.4, 111.0, 53.1, 53.0, 34.7, 31.3; HRMS (EI, m/z): Calculated: 390.21, found: 390.2076 [M^+].

5,5,8,8-Tetramethyl-1,4,5,6,7,8-hexahydro-1,4-epoxyanthracene (31)

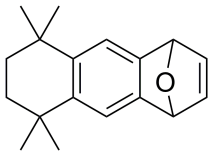

The compound 5,5,8,8-tetramethyl-1,4,5,6,7,8-hexahydro-1,4-epoxyanthracene (**31**) was synthesised according to the general procedure G.P. 1. 6,7-Dibromo-1,1,4,4-tetramethyl-1,2,3,4-tetrahydronaphthalene (**40**) (13.21 g, 38.0 mmol) and anhydrous furan (25 mL, 344 mmol) was dissolved in anhydrous THF (30 mL). n-BuLi (19.84 mL, 50.0 mmol) in anhydrous THF (10.0 mL) was added to yield desired product 5,5,8,8-tetramethyl-1,4,5,6,7,8-hexahydro-1,4-epoxyanthracene (**31**) (7.62 g, 30.0 mmol, 79 %) as a white powder. Mp: 124-126 ºC; ν_{max} (cm^{-1}): 2961, 2920, 2857, 1464, 1360, 1283, 1161, 1001, 968, 868, 853, 833, 694, 660; ^{1}H NMR (500 MHz, $CDCl_3$): δ_H (ppm) = 7.20 (s, 2H, Ar *H*), 6.98 (t, 2H, *J* = 1.0 Hz, C*H*), 5.65 (t, 2H, *J* = 1.0 Hz, C*H*), 1.64 (s, 4H, CH_2), 1.24 (s, 12H, CH_3); ^{13}C NMR (126 MHz, $CDCl_3$) δ_C (ppm) = 145.5, 142.7, 141.1, 118.7, 82.4, 77.2, 35.3, 34.6, 32.0, 31.9; HRMS (EI, m/z): Calculated: 254.17 found: 254.1678 [M^+].

***N*,*N*′-((5*R*,14*R*)-8,8,11,11-Tetramethyl-5,5a,6,8,9,10,11,13,13a,14-decahydro-5,14-[1,2]benzeno-6,13-epoxypentacene-2,18-diyl)dihexanamide (32)**

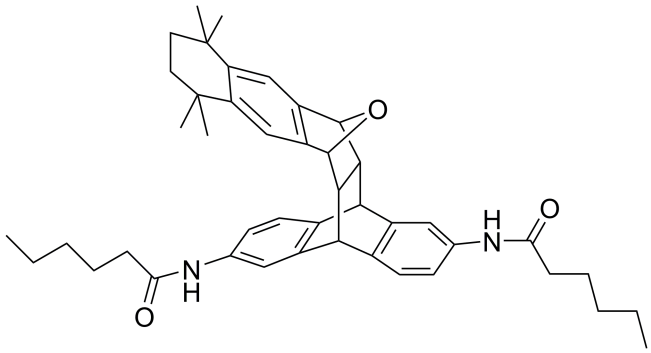

The compound *N*,*N*'-((5*R*,14*R*)-8,8,11,11-tetramethyl-5,5a,6,8,9,10,11,13,13a,14-decahydro-5,14-[1,2]benzeno-6,13-epoxypentacene-2,18-diyl)dihexanamide (**32**) was synthesised according to the general procedure reported by Swager et al.[150] *N*,*N*′-

(anthracene-2,6-diyl)dihexanamide (**61**) (3.00 g, 7.42 mmol) and 5,5,8,8-tetramethyl-1,4,5,6,7,8-hexahydro-1,4-epoxyanthracene (**31**) (1.89 g, 7.42 mmol) was dissolved in DMF (18.0 mL) and heated to 250°C in a microwave reactor for 2 h. After this time the solvent was removed under vacuum and washed with cold chloroform. Dissolved product in hot methanol, filtered off any insoluble material and removed solvent under vacuum. The crude product was recrystallized from acetonitrile to yield *N*,*N*′-((5*R*,14*R*)-8,8,11,11-tetramethyl-5,5a,6,8,9,10,11,13,13a,14-decahydro-5,14-[1,2]benzeno-6,13-epoxypentacene-2,18-diyl)dihexanamide (**32**) (2.60 g, 3.93 mmol, 53 %) as a white solid. Mp: 278-280 ºC; ν_{max} (cm^{-1}): 3283, 2955, 2928, 2859, 2359, 2340, 1676, 1651, 1597, 1537, 1483, 1420, 1267, 1213, 1184, 980, 883, 860, 837, 827, 735, 586, 544; ^{1}H NMR (500 MHz, $(CD_3)_2SO$): δ_H (ppm) = 9.69 (s, 1H, N*H*), 9.68 (s, 1H, N*H*), 7.58 (d, 1H, *J* = 2.0 Hz, Ar *H*), 7.55 (s, 1H, Ar *H*), 7.21-7.09 (m, 6H, Ar *H*), 4.87 (s, 1H, C*H*), 4.86 (s, 1H, C*H*), 4.35 (s, 2H, C*H*), 2.29-2.19 (m, 4H, CH_2), 1.98 (m, 2H, C*H*), 1.62-1.49 (m, 8H, CH_2), 1.37-1.20 (m, 8H, CH_2), 1.17 (s, 12H, CH_3), 0.90-0.81 (m, 6H, CH_3); ^{13}C NMR (126 MHz, $(CD_3)_2SO$) δ_C (ppm) = 171.4, 171.3, 145.3, 144.7, 142.8, 142.3, 139.3, 137.4, 137.2, 136.9, 124.0, 123.8, 116.9, 116.3, 116.2, 115.7, 115.4, 80.9, 80.8, 49.8, 49.4, 46.6, 46.6, 36.9, 36.8, 35.1, 34.5, 32.4, 32.0, 31.4, 31.3, 25.4, 25.3, 22.4, 22.4, 14.3; HRMS (EI, m/z): Calculated: 658.41 found: 658.4133 [M^+].

8,8,11,11-Tetramethyl-5,8,9,10,11,14-hexahydro-5,14-[1,2]benzenopentacene-2,18-diamine (33)

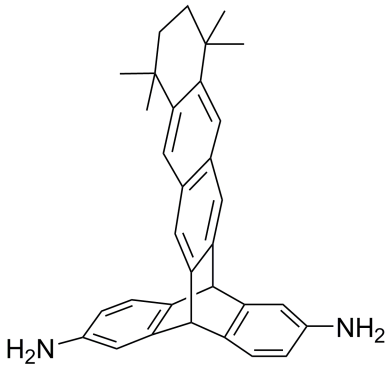

The compound *N*,*N*′-((5*R*,14*R*)-8,8,11,11-tetramethyl-5,5a,6,8,9,10,11,13,13a,14-decahydro-5,14-[1,2]benzeno-6,13-epoxypentacene-2,18-diyl)dihexanamide (**32**) (1.08 g,

1.63 mmol) was dissolved in anhydrous, degassed methanol (40 mL) and conc. HCl (20 mL) was added dropwise and subsequently heated to reflux for 24 h. The resulting precipitate was filtered off and washed with water. Precipitate was suspended in water (100 mL) and neutralised with ammonium hydroxide solution. Filtered off precipitate, washed with water and dried under N_2 to yield 8,8,11,11-tetramethyl-5,8,9,10,11,14-hexahydro-5,14-[1,2]benzenopentacene-2,18-diamine (**33**) (0.55 g, 1.22 mmol, 74 %) as an off white solid. Mp: Above 300 ºC; ν_{max} (cm^{-1}): 3298, 2951, 2928, 1661, 1595, 1533, 1477, 1458, 1410, 1265, 1190, 1109, 910, 841, 814, 748, 727, 637, 529; ^{1}H NMR (500 MHz, $(CD_3)_2SO$): δ_H (ppm) = 7.65 (s, 2H, Ar *H*), 7.60 (s, 2H, Ar *H*), 7.01 (d, 2H, *J* = 7.8 Hz, Ar *H*), 6.65 (d, 2H, *J* = 2.2 Hz, Ar *H*), 6.14 (dd, 2H, *J* = 7.8, 2.2 Hz, Ar *H*), 5.17 (s, 2H, C*H*), 4.82 (*b*s, 4H, NH_2), 1.67 (s, 4H, CH_2), 1.29 (s, 12H, CH_3); ^{13}C NMR (126 MHz, $(CD_3)_2SO$) δ_C (ppm) = 171.1, 146.1, 145.2, 143.4, 143.0, 142.5, 141.3, 139.1, 136.6, 129.5, 51.8, 36.3, 34.6, 34.1, 32.2, 30.8, 24.9, 21.9, 13.9; HRMS (EI, m/z): Calculated: 444.26 found: 444.2530 [M^+].

2,3,6,7-Tetramethoxy-9,10-dimethylanthracene (34)

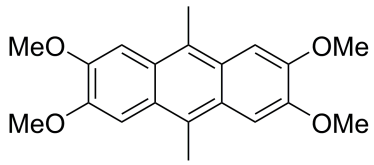

The compound 2,3,6,7-tetramethoxy-9,10-dimethylanthracene (**34**) was synthesised according to the procedure reported by McKeown et al.[173] A solution of veratrole (20 mL, 157.0 mmol), acetaldehyde (8.82 mL, 157.mmol) and CH_3CN (8.19 mL, 157 mmol) was cooled to 0 ºC. To this, *c*H_2SO_4 (75.0 mL) was added drop wise and maintained at 0 ºC for 2 h. The resulting solution was poured onto ice, neutralised with aqueous ammonium hydroxide solution and filtered off. Washed precipitate with water, MeOH and recrystalised from acetone to yield 2,3,6,7-tetramethoxy-9,10-dimethylanthracene (**34**) (5.86 g, 17.95 mmol, 11 %) as an off white solid. Mp: Above 300 ºC; ν_{max} (cm^{-1}): 2995, 2982, 2967, 2957, 2922, 1497, 1468, 1447, 1439, 1381, 1371, 1250, 1209, 1202, 1190, 1163, 1146, 1084, 1030, 959, 893, 822, 750; ^{1}H NMR (500 MHz, $CDCl_3$): δ_H (ppm) = 7.40 (s, 4H, Ar *H*), 4.08 (s, 12H, CH_3), 2.94 (s, 6H, CH_3); ^{13}C NMR (126 MHz, $CDCl_3$) δ_C

(ppm) = 148.9, 126.0, 124.0, 102.8, 55.8, 14.9; LRMS (EI, m/z): Calculated: 326.15 found: 326.1 [M^+].

(2-Chloropropan-2-yl)benzene (35)

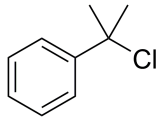

The compound (2-chloropropan-2-yl)benzene (**35**) was synthesised according to the procedure reported by Byrne et al.[174] 2-Phenyl-2-propanol (10.0 g, 73.4 mmol) was dissolved in anhydrous DCM and cooled to 0°C. A solution of $SOCl_2$ (6.93 mL, 95.5 mmol) in anhydrous DCM (10.0 mL) was added drop wise which was stirred at 0°C for 30 mins then allowed to warm to room temperature for 24 h. The resulting solution was poured into ice/water and extracted with DCM (3 x 100 mL), dried over $MgSO_4$ and removed solvent under vacuum to yield (2-chloropropan-2-yl)benzene (**35**) (10.46 g, 67.6 mmol, 92 %) as a light yellow clear oil. ν_{max} (cm^{-1}): 2976, 2361, 2340, 1495, 1447, 1387, 1369, 1260, 1128, 1098, 1074, 1030, 905, 764, 746, 698, 669, 613, 544; ^{1}H NMR (500 MHz, $CDCl_3$): δ_H (ppm) = 7.52-7.49 (m, 2H, Ar *H*), 7.38-7.33 (m, 2H, Ar *H*), 7.27-7.23 (m, 1H, Ar *H*), 1.60 (s, 6H, C*H*$_3$); ^{13}C NMR (126 MHz, $CDCl_3$) δ_C (ppm) = 146.4, 128.4, 127.7, 125.6, 69.8, 34.4; LRMS (EI, m/z): Calculated: 154.05 found: 154.0 [M^+].

1,1,2,2,3,3-Hexamethyl-2,3-dihydro-1*H*-indene (36)

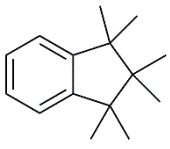

The compound 1,1,2,2,3,3-hexamethyl-2,3-dihydro-1*H*-indene (**36**) was synthesised according to the procedure reported by H. Mayr.[175] (2-Chloropropan-2-yl)benzene (**35**) (17.55 g, 113.5 mmol) and 2,3-dimethyl-2-butene (23.88 g, 284 mmol) was dissolved in anhydrous DCM (100 mL) and cooled to -78°C. $TiCl_4$ (4.31 g, 22.7 mmol) was added

dropwise and left at -78°C for 1 h. The resulting solution was allowed to warm to room temperature, poured into a water:HCL (100 mL:50 mL) solution and extracted with DCM (3 x 100 mL). Dried over $MgSO_4$ and removed solvent under vacuum. Product was purified by distillation to yield 1,1,2,2,3,3-hexamethyl-2,3-dihydro-1*H*-indene (**36**) (19.0 g, 93.9 mmol, 83 %) as a colourless oil. ν_{max} (cm^{-1}): 2982, 2955, 2868, 1481, 1450, 1375, 1368, 1111, 1026, 752; ^{1}H NMR (600 MHz, $CDCl_3$): δ_H (ppm) = 7.20 (m, 2H, Ar *H*), 7.13 (m, 2H, Ar *H*), 1.21 (s, 12H, C*H*$_3$), 0.89 (s, 6H, C*H*$_3$); ^{13}C NMR (151 MHz, $CDCl_3$) δ_C (ppm) = 150.4, 126.6, 122.5, 48.4, 47.7, 27.4, 21.5; LRMS (EI, m/z): Calculated: 202.17 found: 202.1 [M^+].

5,6-Dibromo-1,1,2,2,3,3-hexamethyl-2,3-dihydro-1*H*-indene (37)

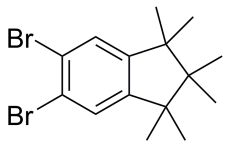

The compound 1,1,2,2,3,3-hexamethyl-2,3-dihydro-1*H*-indene (**36**) (5.0 g, 24.7 mmol) was dissolved in anhydrous DCM (60 mL) and Fe powder (catalytic amount) was added. To this solution, bromine (11.85 g, 74.13 mmol) was added drop wise over 30 mins and was left at room temperature for 4 h. The resulting reaction mixture was poured into water, organic layer was separated and washed with sodium carbonate solution (3 x 100 mL). The organic layer was dried over $MgSO_4$ and solvent removed under vacuum. The crude product was purified by recrystallisation (hexane) to yield 5,6-dibromo-1,1,2,2,3,3-hexamethyl-2,3-dihydro-1*H*-indene (**37**) (4.08 g, 11.33 mmol, 46 %) as a white crystalline solid. Mp: 118-119 ºC; ν_{max} (cm^{-1}): 2982, 2945, 2909, 2868, 1474, 1456, 1449, 1396, 1381, 1368, 1350, 1288, 1161, 1119, 1103, 1067, 872, 854, 756, 673, 584, 538; ^{1}H NMR (500 MHz, $CDCl_3$): δ_H (ppm) = 7.36 (s, 2H, Ar *H*), 1.21 (s, 12H, C*H*$_3$), 0.89 (s, 6H, C*H*$_3$); ^{13}C NMR (126 MHz, $CDCl_3$) δ_C (ppm) = 151.9, 128.0, 122.1, 48.9, 47.7, 27.2, 21.4; LRMS (EI, m/z): Calculated: 357.99 found: 357.9930 [M^+].

2,5-Dichloro-2,5-dimethylhexane (38)

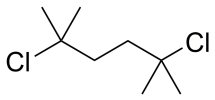

The compound 2,5-dichloro-2,5-dimethylhexane (**38**) was synthesised according to the procedure reported by S. A. Miller.[176] 2,5-Dimethyl-2,5-hexanediol (10.0 g, 68.4 mmol) and *conc.*HCl (150 mL) was combined and left to stir for 24 h. The resulting solid was filtered off, washed with water and recrystallized from methanol to yield 2,5-dichloro-2,5-dimethylhexane (**38**) (8.53 g, 46.60 mmol, 68 %) as a white crystalline solid. Mp: 65-66 ºC (lit[177] 65 ºC); ν_{max} (cm^{-1}): 2997, 2982, 2967, 2957, 2922, 1439, 1381, 1371, 1306, 1250, 1209, 1146, 1084, 957, 822; ^{1}H NMR (400 MHz, $CDCl_3$): δ_H (ppm) = 1.88 (s, 4H, C*H*$_2$), 1.53 (s, 12H, C*H*$_3$); ^{13}C NMR (126 MHz, $CDCl_3$) δ_C (ppm) = 70.5, 41.3, 32.7; LRMS (EI, m/z): Calculated: 182.06 found: 147.1 [M^+- Cl].

1,1,4,4-Tetramethyl-1,2,3,4-tetrahydronaphthalene (39)

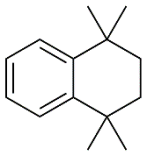

The compound 1,1,4,4-tetramethyl-1,2,3,4-tetrahydronaphthalene (**39**) was prepared according to the procedure reported by H. Toyama.[178] A solution of 2,5-Dichloro-2,5-dimethylhexane (**38**) (20.0 g, 109 mmol) in anhydrous benzene (250 mL, 2.8 mol) was heated to 50°C. To this $AlCl_3$ (5.84 g, 44.0 mmol) was added portion wise over 30 min, which was then left at 50°C for 24 h. The resulting solution was cooled to room temperature, poured into dilute hydrochloric acid and extracted with DCM (3 x 100 mL). The organic layer was washed with water and dilute sodium carbonate solution before being dried over $MgSO_4$. The solvent was removed under vacuum and the resulting orange oil was purified by vacuum distillation to yield 1,1,4,4-tetramethyl-1,2,3,4-tetrahydronaphthalene (**39**) (14.53 g, 77.0 mmol, 71 %) as a colourless oil. ν_{max} (cm^{-1}): 3647, 2959, 2922, 2860, 1487, 1456, 1439, 1362, 1040, 754; ^{1}H NMR (500 MHz, $CDCl_3$):

δ_H (ppm) = 7.33 (dd, 2H, *J* = 6.0, 3.4 Hz, Ar *H*), 7.16 (dd, 2H, *J* = 5.9, 3.4 Hz, Ar *H*), 1.71 (s, 4H, C*H*$_2$), 1.31 (s, 12H, C*H*$_3$); ^{13}C NMR (126 MHz, $CDCl_3$) δ_C (ppm) = 144.8, 126.5, 125.5, 35.1, 34.2, 31.9; LRMS (EI, m/z): Calculated: 188.16 found: 188.1 [M^+].

6,7-Dibromo-1,1,4,4-tetramethyl-1,2,3,4-tetrahydronaphthalene (40)

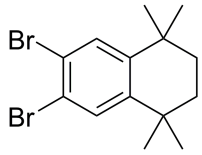

The compound 1,1,4,4-tetramethyl-1,2,3,4-tetrahydronaphthalene (**40**) (23.80 g, 126 mmol) was dissolved in anhydrous DCM (200 mL) and Fe powder (catalytic amount) was added**.** To this solution, bromine (60.60 g, 379 mmol) was added drop wise over 1 h and was left at room temperature for 3 h. The resulting reaction mixture was poured into water, organic layer separated and washed with sodium carbonate solution (3 x 100 mL). The organic layer was dried over $MgSO_4$ and solvent was removed under vacuum. The crude product was purified by column chromatography (Hex) to yield 6,7-dibromo-1,1,4,4-tetramethyl-1,2,3,4-tetrahydronaphthalene (**40**) (33.0 g, 95.0 mmol, 75 %) as a white crystalline solid. Mp: 111-112 ºC; ν_{max} (cm^{-1}): 2953, 2936, 2922, 2862, 1460, 1387, 1362, 1348, 1296, 1261, 1211, 1190, 1132, 1105, 1070, 1047, 1020, 887, 860, 839, 756, 685; ^{1}H NMR (500 MHz, $CDCl_3$): δ_H (ppm) = 7.53 (s, 2H, Ar H), 1.68 (s, 4H, CH_2), 1.28 (s, 12H, CH_3); ^{13}C NMR (126 MHz, $CDCl_3$) δ_C (ppm) = 146.4, 131.8, 121.4, 34.7, 34.3, 31.6; LRMS (EI, m/z): Calculated: 345.9 found: 345.9 [M^+].

(5*s*,12*s*)-2,3,16,17-Tetramethoxy-5,12-dimethyl-5,5a,6,11,11a,12-hexahydro-5,12-[1,2]benzeno-6,11-epoxytetracene (41)

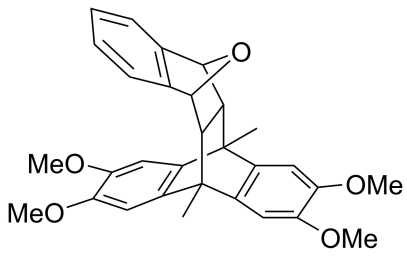

The compound (5*s*,12*s*)-2,3,16,17-tetramethoxy-5,12-dimethyl-5,5a,6,11,11a,12-hexahydro-5,12-[1,2]benzeno-6,11-epoxytetracene (**41**) was synthesised according to the general procedure G.P 2. 2,3,6,7-Tetramethoxy-9,10-dimethylanthracene (**34**) (2.00 g, 6.13 mmol) and 1,4-dihydro-1,4-epoxynaphthalene (**16**) (0.88 g, 6.13 mmol) dissolved in DMF (15.0 mL). Purified by column chromatography DCM/ ethyl acetate (9:1, v/v) to yield (5*s*,12*s*)-2,3,16,17-tetramethoxy-5,12-dimethyl-5,5a,6,11,11a,12-hexahydro-5,12-[1,2]benzeno-6,11-epoxytetracene (**41**) (2.38 g, 5.05 mmol, 83 %) as a light brown crystalline solid. Mp: 110-112 ºC; ν_{max} (cm^{-1}): 2932, 1508, 1485, 1458, 1404, 1331, 1281, 1242, 1223, 1192, 1153, 1045, 1018, 949, 922, 841, 752, 606, 575; ^{1}H NMR (500 MHz, $CDCl_3$): δH (ppm) = 7.13-7.10 (m, 2H, Ar *H*), 7.04-7.01 (m, 2H, Ar *H*), 6.88 (s, 2H, Ar *H*), 6.84 (s, 2H, Ar *H*), 4.99 (s, 2H, C*H*), 3.89 (s, 6H, CH_3), 3.83 (s, 6H, CH_3), 2.08 (s, 6H, CH_3), 2.01 (s, 2H, C*H*); ^{13}C NMR (126 MHz, $CDCl_3$) δC (ppm) =147.1, 147.1, 146.6, 140.5, 136.9, 126.4, 118.7, 106.8, 106.2, 79.8, 77.2, 56.6, 43.2, 17.3; HRMS (EI, m/z): Calculated: 470.21 found: 470.2108 [M^+].

(5*s*,12*s*)-2,3,16,17-Tetramethoxy-5,12-dimethyl-5,12-dihydro-5,12-[1,2]benzenotetracene (42)

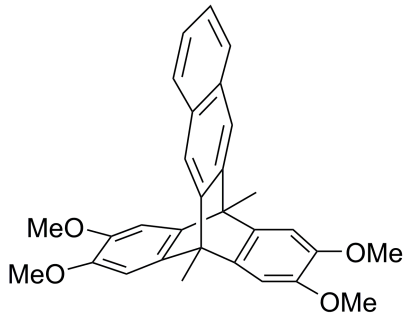

The compound (5*s*,12*s*)-2,3,16,17-tetramethoxy-5,12-dimethyl-5,12-dihydro-5,12-[1,2]benzenotetracene (**42**) was synthesised according to the general procedure G.P. 4. (5*s*,12*s*)-2,3,16,17-Tetramethoxy-5,12-dimethyl-5,5a,6,11,11a,12-hexahydro-5,12-[1,2]benzeno-6,11-epoxytetracene (**41**) (1.87 g, 3.97 mmol), TFA (40.0 mL) combined. Purified by column chromatography DCM/ ethyl acetate (9:1, v/v) to yield (5*s*,12*s*)-2,3,16,17-tetramethoxy-5,12-dimethyl-5,12-dihydro-5,12-[1,2]benzenotetracene (**42**) (1.32 g, 2.91 mmol, 73 %) as a light brown crystalline solid. Mp: 123-125 ºC; ν_{max} (cm^{-1}): 2967,

2936, 1601, 1485, 1458, 1431, 1404, 1281, 1223, 1192, 1165, 1146, 1042, 1018, 945, 883, 860, 756, 617, 579; ^{1}H NMR (500 MHz, $CDCl_3$): δH (ppm) = 7.72-7.68 (m, 2H, Ar *H*), 7.65 (s, 2H, Ar *H*), 7.38-7.34 (m, 2H, Ar *H*), 6.98 (s, 4H, Ar *H*), 3.85 (s, 12H, C*H*$_3$), 2.50 (s, 6H, C*H*$_3$); ^{13}C NMR (126 MHz, $CDCl_3$) δC (ppm) = 146.2, 145.9, 140.8, 131.3, 127.4, 125.7, 118.2, 106.0, 56.4, 47.5, 14.2; HRMS (EI, m/z): Calculated: 452.20 found: 452.1969 [M^+].

(5*s*,12*s*)-5,12-Dimethyl-5,12-dihydro-5,12-[1,2]benzenotetracene-2,3,16,17-tetraol (43)

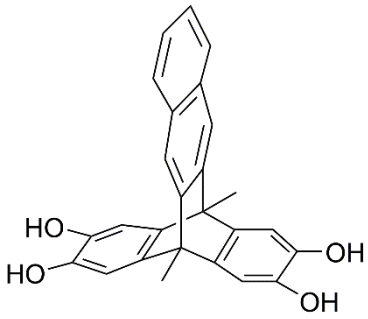

The compound (5*s*,12*s*)-5,12-dimethyl-5,12-dihydro-5,12-[1,2]benzenotetracene-2,3,16,17-tetraol (**43**) was synthesised according to the general procedure G.P 5. (5*s*,12*s*)-2,3,16,17-Tetramethoxy-5,12-dimethyl-5,12-dihydro-5,12-[1,2]benzenotetracene (**42**) (1.32 g, 2.91 mmol) dissolved in anhydrous DCM (40 mL). BBr_3 (2.18 g, 8.74 mmol) was added to yield (5*s*,12*s*)-5,12-dimethyl-5,12-dihydro-5,12-[1,2]benzenotetracene-2,3,16,17-tetraol (**43**) (0.84 g, 2.13 mmol, 73 %) as a white powder. Mp: Above 300 ºC; ν_{max} (cm^{-1}): 3326, 2981, 1695, 1612, 1491, 1440, 1378, 1293, 1248, 1170, 983, 882, 800, 764, 665, 619; ^{1}H NMR (500 MHz, $(CD_3)_2CO$): δH (ppm) = 7.77-7.73 (m, 2H, Ar *H*), 7.67 (s, 2H, Ar *H*), 7.48 (*b*s, 3H, O*H*), 7.37-7.33 (m, 2H, Ar *H*), 6.91 (s, 4H, Ar *H*), 2.34 (s, 6H, C*H*$_3$); ^{13}C NMR (126 MHz, $(CD_3)_2CO$) δC (ppm) =148.0, 142.3, 141.0, 132.3, 128.2, 126.2, 118.5, 109.9, 47.6, 29.8, 14.6; HRMS (EI, m/z): Calculated: 396.14 found: 396.1361 [M^+].

(5*s*,12*s*)-8-(*Tert*-butyl)-2,3,16,17-tetramethoxy-5,12-dimethyl-5,5a,6,11,11a,12-hexahydro-5,12-[1,2]benzeno-6,11-epoxytetracene (44)

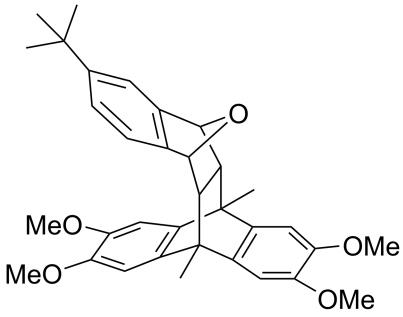

The compound (5*s*,12*s*)-8-(*tert*-butyl)-2,3,16,17-tetramethoxy-5,12-dimethyl-5,5a,6,11,11a,12-hexahydro-5,12-[1,2]benzeno-6,11-epoxytetracene (**44**) was synthesised according to the general procedure G.P 2. 2,3,6,7-Tetramethoxy-9,10-dimethylanthracene (**34**) (2.50 g, 7.66 mmol) and 6-(*tert*-butyl)-1,4-dihydro-1,4-epoxynaphthalene (**28**) (1.53 g, 7.66 mmol) dissolved in DMF (15.0 mL). Purified by column chromatography (DCM) to yield (5*s*,12*s*)-8-(*tert*-butyl)-2,3,16,17-tetramethoxy-5,12-dimethyl-5,5a,6,11,11a,12-hexahydro-5,12-[1,2]benzeno-6,11-epoxytetracene (**44**) (1.87 g, 3.55 mmol, 46 %) as a light brown crystalline solid. Mp: 141-143 ºC; ν_{max} (cm^{-1}): 2961, 1580, 1483, 1460, 1402, 1288, 1240, 1194, 1152, 1045, 1022, 854, 843, 816, 783, 746, 677, 606, 563; ^{1}H NMR (500 MHz, $CDCl_3$): δ_H (ppm) = 7.15 (s, 1H, Ar *H*), 7.06-7.00 (m, 2H, Ar *H*), 6.87 (s, 1H, Ar *H*), 6.86 (s, 1H, Ar *H*), 6.84 (s, 1H, Ar *H*), 6.83 (s, 1H, Ar *H*), 4.96 (s, 1H, C*H*), 4.95 (s, 1H, C*H*), 3.89 (s, 3H, CH_3), 3.88 (s, 3H, CH_3), 3.83 (s, 3H, CH_3), 3.82 (s, 3H, CH_3), 2.08 (s, 3H, CH_3), 2.06 (s, 3H, CH_3), 2.02-1.98 (m, 2H, C*H*), 1.24 (s, 9H, CH_3); ^{13}C NMR (126 MHz, $CDCl_3$) δ_C (ppm) = 149.6, 147.0, 146.8, 146.4, 144.1, 140.4, 136.8, 122.9, 118.0, 115.8, 106.6, 106.6, 106.0, 106.0, 79.8, 79.4, 56.6, 56.5, 56.4-56.3 (cluster of peaks), 43.1, 34.7, 31.6, 17.1; HRMS (EI, m/z): Calculated: 526.27 found: 526.2721 [M^+].

(5*s*,12*s*)-8-(*Tert*-butyl)-2,3,16,17-tetramethoxy-5,12-dimethyl-5,12-dihydro-5,12-[1,2]benzenotetracene (45)

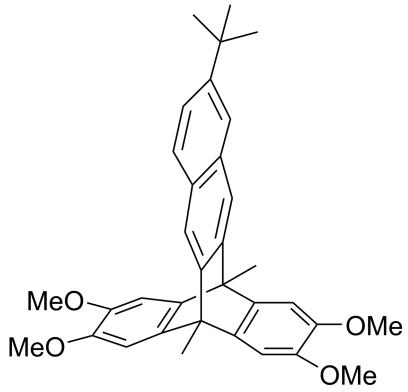

The compound (5*s*,12*s*)-8-(*tert*-butyl)-2,3,16,17-tetramethoxy-5,12-dimethyl-5,12-dihydro-5,12-[1,2]benzenotetracene (**45**) was prepared according to the general procedure G.P 4. (5*s*,12*s*)-8-(*Tert*-butyl)-2,3,16,17-tetramethoxy-5,12-dimethyl-5,5a,6,11,11a,12-hexahydro-5,12-[1,2]benzeno-6,11-epoxytetracene (**44**) (1.87 g, 3.55 mmol) dissolved in TFA (50 mL). Purified by column chromatography to yield (5*s*,12*s*)-8-(*tert*-butyl)-2,3,16,17-tetramethoxy-5,12-dimethyl-5,12-dihydro-5,12-[1,2]benzenotetracene (**45**) (1.65 g, 3.24 mmol, 91 %) as a brown crystalline solid. Mp: 148-150 ºC; ν_{max} (cm^{-1}): 2958.80, 2827.64, 2358.94, 1603, 1582, 1485, 1460, 1435, 1404, 1279, 1225, 1194, 1175, 1150, 1042, 1022, 899, 885, 866, 812, 762, 752, 735, 621, 569; ^{1}H NMR (600 MHz, $CDCl_3$): δ_H (ppm) = 7.66-7.63 (m, 3H, Ar *H*), 7.61 (s, 1H, Ar *H*), 7.45 (dd, 1H, *J* = 8.6, 2.0 Hz, Ar *H*), 6.98 (s, 2H, Ar *H*), 6.97 (s, 2H, Ar *H*), 3.85 (s, 6H, C*H*$_3$), 3.84 (s, 6H, C*H*$_3$), 2.49 (s, 3H, C*H*$_3$), 2.48 (s, 3H, C*H*$_3$), 1.35 (s, 9H, C*H*$_3$); ^{13}C NMR (151 MHz, $CDCl_3$) δ_C (ppm) = 148.5, 146.1, 145.9, 145.3, 140.9, 140.9, 131.1, 129.3, 127.0, 124.4, 122.7, 118.3, 117.7 , 106.0, 55.4, 47.5, 34.7, 31.3, 14.2; HRMS (EI, m/z): Calculated: 508.26 found: 508.2601 [M^+].

(5*s*,12*s*)-8-(*Tert*-butyl)-5,12-dimethyl-5,12-dihydro-5,12-[1,2]benzenotetracene-2,3,16,17-tetraol (46)

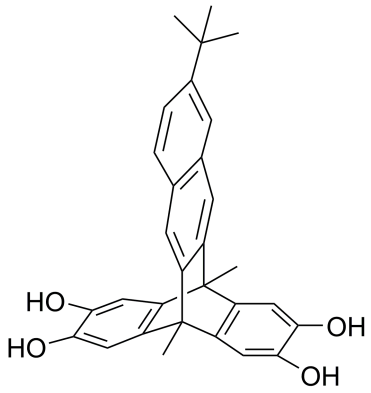

The compound (5*s*,12*s*)-8-(*tert*-butyl)-5,12-dimethyl-5,12-dihydro-5,12-[1,2]benzenotetracene-2,3,16,17-tetraol (**46**) was synthesised according to the general procedure G.P 5. (5*s*,12*s*)-8-(*Tert*-butyl)-2,3,16,17-tetramethoxy-5,12-dimethyl-5,12-dihydro-5,12-[1,2]benzenotetracene (**45**) (1.65 g, 3.24 mmol) dissolved in anhydrous DCM (40 mL). BBr_3 (2.44 g, 9.73 mmol) was added to yield (5*s*,12*s*)-8-(*tert*-butyl)-5,12-dimethyl-5,12-dihydro-5,12-[1,2]benzenotetracene-2,3,16,17-tetraol (**46**) (1.34 g, 2.96 mmol, 91 %) as a white solid. Mp: 280-282 ºC; ν_{max} (cm^{-1}): 3451, 3325, 2965, 1609, 1485, 1449, 1379, 1292, 1128, 984, 899, 878, 810, 760, 633, 617, 608, 422, 413, 401; ^{1}H NMR (600 MHz, $(CD_3)_2CO$): δ_H (ppm) = 7.72 (d, 1H, *J* = 2.0 Hz, Ar *H*), 7.69 (d, 1H, *J* = 8.6 Hz, Ar *H*), 7.65 (s, 1H, Ar *H*), 7.62 (s, 1H, Ar *H*), 7.49 (dd, 1H, *J* = 8.6, 2.0 Hz, Ar *H*), 7.46 (*b*s, 2H, O*H*), 6.90 (s, 2H, Ar *H*), 6.89 (s, 2H, Ar *H*), 2.34 (s, 3H, C*H*$_3$), 2.33 (s, 3H, C*H*$_3$), 1.35 (s, 9H, C*H*$_3$); ^{13}C NMR (151 MHz, $(CD_3)_2CO$) δC (ppm) = 147.85, 146.92, 146.48, 141.31, 140.21, 131.26, 129.42, 127.03, 123.93, 122.61, 117.82, 117.05, 108.93, 46.65, 34.33, 30.70, 13.67; HRMS (EI, m/z): Calculated: 452.20 found: 452.1992 [M^+].

1,1,2,2,3,3-Hexamethyl-2,3,5,8-tetrahydro-1*H*-5,8-epoxycyclopenta[*b*]naphthalene (47)

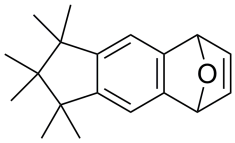

The compound 1,1,2,2,3,3-hexamethyl-2,3,5,8-tetrahydro-1*H*-5,8-epoxycyclopenta[*b*]naphthalene (**47**) was prepared according to the general procedure G.P 1. (**37**) (4.0 g, 11.1 mmol) and anhydrous furan (7.3 mL, 100.0 mmol) dissolved in anhydrous THF (15.0 mL). n-BuLi (5.78 mL, 14.4 mmol) in anhydrous THF (5.0 mL) was added to yield desired product 1,1,2,2,3,3-hexamethyl-2,3,5,8-tetrahydro-1*H*-5,8-epoxycyclopenta[*b*]naphthalene (**47**) (1.68 g, 6.26 mmol, 56 %) as a white powder. Mp: 132-133 ºC; ν_{max} (cm^{-1}): 3003, 2986, 2947, 2864, 1447, 1375, 1368, 1281, 1148, 1123, 999, 897, 889, 866, 849, 772, 748, 704, 652, 613, 550, 538, 527, 505; ^{1}H NMR (500 MHz, $CDCl_3$): δ_H (ppm) = 7.02 (t, 2H, *J* = 1.1 Hz, C*H*), 7.00 (s, 2H, Ar *H*), 5.65 (t, 2H, *J* = 1.1 Hz, C*H*), 1.15 (s, 6H, CH_3), 1.14 (s, 6H, CH_3) 0.86 (s, 3H, CH_3), 0.85 (s, 3H, CH_3); ^{13}C NMR (126 MHz, $CDCl_3$) δ_C (ppm) = 147.5, 146.8, 142.9, 115.1, 82.4, 48.7, 47.3, 27.5, 27.2, 21.7, 21.4; HRMS (EI, m/z): Calculated: 268.18 found: 268.1831 [M^+].

Hexamethylindan adduct (48)

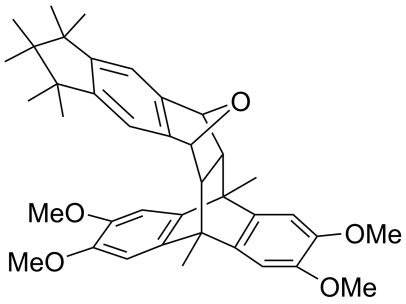

The hexamethylindan adduct (**48**) was prepared according to the general procedure G.P 2. In a sealed vessel, 2,3,6,7-tetramethoxy-9,10-dimethylanthracene (**34**) (2.0 g, 6.13 mmol)

and 1,1,2,2,3,3-hexamethyl-2,3,5,8-tetrahydro-1*H*-5,8-epoxycyclopenta[*b*]naphthalene (**47**) (1.64 g, 6.13 mmol) dissolved in DMF (20.0 mL. Purified by column chromatography ($CHCl_3$) to yield hexamethylindan adduct (**48**) (0.98 g, 1.65 mmol, 54 %) as a light brown crystalline solid. Mp: 125-127 ºC; ν_{max} (cm^{-1}): 2936, 1485, 1458, 1281 1242, 1196, 1150, 1045, 1022, 853, 748, 610, 567; ^{1}H NMR (500 MHz, $CDCl_3$): δ_H (ppm) = 6.87 (s, 2H, Ar *H*), 6.84 (s, 2H, Ar *H*), 6.83 (s, 2H, Ar *H*), 4.92 (s, 2H, C*H*), 3.89 (s, 6H, CH_3), 3.83 (s, 6H, CH_3), 2.07 (s, 6H, CH_3), 2.01 (s, 2H, C*H*), 1.10 (s, 12H, CH_3), 0.81 (s, 3H, CH_3), 0.79 (s, 3H, C*H*); ^{13}C NMR (126 MHz, $CDCl_3$) δ_C (ppm) = 148.6, 147.0, 146.5, 145.9, 140.7, 137.0, 113.1, 106.8, 106.1, 79.8, 56.9, 56.6, 56.5, 48.7, 47.5, 43.3, 27.9, 27.4, 21.8, 21.5, 17.3; HRMS (EI, m/z): Calculated: 594.33 found: 594.3339 [M^+].

(6*s*,11*s*)-8,9,17,18-Tetramethoxy-1,1,2,2,3,3,6,11-octamethyl-2,3,6,11-tetrahydro-1*H*-6,11-[1,2]benzenocyclopenta[*b*]tetracene (49)

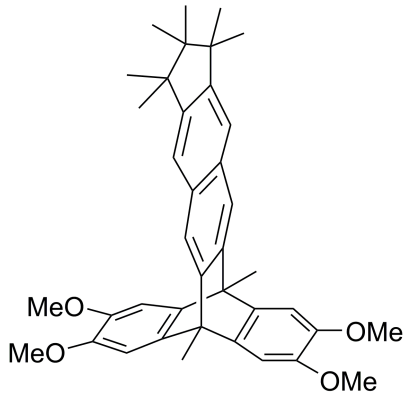

The compound (6*s*,11*s*)-8,9,17,18-tetramethoxy-1,1,2,2,3,3,6,11-octamethyl-2,3,6,11-tetrahydro-1*H*-6,11-[1,2]benzenocyclopenta[*b*]tetracene (**49**) was prepared according to the general procedure G.P 4. Hexamethylindan adduct (**48**) (1.86 g, 3.13 mmol) dissolved in TFA (60 mL). Purified by column chromatography $CHCl_3$/ hexane (1:9, v/v) to yield (6*s*,11*s*)-8,9,17,18-tetramethoxy-1,1,2,2,3,3,6,11-octamethyl-2,3,6,11-tetrahydro-1*H*-6,11-[1,2]benzenocyclopenta[*b*]tetracene (**49**) (1.22 g, 2.12 mmol, 68 %) as a light brown crystalline solid. Mp: 180-182 ºC; ν_{max} (cm^{-1}): 2947, 1485, 1458, 1435, 1404, 1281, 1227, 1165, 1146, 1042, 1022, 899, 752, 621; ^{1}H NMR (500 MHz, $CDCl_3$): δH (ppm) = 7.63 (s, 2H, Ar *H*), 7.44 (s, 2H, Ar *H*), 6.97 (s, 4H, Ar *H*), 3.84 (s, 12H, CH_3), 2.48 (s, 6H, CH_3),

1.24 (s, 12H, CH_3), 0.85 (s, 6H, CH_3); ^{13}C NMR (126 MHz, $CDCl_3$) δC (ppm) = 150.6, 146.3, 145.1, 141.1, 131.2, 120.5, 118.0, 106.2, 56.6, 48.9, 47.6, 47.5, 28.0, 21.5, 14.3; HRMS (EI, m/z): Calculated: 576.32 found: 576.3239 [M^+].

(6*s*,11*s*)-1,1,2,2,3,3,6,11-Octamethyl-2,3,6,11-tetrahydro-1*H*-6,11-[1,2]benzenocyclopenta[*b*]tetracene-8,9,17,18-tetraol (50)

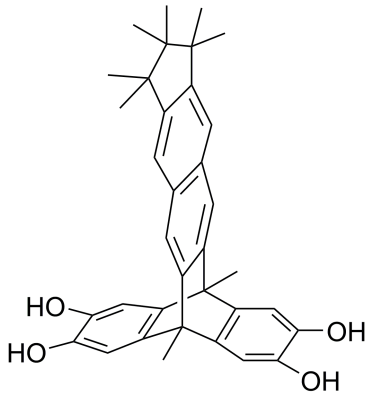

The compound (6*s*,11*s*)-1,1,2,2,3,3,6,11-octamethyl-2,3,6,11-tetrahydro-1*H*-6,11 [1,2]benzenocyclopenta[*b*]tetracene-8,9,17,18-tetraol (**50**) was synthesised according to the general procedure G.P 5. (6*s*,11*s*)-8,9,17,18-Tetramethoxy-1,1,2,2,3,3,6,11-octamethyl-2,3,6,11-tetrahydro-1*H*-6,11 [1,2]benzenocyclopenta[*b*]tetracene (**49**) (1.22 g, 2.12 mmol) dissolved in anhydrous DCM (60 mL). BBr_3 (1.59 g, 6.35 mmol) was added. The crude product purified by reprecipitation from ethyl acetate using hexane to yield (6*s*,11*s*)-1,1,2,2,3,3,6,11-octamethyl-2,3,6,11-tetrahydro-1*H*-6,11 [1,2]benzenocyclopenta[*b*]tetracene-8,9,17,18-tetraol (**50**) (0.43 g, 0.83 mmol, 39 %) as a light brown solid. Mp: Above 300 ºC; ν_{max} (cm^{-1}): 3368, 2955, 1612, 1485, 1447, 1377, 1296, 1169, 984, 903, 876, 837, 814, 760, 621; ^{1}H NMR (500 MHz, $(CD_3)_2CO$): δH (ppm) = 7.61 (s, 2H, Ar *H*), 7.49 (s, 2H, Ar *H*), 7.44 (s, 3H, O*H*), 6.88 (s, 4H, Ar *H*), 2.32 (s, 6H, CH_3), 1.25 (s, 12H, CH_3), 0.87 (s, 6H, CH_3); ^{13}C NMR (126 MHz, $(CD_3)_2CO$) δC (ppm) = 150.6, 146.8, 142.2, 142.1, 141.2, 132.2, 121.2, 118.4, 109.8, 109.7, 49.3, 48.0, 47.5, 29.8, 28.2, 21.8, 14.6; HRMS (EI, m/z): Calculated: 520.26 found: 520.2608 [M^+].

(5*s*,14*s*)-2,3,18,19-Tetramethoxy-5,8,8,11,11,14-hexamethyl-5,5a,6,8,9,10,11,13,13a,14-decahydro-5,14-[1,2]benzeno-6,13-epoxypentacene (51)

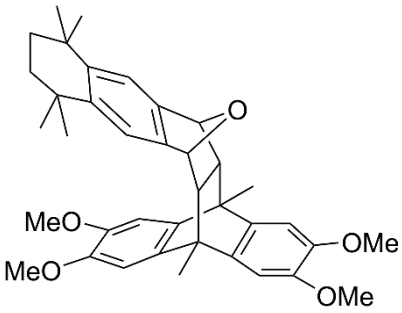

The compound (5*s*,14*s*)-2,3,18,19-tetramethoxy-5,8,8,11,11,14-hexamethyl-5,5a,6,8,9,10,11,13,13a,14-decahydro-5,14-[1,2]benzeno-6,13-epoxypentacene (**51**) was synthesised according to the general procedure G.P 2. 2,3,6,7-Tetramethoxy-9,10-dimethylanthracene (**34**) (2.0 g, 6.0 mmol) and 5,5,8,8-tetramethyl-1,4,5,6,7,8-hexahydro-1,4-epoxyanthracene (**31**) (1.56 g, 6.0 mmol) dissolved in DMF (15.0 mL). Purified by column chromatography DCM/ ethyl acetate (9:1, v/v) to yield (5*s*,14*s*)-2,3,18,19-tetramethoxy-5,8,8,11,11,14-hexamethyl-5,5a,6,8,9,10,11,13,13a,14-decahydro-5,14-[1,2]benzeno-6,13-epoxypentacene (**51**) (2.69 g, 4.62 mmol, 77 %) as a light brown crystalline solid. Mp: 288-290 ºC; ν_{max} (cm^{-1}): 2934, 1506, 1489, 1437, 1404, 1279, 1242, 1227, 1196, 1163, 1049, 1032, 854, 835, 822, 785, 748; ^{1}H NMR (500 MHz, $CDCl_3$): δH (ppm) = 7.03 (s, 2H, Ar *H*), 6.87 (s, 2H, Ar *H*), 6.84 (s, 2H, Ar *H*), 4.92 (s, 2H, C*H*), 3.89 (s, 6H, CH_3), 3.83 (s, 6H, CH_3), 2.07 (s, 6H, CH_3), 1.99 (s, 2H, C*H*), 1.59 (s, 4H, CH_2), 1.19 (s, 12H, CH_3); ^{13}C NMR (126 MHz, $CDCl_3$) δC (ppm) = 146.8, 146.4, 144.1, 142.5, 140.5, 136.8, 116.4, 106.7, 106.0, 79.6, 56.8, 56.4, 56.4, 43.1, 35.2, 34.4, 32.1, 31.9, 17.1; HRMS (EI, m/z): Calculated: 580.32 found: 580.3181 [M^+].

2,3,18,19-Tetramethoxy-5,8,8,11,11,14-hexamethyl-5,8,9,10,11,14-hexahydro-5,14-[1,2]benzenopentacene (52)

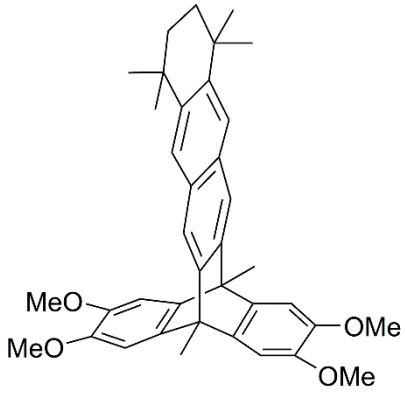

The compound 2,3,18,19-tetramethoxy-5,8,8,11,11,14-hexamethyl-5,8,9,10,11,14-hexahydro-5,14-[1,2]benzenopentacene (**52**) was synthesised according to the general procedure G.P 4. (5*s*,14*s*)-2,3,18,19-Tetramethoxy-5,8,8,11,11,14-hexamethyl-5,5a,6,8,9,10,11,13,13a,14-decahydro-5,14-[1,2]benzeno-6,13-epoxypentacene (**51**) (2.0 g, 3.4 mmol) dissolved in TFA (40 mL). Purified by column chromatography ($CHCl_3$) to yield 2,3,18,19-tetramethoxy-5,8,8,11,11,14-hexamethyl-5,8,9,10,11,14-hexahydro-5,14-[1,2]benzenopentacene (**52**) (1.20 g, 2.1 mmol, 62 %) as a white powder. Mp: Above 300 ºC; ν_{max} (cm^{-1}): 2955, 2928, 2859, 1601, 1489, 1462, 1439, 1404, 1285, 1250, 1165, 1146, 1042, 903, 868, 856, 764, 752, 633, 621, 536; ^{1}H NMR (500 MHz, $CDCl_3$): δH (ppm) = 7.64 (s, 2H, Ar *H*), 7.56 (s, 2H, Ar *H*), 6.96 (s, 4H, Ar *H*), 3.84 (s, 12H, C*H*$_3$), 2.47 (s, 6H, C*H*$_3$), 1.71 (s, 4H, C*H*$_2$), 1.31 (s, 12H, C*H*$_3$); ^{13}C NMR (126 MHz, $CDCl_3$) δC (ppm) = 146.1, 145.0, 143.9, 140.8, 129.5, 124.5, 117.4, 106.0, 56.4, 47.4, 35.1, 34.4, 32.5, 14.2; HRMS (EI, m/z): Calculated: 562.32 found: 562.3069 [M^+].

5,8,8,11,11,14-Hexamethyl-5,8,9,10,11,14-hexahydro-5,14-[1,2]benzenopentacene-2,3,18,19-tetraol (53)

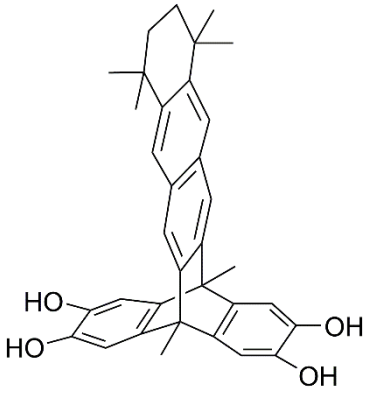

The compound 5,8,8,11,11,14-hexamethyl-5,8,9,10,11,14-hexahydro-5,14-[1,2]benzenopentacene-2,3,18,19-tetraol (**53**) was synthesised according to the general procedure G.P 5. 2,3,18,19-Tetramethoxy-5,8,8,11,11,14-hexamethyl-5,8,9,10,11,14-hexahydro-5,14-[1,2]benzenopentacene (**52**) (1.18 g, 2.09 mmol) dissolved in anhydrous DCM (40 mL). BBr_3 (1.57 g, 6.3 mmol) was added to yield 5,8,8,11,11,14-hexamethyl-5,8,9,10,11,14-hexahydro-5,14-[1,2]benzenopentacene-2,3,18,19-tetraol (**53**) (0.98 g, 1.93 mmol, 92 %) as a white powder. Mp: Above 300 ºC; ν_{max} (cm^{-1}): 3121, 2951, 2228, 1592, 1491, 1442, 1376, 1299, 1265, 1163, 969, 865, 763, 680; ^{1}H NMR (500 MHz, $(CD_3)_2CO$): δH (ppm) = 7.72 (s, 2H, Ar *H*), 7.56 (s, 2H, Ar *H*), 6.88 (s, 4H, Ar *H*), 2.32 (s, 6H, CH_3), 1.73 (s, 4H, CH_2), 1.33 (s, 12H, CH_3); ^{13}C NMR (126 MHz, $(CD_3)_2CO$) δC (ppm) = 146.1, 143.2, 140.2, 129.8, 124.5, 116.9, 108.8, 108.8, 46.6, 35.0, 34.1, 31.8, 13.7; HRMS (EI, m/z): Calculated: 506.25 found: 506.2456 [M^+].

(5*s*,12*s*)-2,3,16,17-Tetramethoxy-5,12-dimethyl-8-(trifluoromethyl)-5,5a,6,11,11a,12-hexahydro-5,12-[1,2]benzeno-6,11-epoxytetracene (54)

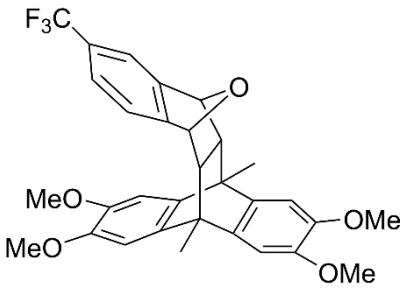

The compound (5*s*,12*s*)-2,3,16,17-tetramethoxy-5,12-dimethyl-8-(trifluoromethyl)-5,5a,6,11,11a,12-hexahydro-5,12-[1,2]benzeno-6,11-epoxytetracene (**54**) was synthesised according to the general procedure G.P 2. 2,3,6,7-Tetramethoxy-9,10-dimethylanthracene (**34**) (2.50 g, 7.66 mmol) and 6-(trifluoromethyl)-1,4-dihydro-1,4-epoxynaphthalene (**25**) (1.63 g, 7.66 mmol) dissolved in DMF (15.0 mL). Purified by column chromatography DCM/ ethyl acetate (95:5, v/v) to yield (5*s*,12*s*)-2,3,16,17-tetramethoxy-5,12-dimethyl-8-(trifluoromethyl)-5,5a,6,11,11a,12-hexahydro-5,12-[1,2]benzeno-6,11-epoxytetracene (**54**) (1.71 g, 3.18 mmol, 41 %) as a light brown crystalline solid. Mp: 138-140 ºC; ν_{max} (cm^{-1}): 2938, 1506, 1485, 1462, 1437, 1404, 1319, 1292, 1279, 1196, 1148, 1113, 1045, 1020, 951, 885, 843, 818, 783, 746, 677, 669, 660, 606, 579; ^{1}H NMR (500 MHz, $CDCl_3$): δ_H (ppm) = 7.37 (s, 1H, Ar *H*), 7.34 (d, 1H, *J* = 7.7 Hz, Ar *H*), 7.23 (d, 1H, *J* = 7.7 Hz, Ar *H*), 6.88 (s, 1H, Ar *H*), 6.87 (s, 1H, Ar *H*), 6.84 (s, 2H, Ar *H*), 5.05 (s, 1H, C*H*), 5.04 (s, 1H, C*H*), 3.89 (s, 3H, CH_3), 3.88 (s, 3H, CH_3), 3.84 (s, 6H, CH_3), 2.08 (s, 6H, CH_3), 2.02 (m, 2H, C*H*); ^{13}C NMR (126 MHz, $CDCl_3$) δ_C (ppm) = 150.7, 147.8, 147.0, 146.5, 140.1, 136.5, 128.9, 128.6, 125.3, 124.0, 123.1, 118.8, 115.7, 106.6, 106.0, 79.5, 56.3, 55.8, 55.7, 43.0, 17.1; HRMS (EI, m/z): Calculated: 538.20 found: 538.1969 [M^+].

(5*s*,12*s*)-5,12-Dimethyl-8-(trifluoromethyl)-5,12-dihydro-5,12-[1,2]benzenotetracene-2,3,16,17-tetraol (55)

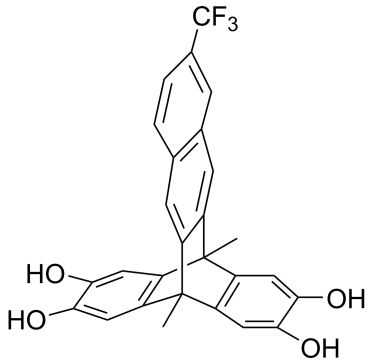

The compound (5*s*,12*s*)-5,12-dimethyl-8-(trifluoromethyl)-5,12-dihydro-5,12-[1,2]benzenotetracene-2,3,16,17-tetraol (**55**) was synthesised according to the general procedure G.P 5. (**54**) (1.39 g, 2.58 mmol) dissolved in anhydrous DCM (40.0 mL). BBr_3

(2.00 g, 8.0 mmol) was added to yield (**55**) (0.58 g, 1.28 mmol, 50 %) as an off white solid. Mp: Above 300°C; ν_{max} (cm^{-1}): 3352, 2970, 1612, 1487, 1443, 1379, 1329, 1298, 1263, 1186, 1155, 1117, 1065, 986, 934, 907, 843, 812, 762, 619, 598; ^{1}H NMR (600 MHz, (CD_3OD): δ_H (ppm) = 8.04 (s, 1H, Ar *H*), 7.85 (d, 1H, *J* = 8.5 Hz, Ar *H*), 7.69 (s, 1H, Ar *H*), 7.66 (s, 1H, Ar *H*), 7.51 (dd, 1H, *J* = 8.5, 1.9 Hz, Ar *H*), 6.84 (s, 4H, Ar *H*), 2.32 (s, 6H, C*H*$_3$); ^{13}C NMR (151 MHz, (CD_3OD) δ_C (ppm) = 149.7, 148.7, 141.4, 139.7, 139.6, 132.8, 130.2, 128.3, 126.5-120.3 (cluster of peaks), 117.8, 117.0, 108.7, 108.7, 60.1, 46.7, 46.6, 13.1; HRMS (EI, m/z): Calculated: 464.12 found: 464.1229 [M^+].

5,7-Bis(trifluoromethyl)-1,4-dihydro-1,4-epoxynaphthalene (56)

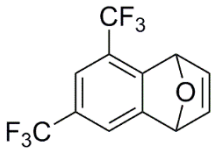

The compound 5,7-bis(trifluoromethyl)-1,4-dihydro-1,4-epoxynaphthalene (**56**) was synthesised according to the general procedure reported by Schlosser.[179] 1,3-Bis(trifluoromethyl)-4-chlorobenzene (10.0 g, 40.2 mmol) was dissolved in anhydrous THF (80 mL) and cooled to -78°C. *n*-butyllithium (20.9 mL, 52.3 mmol), in anhydrous THF (10.0 mL), was added dropwise and left at -78°C for 1 h. The resulting solution was transferred and added dropwise to a solution of anhydrous furan (88 mL, 1.2 mol) and left at room temperature for 24 h. Solvent was removed under vacuum, redissolved in diethyl ether (10.0 mL) and passed through a pad of neutral aluminium (eluent – diethyl ether). Concentrated under vacuum and distilled to yield 5,7-bis(trifluoromethyl)-1,4-dihydro-1,4-epoxynaphthalene (**56**) (3.65 g, 13.0 mmol, 32 %) as a colourless oil. ν_{max} (cm^{-1}): 3036, 1389, 1325, 1287, 1256, 1192, 1175, 1142, 1069, 899, 872, 843, 820, 752, 704, 667, 635, 625; ^{1}H NMR (500 MHz, $CDCl_3$): δ_H (ppm) = 7.60 (s, 1H, Ar *H*), 7.49 (s, 1H, Ar *H*), 7.11 (dd, 1H, *J* = 5.5, 1.9 Hz, C*H*), 7.06 (dd, 1H, *J* = 5.5, 1.9 Hz, C*H*), 6.07 (s, 1H, C*H*), 5.87 (s, 1H, C*H*); ^{13}C NMR (126 MHz, $CDCl_3$) δ_C (ppm) = 152.3, 143.8, 142.1, 129.0 – 119.4 (cluster of peaks), 81.8, 81.4; HRMS (EI, m/z): Calculated: 280.03 found: 280.0317 [M^+].

(5*s*,12*s*)-2,3,16,17-Tetramethoxy-5,12-dimethyl-7,9-bis(trifluoromethyl)-5,5a,6,11,11a,12-hexahydro-5,12-[1,2]benzeno-6,11-epoxytetracene (57)

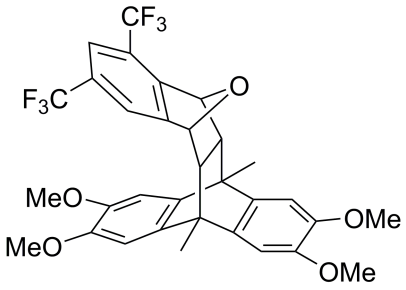

The compound (5*s*,12*s*)-2,3,16,17-tetramethoxy-5,12-dimethyl-7,9-bis(trifluoromethyl)-5,5a,6,11,11a,12-hexahydro-5,12-[1,2]benzeno-6,11-epoxytetracene (**57**) was prepared according to the general procedure G.P 2. 2,3,6,7-Tetramethoxy-9,10-dimethylanthracene (**34**) (1.51 g, 4.6 mmol) and 5,7-bis(trifluoromethyl)-1,4-dihydro-1,4-epoxynaphthalene (**56**) (1.30 g, 4.6 mmol) dissolved in DMF (15.0 mL) to yield (5*s*,12*s*)-2,3,16,17-tetramethoxy-5,12-dimethyl-7,9-bis(trifluoromethyl)-5,5a,6,11,11a,12-hexahydro-5,12-[1,2]benzeno-6,11-epoxytetracene (**57**) (2.23 g, 3.7 mmol, 79 %) as a light brown crystalline solid. Mp: 166-168 ºC; ν_{max} (cm^{-1}): 2965, 2938, 2830, 1506, 1487, 1464, 1404, 1385, 1327, 1277, 1254, 1242, 1194, 1159, 1121, 1074, 1045, 1020, 949, 895, 870, 835, 820, 783, 752, 687, 673, 633, 608, 571; ^{1}H NMR (500 MHz, $CDCl_3$): δ_H (ppm) = 7.56 (s, 1H, Ar *H*), 7.56 (s, 1H, Ar *H*), 6.90 (s, 1H, Ar *H*), 6.88 (s, 1H, Ar *H*), 6.86 (s, 1H, Ar *H*), 6.84 (s, 1H, Ar *H*), 5.31 (s, 1H, C*H*), 5.14 (s, 1H, C*H*), 3.90 (s, 3H, CH_3), 3.90 (s, 3H, CH_3), 3.84 (s, 3H, CH_3), 3.83 (s, 3H, CH_3), 2.09 (s, 3H, CH_3), 2.08 (s, 3H, CH_3), 2.04 – 2.01 (m, 2H, C*H*); ^{13}C NMR (126 MHz, $CDCl_3$) δ_C (ppm) = 149.7, 147.2, 147.1, 146.7, 146.6, 139.8, 136.2, 106.7 - 106.0 (cluster of peaks), 79.3, 79.0, 56.4, 56.4, 56.4, 56.3, 55.5, 54.9, 42.9, 42.9, 17.0, 16.7; HRMS (EI, m/z): Calculated: 606.18 found: 606.1855 [M^+].

(5*s*,12*s*)-2,3,16,17-Tetramethoxy-5,12-dimethyl-7,9-bis(trifluoromethyl)-5,12-dihydro-5,12-[1,2]benzenotetracene (58)

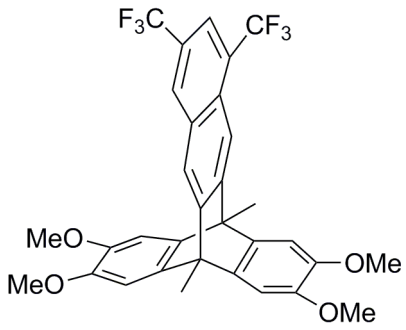

The compound (5*s*,12*s*)-2,3,16,17-tetramethoxy-5,12-dimethyl-7,9-bis(trifluoromethyl)-5,12-dihydro-5,12-[1,2]benzenotetracene (**58**) was preparaed according to the general procedure G.P 4. (5*s*,12*s*)-2,3,16,17-Tetramethoxy-5,12-dimethyl-7,9-bis(trifluoromethyl)-5,5a,6,11,11a,12-hexahydro-5,12-[1,2]benzeno-6,11-epoxytetracene (**57**) (2.20 g, 3.63 mmol) dissolved in CH_3SO_3H (30 mL, 462.0 mmol). Afforded desired product (5*s*,12*s*)-2,3,16,17-tetramethoxy-5,12-dimethyl-7,9-bis(trifluoromethyl)-5,12-dihydro-5,12-[1,2]benzenotetracene (**58**) (1.81 g, 3.1 mmol, 85 %) as a brown crystalline solid. Mp: 138-140 ºC; ν_{max} (cm^{-1}): 2970, 2940, 2830, 1607, 1582, 1487, 1449, 1439, 1406, 1385, 1344, 1275, 1209, 1186, 1152, 1115, 1088, 1042, 1016, 959, 899, 887, 870, 762, 752, 733, 667, 613; ^{1}H NMR (500 MHz, $CDCl_3$): δ_H (ppm) = 8.23 (s, 1H, Ar *H*), 8.05 (s, 1H, Ar *H*), 7.95 (s, 1H, Ar *H*), 7.83 (s, 1H, Ar *H*), 7.01 (s, 2H, Ar *H*), 6.99 (s, 2H, Ar *H*), 3.87 (s, 6H, C*H*$_3$), 3.86 (s, 6H, C*H*$_3$), 2.53 (s, 3H, C*H*$_3$), 2.52 (s, 3H, C*H*$_3$); ^{13}C NMR (126 MHz, $CDCl_3$) δ_C (ppm) = 150.5, 148.5, 146.5, 139.9, 131.3, 129.5 – 120.3 (cluster of peaks), 119.6, 114.6, 106.1, 106.0, 56.4, 56.3, 48.0, 47.5, 14.0; HRMS (EI, m/z): Calculated: 588.17 found: 588.1746 [M^+].

(5*s*,12*s*)-5,12-Dimethyl-7,9-bis(trifluoromethyl)-5,12-dihydro-5,12-[1,2]benzenotetracene-2,3,16,17-tetraol (59)

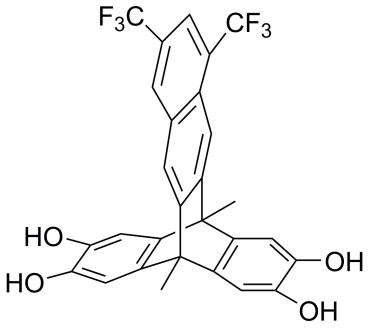

The compound (5*s*,12*s*)-5,12-dimethyl-7,9-bis(trifluoromethyl)-5,12-dihydro-5,12-[1,2]benzenotetracene-2,3,16,17-tetraol (**59**) was synthesised according to the general procedure G.P 5. (5*s*,12*s*)-2,3,16,17-Tetramethoxy-5,12-dimethyl-7,9-bis(trifluoromethyl)-5,12-dihydro-5,12-[1,2]benzenotetracene (**58**) (1.81 g, 3.08 mmol) dissolved in anhydrous DCM (45 mL). BBr_3 (2.31 g, 9.23 mmol) was added to yield (5*s*,12*s*)-5,12-dimethyl-7,9-bis(trifluoromethyl)-5,12-dihydro-5,12-[1,2]benzenotetracene-2,3,16,17-tetraol (**59**) (1.25 g, 2.35 mmol, 76 %) as a white powder. Mp: 248-250 ºC; ν_{max} (cm^{-1}): 3429, 2974, 1614, 1489, 1445, 1383, 1342, 1298, 1277, 1207, 1188, 1157, 1117, 1088, 1015, 988, 957, 924, 903, 889, 880, 841, 775, 762, 669, 617; ^{1}H NMR (500 MHz, $(CD_3)_2CO$: δ_H (ppm) = 8.53 (s, 1H, Ar *H*), 8.08 (s, 1H, Ar *H*), 8.00 (m, 2H, Ar *H*), 7.63 (m, 3H, O*H*), 6.96 (s, 2H, Ar *H*), 6.95 (s, 2H, Ar *H*), 2.39 (s, 6H, CH_3); ^{13}C NMR (126 MHz, $(CD_3)_2CO$) δ_C (ppm) = 153.0, 150.7, 142.7, 140.2, 140.0, 132.5, 131.3, 131.2, 129.1, 127.4, 127.1, 126.5, 126.4, 126.2, 126.1, 124.2, 123.9, 120.6, 114.3, 110.3, 110.2, 48.2, 47.8, 14.3, 14.2; HRMS (EI, m/z): Calculated: 532.11 found: 532.1128 [M^+].

***N*,*N*′-(9,10-dioxo-9,10-dihydroanthracene-2,6-diyl)dihexanamide (60)**

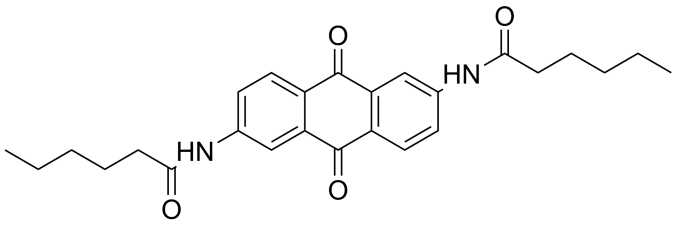

The compound *N*,*N*′-(9,10-dioxo-9,10-dihydroanthracene-2,6-diyl)dihexanamide (**60**) was synthesised according to the procedure reported by R. Kantam et al.[151] 2, 6-Diaminoanthraquinone (20.0 g, 84.0 mmol) and pyridine (88 mL, 1.09 mol) were dissolved in DCM (150 mL). To this, hexanoyl chloride (64.54 mL, 462 mmol) was added drop wise which was left at room temperature for 24 h. The resulting precipitate was filtered off, washed with MeOH (300 mL) and dried to yield *N*,*N*′-(9,10-dioxo-9,10-dihydroanthracene-2,6-diyl)dihexanamide (**60**) (36.1 g, 83.0 mmol, 99 %) as a yellow solid. Mp: Above 300 ºC; ν_{max} (cm^{-1}): 3341, 2943, 1705, 1655, 1570, 1516, 1489, 1466, 1327, 1296, 1246, 1231, 1169, 1142, 1107, 999, 903, 856, 741, 714, 679, 613, 559; ^{1}H NMR (500 MHz, $CDCl_3$): δ_H (ppm) = 10.52 (s, 2H, N*H*), 8.44 (d, 2H, *J* = 2.1 Hz, Ar *H*), 8.15 (d, 2H, *J* = 8.5 Hz, Ar *H*), 8.08 (dd, 2H, *J* = 8.5, 2.1 Hz, Ar *H*), 2.39 (t, 4H, *J* = 7.4 Hz, CH_2), 1.67-1.59 (m, 4H, CH_2), 1.35-1.27 (m, 8H, CH_2), 0.88 (t, 6H, *J* = 6.8 Hz, CH_3); ^{13}C NMR (126 MHz, $CDCl_3$) δ_C (ppm) = 181.3, 172.3, 144.8, 134.3, 128.5, 127.8, 123.3, 115.7, 36.5, 30.8, 24.5, 21.9, 13.8; LRMS (EI, m/z): Calculated: 434.22 found: 434.1 [M^+].

***N*,*N*′-(anthracene-2,6-diyl)dihexanamide (61)**

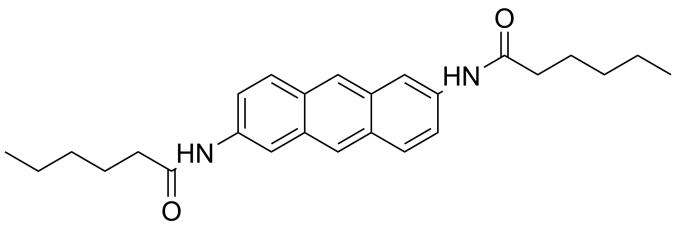

The compound *N*,*N*′-(anthracene-2,6-diyl)dihexanamide (**61**) was prepared according to the procedure reported by R. Kantam et al.[151] *N*,*N*′-(9,10-dioxo-9,10-dihydroanthracene-2,6-diyl)dihexanamide (**60**) (3.0 g, 6.90 mmol), $NaBH_4$ (15.67 g, 414.23 mmol), propan-2-ol (60 mL) and 2M aq. NaOH (4.5 mL, 9.0 mmol) were combined and heated to reflux for 24 h. After this time, poured reaction mixture into water (1 L) and left to stir for 1 h. Filtered off crude product, washed with methanol and dried to yield *N*,*N*′-(anthracene-2,6-diyl)dihexanamide (**61**) (1.82 g, 4.49 mmol, 65 %) as a green powder. Mp: Above 300 ºC; ν_{max} (cm^{-1}): 3248, 2959, 2866, 1651, 1558, 1524, 1474, 1400, 1362, 1281, 1254, 1219, 1204, 1169, 1157, 1065, 984, 903, 872, 849, 837, 826, 748, 698, 656, 633, 571, 517; ^{1}H

NMR (500 MHz, $(CD_3)_2SO$): δH (ppm) = 10.08 (s, 2H, N*H*), 8.46 (s, 2H, Ar *H*), 8.34 (s, 2H, Ar *H*), 7.98 (d, 2H, *J* = 9.2 Hz, Ar *H*), 7.54 (d, 2H, *J* = 9.2 Hz, Ar *H*), 2.39 (s, 4H, CH_2), 1.66 (s, 4H, CH_2), 1.34 (s, 8H, CH_2), 0.91 (s, 6H, CH_3); ^{13}C NMR (126 MHz, $(CD_3)_2SO$) δC (ppm) = 172.6, 135.7, 130.7, 128.9, 128.3, 124.7, 121.0, 113.8, 79.2, 36.5, 30.9, 24.8, 21.9, 13.9; LRMS (EI, m/z): Calculated: 404.25 found: 404.2 [M^+].

General Polymer Procedure 1 (G.P.P 1)

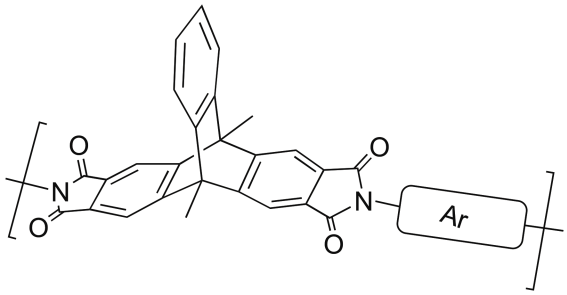

The synthesis of the polyimides **xP1**, **xP2**, **xP3** and **xP4** was conducted according to the procedure reported by Ghanem et al.[143] 9,10-dimethyltriptycene-dianhydride (**x8**) was added to a solution of Et_3N and EtOH and heated to 80°C for 1 h. Solvents were removed and NMP (5 mL) was added. To this, a particular bisamine was added and heated to 80°C for 45 min, before being heated to 190°C over 2 h. Reaction was left at 190°C for 15 min before adding $CHCl_3$ and then EtOH (200 mL). Collected polymer by filtration and washed with acetone. Reprecipitated polymer from $CHCl_3$ by dropwise addition of MeOH (~30 mL) and final reprecipitation in hexane (300 mL). Collected by filtration and refluxed in methanol twice for 16 h, filtered off and dried in a vacuum oven at 120°C for 9 h to yield resulting polyimide.

General Polymer Procedure 2 (G.P.P 2)

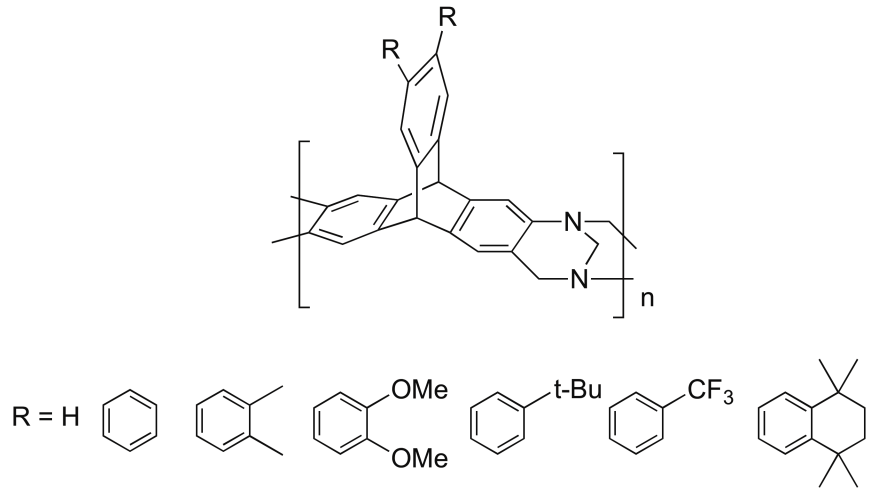

Tröger's Base (TB) polymers were synthesised according to the general procedure reported by McKeown et al.[4] The required bisamine was dissolved in DCM and DMM and resulting solution cooled to 0°C. TFA was added drop wise over 30 mins and stirred for the required time for the polymer solution to become viscous. The viscous yellow mixture was poured into aqueous ammonium hydroxide solution and stirred vigorously for 2 h. Solid was collected by filtration, washed with water and then acetone until washings were clear. The resulting powder was dissolved in chloroform and reprecipitated from methanol. The reprecipitation from chloroform was repeated twice. The crude polymer was dissolved in chloroform (50 mL), added drop wise to hexane and the precipitated powder was filtered off. The polymer was refluxed in methanol twice for 16 h, filtered off and dried in a vacuum oven at 120°C for 9 h to yield resulting TB polymer.

General Polymer Procedure 3 (G.P.P 3)

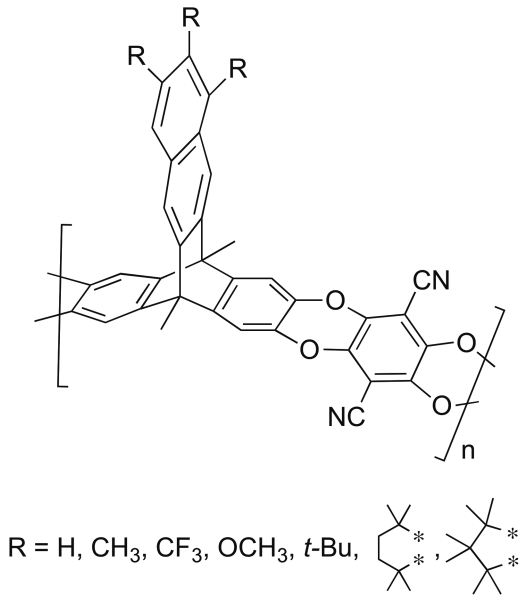

The synthesis of the polybenzodioxane polymers (**P16**, **P17**, **P18**, **P19**, **P20**, **P21)** was conducted according to the procedure reported by Budd et al.[3] The required biscatechol and tetrafluoroterephthalonitrile was dissolved in anhydrous DMF. Once dissolved K_2CO_3 was added and the resulting solution was heated to 65°C for 72 h. After this time, polymer solution was poured into water (~300 mL), acidified with conc. HCl and filtered off. Polymer was washed with water and acetone and dried. Polymer was dissolved in appropriate solvent and reprecipitated into a solution of acetone:methanol (1:2), repeated twice and collected polymer by filtration. Resulting polybenzodioxane polymers were refluxed in methanol twice for 16 h, collected by filtration and dried in vacuum oven at 120°C for 9 h.

P1

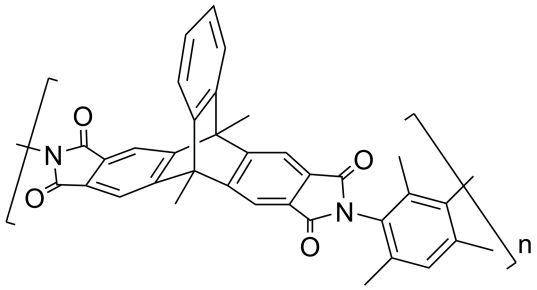

(P1) was synthesised according to the general procedure G.P.P 1. 9,10-dimethyltriptycene-dianhydride (**8**) (1.0 g, 2.37 mmol), Et_3N (1.65 mL, 11.84 mmol) and EtOH (15.0 mL) was combined. 2,4,6-trimethyl-m-phenylenediamine (0.36 g, 2.37 mmol) was added. Polymer was obtained by filtration as an off white powder (0.48 g 0.85 mmol, 36 %). ν_{max} (cm^{-1}): 3480, 2974, 1778, 1717, 1485, 1454, 1346, 1308, 1107, 1030, 777, 745, 625, 613; T_d = 518°C; GPC (Chloroform): M_n = 3,009, M_w = 4,486; BET surface area = 703 m^2g^{-1}; pore volume = 0.4848 cm^3g^{-1} at (P/P_o = 0.9814); ^{1}H NMR (500 MHz, $CDCl_3$) δ 8.03 (*b*s, 4H, Ar *H*), 7.48 (*b*s, 2H, Ar *H*), 7.34-6.88 (m, 3H, Ar *H*), 2.62 (*b*s, 6H, C*H*$_3$), 2.33-1.64 (m, 9H, C*H*$_3$); ^{13}C NMR (126 MHz, $CDCl_3$) δ_c (ppm) = 167.5, 166.9, 154.7, 145.3, 141.6, 138.5, 130.1, 128.7, 127.7, 126.3, 125.6, 123.7, 121.6, 120.5, 116.7, 50.6, 18.3, 17.9, 17.5, 14.1, 13.8, 12.6;

P2

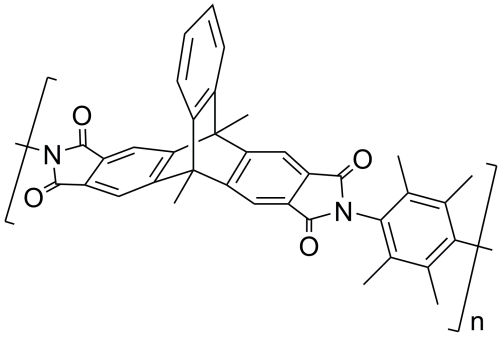

(**P2**) was prepared according to the general procedure G.P.P 1. 9,10-dimethyltriptycene-dianhydride (**8**) (1.03 g, 2.37 mmol), Et_3N (1.65 mL, 11.83 mmol) and EtOH (15.0 mL), NMP (5.0 mL) was combined. 2,3,5,6-tetramethyl-1,4-phenylenediamine (0.39 g, 2.37 mmol) was added. Polymer precipitated out of solution at 165°C to yield an insoluble white polymer (0.14 g, 0.25 mmol, 11 %). ν_{max} (cm^{-1}): 3389, 2972, 1775, 1713, 1454, 1423, 1375, 1348, 1327, 1317, 1263, 1113, 777, 745, 627, 615, 511; T_d = 464°C; BET surface area = 352 m^2g^{-1}; pore volume = 0.2144 cm^3g^{-1} at (P/P_o = 0.9814); Solid state ^{13}C NMR (100 MHz) δ_c (ppm) = 168.4, 156.6, 143.5, 134.9, 133.1, 131.4, 129.9, 120.1, 118.4, 50.7, 15.1, 13.2.

P3

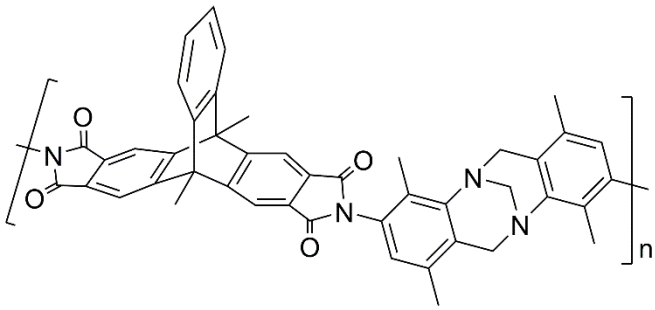

(**P3**) was synthesised according to the general procedure G.P.P 1. 9,10-dimethyltriptycene-dianhydride (**8**) (1.0 g, 2.37 mmol), Et_3N (1.65 mL, 11.84 mmol) and EtOH (15.0 mL). NMP (5.0 mL) was combined. 2,8-diamino-1,4,7,10-tetramethyl-6H,12H-5,11-methanodibenzo[b,f][1,5]dizocine (**9**) (0.73 g, 2.37 mmol) (which was prepared by Michael Lee) was added. Polymer was obtained by filtration as a brown powder (1.0 g, 1.38 mmol, 58 %). ν_{max} (cm^{-1}): 3530, 2930, 1776, 1715, 1474, 1377, 1333, 1225, 1107, 746; T_d = 435°C; GPC (Chloroform): M_n = 21,367, M_w = 38,951; BET surface area = 560 m^2g^{-1}; pore volume = 0.4477 cm^3g^{-1} at (P/P_o = 0.9814); ^1H NMR (500 MHz, $CDCl_3$) δ 7.96 (s, 4H, Ar *H*) 7.45 (s, 2H, Ar *H*) 7.16 (s, 2H, Ar *H*) 6.85 (s, 2H, Ar *H*) 4.42 (d, 2H, C*H*) 4.22 (s, 2H, C*H*) 3.98 (d, 2H, C*H*) 2.61 (s, 6H, C*H*) 2.39 (s, 6H, C*H*) 1.79 (s, 6H, C*H*); ^{13}C NMR (126 MHz, $CDCl_3$) δ_c (ppm) = 167.7, 167.3, 154.4, 147.5, 145.2, 131.8, 131.2, 130.1, 128.7, 127.8, 126.2, 125.7, 121.5, 116.5, 65.6, 53.8, 50.4, 17.1, 17.0, 14.1, 12.8.

P4

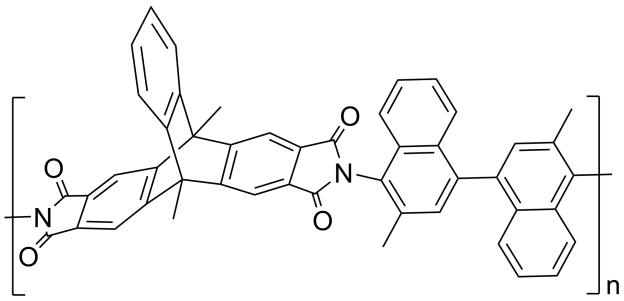

(**P4**) was synthesised according to the general procedure G.P.P 1. 9,10-dimethyltriptycene-dianhydride (**8**) (1.0 g, 2.37 mmol), Et_3N (1.65 mL, 11.83 mmol) and EtOH (15.0 mL), NMP (5.0 mL) was combined. 3,3-dimethylnaphthidine (0.74 g, 2.37 mmol) was added. Polymer was obtained by filtration as a light brown powder (0.450 g, 0.62 mmol, 26 %). ν_{max} (cm^{-1}): 3516, 3013, 1778, 1719, 1456, 1387, 1339, 1107, 876, 773, 743, 627, 613, 596; T_d = 539°C; GPC (Chloroform): M_n = 26,319, M_w = 34,061; BET surface area = 646 m^2g^{-1}; pore volume = 0.4288 cm^3g^{-1} at (P/P_o = 0.9814); ^1H NMR (500 MHz, $CDCl_3$) δ 8.15 (*b*s, 4H, Ar *H*), 7.62-7.36 (m, 10H, Ar *H*), 7.33-7.18 (m, 4H, Ar *H*), 2.74 (*b*s, 6H, C*H*$_3$), 2.36 (*b*s, 6H, C*H*$_3$); ^{13}C NMR (126 MHz, $CDCl_3$) δ_c (ppm) = 167.7, 167.6, 154.8, 145.3, 139.6, 134.8, 132.4, 131.0, 130.6, 130.4, 127.5, 126.5, 126.1, 121.9, 116.9, 50.7, 18.5, 14.3.

P5

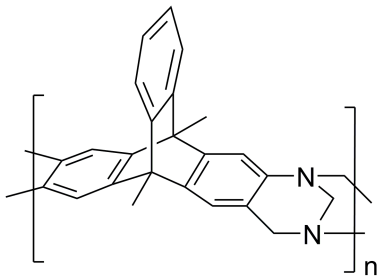

(**P5**) was synthesised according to the general procedure G.P.P 2. (**13**) (1.03 g, 3.30 mmol), DCM (2.0 mL), DMM (1.16 mL, 13.2 mmol) was combined. TFA (8.0 mL) was added and

collected (**P5**) by filtration as an off white powder (2.17 g, 5.31 mmol, 83 %). ν_{max} (cm^{-1}): 3064, 3044, 3011, 2998, 2901, 2850, 1663, 1623, 1575, 1464, 1422, 1339, 1209, 1029, 931; T_d = 413°C; GPC (Chloroform): M_n = 46,215, M_w = 116,000; BET surface area = 926 m^2g^{-1}; pore volume = 0.6532 cm^3g^{-1} at (P/P_o = 0.9814); ^{1}H NMR (400 MHz, $CDCl_3$) δ 6.93 (m, 8H, Ar *H*), 4.46 (*b*s, 2H, C*H*$_2$), 3.92 (*b*s, 4H, C*H*$_2$), 2.19 (m, 6H, C*H*$_3$); Solid state ^{13}C NMR (100 MHz) δ_c (ppm) = 145.0, 124.4, 118.4, 66.9, 58.5, 47.6, 12.9.

P6

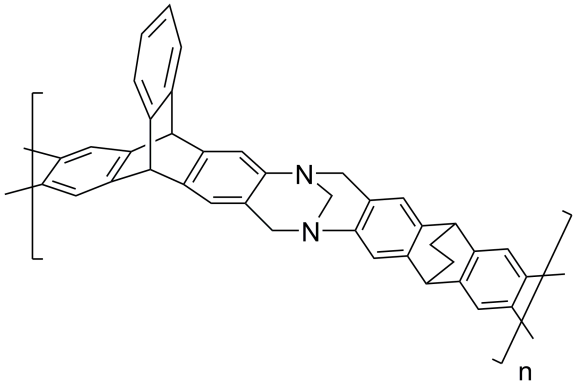

(**P6**) was prepared according to the general procedure G.P.P 2. 2,6(7)-diaminotriptycene (1.03 g, 3.62 mmol), 2,6(7)-diamino-dihydroethanoanthracene (0.86 g, 3.62 mmol), DMM (3.20 mL, 36.2 mmol) was combined. TFA (15.1 mL) was added and collected (**P6**) by filtration as an off white powder (1.56 g, 2.63 mmol, 73 %). ν_{max} (cm^{-1}): 3401, 2941, 1624, 1464, 1420, 1341, 1294, 1211, 1151, 1132, 1105, 1080, 1030, 957, 935, 889, 745, 617, 596, 559; T_d = 289°C; GPC (Chloroform): M_n = 76,095, M_w = 191,000; BET surface area = 855 m^2g^{-1}; pore volume = 0.6212 cm^3g^{-1} at (P/P_o = 0.9814); ^{1}H NMR (500 MHz, $CDCl_3$) δ 7.44-6.49 (m, 12H, Ar *H*), 5.23 (*b*s, 2H, C*H*), 4.54 (*b*s, 2H, C*H*), 3.99 (*b*s, 6H, C*H*$_2$), 1.80 (*b*s, 4H, C*H*$_2$); ^{13}C NMR (126 MHz, $CDCl_3$) δ_c (ppm) = 144.9, 144.0, 142.9, 140.6, 139.5, 125.2, 124.4, 123.2, 121.6, 120.4, 66.7, 58.3, 53.1, 43.4, 26.5

P7

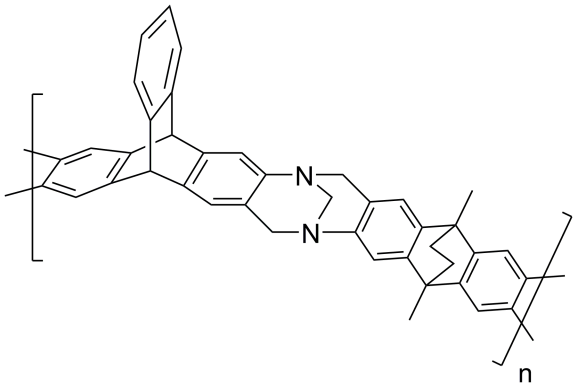

P7 was synthesised according to the general procedure G.P.P 2. 2,6(7)-diaminotriptycene (0.83 g, 2.93 mmol), 2,6(7)-diamino-dimethylethanoanthracene (0.77 g, 2.93 mmol), DMM (2.59 mL, 29.3 mmol) was combined. TFA (12.9 mL) was added and collected (**P7**) by filtration as an off white powder (0.92 g, 1.48 mmol, 51 %). ν_{max} (cm^{-1}): 2957, 2938, 1616, 1462, 1437, 1416, 1375, 1335, 1294, 1204, 1144, 1076, 1069, 986, 951, 920, 893, 745, 617, 596, 573; T_d = 311°C; GPC (Chloroform): M_n = 41,053, M_w = 117,000; BET surface area = 896 m^2g^{-1}; pore volume = 0.7110 cm^3g^{-1} at (P/P_o = 0.9814); ^{1}H NMR (500 MHz, $CDCl_3$) δ 7.48-6.43 (m, 12H, Ar *H*), 5.15 (*b*s, 2H, C*H*), 4.51 (*b*s, 2H, CH_2), 4.02 (*b*s, 4H, CH_2), 2.09-1.02 (m, 10H, CH_3, CH_2); ^{13}C NMR (126 MHz, $CDCl_3$) δ_c (ppm) = 144.9, 144.0, 142.2, 140.5, 125.5, 124.2, 123.3, 121.8, 120.3, 118.6, 117.2, 67.0, 58.5, 53.1, 41.1, 35.5, 18.5.

P8

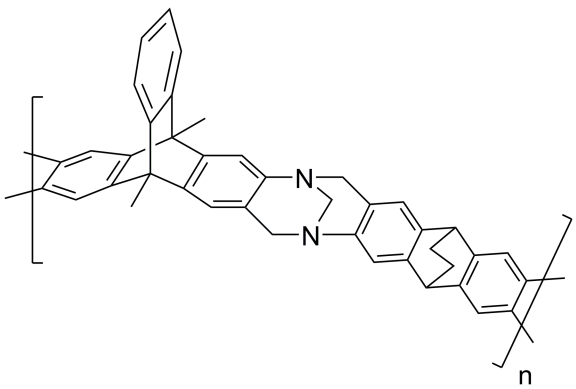

(**P8**) was prepared according to the general procedure G.P.P 2. (**13**) (1.03 g, 3.31 mmol), 2,6(7)-diamino-dihydroethanoanthracene (0.78 g, 3.31 mmol), DMM (2.93 mL, 33.1 mmol) was combined. TFA (14.5 mL) was added and collected (**P8**) by filtration as an off white powder (1.70 g, 2.73 mmol, 83 %). ν_{max} (cm^{-1}): 2941, 1684, 1636, 1472, 1450, 1418, 1375, 1341, 1207, 1132, 984, 912, 891, 745, 623, 604, 559; T_d = 300°C; GPC (Chloroform): M_n = 79,602, M_w = 160,000; BET surface area = 888 m^2g^{-1}; pore volume = 0.6401 cm^3g^{-1} at (P/P_o = 0.9814); ^{1}H NMR (500 MHz, $CDCl_3$) δ 7.61-6.39 (m 12H, Ar *H*), 4.55 (*b*s, 2H, C*H*), 4.05 (*b*s, 6H, CH_2), 2.28 (*b*s, 6H, CH_3), 1.62 (*b*s, 4H, CH_2); ^{13}C NMR (126 MHz, $CDCl_3$) δ_c (ppm) = 147.5, 144.7, 143.6, 139.5, 124.9, 123.8, 121.4, 120.3, 118.9, 117.5, 66.9, 58.5, 47.8, 43.2, 26.5, 13.6.

P9

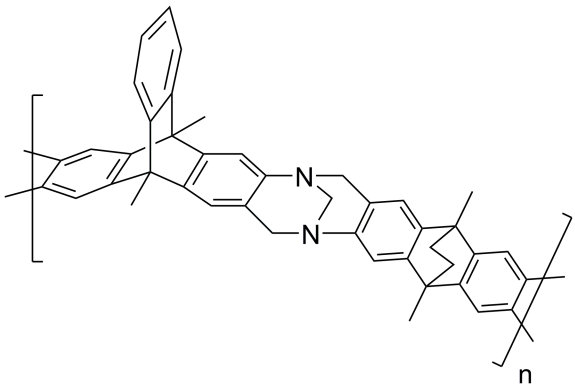

(P9) was prepared according to the general procedure G.P.P 2. (**13**) (1.00 g, 3.20 mmol), 2,6(7)-diamino-dimethylethanoanthracene (0.85 g, 3.20 mmol), DMM (2.83 mL, 32.0 mmol) was combined. TFA (14.8 mL) was added and collected (**P9**) by filtration as an off white polymer (1.43 g, 2.20 mmol, 69 %). ν_{max} (cm^{-1}): 2940, 1450, 1412, 1375, 1329, 1196, 1067, 912, 891, 745, 623, 604; T_d = 311°C; GPC (Chloroform): M_n = 41,871, M_w = 188,000; BET surface area = 952 m^2g^{-1}; pore volume = 0.7672 cm^3g^{-1} at (P/P_o = 0.9814); ^{1}H NMR (500 MHz, $CDCl_3$) δ 7.53-6.39 (m, 12H, Ar *H*), 4.55 (*b*s, 2H, CH_2), 4.04 (*b*s, 4H, CH_2), 2.23 (*b*s, 6H, CH_3), 1.79 (*b*s, 10H, CH_3, CH_2); ^{13}C NMR (126 MHz, $CDCl_3$) δ_c (ppm) = 147.4, 145.0, 144.6, 143.6, 142.1, 124.8, 123.9, 120.3, 118.8, 117.4, 67.0, 58.5, 47.7, 41.1, 35.8, 31.0, 18.5, 13.6.

P10

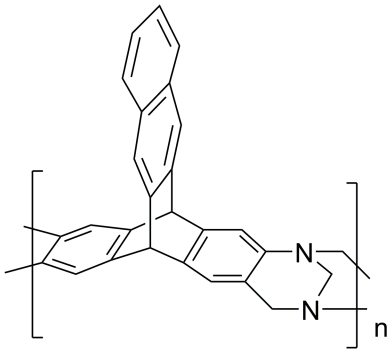

(**P10**) was prepared according to the general procedure G.P.P 2. (**18**) (1.23 g, 3.68 mmol), DMM (1.62 mL, 18.4 mmol) and DCM (2.0 mL) were combined. TFA (9.8 mL) was added and left at room temperature for 24 h. Collected (**P10**) by filtration as an off white powder (1.18 g, 3.19 mmol, 87 %). ν_{max} (cm^{-1}): 3414, 2953, 1680, 1464, 1420, 937, 747; T_d = 465°C; GPC (Chloroform): M_n = 29,014, M_w = 103,000; BET surface area = 868 m^2g^{-1}; pore volume = 0.6189 cm^3g^{-1} at (P/P_o = 0.9814); ^{1}H NMR (500 MHz, $CDCl_3$) δ 7.18 (*b*s, 10H, Ar *H*), 5.11 (*b*s, 2H, C*H*), 4.47 (*b*s, 2H, C*H*), 3.92 (*b*s, 2H, C*H*); ^{13}C NMR (126 MHz, $CDCl_3$) δ_c (ppm) = 145.1, 143.2, 141.6, 139.7, 131.6, 127.4, 125.5, 124.5, 121.3, 120.2, 66.9, 58.4, 52.6.

P11

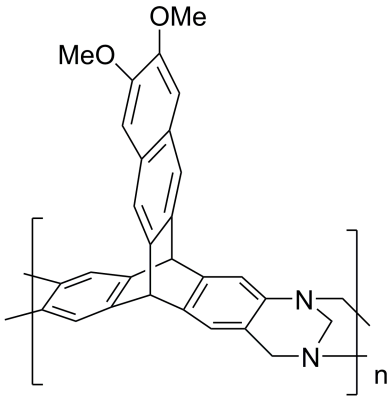

(**P11**) was prepared according to the general procedure G.P.P 2. (**21**) (1.20 g, 3.04 mmol), DMM (1.08 mL, 12.17 mmol) and DCM (2.0 mL) were combined and TFA (9.6 mL) was added. Polymer cross-linked during reaction after 1 h. Collected (**P11**) by filtration as a brown solid (1.00 g, 2.33 mmol, 77 %). ν_{max} (cm^{-1}): 2947, 1684, 1653, 1616, 1464, 1437, 1418, 1339, 1209, 1076, 1024, 934, 895, 542; T_d = 410°C; BET surface area = 384 m^2g^{-1}; pore volume = 0.2631 cm^3g^{-1} at (P/P_o = 0.9814); Solid state ^{13}C NMR (100 MHz) δ_c (ppm) = 149.8, 145.5, 141.7, 127.4, 120.4, 107.1, 67.7, 54.7.

P12

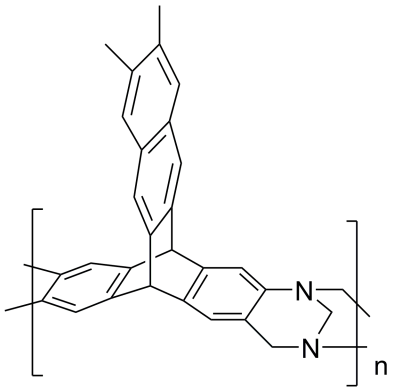

(**P12**) was synthesised according to the general procedure G.P.P 2. (**24**) (1.37 g, 3.77 mmol), DMM (1.67 mL, 18.87 mmol) and DCM (2.0 mL) were combined and TFA (10.9 mL) was added. Polymer cross-linked during reaction after 2.5 h. Collected (**P12**) by filtration as a brown solid (0.72 g, 1.80 mmol, 48 %). ν_{max} (cm^{-1}): 2947, 1717, 1661, 1653, 1464, 1437, 1420, 1404, 1298, 1200, 1150, 932, 895; T_d = 421°C; BET surface area = 729 m^2g^{-1}; pore volume = 0.4627 cm^3g^{-1} at (P/P_o = 0.9814); Solid state ^{13}C NMR (100 MHz) δ_c (ppm) = 175.7, 156.2, 144.9, 141.6, 134.7, 130.6, 121.4, 67.1, 58.1, 53.7, 28.9, 20.2.

P13

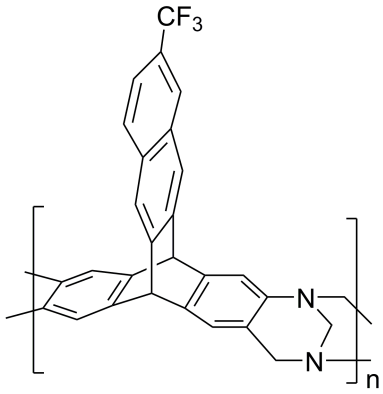

(**P13**) was prepared according to the general procedure G.P.P 2. (**27**) (0.89 g, 2.20 mmol), DMM (0.97 mL, 11.0 mmol) and DCM (1.5 mL) were combined. TFA (7.1 mL) was added and polymer precipitated out of solution after 2 h. Collected (**P13**) by filtration as a light brown powder (0.87 g, 1.98 mmol, 90 %). ν_{max} (cm^{-1}): 2955, 1464, 1456, 1420, 1331, 1306, 1200, 1119, 1074, 1063, 1026, 932, 907, 889, 816, 592; T_d = 458°C; BET surface area = 742 m^2g^{-1}; pore volume = 0.5398 cm^3g^{-1} at (P/P_o = 0.9814); Solid state ^{13}C NMR (100 MHz) δ_c (ppm) = 174.3, 145.5, 140.3, 133.6, 131.4, 125.3, 53.7, 52.8, 47.9, 28.1.

P14

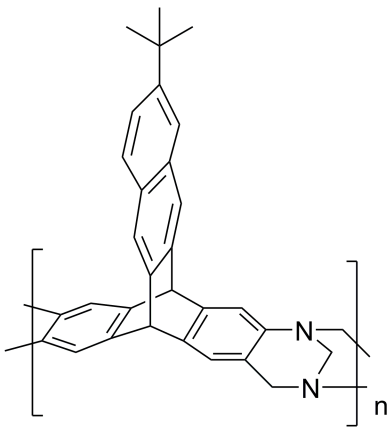

(**P14**) was synthesised according to the general procedure G.P.P 2. (**30**) (1.56 g, 3.99 mmol), DMM (1.76 mL, 19.97 mmol) and DCM (2.0 mL) were combined. TFA (12.5 mL) was added and left at room temperature for 24 h. Collected (**P14**) by filtration as an orange/brown powder (1.20 g, 2.81 mmol, 70 %). ν_{max} (cm^{-1}): 2953, 1616, 1462, 1437, 1420, 1362, 1337, 1209, 1078, 1026, 934, 897, 814, 602; T_d = 446°C; GPC (Chloroform): M_n = 12,097, M_w = 45,000; BET surface area = 856 m^2g^{-1}; pore volume = 0.6475 cm^3g^{-1} at (P/P_o = 0.9814); ^{1}H NMR (500 MHz, $CDCl_3$) δ 7.96-6.42 (m, 9H, Ar *H*), 5.12 (*b*s, 2H, C*H*$_2$), 4.44 (*b*s, 2H, C*H*$_2$), 3.86 (*b*s, 2H, C*H*$_2$), 1.81-0.33 (m, 9H, C*H*$_3$); Solid state ^{13}C NMR (101 MHz, $CDCl_3$) δ_c (ppm) = 145.4, 130.5, 121.4, 67.2, 58.6, 54.6, 31.2.

P15

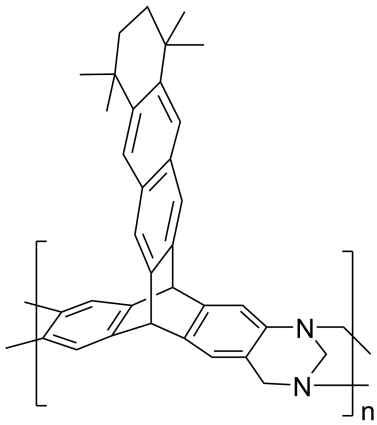

(**P15**) was prepared according to the general procedure G.P.P 2. (**33**) (0.55 g, 1.22 mmol), DMM (0.54 mL, 6.12 mmol) and DCM (1.5 mL) were combined. TFA (4.37 mL) was added and left at room temperature for 2.5 h. Collected (**P15**) by filtration as a yellow powder (0.24 g, 0.49 mmol, 40 %). ν_{max} (cm^{-1}): 2955, 1464, 1437, 1418, 1362, 1339, 1213, 1184, 1107, 1078, 1032, 1022, 935, 903, 615, 604, 534; T_d = 446 °C; BET surface area = 847 m^2g^{-1}; pore volume = 0.6312 cm^3g^{-1} at (P/P_o = 0.9814); ^{1}H NMR (500 MHz, $CDCl_3$) δ 7.61-7.16 (m, 4H, Ar *H*), 7.04-6.83 (m, 2H, Ar *H*), 6.81-6.57 (m, 2H, Ar *H*), 5.24-4.92 (m, 2H, C*H*), 4.42 (*b*s, 2H, C*H*$_2$), 4.15-3.59 (m, 4H, C*H*$_2$), 1.58 (*b*s, 4H, C*H*$_2$), 1.43-0.83 (m, 12H, C*H*$_3$); ^{13}C NMR (126 MHz, $CDCl_3$) δ_c (ppm) = 145.0, 143.4, 140.5, 139.8, 130.0, 124.5, 121.8, 120.4, 58.5, 52.6, 35.2, 34.3, 32.5.

P16

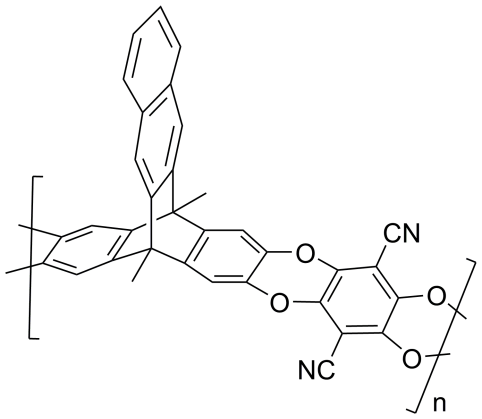

(**P16**) was synthesised according to the general procedure G.P.P 3. (**43**) (0.84 g, 2.13 mmol), tetrafluoroterephthalonitrile (0.43 g, 2.13 mmol), K_2CO_3 (2.35 g, 17.0 mmol) and DMF (15.0 mL) were combined. Collected (**P16**) as a yellow powder (0.86 g, 1.66 mmol, 78 %). ν_{max} (cm^{-1}): 2974, 1435, 1296, 1269, 1007, 885, 752, 582; T_d = 436°C; BET surface area = 791 m^2g^{-1}; pore volume = 0.6050 cm^3g^{-1} at (P/P_o = 0.9814); Solid state ^{13}C NMR (100 MHz) δ_c (ppm) = 144.9, 139.9, 138.2, 131.8, 48.0, 16.4, 13.1.

P17

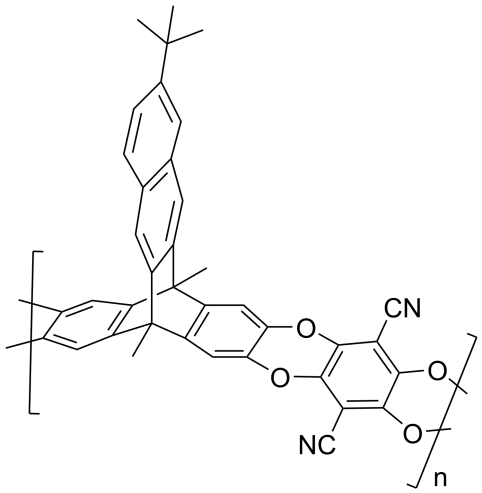

(**P17**) was synthesised according to the general procedure G.P.P 3. (**46**) (1.34 g, 2.96 mmol), tetrafluoroterephthalonitrile (0.59 g, 2.96 mmol), K_2CO_3 (3.27 g, 23.7 mmol) and DMF (15.0 mL) were combined. Collected (**P17**) as a yellow powder (1.27 g, 2.22 mmol, 75 %). ν_{max} (cm^{-1}): 2967, 1437, 1296, 1271, 1179, 1007, 885; T_d = 437°C; BET surface area = 1009 m^2g^{-1}; pore volume = 0.7264 cm^3g^{-1} at (P/P_o = 0.9814); Solid state ^{13}C NMR (100 MHz) δ_c (ppm) = 145.9, 143.3, 142.4, 139.9, 137.9, 132.1, 130.5, 47.8, 34.0, 30.1, 12.6.

P18

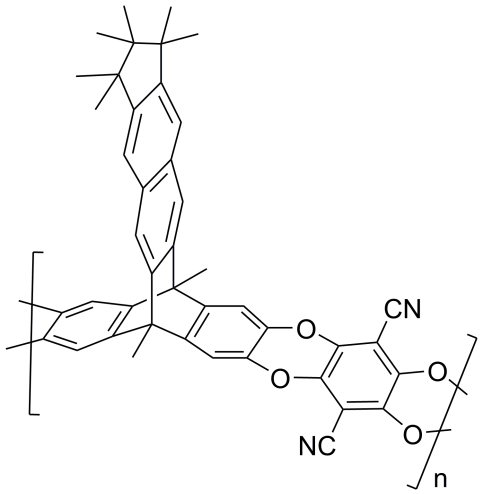

(**P18**) was prepared according to the general procedure G.P.P 3. (**50**) (0.43 g, 0.81 mmol), tetrafluoroterephthalonitrile (0.16 g, 0.81 mmol), K_2CO_3 (0.89 g, 6.47 mmol) and DMF (7.0 mL) were combined. Collected (**P18**) as a yellow powder (0.30 g, 0.47 mmol, 58 %). ν_{max} (cm^{-1}): 2980, 1435, 1396, 1379, 1296, 1271, 1171, 1155, 1005, 903, 883, 752, 552; T_d = 435°C; BET surface area = 1105 m^2g^{-1}; pore volume = 0.8325 cm^3g^{-1} at (P/P_o = 0.9814); Solid state ^{13}C NMR (100 MHz) δ_c (ppm) = 150.4, 146.0, 143.8, 142.0, 140.3, 137.7, 132.3, 119.5, 109.4, 47.4, 26.8, 20.6, 13.7.

P19

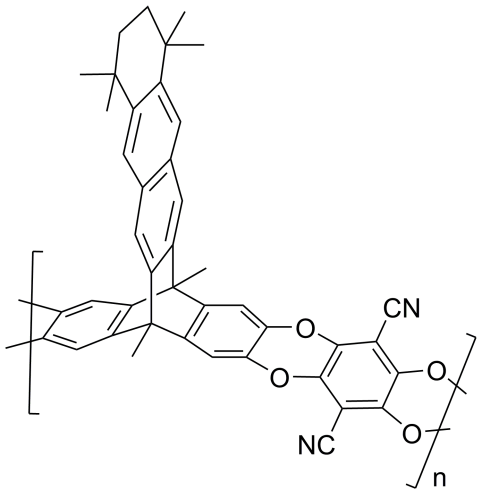

(**P19**) was prepared according to the general procedure G.P.P 3. (**53**) (2.34 g, 4.61 mmol), tetrafluoroterephthalonitrile (0.92 g, 4.61 mmol), K_2CO_3 (5.09 g, 36.9 mmol) and DMF (40.0 mL) were combined. Collected (**P19**) as a yellow powder (1.95 g, 3.11 mmol, 67 %). ν_{max} (cm^{-1}): 2924, 2239, 1740, 1607, 1435, 1385, 1269, 1155, 1005, 905, 883, 750, 669, 538; T_d = 474°C; GPC (Chloroform): M_n = 58,577, M_w = 140,000; BET surface area = 1034 m^2g^{-1}; pore volume = 0.8739 cm^3g^{-1} at (P/P_o = 0.9814); ^{1}H NMR (500 MHz, $CDCl_3$) δ 7.66 (*b*s, 2H, Ar *H*), 7.56 (*b*s, 2H, Ar *H*), 6.96 (*b*s, 4H, Ar *H*), 2.37 (*b*s, 6H, C*H*$_3$), 1.82-1.10 (m, 16H, C*H*$_2$, C*H*$_3$); Solid state ^{13}C NMR (100 MHz) δ_c (ppm) = 143.9, 138.7, 130.5, 124.7, 117.8, 109.1, 94.5, 47.6, 34.3, 12.9.

P20

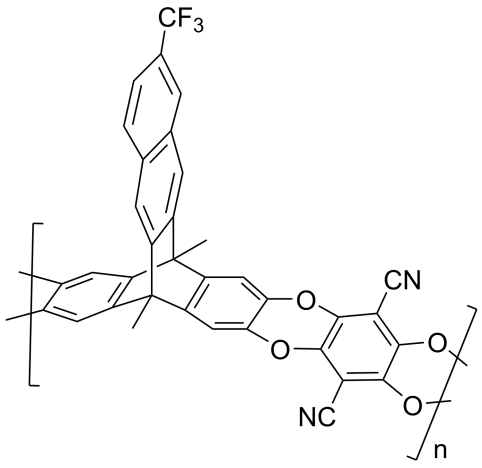

(**P20**) was prepared according to the general procedure G.P.P 3. (**55**) (0.58 g, 1.19 mmol), tetrafluoroterephthalonitrile (0.24 g, 1.19 mmol), K_2CO_3 (1.32 g, 9.52 mmol) and DMF (12.0 mL) were combined. Collected (**P20**) as a yellow powder (0.55 g, 0.94 mmol, 79 %). ν_{max} (cm^{-1}): 2974, 1439, 1329, 1294, 1269, 1186, 1163, 1124, 1067, 1005, 885; T_d = 442°C; BET surface area = 944 m^2g^{-1}; pore volume = 0.7048 cm^3g^{-1} at (P/P_o = 0.9814); ^1H NMR (500 MHz, C_4D_8O) δ 6.33 (*b*s, 1H, Ar *H*), 6.17-5.97 (m, 3H, Ar *H*), 5.74 (*b*s, 1H, Ar *H*), 5.35 (*b*s, 4H, Ar *H*), 0.63 (*b*s, 6H, C*H*$_3$); ^{13}C NMR (126 MHz, C_4D_8O) δ_c (ppm) = 145.8, 140.3, 138.3, 111.4, 95.0, 49.0, 30.8, 14.2.

P21

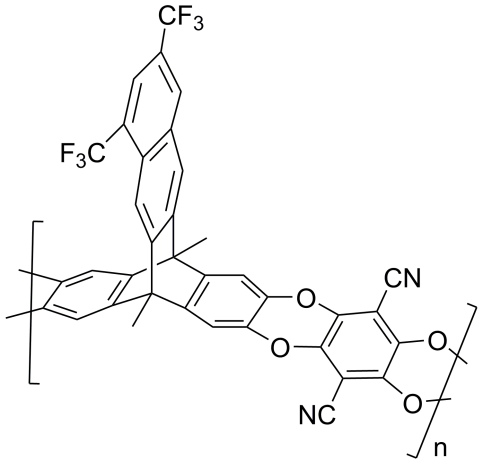

(**P21**) was prepared according to the general procedure G.P.P 3. (**59**) (1.25 g, 2.20 mmol), tetrafluoroterephthalonitrile (0.44 g, 2.20 mmol), K_2CO_3 (2.44 g, 17.6 mmol) and DMF (20.0 mL) were combined. Collected (**P21**) as a yellow powder (1.21 g, 1.85 mmol, 84 %). ν_{max} (cm^{-1}): 2980, 1439, 1298, 1271, 1206, 1188, 1161, 1128, 1088, 1007, 905, 885, 671; T_d = 488°C; BET surface area = 1074 m^2g^{-1}; pore volume = 1.021 cm^3g^{-1} at (P/P_o = 0.9814); ^1H NMR (500 MHz, C_4D_8O) δ 6.68 (*b*s, 1H, Ar *H*), 6.38-6.07 (m, 3H, Ar *H*), 5.40 (*b*s, 4H, Ar *H*), 0.64 (*b*s, 6H, C*H*$_3$); Solid state ^{13}C NMR (100 MHz) δ_c (ppm) = 145.4, 138.2, 131.7, 128.3, 119.4, 109.7, 94.9, 48.0, 12.1.

Bibliography

1. Robeson, L. M., *Journal of Membrane Science* **1991,** *62* (2), 165-185.
2. Robeson, L. M., *Journal of Membrane Science* **2008,** *320* (1–2), 390-400.
3. Budd, P. M.; Elabas, E. S.; Ghanem, B. S.; Makhseed, S.; McKeown, N. B.; Msayib, K. J.; Tattershall, C. E.; Wang, D., *Advanced Materials* **2004,** *16* (5), 456-459.
4. Carta, M.; Malpass-Evans, R.; Croad, M.; Rogan, Y.; Jansen, J. C.; Bernardo, P.; Bazzarelli, F.; McKeown, N. B., *Science* **2013,** *339* (6117), 303-307.
5. Carta, M.; Croad, M.; Malpass-Evans, R.; Jansen, J. C.; Bernardo, P.; Clarizia, G.; Friess, K.; Lanč, M.; McKeown, N. B., *Advanced Materials* **2014**, 3526-3531.
6. Rouquerol, J. A., D.; Fairbridge, C. W.; Everett, D. H.; Haynes, J. H.; Pernicone, N.; Ramsay, J. D. F.; Sing, K. S. W.; Unger, K. K.;, *Pure & Appl. Chem* **1994,** *66* (8), 1739-1758.
7. Zhao, X. S., *Journal of Materials Chemistry* **2006,** *16* (7), 623-625.
8. Rouquerol, F.; Rouquerol, J.; Sing, K., In *Adsorption by Powders and Porous Solids*, Academic Press: London, 1999; pp 1-26.
9. Biniak, S.; Szymański, G.; Siedlewski, J.; Świtkowski, A., *Carbon* **1997,** *35* (12), 1799-1810.
10. Dullien, F. A. L., *Fluid Transport and Pore Structure*. Academic Press: 1992.
11. Abbott, L. J.; McDermott, A. G.; Del Regno, A.; Taylor, R. G. D.; Bezzu, C. G.; Msayib, K. J.; McKeown, N. B.; Siperstein, F. R.; Runt, J.; Colina, C. M., *The Journal of Physical Chemistry B* **2013,** *117* (1), 355-364.
12. Larsen, G. S.; Lin, P.; Hart, K. E.; Colina, C. M., *Macromolecules* **2011,** *44* (17), 6944-6951.
13. Langmuir, I., *Journal of the American Chemical Society* **1916,** *38* (11), 2221-2295.
14. Brunauer, S.; Emmett, P. H.; Teller, E., *Journal of the American Chemical Society* **1938,** *60* (2), 309-319.
15. Ismail, I. M. K., *Carbon* **1990,** *28* (2–3), 423-434.
16. Siemieniewska, *Pure & Appl. Chem* **1985,** *57* (4), 603-619.
17. Wilson, S. T.; Broach;, R. W.; Flanigen;, E. M., *Zeolites in Industrial Separation and Catalysis*. John Wiley & Sons: 2010.
18. Cundy, C. S.; Cox, P. A., *Chemical Reviews* **2003,** *103* (3), 663-702.
19. Rabo, J. A.; Schoonover, M. W., *Applied Catalysis A: General* **2001,** *222* (1–2), 261-275.
20. Barrer, R. M., *Journal of the Chemical Society* **1950,** (0), 2342-2350.
21. Roland, E.; Lutz, W.; Eckehart, R.; Wolfgang, L. Y-Zeolites with high silica/alumina ratios, and high hydrothermal stability 06 Mar 1997
22. Quintelas, C.; Rocha, Z.; Silva, B.; Fonseca, B.; Figueiredo, H.; Tavares, T., *Chemical Engineering Journal* **2009,** *152* (1), 110-115.
23. Yates, D. J. C., *Canadian Journal of Chemistry* **1968,** *46* (10), 1695-1701.
24. Freyhardt, C. C.; Tsapatsis, M.; Lobo, R. F.; Balkus, K. J.; Davis, M. E., *Nature* **1996,** *381* (6580), 295-298.
25. Kristallogr, W. M. M. G. T. K. Z., **1965,** *121* (211).
26. Gualtieri, G. C. A., *American Mineralogist* **1999,** *84*, 112-119.
27. Zhang, L. L.; Zhao, X. S., *Chemical Society Reviews* **2009,** *38* (9), 2520-2531.
28. Sobiesiak, M.; Gawdzik, B.; Puziy, A. M.; Poddubnaya, O. I., *Applied Surface Science* **2010,** *256* (17), 5355-5360.

29. Budd, P. M.; Makhseed, S. M.; Ghanem, B. S.; Msayib, K. J.; Tattershall, C. E.; McKeown, N. B., *Materials Today* **2004,** *7* (4), 40-46.
30. Dekker, M., *Chemistry and physics of carbon: a series of advances*. New York, 2001; Vol. 27.
31. Zhao, Y.; Zhao, L.; Yao, K. X.; Yang, Y.; Zhang, Q.; Han, Y., *Journal of Materials Chemistry* **2012,** *22* (37), 19726-19731.
32. van den Berg, A. W. C.; Arean, C. O., *Chemical Communications* **2008,** (6), 668-681.
33. Hyeon, J. L. J. K. T., *Advanced Materials* **2006,** *18*, 2073-2094.
34. Rodríguez-reinoso, F., *Carbon* **1998,** *36* (3), 159-175.
35. Díaz, U.; Corma, A., *Coordination Chemistry Reviews* **2016,** *311*, 85-124.
36. Ben, T.; Ren, H.; Ma, S.; Cao, D.; Lan, J.; Jing, X.; Wang, W.; Xu, J.; Deng, F.; Simmons, J. M.; Qiu, S.; Zhu, G., *Angewandte Chemie International Edition* **2009,** *48* (50), 9457-9460.
37. Ben, T.; Qiu, S., *CrystEngComm* **2013,** *15* (1), 17-26.
38. Trewin;, A.; Cooper;, A. I., *Angewandte Chemie International Edition* **2010,** *49* (9), 1533-1535.
39. Lan, J.; Cao, D.; Wang, W.; Ben, T.; Zhu, G., *The Journal of Physical Chemistry Letters* **2010,** *1* (6), 978-981.
40. Sun, Y.; Ben, T.; Wang, L.; Qiu, S.; Sun, H., *The Journal of Physical Chemistry Letters* **2010,** *1* (19), 2753-2756.
41. Tsyurupa, S. V. R. V. A. D. M. P. 1969.
42. Tsyurupa, M. P.; Davankov, V. A., *Reactive and Functional Polymers* **2006,** *66* (7), 768-779.
43. Davankov, V. A.; Tsyurupa, M. P., *Reactive Polymers* **1990,** *13* (1), 27-42.
44. Tsyurupa, V. A. D. S. V. R. a. M. P. 1971.
45. Lee, J.-Y.; Wood, C. D.; Bradshaw, D.; Rosseinsky, M. J.; Cooper, A. I., *Chemical Communications* **2006,** (25), 2670-2672.
46. McKeown, N. B.; Budd, P. M., *Macromolecules* **2010,** *43* (12), 5163-5176.
47. Germain, J.; Frechet, J. M. J.; Svec, F., *Journal of Materials Chemistry* **2007,** *17* (47), 4989-4997.
48. Ahn, J.-H.; Jang, J.-E.; Oh, C.-G.; Ihm, S.-K.; Cortez, J.; Sherrington, D. C., *Macromolecules* **2006,** *39* (2), 627-632.
49. Podlesnyuk, V. V.; Hradil, J.; Králová, E., *Reactive and Functional Polymers* **1999,** *42* (3), 181-191.
50. Li, A.; Zhang, Q.; Zhang, G.; Chen, J.; Fei, Z.; Liu, F., *Chemosphere* **2002,** *47* (9), 981-989.
51. Penner;, N. A.; Nesterenko;, P. N.; Ilyin;, M. M.; Tsyurupa;, M. P.; Davankov, V. A., *Chromatographia* **1999,** *50*, 611-620.
52. Martin, C. F.; Stockel, E.; Clowes, R.; Adams, D. J.; Cooper, A. I.; Pis, J. J.; Rubiera, F.; Pevida, C., *Journal of Materials Chemistry* **2011,** *21* (14), 5475-5483.
53. Tsyurupa, M. P.; Davankov, V. A., *Reactive and Functional Polymers* **2002,** *53*, 193.
54. Wood, C. D.; Tan, B.; Trewin, A.; Niu, H.; Bradshaw, D.; Rosseinsky, M. J.; Khimyak, Y. Z.; Campbell, N. L.; Kirk, R.; Stöckel, E.; Cooper, A. I., *Chemistry of Materials* **2007,** *19* (8), 2034-2048.
55. Zhang, G.; Mastalerz, M., *Chemical Society Reviews* **2014,** *43* (6), 1934-1947.
56. Tozawa, T.; Jones, J. T. A.; Swamy, S. I.; Jiang, S.; Adams, D. J.; Shakespeare, S.; Clowes, R.; Bradshaw, D.; Hasell, T.; Chong, S. Y.; Tang, C.; Thompson, S.; Parker, J.;

Trewin, A.; Bacsa, J.; Slawin, A. M. Z.; Steiner, A.; Cooper, A. I., *Nat Mater* **2009,** *8* (12), 973-978.
57. Evans, J. D.; Sumby, C. J.; Doonan, C. J., *Chemistry Letters* **2015,** *44* (5), 582-588.
58. Jin, Y.; Voss, B. A.; Jin, A.; Long, H.; Noble, R. D.; Zhang, W., *Journal of the American Chemical Society* **2011,** *133* (17), 6650-6658.
59. Yoshizawa, M.; Klosterman, J. K.; Fujita, M., *Angewandte Chemie International Edition* **2009,** *48* (19), 3418-3438.
60. Leininger, S.; Olenyuk, B.; Stang, P. J., *Chemical Reviews* **2000,** *100* (3), 853-908.
61. Mal, P.; Breiner, B.; Rissanen, K.; Nitschke, J. R., *Science* **2009,** *324* (5935), 1697-1699.
62. Iyer, K. S.; Norret, M.; Dalgarno, S. J.; Atwood, J. L.; Raston, C. L., *Angewandte Chemie International Edition* **2008,** *47* (34), 6362-6366.
63. Hof, F.; Craig, S. L.; Nuckolls, C.; Rebek, J., *Angewandte Chemie International Edition* **2002,** *41* (9), 1488-1508.
64. Mastalerz, M., *Chemical Communications* **2008,** (39), 4756-4758.
65. Bushell, A. F.; Budd, P. M.; Attfield, M. P.; Jones, J. T. A.; Hasell, T.; Cooper, A. I.; Bernardo, P.; Bazzarelli, F.; Clarizia, G.; Jansen, J. C., *Angewandte Chemie International Edition* **2013,** *52*, 1253-1256.
66. Ghanem, B. S.; Msayib, K. J.; McKeown, N. B.; Harris, K. D. M.; Pan, Z.; Budd, P. M.; Butler, A.; Selbie, J.; Book, D.; Walton, A., *Chemical Communications* **2007,** (1), 67-69.
67. McKeown, N. B.; Budd, P. M., *Encyclopedia of Polymer Science and Technology*. John Wiley and Sons, Inc.: New York, 2009.
68. McKeown, N. B.; Budd, P. M.; Hoek, E. M. V.; Tarabara, V. V., Polymers of Intrinsic Microporosity. In *Encyclopedia of Membrane Science and Technology*, John Wiley & Sons, Inc.: 2013.
69. Hu, Y.; Shiotsuki, M.; Sanda, F.; Freeman, B. D.; Masuda, T., *Macromolecules* **2008,** *41* (22), 8525-8532.
70. Nagai, K.; Masuda, T.; Nakagawa, T.; Freeman, B. D.; Pinnau, I., *Progress in Polymer Science* **2001,** *26* (5), 721-798.
71. Yampolskii, Y., *Macromolecules* **2012,** *45* (8), 3298-3311.
72. Pinnau, I.; Toy, L. G., *Journal of Membrane Science* **1996,** *109* (1), 125-133.
73. Gringolts, M.; Bermeshev, M.; Yampolskii, Y.; Starannikova, L.; Shantarovich, V.; Finkelshtein, E., *Macromolecules* **2010,** *43* (17), 7165-7172.
74. Starannikova, L.; Pilipenko, M.; Belov, N.; Yampolskii, Y.; Gringolts, M.; Finkelshtein, E., *Journal of Membrane Science* **2008,** *323* (1), 134-143.
75. Tanaka, K.; Okano, M.; Toshino, H.; Kita, H.; Okamoto, K. I., *Journal of Polymer Science B Polymer Physics* **1992,** *30* (8), 907-914.
76. Saxman, A. M.; Liepins, R.; Aldissi, M., *Progress in Polymer Science* **1985,** *11* (1–2), 57-89.
77. Masuda, T.; Hasegawa, K.-i.; Higashimura, T., *Macromolecules* **1974,** *7* (6), 728-731.
78. Masuda, T.; Isobe, E.; Higashimura, T.; Takada, K., *Journal of the American Chemical Society* **1983,** *105* (25), 7473-7474.
79. Budd, P. M.; McKeown, N. B., *Polymer Chemistry* **2010,** *1* (1), 63-68.
80. Jia, J.; Baker, G. L., *Journal of Polymer Science B Polymer Physics* **1998,** *36* (6), 959-968.
81. Hofmann, D.; Heuchel, M.; Yampolskii, Y.; Khotimskii, V.; Shantarovich, V., *Macromolecules* **2002,** *35* (6), 2129-2140.

82. Hofmann, D.; Entrialgo-Castano, M.; Lerbret, A.; Heuchel, M.; Yampolskii, Y., *Macromolecules* **2003,** *36* (22), 8528-8538.
83. Morisato, A.; Pinnau, I., *Journal of Membrane Science* **1996,** *121* (2), 243-250.
84. Budd, P. M.; Msayib, K. J.; Tattershall, C. E.; Ghanem, B. S.; Reynolds, K. J.; McKeown, N. B.; Fritsch, D., *Journal of Membrane Science* **2005,** *251* (1–2), 263-269.
85. Wang, Y.; McKeown, N. B.; Msayib, K. J.; Turnbull, G. A.; Samuel, I. D. W., *Sensors* **2011,** *11*, 2478.
86. Budd, P. M.; Ghanem, B. S.; Makhseed, S.; McKeown, N. B.; Msayib, K. J.; Tattershall, C. E., *Chemical Communications* **2004,** (2), 230-231.
87. McKeown, N. B.; Budd, P. M., *Chemical Society Reviews* **2006,** *35* (8), 675-683.
88. Ghanem, B. S.; Swaidan, R.; Litwiller, E.; Pinnau, I., *Advanced Materials* **2014,** *26*, 3688-3692.
89. Rogan, Y.; Starannikova, L.; Ryzhikh, V.; Yampolskii, Y.; Bernardo, P.; Bazzarelli, F.; Jansen, J. C.; McKeown, N. B., *Polymer Chemistry* **2013,** *4* (13), 3813-3820.
90. Calle, M.; Lozano, A. E.; de Abajo, J.; de la Campa, J. G.; Álvarez, C., *Journal of Membrane Science* **2010,** *365* (1–2), 145-153.
91. Ghosh, M. K.; Mittal, K. L., *Polyimides: Fundamentals And Applications*. Marcel Dekker: New York, 1996.
92. Ghanem, B. S.; McKeown, N. B.; Budd, P. M.; Selbie, J. D.; Fritsch, D., *Advanced Materials* **2008,** *20* (14), 2766-2771.
93. Sroog, C. E.; Endrey, A. L.; Abramo, S. V.; Berr, C. E.; Edwards, W. M.; Olivier, K. L., *Journal of Polymer Science A Polymer Chemistry* **1965,** *3* (4), 1373-1390.
94. Sroog, C. E., *Progress in Polymer Science* **1991,** *16* (4), 561-694.
95. Michael, A. M., *Annual Review of Materials Science* **1998,** *28* (1), 599-630.
96. Freeman, B. D., *Macromolecules* **1999,** *32* (2), 375-380.
97. Tröger, J., *Journal für Praktische Chemie* **1887,** *36* (1), 225-245.
98. Sergeyev, S., *Helvetica Chimica Acta* **2009,** *92* (3), 415-444.
99. Spielman, M. A., *Journal of the American Chemical Society* **1935,** *57* (3), 583-585.
100. Wagner, E. C., *Journal of the American Chemical Society* **1935,** *57* (7), 1296-1298.
101. Abella, C. A. M.; Benassi, M.; Santos, L. S.; Eberlin, M. N.; Coelho, F., *The Journal of Organic Chemistry* **2007,** *72* (11), 4048-4054.
102. Rúnarsson, Ö. V.; Artacho, J.; Wärnmark, K., *European Journal of Organic Chemistry* **2012,** *2012* (36), 7015-7041.
103. Larson, S. B.; Wilcox, C. S., *Acta Crystallographica Section C* **1986,** *42* (2), 224-227.
104. Prelog, V.; Wieland, P., *Helvetica Chimica Acta* **1944,** *27* (1), 1127-1134.
105. Wepster, B. M., *Recueil des travaux chimiques des pays-bas* **1953,** *72* (8), 661-672.
106. Marquis, E.; Graton, J.; Berthelot, M.; Planchat, A.; Laurence, C., *Canadian Journal of Chemistry* **2004,** *82* (9), 1413-1422.
107. Poli, E.; Merino, E.; Díaz, U.; Brunel, D.; Corma, A., *The Journal of Physical Chemistry C* **2011,** *115* (15), 7573-7585.
108. Cabrero-Antonino, J. R.; García, T.; Rubio-Marqués, P.; Vidal-Moya, J. A.; Leyva-Pérez, A.; Al-Deyab, S. S.; Al-Resayes, S. I.; Díaz, U.; Corma, A., *ACS Catalysis* **2011,** *1* (2), 147-158.
109. Carta, M.; Croad, M.; Bugler, K.; Msayib, K. J.; McKeown, N. B., *Polymer Chemistry* **2014,** *5* (18), 5262-5266.

110. Rose, I.; Carta, M.; Malpass-Evans, R.; Ferrari, M.-C.; Bernardo, P.; Clarizia, G.; Jansen, J. C.; McKeown, N. B., *ACS Macro Letters* **2015,** *4* (9), 912-915.
111. Paul, D. R.; Yampolskii, Y. P., *Polymeric Gas Separation Membranes*. CRC press: Florida, 1993.
112. Graham, T. P., *Mag.* **1866,** *32*, 402.
113. Koros, W., *Gas Separation, in: Membrane Separation Systems - Recent Developments and Future Directions*. William Andrew Publishing: 1991.
114. Matsuura, T., *Synthetic Membranes and Membrane Separation Processes*. CRC press: Florida, 1993.
115. Sandra, E. K.; Colin, A. S.; Geoff, W. S., *Recent Patents on Chemical Engineering* **2008,** *1* (1), 52-66.
116. Fritzsche, A.; Kurz, J., *The separation of gases by membranes, in: Handbook of industrial membrane technology porter MC*. William Andrew Publishing: 1990.
117. Paul, D.; Yampolskii, Y., *Polymeric gas separation membranes*. CRC Press: 1994.
118. Baker, R. W., *Membrane Technology and Applications*. 2 ed.; John Wiley & Sons, Ltd: California, 2004.
119. Meares, P., *Journal of the American Chemical Society* **1954,** *76* (13), 3415-3422.
120. Meares, P., *Transactions of the Faraday Society* **1957,** *53* (0), 101-106.
121. Meares, P., *Transactions of the Faraday Society* **1958,** *54* (0), 40-46.
122. Vieth, W. R.; Howell, J. M.; Hsieh, J. H., *Journal of Membrane Science* **1976,** *1*, 177-220.
123. Vieth, W. R. A study of polyethylene terephthalate by gas permeation. MIT, 1961.
124. (a) Michaels, A. S.; Vieth, W. R.; Barrie, J. A., *Journal of Applied Physics* **1963,** *34* (1), 1-12; (b) Michaels, A. S.; Vieth, W. R.; Barrie, J. A., *Journal of Applied Physics* **1963,** *34* (1), 13-20.
125. Vieth, W. R.; Sladek, K. J., *Journal of Colloid Science* **1965,** *20* (9), 1014-1033.
126. freeman, B.; Yampolskii, Y., *Membrane Gas Separation*. John Wiley & Sons: New Jersey, 2011.
127. Yampolskii, Y.; Freeman, B., *Membrane Gas Separation*. John Wiley & Sons: 2010.
128. Jansen, J. C.; Friess, K.; Drioli, E., *Journal of Membrane Science* **2011,** *367* (1–2), 141-151.
129. Macchione, M.; Jansen, J. C.; De Luca, G.; Tocci, E.; Longeri, M.; Drioli, E., *Polymer* **2007,** *48* (9), 2619-2635.
130. Carapellucci, R.; Milazzo, A., *Proc. Inst. Mech. Eng. Part A. J. Power Energy* **2003,** *217*, 505-517.
131. Budd, P. M.; McKeown, N. B.; Ghanem, B. S.; Msayib, K. J.; Fritsch, D.; Starannikova, L.; Belov, N.; Sanfirova, O.; Yampolskii, Y.; Shantarovich, V., *Journal of Membrane Science* **2008,** *325* (2), 851-860.
132. Shen, J.; Zhang, Y.; Huang, M.; Wang, W.; Xu, Z.; Yeung, K. W. K.; Yi, C.; Xu, M., *Journal of Polymer Research* **2012,** *19* (5), 1-9.
133. Yang, C.-P.; Hsiao, F.-Z., *Journal of Polymer Research 10* (3), 181-193.
134. Burgoyne;, W. F. Polyimide membrane having improved flux. 4,897,092, Jan. 30, 1990.
135. Wolthuis, E., *The Journal of Organic Chemistry* **1961,** *26* (7), 2215-2220.
136. Shanmugasundaram, M.; Manikandan, S.; Raghunathan, R., *Tetrahedron* **2002,** *58* (5), 997-1003.

137. Van der Eycken, E.; Appukkuttan, P.; De Borggraeve, W.; Dehaen, W.; Dallinger, D.; Kappe, C. O., *The Journal of Organic Chemistry* **2002,** *67* (22), 7904-7907.
138. Loupy, A.; Maurel, F.; Sabatié-Gogová, A., *Tetrahedron* **2004,** *60* (7), 1683-1691.
139. Rybáčková, M.; Bělohradský, M.; Holý, P.; Pohl, R.; Dekoj, V.; Závada, J., *Synthesis* **2007,** *2007*, 1554-1558.
140. Cheng, L.; Xu, Z.; Xiong, X.-q.; Wang, J.-x.; Jing, B., *Chinese Journal of Polymer Science* **2009,** *28* (1), 69-76.
141. Nelleborg, P.; Lund, H.; Eriksen, J., *Tetrahedron Letters* **1985,** *26* (14), 1773-1776.
142. Hart, H.; Bashir-Hashemi, A.; Luo, J.; Meador, M. A., *Tetrahedron* **1986,** *42* (6), 1641-1654.
143. Ghanem, B. S.; McKeown, N. B.; Budd, P. M.; Al-Harbi, N. M.; Fritsch, D.; Heinrich, K.; Starannikova, L.; Tokarev, A.; Yampolskii, Y., *Macromolecules* **2009,** *42* (20), 7881-7888.
144. Kim, K.-J.; So, W.-W.; Moon, S.-J., Preparation of 6FDA-based polyimide membranes for CO2 gas separation. In *Studies in Surface Science and Catalysis*, Sang-Eon Park, J.-S. C.; Kyu-Wan, L., Eds. Elsevier: 2004; Vol. Volume 153, pp 531-534.
145. Kim, T. H.; Koros, W. J.; Husk, G. R.; O'Brien, K. C., *Journal of Membrane Science* **1988,** *37* (1), 45-62.
146. Merkel, T. C.; Freeman, B. D.; Spontak, R. J.; He, Z.; Pinnau, I.; Meakin, P.; Hill, A. J., *Science* **2002,** *296* (5567), 519-522.
147. Taylor, R. G. D.; Carta, M.; Bezzu, C. G.; Walker, J.; Msayib, K. J.; Kariuki, B. M.; McKeown, N. B., *Organic Letters* **2014,** *16* (7), 1848-1851.
148. Malpass-Evans;, R. Microporous Polymers Containing Tertiary Amine Functionality for Gas Separation Membrane Fabrication. Cardiff University, 2014.
149. Alghunaimi, F.; Ghanem, B.; Alaslai, N.; Swaidan, R.; Litwiller, E.; Pinnau, I., *Journal of Membrane Science* **2015,** *490*, 321-327.
150. Sydlik, S. A.; Chen, Z.; Swager, T. M., *Macromolecules* **2011,** *44* (4), 976-980.
151. Kantam, R.; Holland, R.; Khanna, B. P.; Revell, K. D., *Tetrahedron Letters* **2011,** *52* (39), 5083-5085.
152. Carta, M.; Bernardo, P.; Clarizia, G.; Jansen, J. C.; McKeown, N. B., *Macromolecules* **2014,** *47* (23), 8320-8327.
153. Ghanem, B. S.; Swaidan, R.; Ma, X.; Litwiller, E.; Pinnau, I., *Advanced Materials* **2014,** *26* (39), 6696-6700.
154. Fritsch, D.; Bengtson, G.; Carta, M.; McKeown, N. B., *Macromolecular Chemistry and Physics* **2011,** *212* (11), 1137-1146.
155. Carta, M.; Msayib, K. J.; Budd, P. M.; McKeown, N. B., *Organic Letters* **2008,** *10* (13), 2641-2643.
156. Ghanem, B. S.; Hashem, M.; Harris, K. D. M.; Msayib, K. J.; Xu, M.; Budd, P. M.; Chaukura, N.; Book, D.; Tedds, S.; Walton, A.; McKeown, N. B., *Macromolecules* **2010,** *43* (12), 5287-5294.
157. Bezzu, C. G.; Carta, M.; Tonkins, A.; Jansen, J. C.; Bernardo, P.; Bazzarelli, F.; McKeown, N. B., *Advanced Materials* **2012,** *24* (44), 5930-5933.
158. Pinnau, I.; Casillas, C. G.; Morisato, A.; Freeman, B. D., *J. Polym. Sci. Part B: Polym. Phys.* **1997,** *35*, 1483.
159. Starannikova, L.; Khodzhaeva, V.; Yampolskii, Y., *J. Membr. Sci* **2004,** *244*, 183.
160. Cheng;, L.; Liu;, J.; Xu, H. Synthesis method for 2,3,6,7-triptycene tetracarboxylic dianhydride. 2012.

161. Luo, R.; Liao, J.; Xie, L.; Tang, W.; Chan, A. S. C., *Chemical Communications* **2013,** *49* (85), 9959-9961.
162. He, N.; Chen, Y.; Doyle, J.; Liu, Y.; Blau, W. J., *Dyes and Pigments* **2008,** *76* (2), 569-573.
163. Wang, X.; Zhang, Y.; Sun, X.; Bian, Y.; Ma, C.; Jiang, J., *Inorganic Chemistry* **2007,** *46* (17), 7136-7141.
164. Meier, H.; Rose, B., *Liebigs Annalen* **1997,** *1997* (4), 663-669.
165. Guenzi, A.; Johnson, C. A.; Cozzi, F.; Mislow, K., *Journal of the American Chemical Society* **1983,** *105* (6), 1438-1448.
166. Friedman, L.; Logullo, F. M., *Journal of the American Chemical Society* **1963,** *85* (10), 1549-1549.
167. Naghipur, A.; Reszka, K.; Sapse, A. M.; Lown, J. W., *Journal of the American Chemical Society* **1989,** *111* (1), 258-268.
168. Crivello, J. V., *The Journal of Organic Chemistry* **1981,** *46* (15), 3056-3060.
169. Furst, A.; Moore, R. E., *Journal of the American Chemical Society* **1957,** *79* (20), 5492-5493.
170. Rabjohns, M. A.; Hodge, P.; Lovell, P. A., *Polymer* **1997,** *38* (13), 3395-3407.
171. Lautens, M.; Fagnou, K.; Yang, D., *Journal of the American Chemical Society* **2003,** *125* (48), 14884-14892.
172. Bailly, F.; Cottet, F.; Schlosser, M., *Synthesis* **2005,** *2005* (05), 791-797.
173. Hagiwara, K.; Otsuki, M.; Akita, M.; Yoshizawa, M., *Chemical Communications* **2015,** *51* (52), 10451-10454.
174. Byrne, C. J.; Happer, D. A. R.; Hartshorn, M. P.; Powell, H. K. J., *Journal of the Chemical Society, Perkin Transactions 2* **1987,** (11), 1649-1653.
175. Baran, J.; Mayr, H., *The Journal of Organic Chemistry* **1988,** *53* (19), 4626-4628.
176. Irwin, L. J.; Reibenspies, J. H.; Miller, S. A., *Journal of the American Chemical Society* **2004,** *126* (51), 16716-16717.
177. Maignan, J.; Malle, G.; Deflandre, A.; Lang, G., New derivatives of 5,6,7,8-tetrahydro-1-naphthalenol, a process for their preparation and cosmetic and pharmaceutical compositions containing them. Google Patents: 1991.
178. Toyama, H.; Nakamura, M.; Nakamura, M.; Matsumoto, Y.; Nakagomi, M.; Hashimoto, Y., *Bioorganic & Medicinal Chemistry* **2014,** *22* (6), 1948-1959.
179. Bailly, F.; Cottet, F.; Schlosser, M., *Synthesis* **2005,** *2005* (05), 791-797.